PARTICLE SWARM OPTIMIZATION METHOD FOR ENERGY MANAGEMENT OF THE HYBRID SYSTEM OF AN ELECTRIC VEHICLE CHARGING STATION

by

OLUKOREDE TIJANI ADENUGA

Thesis submitted in fulfillment of the requirements for the degree

Doctor of Engineering: Electrical Engineering

in the Faculty of Engineering and Built in Environment

at the Cape Peninsula University of Technology

Supervisor: Professor Senthil Krishnamurthy

Bellville
June 2024

DECLARATION

I, Olukorede Tijani Adenuga, declare that this thesis is my own work and has not been submitted for academic assessment towards any qualification. Furthermore, it expresses my own views, not those of the Cape Peninsula University of Technology.

03/06/2024

Signed **Date**

ABSTRACT

Renewable energy sources (RES) are erratic, while its variability and intermittency limit energy supply once the grid is operating in islanded mode. High penetration rate challenges for renewable energy demands, such as frequency reserves reduction, voltage profile deterioration, inductive loading, and supply-demand balance aggregation/matching are difficult to achieve in practice.. However, the use of renewable energy resources complicates the optimization of nonlinear control variables. Metaheuristic approaches can efficiently solve high-dimensional economic dispatch (ED) issues. Renewables-incorporated ED problems are currently receiving a lot of attention as a way to deal with the challenges of an energy crisis and the environment, and they are being solved utilizing the PSO method. In this vein, the charging infrastructure required by electric vehicles is a fundamental challenge that must be addressed before large-scale deployment of RESs can take place.

The thesis developed Particle Swarm Optimisation (PSO) method for energy management of the hybrid system of an electric vehicle charging station (EVCS). The PSO provide the best value for uncertainty cost functions for both RESs and electric vehicle charging stations considering active power loss, reactive power loss operation cost, power flow, and voltage deviation in the thesis. The power generation problem for committed generators is scheduled to meet obligatory load demand while satisfying the inequality and equality constraints. The thesis provides economic power dispatch (EPD) and optimal power flow (OPF) optimization solutions based on uncertainty costs for renewable generation and its application on economic dispatch.

The most important contribution of the thesis is the analysis and investigation of the optimization effect of PSO method for the inclusion in the economic dispatch of renewable energy generation plants in energy management strategies to select the nonlinear optimization control variables, objective function and techniques are considered highly capable of solving high-dimensional ED problems with less computational time. The EPD problems are solved by implementing the developed PSO algorithm simulation on grid-tied-RES diffusion to address supply-demand balance aggregation/matching and uncertainty costs for renewable generation to enable lower power demand

from the energy storage systems (ESSs). The developed PSO method handles the co-optimization using a RES uncertainty cost functions using the B-loss transmission coefficient approach to estimate operational costs for allocated generation unit's power values.

PSO algorithms in the thesis applied uncertainty cost function with and without RESs, test cases where EVCSs loading were integrated with optimally sized RESs in the IEEE 14-bus, IEEE 30-bus and IEEE 118-bus distribution testbed. The developed PSO methods and algorithms can be useful for the resolution of numerous energy management problems in smart grid applications, provincial and national control centers, and research and educational institutions.

Keywords: Renewable energy sources; Economic power dispatch; Particle Swarm Optimisation

ACKNOWLEDGEMENTS

The student is profoundly obligated to Cape Peninsula University of Technology (CPUT) support, guidiance from Centre for Substation Automation and Energy Management Systems (CSAEMS) team, and the Centre for Postgraduate Studies.

I sincerely express my appreciation and gratitude to My Supervisor, Professor Senthil Krishnamurthy, whose academic guidance and scientific contributions were crucial through the entire duration of this research, and Dr. Oluwadamilare Bode Adewuyi, for their encouraging attitude towards the finalization of the thesis.

My heartfelt gratitude is extended to the entire faculty of Electrical, Electronics, and Computer Engineering Department at Cape Peninsula University of Technology for their continual support and ideas throughout the project. The team have been quite helpful and supportive of this research, and Ms Phaphama Panda (Administrator, Department of Electrical Engineering, CPUT) deserves special mention.

Special thanks go to Idowu Oluwabunmi, my lovely wife and daughters; your existence as family members validates the efforts towards the thesis deliverable, adoption of a never-say-die attitude and the socially acceptable behavior. Keep you all in mind that I am a father, a guide and refence point, are responsible for the flawless curve of the soft grin that I usually exhibit. Apologies for all of the quality family time that we missed while conducting this research. Finally, I thank the ALMIGHTY ALLAH for allowing me to observe the thesis completion.

DEDICATION

This study is dedicated to my beloved wife Idowu Oluwabunmi and our daughters, Adedamola Aliyah, Adeola Alimaa, Adeshile Aisha and Adebola Azeezat for the time they gave me to explore the arena of academia. You are All a secure refuge and a pleasure to my sisters, brothers and my late parents for their encouragement and advisory support.

To Almighty Allah granted wisdom, privilege, direction and for mercies of existence, I will ever be indebted.

TABLE OF CONTENTS

DECLARATION		i
ABSTRACT		ii
ACKNOWLEDGEMENTS		iv
DEDICATION		v
TABLE OF CONTENTS		vi
LISTS OF FIGURES		x
LISTS OF TABLES		xiii
GLOSSARY		xiv
TERMS/ACRONYMS/ABBREVIATIONS DEFINITION/EXPLANATION		xvii
MATHEMATICAL NOTATIONS		xvi
CHAPTER ONE INTRODUCTION		1
1.1	Introduction	1
1.2	Problem Overview	2
1.3	Statement of the problem	3
1.4	Research Aim and Objectives	5
1.5	Hypothesis	6
1.6	Delimitation of research	7
1.7	Assumptions	8
1.8	The deliverables of the thesis	8
1.9	Chapter breakdown	9
1.10	Chapter Summary	10
CHAPTER TWO LITERATURE REVIEW ON ENERGY MANAGEMENT FOR HYBRID SYSTEMS OF AN ELECTRIC VEHICLE CHARGING STATION		12
2.1	Introduction	12
2.2	A Survey of Energy Management for Hybrid System	14
2.3	Literature Survey on Energy Management Approach for Hybrid System	17
2.3.1	Review Findings on Energy Management System	18
2.4	A Review of Classical Optimisation Methods for Energy Management of the Hybrid System	18
2.4.1	Dynamic programming	19
2.4.1.1	Review discussion on DP	20
2.4.2	Linear Programming (LP) And Nonlinear Programming (NLP) Methods	21
2.4.2.1	Review discussion on LP	21
2.4.3	Mixed Integer Programming (MILP) Methods	22
2.4.3.1	Review discussion on MINLP	24
2.5	Review of Meta-Heuristics or Evolutionary Computation Optimisation Methods for Energy Management Systems	24
2.6	Swarm Intelligence Algorithms	26
2.6.1	Genetic Algorithm	26
2.6.2	Ant Colony Optimization	27
2.6.3	Particle Swarm Optimization	28
2.6.4	Differential Evolution	29
2.6.5	Artificial Bee Colony	30
2.6.6	Cuckoo Search Algorithm	30
2.6.7	Review discussion on Meta-Heuristics	31
2.6.8	Review findings on Meta-Heuristics or Evolutionary Computation Optimisation Methods for Energy Management Systems	33

2.7	Optimization Application Methods for Power Systems	34
2.8	Particle Swarm Optimization and its Applications for Power Systems	35
2.9	Chapter Summary	37
CHAPTER THREE DEVELOPMENT OF MINLP FOR ECONOMIC DISPATCH PROBLEM OF THE HYBRID SYSTEM WITH ELECTRIC VEHICLE CHARGING STATION		39
3.1	Introduction	39
3.2	Formulation of an optimization problem for energy management of the RES hybrid system	39
3.2.1	Constraints and Variable Limits	42
3.2.2	EMS MINLP Classical Algorithm	44
3.3	EMS MINLP Simulation Results and Discussion	45
CHAPTER FOUR PSO METHOD FOR ECONOMIC POWER DISPATCH PROBLEM OF A GRID-TIED RES-BASED-HS SYSTEM		52
4.1	Introduction	52
4.2	Economic Power Dispatch Problem	52
4.3	Particle Search Optimisation Model Formulation EPD Problem	53
4.4	Economic power dispatch problem with a fuel cost objective function	54
4.4.1	PSO's method for the solution of the economic power dispatch	55
4.4.2	PSO Algorithm Steps to solve EPD problems (Heris, 2016)	62
4.5	Developed PSO Method Application for solving EPD problem	63
4.5.1	Test system 1: IEEE 14-bus, IEEE 30-bus and IEEE 118-bus distribution testbed with 3, 6, and 15 generator units using zero RESs cost coefficients	63
4.5.1.1	Case 1: 3-unit generator demand of 850 MW	63
4.5.1.2	Case 2: 6-unit generator system with demand of 1263 MW	64
4.5.1.3	Case 3: 15-unit generator demand of 2630 MW	65
4.5.2	Test system 2: IEEE 14-bus, IEEE 30-bus and IEEE 118-bus distribution testbed with 3, 6, and 15 generator units using Monte Carlo uncertainty cost coefficients for RESs (Mart´ınez, 2018)	67
4.5.2.1	Case 4: 4.5.1.1 3-unit generator demand of 850 MW with RESs using Monte Carlo uncertainty cost functions	69
4.5.2.2	Case 5: 6-unit generator demand of 1263 MW with RESs using Monte Carlo uncertainty cost functions	70
4.5.3.3	Case 6: 15-unit generator demand of 2630 MW with RESs Monte Carlo uncertainty cost functions	71
4.6	Results Discussion	74
4.7	Chapter Summary	74
CHAPTER FIVE PSO METHOD FOR HYBRID SYSTEM WITH ELECTRIC VEHICLE CHARGING STATION		75
5.1	Introduction	75
5.2	Energy Management of The Hybrid System	76
5.3	Energy Management for the Hybrid System of an EVCS	77
5.4	Hybrid System of An Electric Vehicle Charging Station	78
5.5	Energy management strategies at an electric vehicle charging station	79
5.6	Optimal Active–Reactive Power Flow Considering RESs and EV charging stations station using multi-objective PSO optimization	81
5.6.1	Equality constraints considered with a power flow inside the optimization Algorithm	82

5.6.2	Inequality Constraints Related to the Fitness Function Inside of the Optimization Algorithm	82
5.6.3	Electric Vehicle Charging Station Load Profiles-Based Methods	83
5.7	Particle Swarm Optimization for Hybrid Systems of An Electric Vehicle Charging Station	84
5.8	Results of Optimal Active–Reactive Power Flow Considering RESs and EV Charging Stations using multi-objective PSO Algorithm	87
5.9	Validation of optimal active–reactive power flow considering RESs and EVCS using PSO algorithm on IEEE 14, IEEE 30 and IEEE 118 bus network	91
5.9.1	IEEE 14 bus test system	91
5.9.2	IEEE 30 bus test system	91
5.9.3	IEEE 118 bus test system	92
5.9.4	IEEE 14, IEEE 30 and IEEE 118 Classification of Buses	92
5.9.5	IEEE 14, IEEE 30 and IEEE 118 bus test analytical algorithm	92
5.10	Results of IEEE 30 Distribution Test Bus with RESs and EVCS (NHTS, 2024)	96
5.10.1	Test system 1: IEEE 14 using zero cost coefficients for RESs and Monte Carlo cost coefficients for RESs with optimal EVCS load demand	96
5.10.2	Results of IEEE 14-bus testbed without using and using RESs Data	97
5.10.3	Discussion of Results of IEEE 14-bus testbed without using and using RESs Data	98
5.10.4	Test system 2: IEEE 30 using Monte Carlo cost coefficients for RESs with optimal EVCS load demand	98
5.10.5	Results of IEEE 30-bus testbed without using and using RESs Data	100
5.10.6	Discussion of Results of IEEE 30-bus testbed without using and using RESs Data,	
5.10.7	Test system 3: IEEE 118 using Monte Carlo uncertainty cost coefficients for RESs with optimal EVCS load demand	101
5.10.8	Results of IEEE 118-bus testbed without using and using RESs Data	104
5.10.9	Discussion of Results of IEEE 118-bus testbed without using and using RESs Data	
5.11	Chapter Summary	104
CHAPTER SIX CONCLUSION AND FUTURE RECOMMENDATIONS		106
6.1	Introduction	106
6.2	Aim and Objectives of the research	106
6.3	Thesis deliverables	107
6.3.1	Comprehensive literature study and review of the main aspects of the optimization methods for the Hybrid energy management with Electric Vehicles	107
6.3.2	Theoretical development and design of the algorithms used in solving the dispatch optimization problem of the grid-tied RES hybrid system	108
6.3.2.1	MNLIP method for the Economic dispatch of the grid-tied RES hybrid system	108
6.3.2.2	PSO method for the Economic dispatch of the grid-tied RES hybrid system	109
6.3.2.3	PSO method for the Economic dispatch of the grid-tied RES hybrid system with Electric Vehicles	109
6.3.3	Software development for the implementation of the developed MLIP & PSO algorithms	110
6.4	Contribution of the Thesis	112

6.5	Possible applications of the research outputs	113
6.6	Future research	114
6.7	Publication	114
BIBLIOGRAPHY		114
APPENDICES		141
A.	MINLP SCRIPTS FOR ENERGY MANAGEMENT SYSTEM FOR HYBRID SYSTEM	141
B.	PSO METHOD FOR ECONOMIC POWER DISPATCH PROBLEM OF A GRID- TIED RES-BASED-HS SYSTEM SCRIPTS	149
C.	SCRIPTS FOR PSO METHOD FOR ENERGY MANAGEMENT OF THE HYBRID SYSTEM OF AN ELECTRIC VEHICLE CHARGING STATION	155
D.	PSO SCRIPTS FOR PV-Bat-Grid ENERGY MANAGEMENT OF THE HYBRID SYSTEM	176

LISTS OF FIGURES

Figure 1.1.	The schematic diagram for a hybrid energy management enabled with an electric charging station	3
Figure 2.1.	Number of energy management publications for hybrid system year-wise	13
Figure 2.2.	Number of energy management for hybrid system publications year-wise	16
Figure 2.3.	Number of reviewed publications based on the application domain, objective functions, and constraints against year of publication	16
Figure 2.4.	Number of reviewed publications against country of origin	18
Figure 2.5.	Solution methods from literature review for optimal economic power dispatch and power flow problem	19
Figure 3.1.	Flowchart for MINLP Classical Algorithm	45
Figure 3.2.	ESS SOC% simulation: (a) battery energy loss during clear days in the heuristics method simulation; (b) energy availability increases with peak during cloudy days in the optimal approach	46
Figure 3.3.	ESS SOC % simulation: (a) battery energy reduction during clear days in the heuristics approach simulation; (b) energy availability rises with peak during cloudy days in the optimised-based approach	47
Figure 3.4.	Voltage simulation: (a) less than 5000 V battery energy during clear days in the heuristics method simulation; (b) more than 5000V peak energy availability during cloudy days in the optimal approach	48
Figure 3.5.	Grid cost simulation: (a) loss of grid supply and cost of ESS	49
Figure 3.6.	Flowchart for EPD problems solution using PSO method	49
Figure 3.7.	Energy management strategies of grid-tied HS	50
Figure 3.8.	Grid-tied HS Energy management at EV charging station loading	50
Figure 4.1.	Flowchart for using the PSO algorithm to solve EPD problems	60
Figure 4.2.	Flowchart for EPD problems solution using PSO method continuation	61
Figure 4.3.	3-Unit testbed simulation for EPD (best cost) (a) minimum cost (best cost) 3 thermal units convergence; (b) minimum cost (best cost) 2 thermal and 1 solar PV units convergence	64
Figure 4.4.	6-Unit testbed simulation for EPD (best cost) (a) minimum cost (best cost) 6 thermal units convergence; (b) minimum cost (best cost) 2 thermal and 4 solar PV units convergence	65
Figure 4.5.	15-Unit testbed simulation for EPD (best cost) (a) minimum cost (best cost) 15 thermal units convergence; (b) minimum cost (best cost) 7 thermal and 8 solar PV units convergence	67
Figure 4.6.	6-Unit with RESs cost coefficient data testbed simulation for EPD (best cost) (a) minimum cost (best cost) 6 thermal units convergence; (b) minimum cost (best cost) 2 thermal and 4 solar PV units convergence	69
Figure 4.7.	6-Units EPD simulation for the minimum cost (best cost) Fuel cost coefficients with RESs (a) convergence of the minimum cost (best cost) 6 thermal units; (b) second run convergence of the minimum cost (best cost) for 2 thermal and 4 solar PV units.	71
Figure 4.8.	15-Unit with RESs cost coefficient data testbed simulation for EPD (best cost) (a) minimum cost (best cost) 15 thermal units convergence; (b) minimum cost (best cost) 7 thermal and 8 solar PV units convergence	73
Figure 5.1.	Energy Management structure for the Hybrid System of an EVCS	78
Figure 5.2.	Energy management strategies at EV charging station	81
Figure 5.3.	Energy management strategies at EV charging station flowchart	87
Figure 5.4.	Best Total System Cost at Buses without optimal EVCS demand	88

Figure 5.5.	Voltage profile at Buses without optimal EVCS demand	88
Figure 5.6.	Apparent Line Power Flow without optimal EVCS demand	89
Figure 5.7.	Real Power Loss without optimal EVCS demand	89
Figure 5.8.	Reactive Power Loss without optimal EVCS demand	90
Figure 5.9.	IEEE 14 Best Total System Cost at Buses with optimal EVCS load demand (a) using zero cost coefficients for RESs (b) using Monte Carlo uncertainty cost coefficients for RESs	96
Figure 5.10.	IEEE 14 Bus Voltage profile with optimal EVCS load demand (a) using zero cost coefficients for RESs (b) using Monte Carlo uncertainty cost coefficients for RESs	96.
Figure 5.11.	IEEE 14 Apparent Line Power Flow with optimal EVCS load demand (a) using zero cost coefficients for RESs (b) using Monte Carlo uncertainty cost coefficients for RESs	96
Figure 5.12.	IEEE 14 Real Power Loss with optimal EVCS load demand (a) using zero cost coefficients for RESs (b) using Monte Carlo uncertainty cost coefficients for RESs	97
Figure 5.13.	IEEE 14 Reactive Power Loss with optimal EVCS load demand (a) using zero cost coefficients for RESs (b) using Monte Carlo uncertainty cost coefficients for RESs	97
Figure 5.14.	Simulated Model of IEEE 14-bus system with Optimal RESs and EV Location	97
Figure 5.15.	IEEE 30 Best Total System Cost at Buses with optimal EVCS load demand (a) using zero cost coefficients for RESs (b) using Monte Carlo uncertainty cost coefficients for RESs	98
Figure 5.16.	IEEE 30 Bus Voltage profile with optimal EVCS load demand (a) using zero cost coefficients for RESs (b) using Monte Carlo uncertainty cost coefficients for RESs	99
Figure 5.17.	IEEE 30 Apparent Line Power Flow with optimal EVCS load demand (a) using zero cost coefficients for RESs (b) using Monte Carlo uncertainty cost coefficients for RESs	99
Figure 5.18.	IEEE 30 Real Power Loss with optimal EVCS load demand (a) using zero cost coefficients for RESs (b) using Monte Carlo uncertainty cost coefficients for RESs	100
Figure 5.19.	IEEE 30 Reactive Power Loss with optimal EVCS load demand (a) using zero cost coefficients for RESs (b) using Monte Carlo uncertainty cost coefficients for RESs	100
Figure 5.20.	Simulated Model of IEEE 30-bus with Optimal RESs and EV Location	101
Figure 5.21.	IEEE 118 Best Total System Cost at Buses with optimal EVCS load demand (a) using zero cost coefficients for RESs (b) using Monte Carlo uncertainty cost coefficients for RESs	101
Figure 5.22.	IEEE 118 Bus Voltage profile with EVCS loading demand (a) using zero cost coefficients for RESs (b) using Monte Carlo uncertainty cost coefficients for RESs	102
Figure 5.23.	IEEE 118 Apparent Line Power Flow with optimal EVCS load demand (a) using zero cost coefficients for RESs (b) using Monte Carlo uncertainty cost coefficients for RESs	102
Figure 5.24.	IEEE 118 Real Power Loss with optimal EVCS load demand (a) using zero cost coefficients for RESs (b) using Monte Carlo uncertainty cost coefficients for RESs	103
Figure 5.25.	IEEE 118 Reactive Power Loss with optimal EVCS load demand (a) using zero cost coefficients for RESs (b) using Monte Carlo uncertainty cost coefficients for RESs	103

LISTS OF TABLES

Table 2.1.	Table 2.1. Number of energy management for hybrid system publications year-wise	15
Table 2.2.	Meta-Heuristics or Evolutionary Computation Optimisation Methods for Energy Management Systems Considering RESs and EVs	31
Table 4.1.	IEEE 30-bus cost coefficient data of 6-Unit testbed (Heris, 2016; Al-Roomi, 2016; Gaing, 2003)	63
Table 4.2.	IEEE 30 Bus System Cost Data and Power Constraints Of 6-Unit System Data (Heris, 2016; Al-Roomi, 2016; Gaing, 2003)	64
Table 4.3.	IEEE 118-bus cost coefficient data of 15-Unit testbed (Heris, 2016; Al-Roomi, 2016; Gaing, 2003; Yoshida et al., 2000)	65
Table 4.4.	IEEE 14-bus of 3-Unit with RESs cost coefficient data (Heris, 2016; Al-Roomi, 2016; Gaing, 2003; Yoshida et al., 2000)	69
Table 4.5.	IEEE 30 Bus System Cost Data and Power Constraints Of 6-Unit System Data (Heris, 2016; Al-Roomi, 2016, Gaing, 2003)	70
Table 4.6.	IEEE 118-bus of 15-Unit with RESs cost coefficient data (Heris, 2016; Al-Roomi, 2016; Gaing, 2003; Yoshida et al., 2000)	71
Table 4.7.	Comparative results of simulated IEEE 14-bus and 30-bus test of committed units with buses and transmission lines system data	73
Table 5.1.	Parameters for Charging Load Model by EV Consumer Classes and Type	84
Table 5.2.	IEEE 14-bus 3-Unit cost data and constraints (Heris, 2016; Al-Roomi, 2016, Gaing, 2003)	85
Table 5.3.	IEEE 30-bus 6-Unit cost data and constraints (Heris, 2016; Al-Roomi, 2016, Gaing, 2003)	85
Table 5.4.	IEEE 118 Bus 15-Unit cost data and constraints (Heris, 2016; Al-Roomi, 2016, Gaing, 2003)	85
Table 5.5.	Load bus data for the IEEE 14-bus testbed using NR method (Al-Roomi, 2015; Olcay et al., 2023)	93
Table 5.6.	IEEE 30-bus Load data using the NR method (Al-Roomi, 2015; Olcay et al., 2023)	94
Table 5.7.	IEEE 118-bus selected Load data using the NR method (Al-Roomi, 2015; Olcay et al., 2023)	95
Table 5.8.	Compared Results of IEEE 14-bus system	97
Table 5.9.	Compared Results of IEEE 30-bus system	100
Table 5.10.	Compared Results of IEEE 118-bus system	104
Table 6.1	Software programs developed and implemented in this thesis	111

GLOSSARY

TERMS/ACRONYMS/ABBREVIATIONS	DEFINITION/EXPLANATION
ACO	Ant Colony Optimization
AEs	Algebraic Equations
AI	Artificial Intelligence
B&B	Branch-and-bound
B&C	Branch-and-cut
BN	Bayesian network
BO	Butterfly Optimization
COESS	Cost of energy storage system
DAEs	Differential Algebraic Equations
DE	Differential Evolution
DES	Distributed Energy System
DGs	Distributed Generators
DP	Dynamic Programming
DR	Down-ramp
DRPs	Demand Response Programs
EAs	Evolutionary Algorithms
EMS	Energy Management System
EP	Evolution Programming
EPD	Economic dispatch problem
ES	Evolution Strategy
ESL	Ensemble machine learning
ESS	Energy storage system
EV	Electric vehicle
EVCS	Electric vehicle charging station
FCS	Fuel cell stack
FMINCON	Find minimum of constrained nonlinear multivariable function
GA	Genetic Algorithm
GS	Gauss-Seidel
GTO	Gorilla Troop Optimizer
GWO	Grey Wolf Optimization

HS	Hybrid system
IEA	International Energy Agency
ISO	Independent System Operator
ISO	International Organization for Standard
LGS	Total number of renewable energy resources (RESs)
LP	Linear Programming
MC	Monte-Carlo
MILP	Mixed Integer Linear Programming
MINLP	Mixed Integer Nonlinear Programming
NHTS	National Household Travel Survey
NLP	Non-linear programming
NR	Newton-Raphson
OPF	Optimal power flow
POAs	Population-Based Optimization Algorithms
PSO	Particle Swarm Optimization
PST	Power System Toolkit
PV	Photovoltaic
QP	Quadratic Programming
RESs	Renewable energy sources
RO	Robust optimization
SA	Simulated Annealing
SIAs	Swarm Intelligence Algorithms
SoC	State of charge
T&D	Transmission-and-Distribution
TAC	Total Annual Cost
TLLs	Transmission Line Losses
TSO	Transient Search Optimisation
UC	Unit commitment
UCF	Uncertainty Cost Function
UR	Up-ramp
VSI	Voltage Stability Index
WT	Wind turbine

MATHEMATICAL NOTATIONS

SYMBOLS / LETTERS	DEFINITION/EXPLANATION
a_i, b_i, c_i	Cost coefficients of generating for unit i
α^{bat}	Maintenance coefficient
$B_{i,j}, B_{0i,}, B_{00}$	Transmission loss coefficients
β^{bat}	Value depreciation coefficient
$C_{evcs(t)}$	Battery capacity, t is the current time
$C_G(P_{Gi})$	Grid cost function
C_t^{RES}	RESs social cost
$c_i(t)$	Cost of unit i in time period t
C_{PVi} and C_{dm}	PV ith and wind mth operating cost
$C_V(P_{RESi})$	Cost functions for the RES generator
$C_r(P_{ri})$	Grid transmission line spinning reserve operating cost
E_{batt}	Battery model equation
F_T	EPD fuel cost
F_c	Total Fuel Cost
$F_i(P_{Gi})$	Fuel cost of the generator
$g_{ij}$and B_{ij}	Conductance and susceptance of branch between buses I, j
n	Number of the members in one particle and it is equal to the total number of generators
N_1	Number of network branches
N_B	Number of load buses, i.e., buses with P_{di} greater than zero
N_G	Number of generating units
P_i	Active power generation of unit i
P_j	Active power generation of unit j
P_D	Total power demand of the system
P_G	Total power generation of the system
P_{PVi}^t	PV ith output power at time t horizon
P_{PVmin}^t and P_{PVmax}^t	Maximum and Minimum power of the ith PV system
$P_{evcs(t)}$	EVCS charging power
P_{gi} and P_{di}	Active power generated and demanded by bus i

P_i	Active power generation of unit i
P_i, max	Maximum value of real power allowed at generator i
P_i, min	Minimum value of real power allowed at generator i
P_{pd}	Power produced by the slack bus generator
P_{Ui}	Real power generation of conventional generators
P_{mi}	Real power generation of wind turbine generators
P_{ri}	Real power generation of grid transmission line spinning
P_t^{bat}	Power supplied (discharging) or stored (recharging) of the
$\sum_{\substack{i=1 \\ i \neq d}}^{n} P_{pi}$	Total active power of the power system excluding the slack
v_i and v_J	Voltage magnitudes at buses i and j,
θ_{ij}	Load angle difference between buses i and j
Q_{gi} and Q_{di}	Reactive power generated and needed by bus i
$SOC_{evcs(\max)}$	EVCS maximum state of charge
$SOC_{evcs(t)}$	Current charging station state of charge
tdi	Departure time
v_i and v_J	Voltage magnitudes at buses i and j
$V_{pi}^{min}, V_{pi}^{max}$	Computed minimum and maximum velocities
$x_i(t)$	Power output of unit i time t
$Y_i(t)$	Fixed power output of unit i,0, variable
Δt	Controlled EMS's EV charging strategy to maximize solar energy consumption
γ	Percentage renewable-based penalty requirement on grid transmission line

CHAPTER ONE

INTRODUCTION

1.1 Introduction

The never-ending load shedding has been progressively unswerving and is likely to linger over the coming years in South Africa. The augmented usage of coal for power generation has brought about a rising concern for the environmental impact. The erratic nature of RESs introduces uncertainty in grid-tied configuration and reliability. The International Energy Agency (IEA) projects yearly energy demand growth by any nation at 1.5% from 2007 to 2030 (REN21,2017), while the International Organization for Standards (ISO) established values to sustain energy resource and efficiency drifts towards technology for energy reduction by 50% (IEA, 2012). Hybrid systems have been pronounced as one of the noteworthy enablers for a future smart grid, which involves power-distributed schemes integration with RESs and their controllable loads. The integration of RESs and controllable loads brings remarkable prospects for reliable efficient energy usage, and increased sustainability, either with or without the grid-tied arrangement. Exploration of the efficient energy baseline could help proposed grid-tied energy generation configuration, life cycle cost, and continuous improvement practices in energy resources usage (Adenuga, et.al., 2019). However, RES variability and intermittency limit energy supply once the grid is operating in islanded mode. High penetration rate challenges for renewable energy demands, such as frequency reserves reduction, voltage profile deterioration, inductive loading, and supply-demand balance aggregation/matching are difficult to achieve in practice. Optimization algorithm model for daily economic power dispatch operation with energy storage discharging and charging power, the maximum discharge depth and current SoC (state of charge), and mismatching between capacity utilization and operational need are additional challenges (Fan et.al., 2019). To maintain system stability, and supply-demand balance challenges, this thesis proposes particle swarm optimization methods for hybrid system energy management of an electric vehicle charging station, while minimizing operational cost constraints, economic dispatch problem , and maximizing optimal power flow (OPF). This chapter presents synopsis of the problem in section 1.2, statement of the problem is described in section 1.3, the research aims and objectives are stated in section 1.4, the hypothesis, assumptions and delimitations of the research, are presented in sections 1.5 – 1.7, thesis deliverables and chapter break down are described in sections 1.8 – 1.9 respectively, and conclusions is specified in section 1.10.

1.2 Problem Overview

The indeterminate renewable energy source's behavior depends naturally on stirring weather conditions, fluctuating irradiance, and light strength phenomena. These inadequacies make RES integration thought-provoking and uneconomical into electrical grids energy dispatch that are coordinated by fuel-based generations. A unique pragmatic method is to rise above the inadequacies through grid-tied dispatchable RES. Integration of RESs with complex seasonal variations is valuable in use with existing conventional power generation sources, making the hybrid system operating strategy an inspiring area of research. The cost coefficient characteristics of each RES generator also have inherent nonlinear functions. Underneath energy demand-supply balancing constraints are lower and upper generators operational limitations, while power dispatch optimization problem has exclusively used the quadratic cost functions but the non-inclusion of quadratic uncertainty cost function for renewable energy is rare. The hybrid system (HS) has an inherent intermittent nature of RESs which makes more RES power supply uncertain, which has negative effects on load profiles, quadratic equality constraint, and grid steadiness. The grid-tied HS operates more steadily under distorted loading conditions in comparison to established grid-thermal systems. The difficulties in achieving a high penetration rate for RESs include the need for prior knowledge of the underlying stochastic methods to achieve grid-tied feeder loss impacts, energy demand to optimize usage, controlled operation of EVCS, and peak demand limit of EV charging stations. Hybrid system energy management enabled with electric charging stations (Figure 1.1) presents grid integration of RESs and optimal electric vehicle charging station arrangements, including uncertainties like imprecise energy demand optimization and generation. To minimize the power system protection activating risk while ensuring that the charging demand is met and costs are kept to a minimum, the thesis analyze the penetration of RES with EV charging stations power losses, voltage variances, and proposes a solution to the minimum total operating cost objective function problem. Some of the most important contributions of this thesis are summarized in the following objectives:

1. Analysis of energy management strategies for a hybrid system of electric vehicle charging stations to select the nonlinear optimization control variables, objective function and techniques that are considered highly capable of solving high-dimensional ED problems with less computational time.
2. Formulation of renewable energy generation uncertainty cost function from the reviewed literatures and investigation of the best value for uncertainty cost

functions for both RESs and electric vehicle charging stations considering active power loss, reactive power loss operation cost, power flow, and voltage deviation.

3. Analysis and investigation of the optimization effect of PSO method for the inclusion in the economic dispatch of renewable energy generation plants in energy management strategies to select the nonlinear optimization control variables, objective function and techniques are considered highly capable of solving high-dimensional ED problems with less computational time..
4. Minimization of power losses on the distribution grid due to non-linear behavior by adopting electric vehicles as a more cost-effective method of transportation.
5. Use of MINLP method for energy management strategies of the hybrid system and particle swarm optimization for the inclusion in the economic dispatch of renewable energy generation plants.in energy management strategies of an electric vehicle charging station to reach convergence quickly and accurately.
6. Use of IEEE 14-bus, IEEE 30-bus and IEEE 118-bus distribution testbed to demonstrate the suggested approach validity and identifying the optimal EV charging stations locations on the distribution testbed.

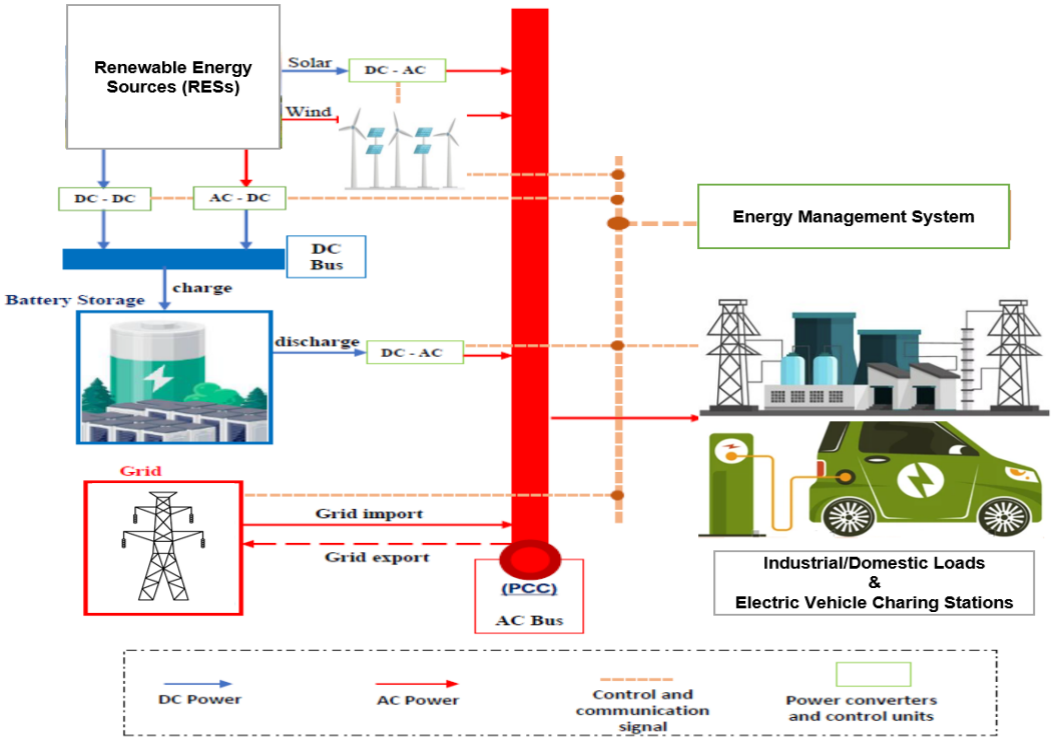

Figure 1.1. The schematic diagram for a hybrid energy management enabled with an electric charging station.

1.3 Statement of the problem

The foremost problem is:

- Renewable energy sources (RESs) supply is uncertain, as are the quadratic uncertainty cost functions for RESs generation employed in grid-integrated RES subsystems. However, optimization approaches can effectively address key challenges in the power system's economic efficiency that depend on three key problems which depend on economic power dispatch (EPD), and optimal power flow (OPF).
- The electric vehicle charging station (EVCS) required by electric vehicles poses a fundamental problem that must be overcome before large-scale deployment of RESs can occur. This makes the optimization problem relevant to hybrid systems with integrated RES subsystems.

To solve the problems using a particle swarm optimization technique that is appropriate to the requirements of hybrid system energy management while reducing voltage fluctuations, feeder losses impact, and peak demand limit due to EVCS non-linear behavior. To complete the thesis's investigations, two sorts of research subproblems are solved namely design and implementation sub-problems.

1.3.1 Research Questions

1. How can the particle swarm optimization method be modeled for grid-tied RES hybrid systems in the future smart distribution system, dominated by being defined for economic power dispatch?
2. How accurately can PSO method provide optimized solution based on objective function and as per set constraints for grid-tied RES hybrid system when the disturbance of electric charging station at distribution bus is simulated?
3. Is it computationally efficient and practicable to apply metaheuristic approach to perform in a computerized way using Matlab for IEEE 14-bus, IEEE 30-bus and IEEE 118-bus distribution testbed?

1.3.1 Design sub-problems

Sub-problem 1: The short-term power variations caused by RES generators may exceed grid ramping capacity. The thesis explores deeper into EPD problems by considering RES integration, power variations, energy storage systems capacity, and scheduling preferences.

Sub-problem 2: Formulation of an optimization objective functions to minimize the committed generators total operational cost while observing power flow network constraints and maintaining EPD at the transmission level.

Sub-problem 3: Development of PSO method for single and multi-objective economic power dispatch functions using uncertainty cost functions for RESs generation.

Sub-problem 4: Simulation of grid-tied-RES hybrid system to address formulations of power balance variations, as well as the provision of uncertainty cost from spinning reserves by allowing reduced grid power demand from ESSs supply to an electric vehicle charging station.

Sub-problem 5: The developed PSO method tackles employs an uncertainty cost function of RESs to minimize the generation unit's operational costs and the B-loss coefficient optimization approach to estimate transmission losses.

1.3.2 Sub-problems on implementation

Sub-problem 6: Algorithm development in Matlab implementation in the use of uncertainty cost functions for PSO's methods to solve EPD problems in RESs generation.

Sub-problem 7: A PSO algorithm to minimize power losses by the adoption of EVs as a more cost-effective method of transportation on the distribution grid, presents problem such as power loss and voltage fluctuations due to non-linear behavior.

Sub-problem 8: Proposed Co-Optimization algorithm, PSO for EPD and MINLP for EMS.

Sub-problem 9: Validate the simulation results of the developed MINLP and PSO algorithm for the considered three Case studies 3-unit, 6-unit, and 15-unit generator system using IEEE 14-bus, IEEE 30-bus and IEEE 118-bus distribution testbed cost data.

1.4 Research Aim and Objectives

Electric utility schemes are integrated to lower power generation costs, high dependability, and enhanced operating conditions, reserve sharing, increased firmness, and emergency operations. The hybrid system can be divided into single or several areas depending on the system's complexity. Given the literature, the EPD problem has been solved successively for complex power systems. Grid energy management requires real-

time EPD solutions for decision-making on hybrid systems and distribution networks. Based on the preceding, formulations of multi-objective EPD problems and new AI methods for solving these problems are required. The thesis's aim and objectives are:

1.4.1 Aim

A novel particle swarm optimization and mixed inter nonlinear programming methods are developed and simulation results are validated for the considered hybrid system energy management of an electric vehicle charging station usecase scenarios .

1.4.2 Objectives

i. Review existing AI methods on a set of rules and software applications for solving economic power dispatch problems.
ii. Identify energy management dispatch-optimizer objective functions and constraints for hybrid system energy management of the electric vehicle charging station.
iii. Develop the energy management strategies for a hybrid system of an electric vehicle that is comprised of a photovoltaic, wind, and energy storage system using a MINLP.
iv. Determine an uncertainty cost function for renewable energy sources based on literature and analyze its impact on EPD.
v. Develop PSO method for hybrid system energy management of an electric vehicle charging station.
vi. Develop a particle swarm optimization method that employs a RESs uncertainty cost function to minimize the generator unit's operational costs while minimizing the transmission losses.
vii. Validate the simulations results of the developed PSO methods for hybrid system energy management of an electric vehicle charging station using IEEE 14-bus, IEEE 30-bus and IEEE 118-bus distribution testbed.

1.5 Hypothesis

The real-time energy supply-demand balance and power flow problem among various renewable energy sources is hypothesized to be:

H1 - The PV's power and WTs will be set to maximum values to observe the load storing the surplus power in the battery.

H2 - When the energy supply-demand balancing and power flow problem is equal to the provided power by PV and WT sources, both sources will continue to supply the required energy by the load.

H3 - Describes a precise approach for addressing optimal dispatch problems to fill the power deficit of PVs, WTs, and grid-tied supply situations.

1.6 Delimitation of research

The exploration will be limited to the development of PSO methods and will not contain any other prevailing optimization methods but instead examine using survey to justify selection of the adopted method. The adoption of uncertainty cost function for renewable energy sources will be based on a literature review and will not include the monte-carlo simulation for the economic power dispatch problems.

Some of the PSO delimitations are listed as:

Convergence to Local Optima: PSO may converge prematurely to local optima, especially in multimodal and complex search spaces. This can lead to suboptimal solutions, particularly when the particles get stuck in narrow regions of the solution space.

Parameter Sensitivity: PSO performance heavily depends on the setting of its parameters, such as the cognitive and social components, inertia weight, and acceleration coefficients. Tuning these parameters for optimal performance can be challenging and problem-specific.

Limited Exploration: PSO's exploration capability may be limited, particularly with high-dimensional and non-linear problems. It might struggle to adequately explore the entire search space, leading to a lack of diversity in the solutions found.

Premature Convergence: PSO can converge prematurely, especially when the search space is dynamic or changes over time. It might struggle to adapt to such changes effectively, resulting in stagnation or convergence to suboptimal solutions.

Difficulty in Handling Constraints: PSO's original formulation does not inherently handle constraints. While various approaches have been proposed to address constraint handling in PSO, such as penalty functions or repair mechanisms, integrating constraints can be complex and may affect the algorithm's performance.

Computational Complexity: PSO's computational complexity are relatively high, specifically for large-scale RES integration. The algorithm's efficiency may decrease significantly as the dimensionality of the problem increases.

Limited Scalability: PSOs may face scalability issues when dealing with very large-scale RES integration problems or problems with a large number of constraints. It might struggle to maintain diversity and explore the solution space effectively in such scenarios.

Lack of Robustness: PSO's performance can be sensitive to the problem characteristics, initialization, and random factors. It might not always guarantee consistent results across different runs or problem instances.

Dependence on Initialization: PSO's performance can be influenced by the initial positions and velocities of particles. In some cases, poor initialization may lead to convergence to suboptimal solutions or hinder exploration.

Despite these limitations, PSO remains a popular and widely used optimization technique due to its simplicity, ease of implementation, and ability to find good solutions in various problem domains. In this study work, the PSO method is used to investigate hybrid system energy management of an electric vehicle charging station.

1.7 Assumptions

The study relies on the ensuing assumptions to solve the economic power dispatch problem:

- The hybrid system power demand is assumed to be continual for a set measurement of time to simplify the problem. However, power demand varies in according to the load absorbed by clientele.
- In the economic power dispatch problem, transmission losses are typically expressed as a generator power outputs quadratic function of using Kron's formulae (Dhillon et al, 1994). However, power flow equations are calculated using the power system's active power transmission losses.
- PSO approach requires an initial acceleration factors estimation, random numbers, and inertia constant to begin the search process.
- Metaheuristic PSO algorithm does not apply the gradient technique, therefore, cannot guarantee an optimal solution.

1.8 The deliverables of the thesis

The economic power dispatch optimization for definite system are based on a realistic methodological collection of grid-tied apparatuses (RES, ESS and EVCS Load) economic models with network operator schedule strategies and mechanisms for

changing sun irradiation, wind speed, EVCS load, and dynamic electricity profiles. In this thesis scope, the deliverables are grouped as follows:

- The study involves the development of novel MINLP algorithms to solve hybrid system network objective functions and constraint limitations to minimize the committed generators total operational cost and reduce grid's dependency, grid voltage, power flow and maximize renewable energy source application. This is accomplished by applying MINLP solver with a grid-tied RES HS network scheme, since the constraints are nonlinear, they are considered in mathematical calculation through an iterative procedure for the MINLP solver in separately until the anticipated voltage and power flow supplies are met. The investigation in the Matlab is robust enough to attempt varied stratagems for setting probable demand and EVCS loading violations on the grid distribution bus while concurrently deriving optimized RES and ESS dispatch, which makes it suited for handling a high RES units' integration in future networks. These strategies include iteratively changing MINLP constraints from RES power dispatch.
- The thesis second significant contribution originates from PSO algorithm development, which solves EPD optimization problems in a grid-tied RES hybrid system. The novelty of the PSO method is in an optimization mechanism that incorporates the network constraints impact on the economic dispatch problem. In addition, the RESs uncertainty cost function from the conducted literature review using simulated Monte Carlo RESs uncertainty fuel cost function from the conducted literature review is applied to optimize power flow active and reactive power losses, and voltage by integrating grid-tied RES to guarantee a fast convergence for the best possible output.
- The last contribution is the development of particle swarm optimization method that employs a RESs uncertainty cost function is to minimize the unit's operational costs while minimizing the transmission losses and validation of the developed PSO methods for hybrid system energy management of an electric vehicle charging station using IEEE 14-bus, IEEE 30-bus and IEEE 118-bus distribution testbed to reduce active, reactive power losses, voltage and power flow of the EVCS.

1.9 Chapter breakdown

The thesis is comprised of six chapters highlighted as follows:

Chapter 1 describe the problem overview and statement of the problem. The chapter includes the study aim and objectives, hypothesis, research limitations, assumptions, and the thesis deliverables.

Chapter 2 presents a literature survey of hybrid system energy management publication year wise, application domain, objective functions and constraints against year of publication. It surveys the unique properties of numerous classical, heuristic, metaheuristics for solving the economic power dispatch problem.

Chapter 3 presents a MINLP method developed to solve grid-tied RES hybrid system network objective functions and constraint limitations for economic power dispatch problems. The developed MINLP algorithms can lower total operating costs and grid dependency, optimal power flow, losses and voltage on the grid and exploring renewable energy source usage by electric vehicle charging stations. The proposed approach, which is based on the energy management of hybrid system strategies for grid-tied RES systems, is capable of resolving EVCS loading strategies through optimal power losses in determining the probable EVCS loading on grid-tied RES.

Chapter 4 introduces the particle swarm optimization and outlines how it was developed for the EPD problem. The PSO algorithm is tested using multiple IEEE 14-bus, IEEE 30-bus and IEEE 118-bus distribution testbed benchmark models in Matlab environment.

Chapter 5 provides the PSO method for a hybrid system with an electric vehicle charging station. The developed PSO method has successfully demonstrated EVCS load modeling operational cost reduction using parameters for charging load model by EV consumer classes and type, and NHTS 2023 data of EV Class, variables such as the number of EVs being total charging current, arrival rate, and parking rate time.

Chapter 6 discusses the thesis conclusion and concludes with theoretical development of MINLP and PSO applications for hybrid grid-tied RES, software development and possible applications of the research outputs with future research and a list of author publications.

1.10 Chapter Summary

This chapter discusses the problem statement and provides background on the study. The chapter content provides the research aim, objectives, assumptions and project

deliverables. The thesis outline and deliverables are stated. To have a thorough understanding of the problem, it is necessary to research the literature, particularly those that present algorithms for solving single or multi-objective EPD functions utilizing classical and meta-heuristic optimization. Chapter 2 provides overview of literature on hybrid system energy management of an electric vehicle charging station.

CHAPTER TWO

LITERATURE REVIEW ON ENERGY MANAGEMENT FOR HYBRID SYSTEMS OF AN ELECTRIC VEHICLE CHARGING STATION

2.1 Introduction

The diffusion of renewable energy into the grid has attracted lots of interest. Insufficient power generation in developing nations frequently results in an unstable electrical grid with outages as systems operate in a limited state (Masrur et al., 2021). Utilities are choosing to integrate RESs into the grid to meet the demand for a cleaner generation. One of the key structures for a future smart grid is the integration of low-voltage distributed systems with RESs and hybrid systems with or without grid connection (Rolan et al., 2022; Almi et al., 2019). The recurrent nature of RESs introduces uncertainty in the microgrid configuration, which distorts grid-tied reliability. The energy management approach encompasses the foundation of the dynamics of energy resources by determining when to use or turn off the grid based on the availability of renewable penetration rates, such as energy dispatch scheduling, frequency reserve reduction during inductive loading, deteriorated voltage profiles, and transmission line congestions (Adenuga and Krishnamurthy, 2023; Shaffer et al., 2015). The mismatch between the generator's capacity utilization and operational needs is a supplementary challenge. Captive energy resources require coordination within identified, defined boundaries regarding objective function and constraint formulation. The instability and erratic nature of RESs, as well as restrictions on the energy supply, pose serious problems. The difficulty in predicting the energy demands of RES is difficult to perform in practice, coupled with some of the challenges of high RES penetration rates, such as frequency reserve reduction during inductive loading. The deterioration of voltage profiles; supply-demand balance aggregation/matching; economic dispatch; and current SoC (state of charge) with maximum discharge depth (Fan et al., 2019).

The EMS is a crucial smart grid module that offers all the functionality required to guarantee the supply of energy at the lowest possible generation operational costs from both distribution and transmission (Garcia Vera et al., 2019). It also helps to schedule the electricity real-time cost by maximizing power consumption. A remarkable number of research studies employ EMS optimization algorithms to reduce costs by considering active energy rates and the best use of power (Khorram et al., 2018). The bidirectional energy flow between the EMS and energy storage systems, such as hybrid energy availability, and the dynamic grid power price change are not considered by these techniques (Mehdi et al., 2023; Li et al., 2022). A sustainable EMS is developed through optimal simulations using economic power dispatch, power flow, and supply-demand

balance aggregation/matching approaches for an existing power system (Ouyang et al., 2022; Islam et al., 2022).

The hybrid system is made more uncertain by the irregular RESs nature, which has undesirable effects on grid stability, RES load profiles, and the quadratic equality constraint. The difficulties in achieving a high penetration rate for renewable energy sources include the need for prior knowledge of the underlying stochastic processes in the hybrid system state to achieve AI monitoring of electric vehicles.

Electric vehicle-enabled hybrid systems (Figure 2.1) present grid integration of renewable energy and optimal energy monitoring system scheme challenges, including instability, integrability, modularity, dependability, interoperability, and uncertainties like imprecise optimization of energy demand and generation. Optimization-based energy management will offer artificial intelligence (AI) that needs autonomy, intellect, and proprietary protocols to interface with coordinated EV charging in a heterogeneous way. The grid-connected HS operates more steadily under unbalanced loading conditions in comparison to traditional grid-interfaced hybrid renewable energy systems.

The objective of Chapter 2 is to conduct a literature survey of hybrid system energy management publications year-wise for a period of 12 years, from 2013 to 2024, covering application domains, objective functions, constraints, and the existing approach for the solution of these economic dispatch challenges. The schematic diagram for a hybrid energy system with EVCS grid integration is shown in Figure 2.1.

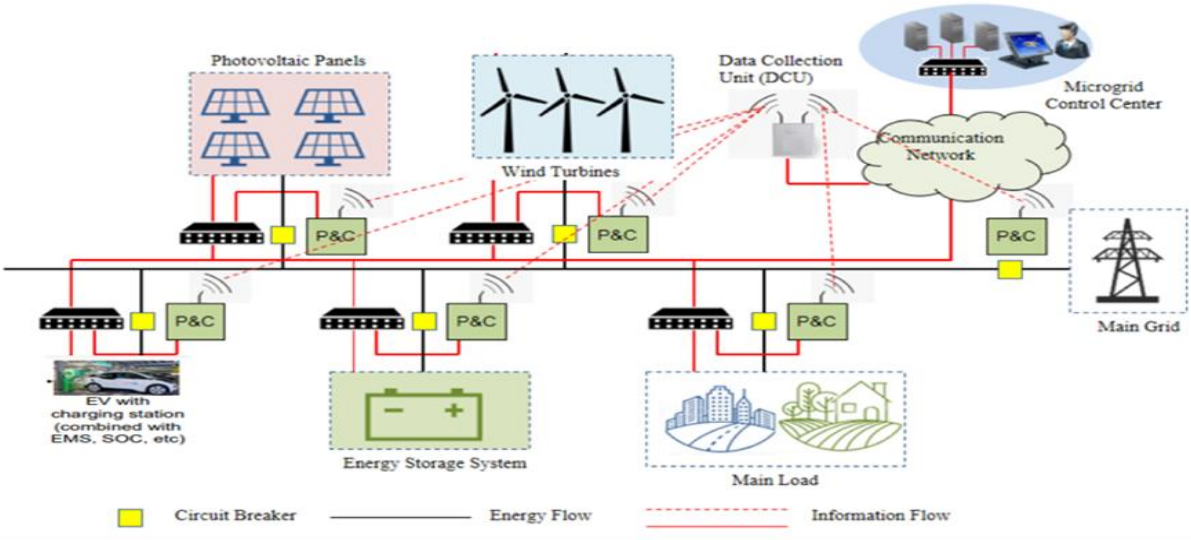

Figure 2.1. Schematic diagram for a hybrid energy system with EVCS grid integration.

2.2 A Survey of Energy Management for Hybrid System

Energy management and usage in various engineering domains have a significant increase in energy studies over the past ten years (Adenuga et al., 2020). However,

many nations constantly enhance renewable energy targets for various factors such as reduction of frequency reserves during inductive loading, deteriorated voltage profiles, congestions in transmission lines, and mismatching between energy cost, capacity utilization, and operational need. Coordination within predetermined limitations is necessary for the balancing of captive energy sources and operational goals of the optimized energy management system to regulate, improve, and keep track of the hybrid solar PV systems (Yu et al., 2021), wind turbine energy generation (Zhang et al., 2021), battery grid, and electric vehicle (EV) systems (Jamborsalamati et al., 2020). Coordination within predetermined bounds is necessary for balancing captive energy sources (Modise et al., 2021). Decentralizing energy production to bring it closer to consumers would increase system efficiency and dependability (Ton and Smith, 2012). Solar panels, wind turbines, supercapacitor batteries, and converters, as well as the connectivity of connected loads as a single controlled entity, offer an effective solution in the integration of diverse RESs with ESS (Bigdeli, 2015). In the past ten years, the use of fuel cell stacks (FCS), which use chemical reactions to convert hydrogen into electricity instead of using internal combustion engines to produce heat and water as waste products, has grown in popularity (Meiling et al., 2019). FCSs are anticipated to have a significant role on reliability improvement, the resilience of modern distribution systems, safety, high-power density, cleanliness, and adaptability of energy generation, particularly in hybrid energy systems (Blaabjerg et al., 2017). However, the lack of significant FCS application in microgrids drives the research and design of FCS-based microgrids, as well as the possible difficulties (Abdellatif Elmouatamid et al., 2021). With the benefits of combining the two technologies from PVs and WTs in hybrid energy integration, the hybridization energy management and control system requirements for resilience, dependability, and grid safety have grown to become more pressing (Lakshminarayanan et al., 2019). Renewable energy penetration poses substantial hurdles in the normal operation of distribution systems, which were often designed to manage only passive loads and networks (e.g., voltage variation, protection malfunction, etc.) (Naidu et al., 2018). Energy management systems studies in hybrid systems have been the subject of numerous research investigations with varying degrees of success. However, most studies primarily used simulation, with little focus on the testing or real-world implementations of the EMS. Fuzzy logic schemes, simple control algorithms, convex optimization, classical-based algorithms, model predictive control, dynamic tools, optimal control algorithms, hybrid control strategies, etc. EMS control system applications are not remarkably impressive when judging the effectiveness of the converters during hardware testing (Sulaiman et al., 2015). Table 2.1 presents the number of energy management hybrid system publications per year, and Figure 2.2

illustrates the hybrid system energy management publications. Figure 2.3 provides a synopsis of literature in the last 10 years based on objectives, functions, constraints, and application domains, showing limited studies on energy management system research in power flow balance, supply and demand balance, and electric vehicles. 182 publications are considered in the survey; publications year-wise were analyzed and shown in Table 2.1, with graphical depictions shown in Figure 2.1 and Figure 2.2.

Table 2.1. Number of energy management publications for hybrid system year-wise

Reference	Publication Year	Publication Number
(Nguyen and Le, 2013)	2013	1
(Fernandes et al., 2014), (Ishigaki et al., 2014), (Igualada et al., 2014)	2014	3
(Arash Dizqah et al., 2015), (Shi et al., 2015), (Song et al., 2015), (An and Quoc-Tuan, 2015), (Dizqah et al., 2015)	2015	5
(Abrishambaf et al., 2016), (Akhtar et al., 2016), (Luna et al., 2016), (Koubaa and Krichen, 2016), (Lin et al., 2016), (Sai Thirumala Baba and Srinivas, 2016), (Lv and Qian, 2016)	2016	7
(Ahmad et al., 2017), (Li et al., 2017), (Anglani et al., 2017), (Sunny and Thomas, 2017), (Shayeghi et al., 2017), (Marzband et al., 2017)	2017	6
(Khorram et al., 2018), (Ghasemi. and Enayatzare, 2018), (Shafie-Khah and Siano, 2018), (Byrne et al., 2018), (Şengör et al., 2018), (Wang et al., 2018), (Hu et al., 2018), (Hussain et al., 2018), (Yuan et al., 2018),	2018	9
(Gielen et al., 2019), (Garcia Vera et al., 2019), (Eslami and Kamarposhti, 2019), (Li et al., 2019), (Shekari et al., 2019), (Jaurola et al., 2019), (Lai and Illindala, 2019), (Karmellos. and Mavrotas, 2019), (Khan et al., 2018)	2019	10
(Cecilia et al., 2020), (Wu et al., 2020), (Gbadegesin, 2020), (Mandal and Mandal, 2020), (Gao and Fu, 2020), (Hamid and Shahram, 2020), (Murty and Kumar, 2020), (Dorahaki et al., 2020), (Prudhviraj et al., 2020), (Wang et al., 2020),	2020	10
(Ahmadi et al., 2021), (Barua and Mohammad, 2021), (Peilin et al., 2021), (Adefarati et al., 2021), (Shahrabi et al., 2021), (Kumar. and Tyagi, 2021), (Phani Raghav et al., 2021), (Dinh and Kim, 2021), (Naz et al., 2021), (Ghiasi et al., 2021), (Fouladfar et al., 2021), (Alhasnawi et al., 2021)	2021	12
(Xie et al., 2022), (Nyong-Bassey, 2022), (Erenoğlu et al., 2022), (Fathy et al., 2022), (Gomes et al., 2022), (Nasir et al., 2022), (Cao et al., 2022)	2022	7
(Karmaker et al., 2023), (Kamal et al., 2023), (Boqtob et al., 2023), (Ebeed et al., 2023), (Hai et al., 2023), (Esmaeili et al., 2023, (Nassaret al., 2023), (Singh et al., 2023)	2023	8
(Keshta et al., 2024), (Habibi et al., 2024), (Ndeke et al., 2024) ;(Li et al., 2024), (Sheng et al., 2024)	2024	5

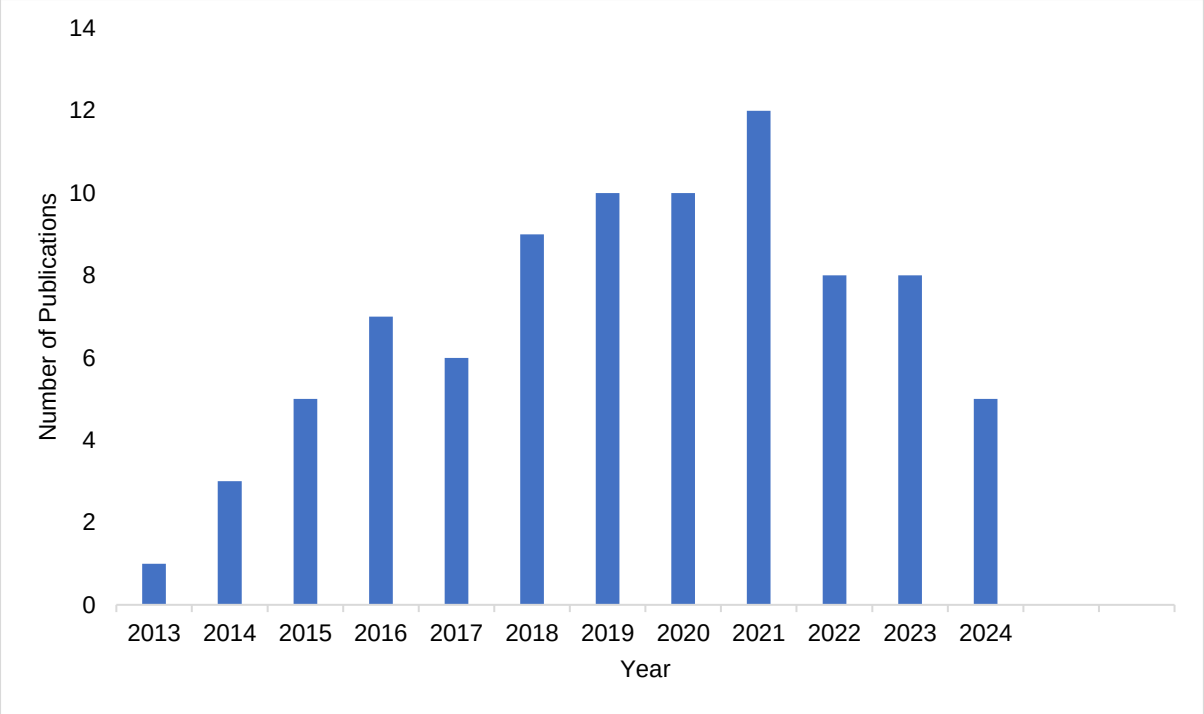

Figure 2.2. Number of energy management for hybrid system publications year-wise

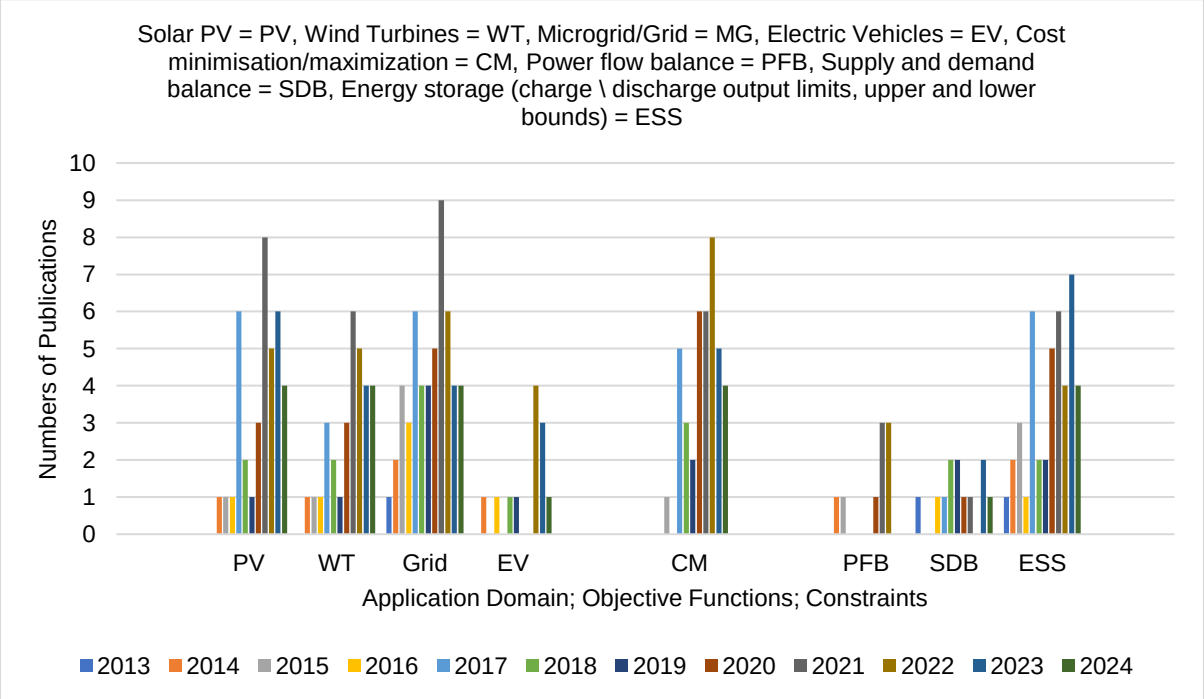

Figure 2.3. Number of reviewed publications based on the application domain, objective functions, and constraints against year of publication

2.3 Literature Survey on Energy Management Approach for Hybrid Systems

Numerous studies on energy management approaches have been conducted from various hybrid system viewpoints to utilize RESs as effectively as possible while finding the minimum cost function. Therefore, a comprehensive understanding of the entire process necessitates computational portions of data obtained from a broad power system. To achieve power balancing in energy systems, a range of technologies employ both monitoring and controlling the energy produced or used at the consumer level (Filho et al., 2019). The demand load and the energy sources relationship are under the control of EMSs. To optimize energy utilization, the approaches under review do not reflect two-way power flow between solar PV, WT, EMSs, and ESS and dynamic change in the price of grid power. Several years ago, networked microgrid systems were developed with many benefits to increase grid stability, distribution, and resiliency (Li et al., 2017). Researchers pay a lot of attention to optimization-based tactics because they use numerical or analytical algorithms to produce optimal or unsatisfactory results (Adefarati et al., 2021). Data collection from the EMS and computational resources are needed to have a comprehensive understanding of the entire process and find a minimal cost function while considering several restrictions. The designed variables must be met by operational cost constraints in real-world circumstances to maintain system stability and reduce environmental degradation. A priori generation from the global optimization model specification and experimental applications to discover and find errors has been categorized in previous research studies (Yuan et al., 2018). The proposed research requires complete hybrid system knowledge of precise load variations to achieve a global optimum solution. The designer's control strategy aims at the consideration of restrictions that are better suited to early-stage designing, energy dispatch issues, and real-time testing alternatives (Sundstroom and Stefanopoulou, 2006). It is mostly used for real-time power splitting, regulating, protection, etc., and is capable of handling pulsed loads, uncertainty, and long-term disruptions from centralized distributed energy systems, energy storage, photovoltaic, and WT system safety and efficiency.

The authors surveyed the number of review papers (Elsevier, Springer, SAGE, Emerald, Francis, IJIMS, Wiley, etc.) based on the Scopus database. The first-dimension findings show the number of publications that covered various journal papers between 2013 and 2022. Based on publication numbers by country of origin, second-dimension results (Figure 2.4) showed that China accounted for 13.2% of EMS's research output, Iran for 10.8%, India for 8.4%, the USA for 7.2%, the UK and Pakistan at 6.0%, placing them in a fifth position on the lists.

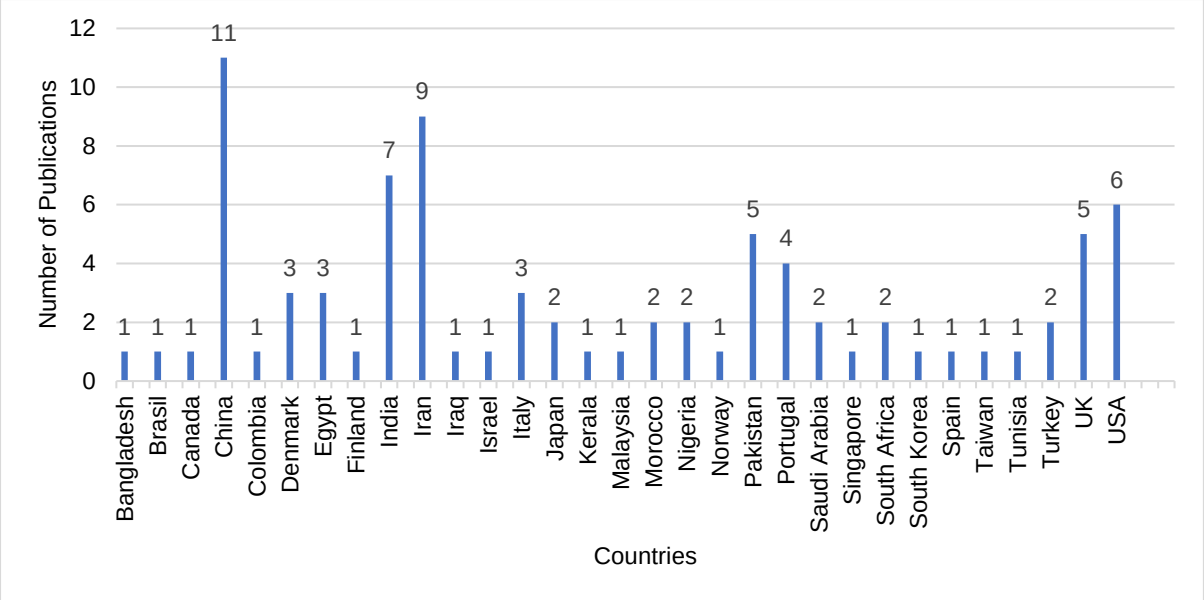

Figure 2.4. Number of reviewed publications against country of origin

2.3.1 Review Findings on Energy Management System

Based on the Scopus database, the authors examined the review paper numbers (Elsevier, Springer, SAGE, Emerald, Francis, IJIMS, Wiley, etc.). The first-dimension results reveal how many publications covered different journal papers between 2013 and 2022. The second-dimension results (Figure 2.4) were based on the number of publications broken down by country of origin, with China accounting for 13.2% of EMS's research output, Iran for 10.8%, India for 8.4%, the USA for 7.2%, the UK and Pakistan at 6.0%, placing them in fifth place on the lists. The third dimension (Figure 2.4) was based on the number of articles on EMS in IEEE Access journals at 4.2%, with Energies journal at 18.1% the highest. The fourth dimension demonstrates how EMSs have developed over time, from being merely a concept to being put into practice. The important discoveries are relevant to EMSs since it is clear that research is progressing from concept to realization of the identified research gap. The MINLP optimization method for hybrid system energy management is presented in Chapter 3 of the thesis.

2.4 A Review of Classical Optimisation Methods Hybrid System Energy Management of the

There are several optimization techniques today that fit strategies to decrease costs, which can broadly be categorized into two optimizations: classical and meta-heuristic algorithms. In the 20th century, dynamic programming (DP), linear programming, non-linear programming, and mixed integer linear programming algorithm approaches have made remarkable strides as classical techniques. The analytical characteristics of the

problem are used by classical optimization techniques to produce a series convergence for a globally optimal solution. Figure 2.5 provides the classical and meta-heuristics review structure considered in the energy management of the economic dispatch problem with electric vehicles.

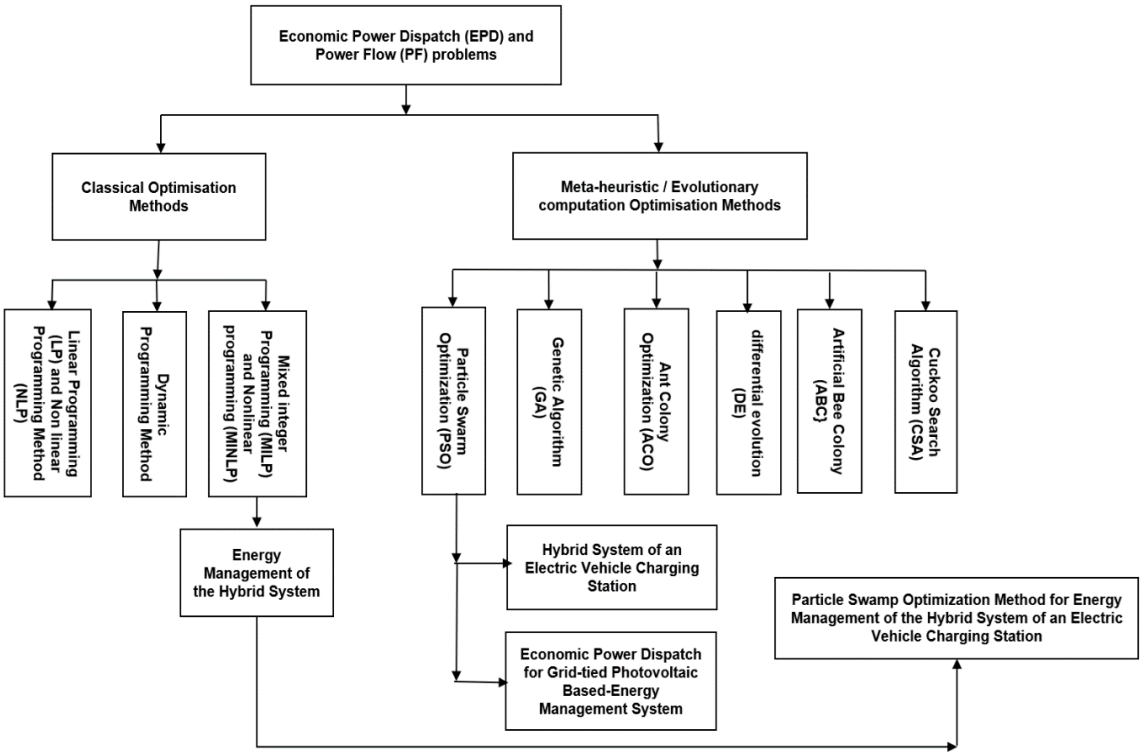

Figure 2.5. Solution methods from literature review for optimal economic power dispatch and power flow problem

2.4.1 Dynamic programming

Dynamic programming (DP) is the most effective mathematical method, which can resolve optimization complications and produce efficient solutions while solving other energy management challenges. It makes intelligent decisions at each phase of a multi-step problem by methodically analyzing a huge number of potential decisions and reducing the overall cost of all decisions. DP used recursive algorithms to solve computational issues by subdividing the problem supplied by solutions (Derong Liu et al., 2020; Djete et al., 2022). DP algorithm applications come in the form of Knapsack, Fibonacci Series, and Coin Change complex problems, etc. The Bellman issue illustrates that dynamic programming is the most effective mathematical method that can solve several optimization challenges and produce the most efficient solution. It makes intelligent decisions at each phase of a multi-step problem by methodically analyzing a huge number of potential decisions and reducing the overall cost of all decisions. are in DP solved computational issues also used recursive algorithms by subdividing the

problem supplied by solutions (Derong Liu et al., 2020; Djete et al., 2022). The Bellman problem illustrates a DP optimization approach, as given in Equations (2.1) and (2.2):

$$V(x_0) = max\{F(x_0, a_0) + \beta V(x_1)\} \quad (2.1)$$

Subject to constraints:

$$a_0 \in \Gamma(x_0), x_1 = \mathrm{T}(x_0, a_0) \quad (2.2)$$

2.4.1.1 Review discussion on DP

To implement DP, a mathematical model must have well-defined choice variables, constraints, and parameters as an entire power demand a priori. In addition, power requires prior knowledge, which is not always possible in practical applications to serve as a benchmark for improvement. It should be emphasized that DP may sometimes handle these challenging issues while it may need a significant amount of computation and may not be able to handle situations where there are time coupling restrictions.

2.4.2 Linear Programming (LP) and Nonlinear Programming (NLP) Methods

The simplest classical optimization technique, linear programming, determines many system parameters first-order to be optimized. The linear programming technique analyze mathematical frameworks using several variables and a and a single degree of freedom linear function to find optimal solutions, such as those with the lowest cost or highest profit (Vanderbei, 2020; Wu and Lisser, 2022). The LP approach optimizes the linear objective function value based on cost, subject to equality and inequality constraints. An LP problem uses input parameters, objective functions, constraints, and decision variables to solve an optimization issue. Equations (2.3–2.5) provide a generic formula for solving an optimization issue.

$$f_x^T \quad (2.3)$$

subject to constraints

$$Ax \leq b \quad (2.4)$$

$$x \geq 0 \quad (2.5)$$

Quadratic programming (QP) is a specific simple NLP type and seen as the most recurrently used real-world algorithm in optimization due to the system states quadratic relationships between diesel generator fuel consumption, produced power quadratic function (Xu et al. 2019), and quadratic cost functions in multi-objective function

optimization. Additionally, a specific form of convex optimization can resolve the QP problem with conflicting objectives (Hossain and Ginn, 2017). Some simplifications are needed when creating a mathematical model for a hybrid energy system; they may be connected to avoiding the usage of integer variables, failing to consider supply-demand performance, the dynamic nature of the power flow issue, cost-effective power dispatch, etc. According to Karamellos et al. (2019), the framework for multi-objective (MO) comparison and design of distributed energy systems optimization usage is an objective function when designing distributed energy systems (DES) for total annual cost and carbon emissions.

2.4.2.1 Review discussion on LP

Numerous engineering disciplines have made extensive use of LP, incorporating power flow, energy management, and others (Asghari et al., 2022). However, the industry rarely employs LP owing to the complexity and nonlinear nature of the EMS-based derivative methods. NLP approaches are thereby adopted to linearize the complexity of nonlinear problems. However, whether NLP issues are parallel, sequential, or multi-objective, linearization could lead to enlarged processing complexity or dynamic responses capturing failures.

2.4.3 Mixed Integer Programming (MILP) Methods

Mixed-integer programming (MILP) is suitable for describing linear variables. It could be the case in some cases, where an integer linear program refers to a program with all important variables that are integers. MILP can deal with issues involving millions of variables, while mixed integer nonlinear programming techniques are the most challenging classical optimization methods type, which have lately begun to advance. It can be a huge advancement if MINLP issues might be solved by MILP solvers globally, even with the present advancements in MINLP solvers. Theoretically, approximating the MINLP problem can be accomplished by a MILP, but doing so will likely be more difficult than doing it for the original problem with a MINLP solver. It is significant that some real-world application variables must be integers or binary. These issues, known as integer programming issues, fall under the MILP categories (Li et al., 2020) and MINLP (Li et al., 2020; Sahinidis, 2019). The main factors that cause a mixed-integer problem quantity can only be integers, such as RESs and batteries (Baldi et al., 2016). Numerous engineering design issues represent discrete decisions by capturing complicated nonlinear behavior in the objective function and/or restrictions of processes and integer variables. They are founded on heuristic or hybrid mathematical and heuristic

methodologies. This comprises various energy sources and types with various economies of scale over fixed charges, decomposition, convexification, deterministic decomposition, and local and global solutions stochastic algorithms (Barbato and Capone, 2014).

It is unavoidable to have an optimization procedure in place due to the irregular RESs nature and other devices nonlinear properties; simple, uncomplicated decisions lead to extremely poor management. Mixed-integer linear programming and mixed-integer nonlinear programming are both extensively used in this context (Prudhviraj et al., 2020). The solution techniques rely on implied enumeration, which has a high real-world computing cost, though algorithms to obtain accurate integer programming problems solutions have substantially improved over the years. For energy system optimization, MILP is frequently used to find solutions to issues based on the design of plants. Numerous issues can be modified to work with MILP. Piecewise linear functions can be used to approximate nonlinear ones (Taslimi et al., 2021), and logical operators and the products of integer variables can be used (Alkhalifa and Mittelmann, 2022). The issue becomes increasingly difficult with the frequent need for additional constraints or decision variables (Burlacu et al., 2020).

The full MINLP high computational cost in large-scale systems with potential continuous variables, as well as nonlinear objective and constraint functions, has motivated researchers to consider nonstop approximate problem formulation (Sitek and Wikarek, 2018). The disadvantage of this strategy is that, in many circumstances, it may be challenging to achieve the nonstop solution's viability by controlling variable values round off that must be essential to the bordering integer values. Additionally, the rounded-off solution's objective value may differ greatly from the continuous optimal solution (Kleinert et al., 2021). These factors, together with the improvements in the processing power of contemporary computers, have improved the class of problem controllability and sparked an interest in finding effective algorithms to handle the entire MINLP (Pappas et al., 2021). The branch-and-bound technique, developed by Nikolaos and Sahinidis (2019) to handle integer LP issues, was advanced to extended MINLP solutions. It is the most often used optimization approach for MINLP. When using the B&B method to solve mixed integer linear programming (MIP) issues, an indirect approach is used to first acquire a nonstop optimal solution by reducing integrality constraints. From there, the integrality constraints are gradually re-enforced to obtain an optimal integer solution. The algorithm is denoted as branching and bounding, where the upper bound is the up-to-date optimal integer value without any alternatives of a possible better optimal solution. For a given nonstop optimal solution, the associated feasible integer solutions are evaluated for their optimality.

The following study adopted convex MINLP, resting on the energy system mixed-integer quadratic program with storage, and found a near-optimal solution for online heuristic branch and bound model implementation facilitation (Leyffer and Linderoth, 2007). For complex, wide-ranging research with numerous objectives resolution for integration while using evolutionary algorithm guides for various optimizations, whether deterministic or metaheuristic (Montero et al., 2022), it has been well established and exhaustively reviewed in many references. A thorough explanation of the most efficient nonstop optimization techniques (Glover and Kochenberger, 2003), an all-encompassing review of method engineering mathematical optimization (Nocedaland and Wright, 2006), recent developments in global optimization (Biegler and Grossmann, 2004), and bound-constrained derivative permitted optimization algorithms (Wang et al., 2019), which serve as the foundation for widely used metaheuristic and deterministic algorithms related to optimization resolution in the review.

2.4.3.1 Review discussion on MINLP

We covered classical optimization techniques, their benefits, and shortcomings, with an emphasis on a full comparison of the essential elements of the computational cost of systems with potentially nonstop mixed integer variables, as well as nonlinear objective functions and constraints. The thesis adopted the convexity of MINLP, which rests on an energy system quadratic program mixed-integer with an energy storage system, to find a near-optimal heuristic solution for branch and bound development in the online implementation model facility. The centralized branch and cut approach, often known as developed integer programming from history, indicates formulation tightening in addition to further validity variations in branching or cutting that are placed at the branch and bound tree nodes. The energy supply-demand balancing variables and power flow within real-time integrated grid-tied RESs were motivated by this study.

2.5 Review of Meta-Heuristics or Evolutionary Computation Optimisation Methods for Energy Management Systems

The application of population-based optimization algorithms (POAs) is still in its very early stages and is lacking in real-world experience with grid integration for electric vehicles. Because POAs are relatively new technologies, it is difficult to gauge how prepared businesses are to adopt and use them. While methods for evaluating digitalization readiness and even maturity are well-established and covered in the literature, methods for addressing POA implementation in the hybrid system with grid integration are still in their infancy. The review aims to categorize the existing studies

that have been researched in the literature for a variety of reasons, including decreasing operation costs, increasing RE energy penetration battery life, decreasing operational costs and environmental pollution, and enhancing system stability and dependability.

Optimization is significant in methodical research, industry, and resource utilization because many real-world optimization task issues are treated as gradient-based methods in mathematical programming approaches that are no longer abundantly effective in multi-modality complex optimization handling and noise cut-out. Different types of population-based algorithms have emerged as viable solutions to the listed difficulties. In POAs, several entities collaborate in searching the resolution space universally using selection operators, mutation and crossover mechanisms, learning, and knowledge sharing. In addition, more or one operator's unpredictability allows POAs to explore better search space and outpace the local optimal points. POAs have three key qualities that set them apart from other optimization procedures. First is the searching of the solution space from several points at the same time. Second is the provision of knowledge sharing mechanisms for interactive learning among learning agents with different search behavioral approaches. Third, POAs are unpredictable because they are recurrently integrated stochastically into search behaviors. POAs can be broadly classified into EAs (evolutionary algorithms) and SIAs (swarm intelligence algorithms). Classical and widespread EAs include GA (genetic algorithm) (Janjic et al., 2017; Ahmad et al., 2018; Luo and Qiu, 2020), ES (evolution strategy), EP (evolution programming), and DE (differential evolution) (Ahmad et al., 2018). In addition, popular SIAs include meta-heuristic methods commonly used in optimization research, including GA, PSO, SA (simulated annealing), ACO (ant colony optimization), and several others (Wang et al., 2020; Gong et al., 2018). Injeti and Thunuguntla (2020) used PSO and BO (butterfly optimization) algorithms to optimize distributed generator combinations in radial distribution with plug-in EV systems. The aim is to minimize active daily power losses and develop a voltage profiling system. The study used a backward-forward power flow to assess radial distribution system daily bus voltages and power losses. POAs are renowned for tackling optimization objectives size and/or constraints, which may not always be differentiable and/or incessantly include randomness, disordered instabilities, and complex non-linear dynamics. Metaheuristics' feasibility is determined by their ease of formulation, ability to handle non-linear or discontinuous objective functions and constraints, and ability to solve complex computational snags. However, there are substantial problems with how they should be handled. Adding variables and limitations might slow down the process, leading to premature convergence and local minima or maxima (Nocedal et al., 2006; Biegler et al., 2004). Meta-heuristic approaches can be classified into countless groupings based on their natural stimulus to effectively tackle

EVCS-related optimization challenges. One prominent grouping is swarm intelligence algorithms, which draw stimulus from the cooperative comportment of social bird flocks, insect colonies, or animal herds. Swarm intelligence-based (SI) algorithms reviewed in the next section simulate the natural swarms self-organizing and observed collective behavior in solving complex optimization problems.

2.6 Swarm Intelligence Algorithms

There are several SI-based algorithms today that fit strategies to decrease costs, including their prominent versions, applications, advantages, and disadvantages. These methods include PSO, GA, DE, ACO (ant colony optimization), ABC (artificial bee colony), and the CSA (cockoo search algorithm). The optimization approaches leverage the problem's analytical properties to generate a series of points that converge to a globally optimal solution.

2.6.1 Genetic Algorithm

GA as a search optimization algorithm's basic concept was based on natural selection process mechanics, which were introduced in 1975 by John Holland (Ma, 2024; Albadr et al., 2020). The GA algorithm mimics 'the survival of the fittest' concept, which simulates observed natural system dynamics in which the strong adapt and live while the weak die. GA is a population-based strategy that employs specified genetic operators graded according to solution fitness, such as mutation, crossover, and reproduction (Lim et al., 2017). Chromosomes reflect the members of the population in a set of strings based on information from the preceding population's fittest chromosomes. GA provides possible solutions for an initial population and recombines them into more capable parts of the search space to steer their individual searches. These possible solutions, which are rarely referred to as genotype, are encoded as a chromosome and are measured for fitness using a fitness function. The fitness function value of a chromosome determines its ability to carry and create progeny. Maximization problems exhibit a high fitness value for a better solution, but minimization problems show a low fitness value for the same answer. GA consists of five key components: a random number generator, a reproduction process, a fitness evaluation unit, a crossover process, and a mutation operation. The reproduction process picks the population's fittest candidates, while the crossover process combines the fittest chromosomes and passes superior genes to the next generation, and mutation modifies genes in a chromosome (Ma, 2024; Albadr et al., 2020). The GA operation begins with a heuristic random selection of an initial population. The fitness function analyzes and ranks population members according to their

performance. After all of the population members have been examined, lower-ranking chromosomes are removed, and the residual populations are used to reproduce. Another possible selection strategy is pseudo-random selection, which gives lower-ranking chromosomes a chance to be selected for reproduction. The crossover stage randomly chooses two members of the remaining population (the fittest chromosomes) and swaps and mates them. The final step in GA is mutation, which includes using a mutation operator to randomly change a gene on a chromosome. Mutation is an important stage in GA since it ensures that all regions of the problem space are accessible. Elitism is utilized to keep the population's best solution from being eliminated throughout the crossover and mutation phases. Elitism ensures that the future generation has the same level of fitness as the current generation. The examination and production of new populations will continue until the best answer is found. GA is advantageous in that it requires only a few parameters sets and begins with a set of alternatives rather than a single one. The downside of GA is that the crossover and mutation processes are random, which causes slow convergence to optimal values. Several researchers conducted tests to increase optimal value performance, which resulted in a variety of alternate crossover and mutation pathways.

2.6.2 Ant Colony Optimization

Marco Dorigo proposed Ant Colony Optimization in 1992, based on the foraging behavior of the Ant System. The ACO algorithm is made up of four basic components: ant, pheromone, daemon action, and decentralized control. Ants are utilized as fictitious search agents to simulate exploration and exploitation. In real life, ants spread pheromones along their journey path, which evaporate and alter intensity over time. The amounts of these pheromones in the search space reflect the intensity of the trail, which can be regarded as the system's global memory (Sihotang, 2021). Global information acts collect inspiration, something a single ant cannot accomplish, and utilize the knowledge to choose the pheromone to help the convergence. The decentralized control in ACO is utilized to make the algorithm adaptable and robust in a dynamic environment, resulting in the ant failure supplied by such a system in the event of ant loss. In the initial phase, an agent (ant) moves randomly from the nest near the source and returns; the mid-range status involves several executed iterations in which ants learn multiple probable paths between the nest and the source, and the final outcomes of the ACO algorithm contribute to a cooperative interaction that results in the emergence of the shortest path (Liu et al., 2023; Kassim, 2022). ACO, unlike other evolutionary techniques, provides positive feedback, resulting in faster solution finding and distributed processing, avoiding premature convergence. Nonetheless, ACO has limitations, such as slower

convergence and the lack of a centralized processor to lead it toward good solutions as compared to other heuristic-based techniques. Although the timing of convergence is unknown, it is guaranteed. Another disadvantage of ACO is its low performance when working with huge search spaces. ACO has been used to solve a variety of optimization problems with the goal of improving overall performance, and several ACO versions have been developed. Dorigo and Gambardella enhanced ACO variations by increasing the state transition rule and pheromone, culminating in the Ant Colony System in local search processes (Dorigo and Gambardella, 2009). ACS uses a global centrally to maximize convergence time efficiency when GA is re-initialized, updates the pheromone approach, and concentrates the search within the best identified solution. To find the local minima of an ant-generated solution, a local optimization heuristic based on an edge exchange approach such as 2-opt, 3-opt, or Lin-Kernighan is utilized. The combination of novel pheromone management, new state transition, and local search algorithms has resulted in a variant of ACO for TSP difficulties (Tuani et al., 2020). The pheromone employs either the global-best approach or the iteration-best technique, but allows the ant with the best solution to apply the pheromone without regard for other ants in the same iteration ("Finding the best strategy in 2-player games through iteration," 2023).

2.6.3 Particle Swarm Optimization

Kennedy and Eberhart invented PSO in 1995 as an optimization technique that uses the flocking behavior of birds and fish to direct particles in their quest for global optimal solutions. PSO is defined as ducking the swarming local flock mates, aligning towards the average local flock mate's direction, and cohesion towards the average PSO position by searching an entire high-dimensional problem space as a robust stochastic optimization technique-based intelligence and swarm movement. PSO solves problems using the concept of social interaction rather than using the problem's gradient or requiring the optimization problem to be differential, as traditional optimization methods do (Dinc Yalcin and Curtis, 2024). PSO parameters include the go-between's position, velocity, particles in the solution space, and its surroundings. The PSO method starts with population initialization, then calculates each particle's fitness values, then updates individual and global bests, particle position, and velocity, and repeats until convergence (Rivera et al., 2023). The convergence is accomplished through particle attraction to the particle with the best solution. The PSO algorithm is straightforward to construct, requiring just a few parameters to be defined, effective in global search, insensitive to design variable scaling, and readily parallelized (Koyuncu & Ceylan, 2018). PSO converges quickly and prematurely in mid-optimal searches but slowly in refined searches. There are several approaches for improving PSOs using population sizes that

can boost the possibility of faster and more exact convergence. A second strategy is to strike a balance between exploration and exploitation at the start of an iteration, which increases the likelihood of discovering a solution close to the global optimum. Meanwhile, high exploitation would allow particles at the end of the iteration to select the most exact answer inside the promising area. A sub-swarm strategy is now frequently used as an alternative method for improving PSO performance. Allocating separate objectives to each subswarm may enhance PSO performance in multi-objective problems (Selvaraj and Choi, 2022). Another method for improving PSO performance is to change the dynamic velocity equation to move particles in numerous directions, resulting in faster convergence to a global optimum.

2.6.4 Differential Evolution

DE is a population-based method that uses the same operators as GA: crossover, selection, and mutation. The primary distinction is that DE uses mutation operations while GA uses crossover operations to provide superior solutions. Storn and Price invented the DE algorithm in 1997, and it employs mutation as a search mechanism and the selection operation to narrow the search to potential regions in the search space (Khan and Malik, 2017). DE uses iteratively generating a target vector to contain the search space solution; the mutant vector is the target vector mutation; and the trail vector is the resulting vector of the crossover operation between the target and mutant vectors, which are similar to GA with only minor differences. DE starts with population initialization, then evaluates to find the population's fittest members. Later, additional parameter vectors are created by adding the weighted difference of the two population vectors to the third vector. This stage is referred to as mutation. During the crossover, the vector is mixed, and the algorithm makes a final pick. To comprehend the distinctions between DE and GA, a more in-depth analysis of DE's three main operators is required. In DE, all solutions in the population have an equal probability of being chosen as parents, regardless of their fitness level. The most notable distinction between DE and GA procedures is determined only after the mutation and crossover processes. The exploitation behavior occurs when the difference between two solution vectors is minimal, whereas the exploration behavior occurs when the difference is high. DE is advantageous in terms of increasing local search capability and preserving population diversity, but it suffers from slow convergence and instability.

2.6.5 Artificial Bee Colony

Dervis Karaboga proposed the artificial bee colony in 2005. It is recognized as one of the most popular swarm intelligence algorithms and performs well when compared to other methodologies. The ABC algorithm is stimulated by the real honey bee's intelligent behavior in sourcing food, identified as nectar, and information is shared in the nest about food sources among other bees. Each bee has dissimilar tasks allocated to them to complete the algorithm's process. The algorithm is easy and simple to implement as DE and PSO are categorized as artificial agents known as: 1. employed bees with food source focus, retaining food source locality in their memories and equal to food source numbers, with each employed bee linked with a single food source; 2. the onlooker bee receives food source information in the hive from the employed bee; and 3. the scout bee is in charge of discovering new food sources and nectar.

2.6.6 Cuckoo Search Algorithm

Yang and Deb introduced the Cuckoo search algorithm in 2009. It is one of the newest metaheuristic approaches. CSA algorithm is stimulated by cuckoo species behavior, such as Lévy flight characteristics, fruit flies, brood parasites, and some birds. CSA employs three basic implementation operations rules. First, in each cycle, each cuckoo is allowed to lay one egg and choose a cuckoo nest at random. Second, high-quality nests and eggs are passed on to future generations. Third, the number of available host nests is set, and the deposited egg is discovered by a host bird based on cuckoo probabilities. The CSA algorithm can be extended to the point where each nest contains many eggs, which is helpful for multi-objective function problems and requires fewer parameters to be fine-tuned than other algorithms. CSA has an impermeable convergence rate to the parameter; hence, fine-tuning the parameters is unnecessary on some occasions. The swarm has the option of abandoning the nest or destroying the egg and starting over. The assumption can be approximated as a fraction, and the total parameter of the nests is replaced by new nests with a random solution.

2.6.7 Review discussion on Meta-Heuristics

Since the early 1960s, many swarm optimization algorithms have been devised, including evolutionary programming and the most current particle swarm optimization. All of these methods have proven capable of solving a wide range of optimization issues. This thesis gives a thorough examination of well-known optimization algorithms. Selected algorithms are briefly presented and thoroughly compared to one another, with a discussion of their benefits and drawbacks. When compared to other methodologies,

the results show that Differential Evolution (DE) has the greatest overall advantage, followed by Particle Swarm Optimization (PSO).

PSO tends to converge fast and prematurely in mid-optimum searches, as well as slowly in refined searches. There are numerous techniques for PSO improvement involving population sizes; this may improve the chance of faster and more exact convergence. A second approach is to strike a balance between exploration and exploitation at the outset of an iteration, increasing the chances of finding a solution that is near the global optimum.

Table 2.2. Meta-Heuristics or Evolutionary Computation Optimisation Methods for Energy Management Systems Considering RESs and EVs

Reference	Optimization technique	Objectives function	Power System considered
Janjic et al., 2017	Genetic Algorithm	Minimize EV owner costs and secondary frequency regulation, maximize charging station efficiency and total investment.	Frequency control for commercial electric car fleets
Gong et al., 2018	Particle Swarm Optimisation	Minimize voltage deviations and losses	Optimization of electric vehicle charging impact on distribution systems.
Ahmad et al., 2018	Differential Evolution and Genetic Algorithm	Minimizing distribution losses and lowering aggregator charging costs for EVs.	Review of Electric Vehicle Charging Techniques and Technology Evolution
Cui et al., 2019	Robust optimization	Minimize the power loss, high voltages, charging cost, and load fluctuation.	Methods for placing an electric vehicle charging station.
Chung et al., 2019	Ensemble machine learning	Minimize load variance while lowering EV charging costs.	User behavior prediction algorithm for electric vehicle
Luo and Qiu, 2020	Genetic Algorithm	Minimize traveling, cost of annual construction time opportunity and operational costs	Sustainable Cities' Approach to Locating Electric Vehicle Charging Stations
Hongtao et al., 2020	Bayesian network	Reduction of EV charging costs on traffic route	Comparison of EV charging cost without charging behavior and renewable integration
Farshad et al., 2021	NSGA-II-based method and Monte-Carlo method	Minimize electric vehicle charging costs	Optimization approach for energy cost, the state of charge of an EV battery and load demand,
Ahmad et al., 2022	grey wolf optimization	Minimization of land cost, power loss, and electric vehicle population	Fast electric vehicle charging station optimization

(Sultana et al., 2022)	Particle Swarm Optimization algorithm	Minimizing energy loss cost	EVCS efficient location allocation
(Ahmadi et al., 2022)	demand response programs (DRPs),	Minimizing energy cost	PEV parking lot's new model
(Ahmad et al., 2022)	Gorilla Troop Optimizer (GTO) algorithm	Minimizing total voltage deviation and power loss	EVCS operation Efficiency of battery energy storage systems
(Krishnamurthy et al., 2023)	modified teaching-learning-based optimization	Minimizing the power loss index and cost, while maximizing the voltage stability and reliability index.	EVCI Infrastructure Sizing and Placement

Furthermore, the paucity of charging stations restricts the quick adoption of EVs as a more cost-effective method of transportation, particularly in developing nations. As a result, EV owners recharge their batteries via their home connection, causing a considerable system loss in the power sector and a lower profitability index (Sivaraman and Sharmeela, 2021). Because of their nonlinear behavior, many EV chargers produce power quality issues on the distribution grid, including voltage fluctuations, harmonics, and power loss (Surbhi et al., 2020). Power quality difficulties in the distribution network are associated with unorganized and inefficient EV charging procedures (Sridevi et al., 2022). These issues can be addressed by changing charging patterns (Qiyun, 2018), upgrading converter topologies (Radha and Singh, 2019), incorporating renewable resources (Ashish Kumar et al., 2019), and implementing energy management strategies (Viet Thang et al., 2019). Despite renewable power-generation intermittent nature and the high infrastructure capital requirements, these RE have gained in popularity due to their low cost, environmental benefits, and low maintenance requirements (Wang, 2020). Furthermore, power quality difficulties in the distribution network were created by chaotic and inefficient EV charging plans. The risks of integrating renewable energy for EV charging must be considered to improve dependability (Ekramul et al., 2017). As a result, an energy management strategy is required for EV charging in order to maximize renewable use. Research has been undertaken on EVCS optimization, considering location, EV power demand, charging priority, and charging duration (Shahid et al., 2020). Although solar energy is an essential source of electricity generation, it can only be harvested for a few hours every day (Natasha and Warren, 2020). However, the lack of an energy management system significantly limits hybrid power generation for EV charging. More research is needed to optimize the EVCS in terms of charging period (peak/off-peak hour), renewable energy generation, EV power consumption, and real-

time charging cost. The review in this chapter examines numerous approaches for the optimization of EVCS, including meta-heuristics or evolutionary computation optimization methods for energy management systems considering RESs and EVCS as applicable to the distribution network and the EV user tactic with diverse objective functions, constraints, and combinations. Hence, this chapter has addressed the review of the sizing approach and optimal citation for charging stations with EMSs and RESs integration to reduce the peak EV demand from the grid. In addition, various EVCS placement optimization algorithms using objective functions are discussed. This review study examines the consequences of EV loads on the environment, distribution system, and economics. The charging control, charging procedures, and coordinated power flow in the distribution network with EVCS are also investigated.

2.6.8 Review findings on Meta-Heuristics or Evolutionary Computation Optimisation Methods for Energy Management Systems

Despite the significant computerization potential, grid-tied RES integration and optimal energy management strategies of a hybrid system design for AI applications are still in their early stages, with little practical knowledge and execution. One of the primary reasons for the knowledge gap is the companies' readiness to adopt new AI technology. While ways to measure preparedness and even maturity in terms of digitalization or Industry 4.0 are well established and debated in the literature, approaches to AI deployment are still in their early stages in a hybrid system with an electric vehicle charging station. Despite the advancements in understanding meta-heuristic/evolutionary optimization algorithms in the context of power systems, the grid-tied RES application of EV integration and optimal energy management strategies of a hybrid system design that systematically addresses the operational cost reduction in EVCS is lacking. Addressing this gap, this thesis chapter presents a review of meta-heuristics or evolutionary computation optimization methods for energy management systems. The review covers 2017 to 2023, with an 11.7% study relevant to using PSO differently for EVCS efficient location in 2018 and electric vehicle charging stations optimal distribution system impacts in 2022, while the thesis explores both studies as a single research project. The second dimension of the review result is objective functions that demonstrate minimizing voltage deviations and losses and minimizing energy loss costs are applied differently in the study, while the thesis explores both in a single study. The integration of a Particle Swarm Optimization algorithm enables the optimization of operational cost, contributing to a judicious and cost-effective deployment strategy. However, EMS has evolved over time from being merely a concept to being put into

practice. The important discoveries are relevant to EMS since it is clear that research is progressing from concept to realization. In Chapter 4 of the thesis, we provide a PSO implementation technique for energy management of an electric vehicle charging station's hybrid energy system, based on a review of the literature on technological adoption and the implementation of AI methods.

2.7 Optimization Application Methods for Power Systems

Optimization is a systematic expedition for better solutions or designs that humans may not be able to discover through intuition, experience, or trial and error. Optimization can not only improve performance but also support until now unknown skills. Computers are essential to fully utilizing optimization capabilities in practice. Optimization research often requires both theoretical considerations for developing novel optimization strategies and evaluating existing ones (Gürdal et al., 1999), and computational approaches frequently focus on understanding different search algorithms. Theoretical approaches are important. Power system planning aims to optimize generation and transmission strategies for optimum system utilization. Conventional power plants are expensive to operate due to high energy prices and maintenance expenditures. Conventional power plants require lengthy transmission lines that carry power from producers to consumers due to their remote locations. The EPD issue, like most complicated engineering optimization problems, exhibits nonlinear and nonconvex properties. Computational approaches may not produce a global extremum due to the presence of multiple local extrema, making getting an optimal solution challenging. Modern power systems require optimal energy efficiency due to scarcity of resources, rising generation costs, and rising demand. Economic power dispatch process of allocating generating units to supply the system load efficiently while meeting restrictions. The EPD aims to lower power generation costs while balancing equality and inequality constraints. In EPD situations, the generating unit cost function is sometimes referred to as a quadratic function. Thermal generating units may have restricted operating zones between the lowest and maximum power outputs due to physical constraints on power plant components. The gasoline cost curve for a unit with prohibited operation zones resulting from the physical limits of power plant components is discontinuous. Prohibited operating zones for separate generators create a solution space with disjointed, feasible sections. Committed thermal units have a limited working range due to ramp-rate constraints between two phases. The generation rate can fluctuate based on unit ramp-rate constraints. Unit input-output curves are not monotonically growing. Physical restrictions may cause instability during operation with certain loads. To prevent instability, the notion of forbidden operation zones was devised. Avoid using thermal units to generate power

in forbidden locations. Energy management plans improve the efficiency of transmission system facilities, both old and new. OPF analysis is used by system operators to reduce grid-wide generation costs and losses while meeting operational constraints like generation-load balance, bus voltage limits, and transmission line congestion. A power grid is an interconnected system that dynamically dispatches generation to meet changing load demand. Solving the OPF fault caused by an independent system operator may violate unit confidentiality in an energy-driven market, such as disclosing load aggregator demand and generator costs. The second issue is the nonconvexity of the OPF problem. Linearizing the OPF problem in big networks can be computationally difficult, especially with additional decision variables and price-responsive load aggregators in the energy market. Uncertainty in renewable energy threatens the generation load balance, especially since the ISO lacks reliable historical generation data from privately owned renewable plants. Global optimization has gained popularity over the past decade, with many deterministic and stochastic methods developed for continuous domain optimization. Mathematical methods may not provide global optimal solutions for practical economic dispatch problems due to limitations. Evolutionary computation provides distinct advantages over other stochastic techniques, including stable performance and global search capabilities. Despite substantial research, consistent solutions for solving the realistic economic dispatch problem continue to evolve. If computations were performed point by point, a solution to the problem of load dispatch optimization would be extremely complex and time-consuming. Therefore, a rapid approach is necessary for this purpose. Nonlinear thermal generating units necessitate unique strategies for efficient generation scheduling in nonconvex economic dispatch problems. This thesis uses particle swamp optimization to solve economic power dispatch problems with uncertain RES quadratic cost functions using Monte Carlo simulation from reviewed literature.

2.8 Particle Swarm Optimization and its Applications for Power Systems

The proposed solutions was evaluated against a typical PSO algorithm to demonstrate their efficiency. After validation, the optimal method is chosen and used to resolve a reactive market clearing issue. Power systems rely heavily on adequate reactive power supplies. Reactive power supplies improve the overall power system stability, energy loss, and voltage profile by providing adequate reactive power helps reduce energy loss, increase stability margins, and enhance the voltage profile. Before reorganization, the government only operated the generation section. Power system operators have complete control over the scheduling of power plants. electricity system operators had full ability to schedule active and reactive electricity for all power plants owned by the

government. Within these strategies, the procedure is carried out to minimize the total cost of operation. Power system reform aims to improve efficiency, increase competition, and determine the true cost of generating electricity. In reorganized power networks, power generation is privatized. The independent system operator has responsibility for properly functioning the functioning the electricity system. The private nature of power plants limits the independent system operator's scheduling authority. Under this scenario, power plants should submit energy-selling proposals to the independent system operator. Furthermore, all energy consumers should submit purchase offers to the independent system operator. The independent system operator clarifies the energy market based on proposals from both consumers and producers (Davarzani et al., 2020). An insufficient reactive power supply can induce voltage collapse in power systems. The PSO method is composed of two core equations. The velocity equation (Equation 2.1) states that each particle in the swarm adjusts its velocity based on the computed values of the individual and global best solutions, as well as its current position. The PSO algorithm consists of a velocity equation (Equation 2.1) that indicates each particle in the swarm adjustment towards the computed velocity values and global best solutions, and the present position of individual and social acceleration factors represented by coefficients $c_1$and c_2, with c_1 represent local particle's confidence and c_2 representing a neighboring particle's confidence. Random numbers represent the stochastic influence of cognitive and social processes r_{1k}^i and r_{2k}^i. To define PSO, stochastic vector $v_k^i$is given by

$$v_k^i = c_1 r_{1k}^i \left(\mathcal{P}_k^i - x_k^i\right) + c_2 r_{2k}^i \left(\mathcal{P}_k^g - x_k^i\right) \quad (2.1)$$

r_{1k}^i and r_{2k}^i are two uniform random scalar integers between 0 and 1 that change with each iteration k and solar PV generation source i in the swarm. Thus, r_{1k}^i and r_{2k}^i scale the magnitudes of the cognitive and transmission line powers, $c_1 r_{1k}^i \left(\mathcal{P}_k^i - x_k^i\right)$ and $c_2 r_{2k}^i \left(\mathcal{P}_k^g - x_k^i\right)$. The stochastic contribution v_k^i in the instantaneous search domain. Cognitive vector $\mathcal{P}_k^i - x_k^i$ and transmitted power $\mathcal{P}_k^g - x_k^i$ denote solar generator's position distance directions and x_k^i to best location for solar generator $\mathcal{P}_k^i$, and global best location $\mathcal{P}_k^g$, respectively. Cognitive and transferable abilities may be normal or parallel to each other. Suppose the cognitive vector $\mathcal{P}_k^i - x_k^i$ and transmitted powers $(\mathcal{P}_k^g - x_k^i)$ are not parallel, equation (2.2) can be understood as the vector equation of a bound plane $\mathcal{P}_k^i$ in an n-dimensional space. The plane is constrained by the lengths of the cognitive and social vectors that are scaled separately by the finite scalars $c_1 r_{1k}^i$ and

$c_2 r_{2k}^i$. Calculate the angle $\bar{\theta}$ between the cognitive vector $\mathcal{P}_k^i - x_k^i$ and the transmitted powers $(\mathcal{P}_k^g - x_k^i)$.

$$\bar{\theta} = \cos^{-1}\left(\frac{\left|(\mathcal{P}_k^i - x_k^i) * (\mathcal{P}_k^g - x_k^i)\right|}{\|(\mathcal{P}_k^i - x_k^i)\|\|(\mathcal{P}_k^g - x_k^i)\|}\right) \tag{2.2}$$

If $\bar{\theta} = 0$, the vectors $(\mathcal{P}_k^i - x_k^i)$ and $(\mathcal{P}_k^g - x_k^i)$are parallel; when $\bar{\theta} = 90$, the vectors $(\mathcal{P}_k^i - x_k^i)$ and $(\mathcal{P}_k^g - x_k^i)$ are perpendicular. Scaling each RES generator source individually, the component of $(\mathcal{P}_k^i - x_k^i))$ and $(\mathcal{P}_k^g - x_k^i)$ is substituted by scalar random values in the stochastic vector from r_{1k}^i and r_{2k}^i to $\mathcal{R}_{1k}^i$ and $\mathcal{R}_{2k}^i$.

$$v_k^i = c_1 \mathcal{R}_{1k}^i \left(\mathcal{P}_k^i - x_k^i\right) + c_2 \mathcal{R}_{2k}^i \left(\mathcal{P}_k^g - x_k^i\right) \tag{2.3}$$

The $\mathcal{R}_{mk}^i$ random diagonal matrices are expressed formally as

$$\mathcal{R}_{mk}^i = \begin{bmatrix} \mathcal{P}_{11k}^i & 0 & \dots & 0 \\ 0 & \mathcal{P}_{22k}^i & \dots & 0 \\ \vdots & \vdots & \ddots & \vdots \\ 0 & \dots & \dots & \mathcal{P}_{nnk}^i \end{bmatrix}, \qquad \mathrm{m} = 1,2, \tag{2.4}$$

For independently scaled RES generator sources, use $0 < \mathcal{P}_{jjk}^i < 1,\ j = 1, \dots \dots \dots, n$.

2.9 Chapter Summary

The survey examined the number of peer-reviewed publications covering the different journal articles, including Elsevier, Springer, SAGE, Emerald, Francis, IJIMS, MDPI, Wiley, and others, between 2013 and 2022. A comparison of traditional and heuristic optimization methods for energy management for hybrid systems of an electric vehicle charging station provides review findings for the method considered. An optimization review describes the pros and cons of conventional and heuristic methods that have been proven to be reliable, efficient, rapid, and very upfront to algorithmically implemented, but with exertion in dealing with inequality constraints, lack of convergence, and global optimality properties. In some instances, non-conventional or heuristic optimization techniques can achieve global convergence and global optimality independently of the problem formulation and their natural ability to handle discrete variables, but their effectiveness and efficiency weigh heavily on parameter selection and relatively incur a greater computational expense. The optimization method in the thesis review shows that the PSO and MINLP co-optimization methods can be used for hybrid

system energy management to determine the optimal power flow of the hybrid system of an electric charging station separately. The time interval for using MINLP for modeling as classical convex optimization methods is an iterative process for the costs of each possible RES output with a possible combined aggregate output. Mixed-integer nonlinear programming modeling will be explored to solve an envisaged optimization problem by calculating an optimal solution that minimizes a generated set of objective functions weighted to compute the importance of definite constraints. External constraints about the future dynamic cycle or internal constraints may be added to the objective function set for solving the optimization problem and calculation of the control input as different energy sources. The problem formulation, input and output variables, system modeling, and considered optimization horizon will help determine a new taxonomy for optimization-based energy management. Without the linear objective, the optimal solution may be interior to the convex hull, which will exclude solutions from constraints enforcement relaxations (i.e., computation for a lower bound on the optimum value) that are not feasible for MINLP. The heuristic search optimization method will be explored for the nonconvex PSO technique for hybrid system energy management of an electric vehicle charging station. The heuristics optimization techniques require the strategy for optimum-seeking solutions using search point algorithms to be modeled in MATLAB. It involves a stochastic process for global convergence to search for characteristics of one-point existence. The optimal resolution depends on the heuristic algorithm parameter choices, considering the non-convex nature of the objective function.

Economic dispatch in engineering is a power systems problematic optimization aimed at determining the most economical way to allocate a set of power output from generators to meet the demand while various operational constraints are satisfied. The next chapter provides the MINLP formulations applied to the economic dispatch problem with hybrid energy resources.

CHAPTER THREE

DEVELOPMENT OF MINLP FOR ECONOMIC DISPATCH PROBLEM OF THE HYBRID SYSTEM WITH ELECTRIC VEHICLE CHARGING STATION

3.1 Introduction

The objective of this chapter is to develop the energy management dispatch-optimizer strategies for a hybrid system of an electric vehicle that is comprised of a photovoltaic, wind, and energy storage system for the economic dispatch problem using a MINLP based on results from a literature review of single and multi-objective objective functions. The study adopted a convex multi-integer nonlinear programming (MINLP) algorithm from mathematical techniques, which rests on mixed-integer quadratic programming, and found a near-optimal solution to facilitate simulation implementation in the branch-and-bound model application (Leyffer and Linderoth, 2007). Throughout the history of integer programming, the fundamental branch-and-cut (B&C) has been developed to identify additional valid inequalities or cuts at the nodes of the branch-and-bound tree. This study motivated the variables used to control the energy supply-demand balance problem in grid-tied RESs in real time. The noteworthy contributions outlined in the thesis chapter are:

i. Formulation of economic dispatch problem for the hybrid systems energy management strategies for EVCS.
ii. Examine the problem of minimizing power losses by merging EVs and RES to achieve the highest feasible active power output from RESs in voltage terms and power distribution loss coefficients.

The chapter discusses the formulation of MINLP of EMS for the RES hybrid system in Section 3.2; Section 3.3 presents EMS simulation results and discussion; and section 3.4 is the conclusion.

3.2 Formulation of an optimization problem for energy management of the RES hybrid system

The modeling of the optimal linear objective function's input in a mathematical way is guided by the work of (Leyffer and Linderoth, 2018):

$$\text{Min} \sum_{i=1}^{N}[\sum_{t=1}^{T} c_i(t) \times x_i(t) + F_i Y_i] \quad (3.1)$$

Where $\mathrm{N} = \text{Total number of renewable energy resources (RESs)};$

$\mathrm{i} = \text{Unit number}$

$\mathrm{t} = \text{Time period}$

$c_i(t) = Cost\ of\ unit\ i\ in\ time\ period\ t$

$x_i(t) = Power\ output\ of\ unit\ i\ time\ t$

$Fixed\ cost\ of\ unit\ i$

$Y_i(t) = Fixed\ power\ output\ of\ unit\ i, 0, variable$

The objective function to reduce nPV generating costs and m loads are

$$\text{Minimize} C_{PV} = \sum_{t=1}^{k} \left[\sum_{i=1}^{Ns} P_{PVi}^{t} C_{PVi} + P_s^t C_s^t\right] \quad (3.2)$$

Subjected to $P_{PVmin}^{t} \leq P_{PVi}^{t} \leq P_{PVmax}^{t}$

Similarly, the objective function to reduce WT nWT generating costs and m loads may be,

$$\text{Minimize} C_w = \sum_{t=1}^{k} \left[\sum_{m=1}^{Nw} P_m^{sc} C_{dm} + P_s^t C_s^t\right] \quad (3.3)$$

Subjected to $P_m^{min} \leq P_m \leq P_m^{max}$

Where C_{PV} and C_w is the solar PV and wind turbine cost,

P_{PVi}^{t} is the PV ith output power at time t horizon,

C_{PVi} and C_{dm} are the PV ith and wind mth operating cost,

P_s^t and C_s^t is the cost of distribution network and operation cost at time t,

P_{PVmin}^{t} and P_{PVmax}^{t} is the maximum and minimum power of the ith PV system.

Equations (3.4) and (3.5) describe the explicit battery operating cost model while charging and discharging:

$$C_{charging} = C_{bat}^{C} + C_{bat}^{C,max} \quad (3.4)$$

$$C_{discharging} = P_{bat}^{D} + P_{bat}^{D,max} \quad (3.5)$$

Subject to ESS power charging or discharging constraints.

$$P_{ess}^{min} \leq P_{ess} \leq P_{ess}^{max} \quad (3.6)$$

Equations (3.7) and (3.8) provide the objective function used in Equation (3.1) to minimize the overall operational cost of renewable energy production while accounting for uncertainty restrictions. These models will be generated in real-time, with intra-hour dispatch intervals, while accounting for operating and security limits using the guided model.

$$\sum_{t=1}^{Nsub} \sum_{i=1}^{Ng} C_{Gi}(P_{Gi}) + \sum_{t=1}^{Nsub} \sum_{i=1}^{Nw} C_j R + C_j P + \sum_{t=1}^{Nsub} \sum_{i=1}^{Ns} C_l R + C_l P \quad (3.7)$$

Subjected to

$$\max\left[P_{Gc}^{min}, P_{Gi}^{T-1} - R_{Gi}^{down}\right] \leq P_{Gi} \leq \min\left[P_{Gi}^{max}, P_{Gi}^{T-1} + R_{Gi}^{down}\right] \; V_{Dk}^{min} \leq V_{Dk}^{max} \quad (3.8)$$

The MINLP mathematical modeling solvers to compute the optimum objective function's lower bound on the inputs is derived by widening feasible sets and ignoring restrictions.

$$Z_{MINLP} = \min_{x} f(x) \leq \eta \tag{3.9}$$

η is the batteries charging and discharging efficiencies, subject to g as $0 \leq P_{bt}^{C} \leq P_{bt}^{C,max} u_{bt}^{C}$ or $0 \leq P_{bt}^{D} \leq P_{bt}^{D,max} u_{bt}^{D}$ while f(x) is a cost function (minimization) or a grid function (maximization) for an ideal solution.

$$x \in X \ , \ x_{\boldsymbol{I}} \in \mathbb{Z}^{/\mathbf{I}/} \text{for all i} \in \text{I} \tag{3.10}$$

The expected energy storage of a PV/WT variable is constrained by the real power output of the convex function $f(x): \mathbb{R}^n \rightarrow \mathbb{R}$, $g: \mathbb{R}^n \rightarrow \mathbb{R}^m$ of the charging or discharging of the battery given as

$$E_{bt} = E_{b,t-1} + P_{bt}^{C} \eta_b^{C} \Delta t - P_{bt}^{D} \frac{1}{\eta_b^{D}} \Delta t \tag{3.11}$$

Giving the constraints to ensure that battery energy does not exceed storage capacity E_b^{cap} as $0 \leq E_{bt} \leq E_b^{cap}$. $P_{bt} = P_{bt}^{D} - P_{bt}^{C}$ as total power. We have a convex MINLP, if f and g are convex functions. If f and g are not convex, then we have a nonconvex MINLP. In the adopted approach g are convex functions but nonlinear. Dropping integrality in convex results in nonlinear relaxation (removing some constraints). The ideal relaxation is the convex hull of feasible locations, while maximizing a linear function over a convex set solves the problem.

3.2.1 Constraints and Variable Limits

Having constraints $0 \leq E_{bt} \leq E_b^{cap}$ that ensures the energy in the battery does not surpass the storage capacity E_b^{cap}, total power $P_{bt} = P_{bt}^{D} - P_{bt}^{C}$. The battery's state of charge (SOC) indicates its behavior in percentage terms and can be represented as follows. The level of charge and associated limits are explained for both battery energy storage systems and deployed electric vehicle battery systems, by

$$SOC(h) = SOC(h-1) + n_{charge} \, X \, E_{charge}(h) - \frac{E_{discharge}(h)}{n_{charge}} \tag{3.12}$$

$$SOC(h) = SOC_{initial} \tag{3.13}$$

$$SOC(h) \leq SOC^{max} \tag{3.14}$$

$$SOC(h) \leq SOC^{min} \tag{3.15}$$

$$E_{charge}{}^{h} \geq E_{change}^{min_{charge}} \tag{3.16}$$

$$E_{charge}{}^{h} \geq E_{change}^{max_{charge}} \tag{3.17}$$

$$E_{discharge}{}^{h} \geq E_{dischange}^{min_{discharge}} \quad (3.18)$$

$$E_{discharge}{}^{h} \geq E_{dischange}^{max_{discharge}} \quad (3.19)$$

$$U_{charge}(h) + U_{discharge}(h) \leq 1 \quad (3.20)$$

1. If the battery is charged:

$$SOC_{(t+1)} = SOC_{(t)} + \frac{\Delta t + \eta_{charge}}{E_{nom}} X(P_{Charge(t)}) \quad (3.21)$$

With

$$P_{Charge(t)} = P_{PV->batt} + P_{Grid->batt(t)} \quad (3.22)$$

2. If the battery is discharged:

$$SOC_{(t+1)} = SOC_{(t)} - \frac{\Delta t}{E_{nom}\, X\, \eta_{discharge}} X(P_{Discharge(t)}) \quad (3.23)$$

$$P_{Discharge(t)} = P_{batt->L(t)} + P_{batt->Grid(t)} \quad (3.24)$$

where the amount of energy stored is SOC; $P_{Charge(t)}$ is battery charging power, while $P_{Discharge(t)}$ is battery discharging power. $\eta_{charge\ and}\, \eta_{discharge}$ are battery's charging and discharging efficiencies respectively; E_{nom}. is system nominal energy, while $P_{Grid->batt(t)}$ is the battery charge electricity imported from the grid; $P_{PV->batt}$ is the solar PV power to charge the battery. $P_{batt->L(t)}$, represents the battery electricity for load supply, while $P_{batt->Grid(t)}$ represents power exports to the grid.

The ideal cost is the applied optimal controlled grid energy cost, whereas the baseline cost is the consumer tariff if no optimization was applied. The tariff remarks the imported grid energy used to power the load and battery storage system. The surplus of PV, WT, and storage energy sold to the utility grid is considered income. The cost savings computation is shown in equation (3.41):

$$\underbrace{\underbrace{Min}_{x}}_{\underbrace{Max}_{x}} F(x), subject\ to \begin{cases} c(x) \leq 0, \\ c_{eq}(x) \\ Ax \leq b, \\ A_{eq}x = b_{eq} \\ lb \leq x \leq ub \end{cases} \quad (3.25)$$

Where $F(x)$ denote the objective function; $c(x)$ and $c_{eq}(x)$ are linear and non-linear functions; A and B are the inequality constraints coefficients; $A_{eq}\ and\ b_{eq}$ is the equality constraints coefficient.

Equality Constraints

$$\begin{bmatrix} \overbrace{\begin{matrix} I_{NXN} & I_{NXN} & O_{NXN} \\ O_{NXN} & Y_{NXN} & \emptyset_{NXN} \end{matrix}}^{A_{eq}} \end{bmatrix} X \overbrace{\begin{matrix} P_{load}(1:N) - P_{RES}(1-N) \\ E_{batt(1)} \\ 0_{N-1} \end{matrix}}^{b_{eq}} \quad (3.26)$$

$$Y_{3X3} = \begin{bmatrix} 0 & 0 & 0 \\ \Delta t & 0 & 0 \\ 0 & \Delta t & 0 \end{bmatrix} \qquad Y_{3X3} = \begin{bmatrix} 1 & 0 & 0 \\ -1 & 1 & 0 \\ 0 & -1 & 1 \end{bmatrix} \quad (3.27)$$

Inequality Constraints

$$\begin{bmatrix} \overbrace{\begin{matrix} O_{NXN} & I_{NXN} & O_{NXN} \\ O_{NXN} & -I_{NXN} & O_{NXN} \\ O_{NXN} & O_{NXN} & I_{NXN} \\ O_{NXN} & O_{NXN} & -1_{NXN} \end{matrix}}^{A} \end{bmatrix} X \geq \overbrace{\begin{matrix} P_{max} \\ -P_{min} \\ E_{max} \\ -E_{max} \end{matrix}}^{b_{eq}} \quad (3.28)$$

$$C_t^{bat} = \alpha^{bat} X P_t^{bat} + \beta^{bat} X P_t^{bat} + \gamma^{bat} X P_t^{bat}, \forall t \in T \quad (3.29)$$

P_t^{bat}: Power supplied (discharging) or stored (recharging) of the battery at the time t.

γ^{bat}: the coefficient for pollution treatment cost

α^{bat}: Maintenance coefficient

β^{bat}: Value depreciation coefficient

C_t^{RES}: RESs social cost

Since this ESS does not emit any greenhouse gases, the value of γ^{bat} is zero.

Dispatchable RE function is

$$C_t^{MT+FC} = C_t^{MT} + C_t^{FA} \quad (3.30)$$

The grid social cost function can be formulated as follows:

$$C_t^{Total} = C_t^{MT+FC} + C_t^{RES} + C_t^{grid} + C_t^{bat} \quad (3.31)$$

3.2.2 EMS MINLP Classical Algorithm

Step 1 - Input decision variables to optimise usage of energy storage Ppv, N, Pload, dt, Cost, Einit, EWeight, MinMaxbattery)

N - Number of discrete steps horizon
dt - Optimization calls time [s]
Ppv - Solar PV power [W]
Pload - Grid load power [W]
Einit - Battery initial energy [J]
EbattV – Battery voltage [V]
Cost - Grid Charge Cost [$/kWh]
EWeight - Energy storage weight
MinMaxbattery - Battery min/max

Step 2 – Confirm battery/grid power differencial (d) = Pload - Ppv

Step 3 – Minimize grid energy cost from the objective optimization calls time * grid charge cost *Pgrid – Energy storage weight * Battery voltage

Step 4 - Battery input/output power Optimconstr(N) = constraints. energyBalance

Step 5 – Power from PV, grid, and battery Ppv+PgridV+PbattV-Pload = constraints.loadBalan.

Step 6 - Battery SOC Energy constraints

Step 7 - Perform Linear programming optimization

Step 8 – Sub-matrices for optimization constraints

Step 9 - Optimoptions(prob.optimoptions,) = Options for Linear Program

Step 10- Parsing the optimization results

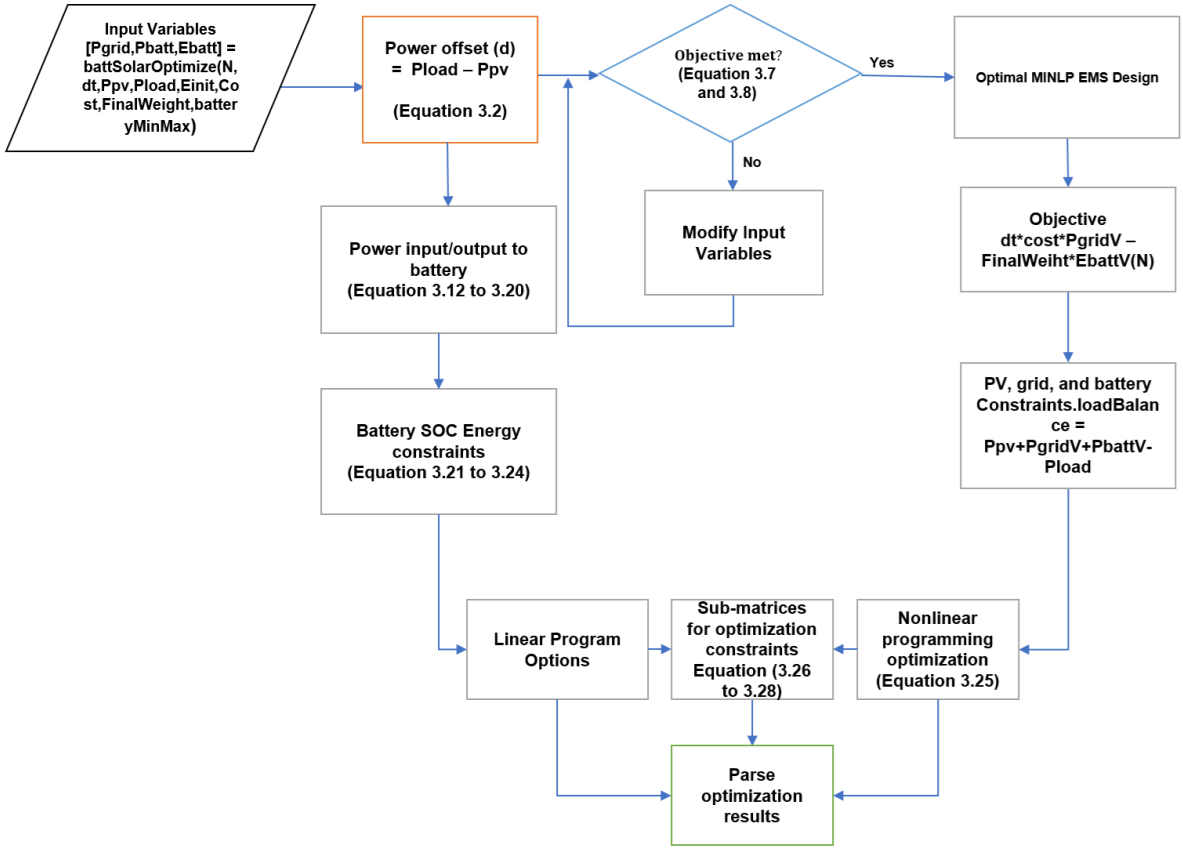

Figure 3.1. Flowchart for MINLP Classical Algorithm

3.3 EMS MINLP Simulation Results and Discussion

The thesis's objective on the identification of energy management for hybrid system's objective functions and constraints was answered in the chapter. Subsequently, the approach was implemented in MATLAB with FMINCON (Find minimum of constrained nonlinear multivariable function) optimization solver to resolve the MINLP problem. The

power output of the solar PV model against the load demand on an hourly basis. The everyday hybrid system operational behavior is the main subject of chapter 3. The solar PV power output is mostly determined by the various irradiance values estimation, necessitating the use of an appropriate functional model. Before using the MATLAB program, data from the seasonal sun irradiance model was obtained through simulation. This function evaluates a solar PV's output based on cloudy and clear days, it calculates the overall solar PV systems output. Next, the cost function is compared without taking into consideration the battery's daily operating costs. The FMINCON approach is used in MATLAB to tackle the optimization problem. Monthly energy consumption exceeds 500 kWh, and the load demand profile represented in Figure 3.2 reaches a peak of 800 kWh during the peak price period.

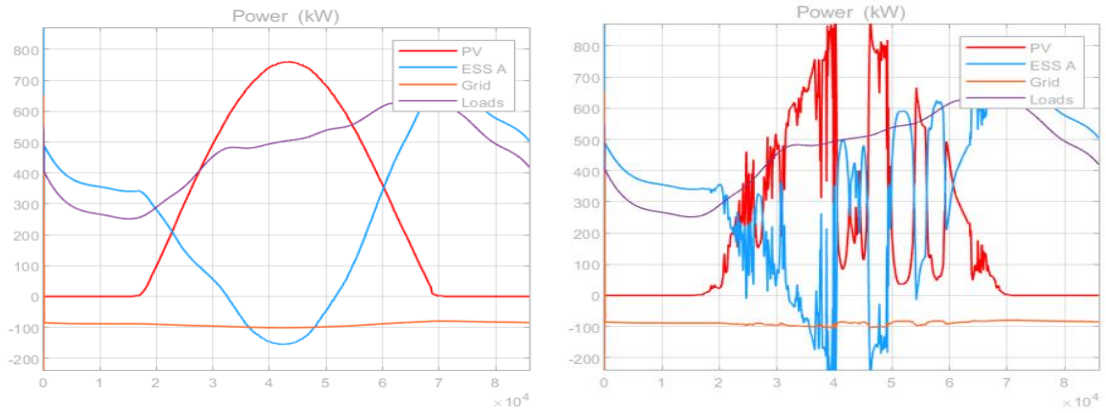

(a) (b)

Figure 3.2. Simulated power generation: (a) energy availability of 500 kWh during clear days in the heuristics method simulation; (b) energy availability with peak of 800 kWh during cloudy days in the optimal approach.

As seen in Figure 3.2, when the demand is at its highest and between the hours of 22 and 5, the RES is at its lowest, and the solar PV power along with battery power are sufficient to meet the client's needs. The battery is charging during the day using RES power and at night using utility power, particularly throughout the off-peak price period. When the SOC rises to meet the load needs during times of high demand, battery power plays a significant role. When the demand is at its highest and between the hours of 22 and 5, the RES is at its lowest, and the solar PV power along with battery power are sufficient to meet the client's needs. Furthermore, only a little amount of power is produced during off-peak hours, and the system does not send any electricity to the demand during the peak pricing time interval. However, enough power is produced from grid-tied HS to make up the difference during the day. The surplus energy transmitted to the grid during the day generates a sizeable profit. The decline in the SOC (Figure 3.3) can be attributed to a low surplus of energy storage that is utility grid export, particularly during peak pricing periods. The ESS takes data from EMS optimization directives and

then performs energy generation and load balancing tasks in either off-grid or grid-connected mode. The ESS is crucial for demand-side management. This simulation model utilized two forms of EMS: heuristics and the linear optimization approach. Equations (3.21–3.24) are used to compute the SoC energy limitations of the battery limits. While SoC cannot be measured directly, it can be estimated and monitored via SOC techniques. The charge and discharge rate. The charging and discharging rate restrictions are then determined using equation (3.51-3.54). When the SoC reaches its maximum storage capacity (SoC = maximum SoC), the discrete solar PV power follows the EMS's mode recommendations. The energy constraints are kept between 20% and 80% on the battery SoC, which will improve battery health and lifespan. The starting battery energy, Emax, is computed with a 50% SoC assumption for the ideal situation. However, in this proposed grid, a battery with the lowest 10% SoC energy is employed, allowing any extra saved energy to be transferred into the grid-tied transmission bus as needed.

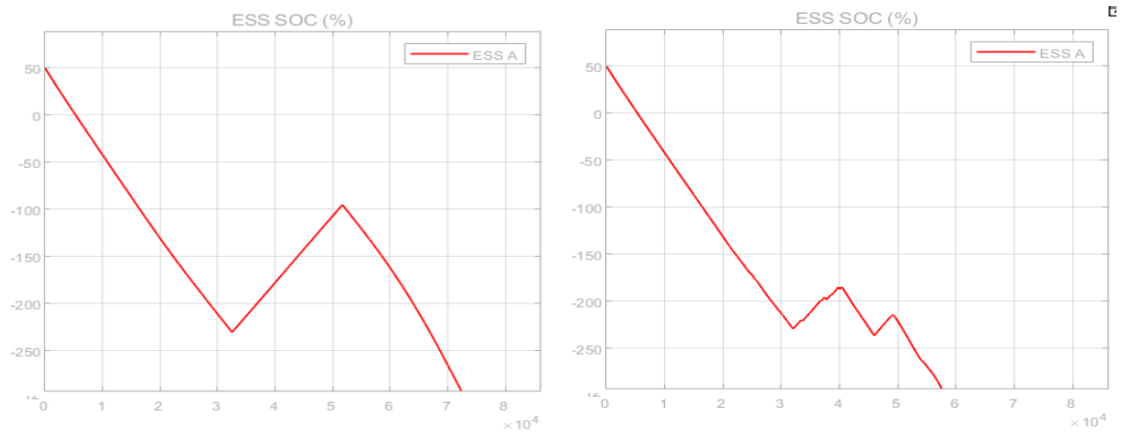

(a) (b)

Figure 3.3. ESS SOC% simulation: (a) battery energy loss during clear days in the heuristics method simulation; (b) energy availability increases with peak during cloudy days in the optimal approach.

The author modified the work of (Velamuri, et. al., 2025; Xinyang et al., 2021; Meryeme et al., 2022) on the grid-tied solar PV and grid patterns hybrid energy systems operational behavior and co-optimization approach (EPD & EMS), using the following data (Vrms =5000 Figure 3.4), 60 Hz, with an initial power of 10 MW) in a MATLAB environment using the FMINCON algorithm. The operational cost over a 24-hour schedule with solar PV rms = 6600, phase angle = 0.007, beginning power 10 MW. ESS capacity = 25000 kwh, the minimum discharge rate of Pmin = 400 kw, and the maximum charge rate of Pmax = 400 kWh both in the negative and positive. battery capacity is 3.6 MW, SOC range between 20% and 80%.

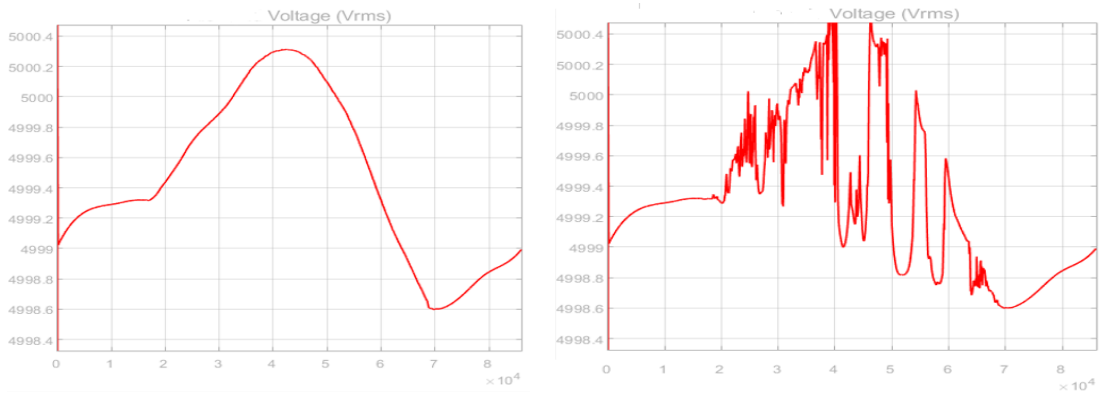

(a) (b)

Figure 3.4. Voltage simulation: (a) less than 5000 V battery energy during clear days in the heuristics method simulation; (b) more than 5000V peak energy availability during cloudy days in the optimal approach.

The of grid electricity cost is the model cost after optimization, whereas the consumer baseline cost is tariff if no optimization is done. The tariff specifies the load grid purchased power and ESS. Figures 3.6 and 3.6 show the cost-savings computations. The optimal system size is: Npv (Solar PV power) = 6600 Watts, Ngrid (Grid load power) = 6600 Watts and EbattV (Battery voltage) =6600

with the LGS – loss of grid supply = 0.017% and,

COESS – cost of energy storage system = $594.00

Compute in 0.19 s

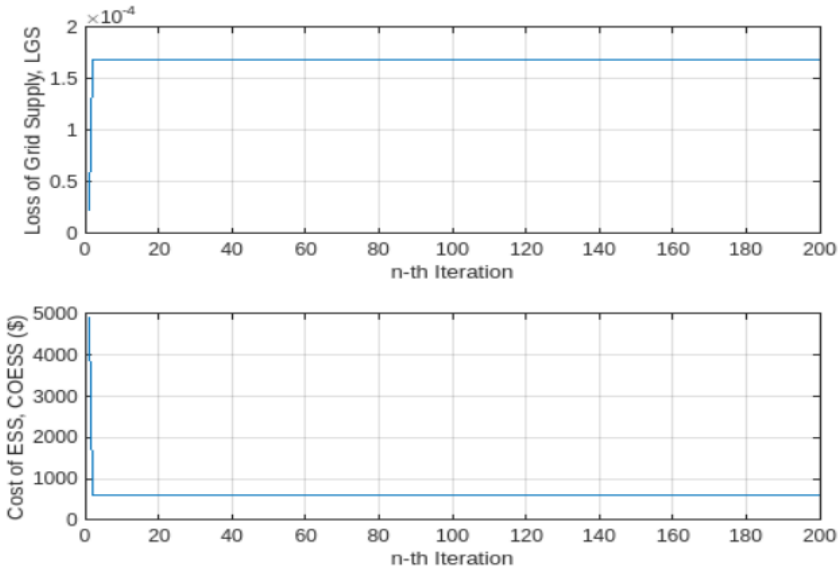

Figure 3.5. Grid cost simulation: (a) loss of grid supply and cost of ESS

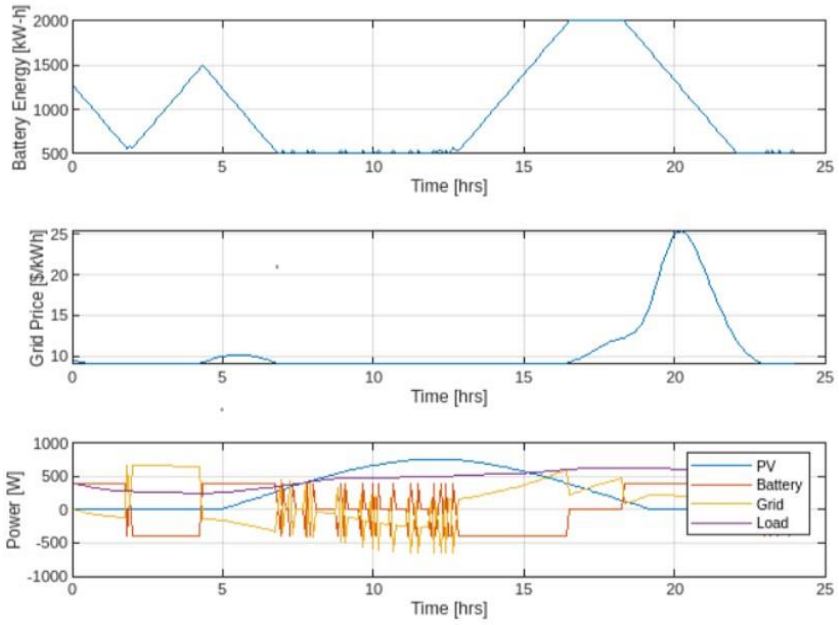

Figure 3.6. MINLP cumulative grid cost and usage simulation approach

The committed RESs unit's energy management results of in EVCSs load demand are presented in Figure 3.7. Prioritizing RESs usage due to low marginal costs is higher and possible when solar PV generation can supply EVCS loads from 06:00 to 19:00 hours. In this instance, wind turbine power is switched off, and no energy dispatch from the grid. When marginal costs of WTs are higher than the grid electricity price, power demands will be from the grid, as shown in EVCS loading diagram, from 0:01 to 6:00 hours in the Figure 3.8.

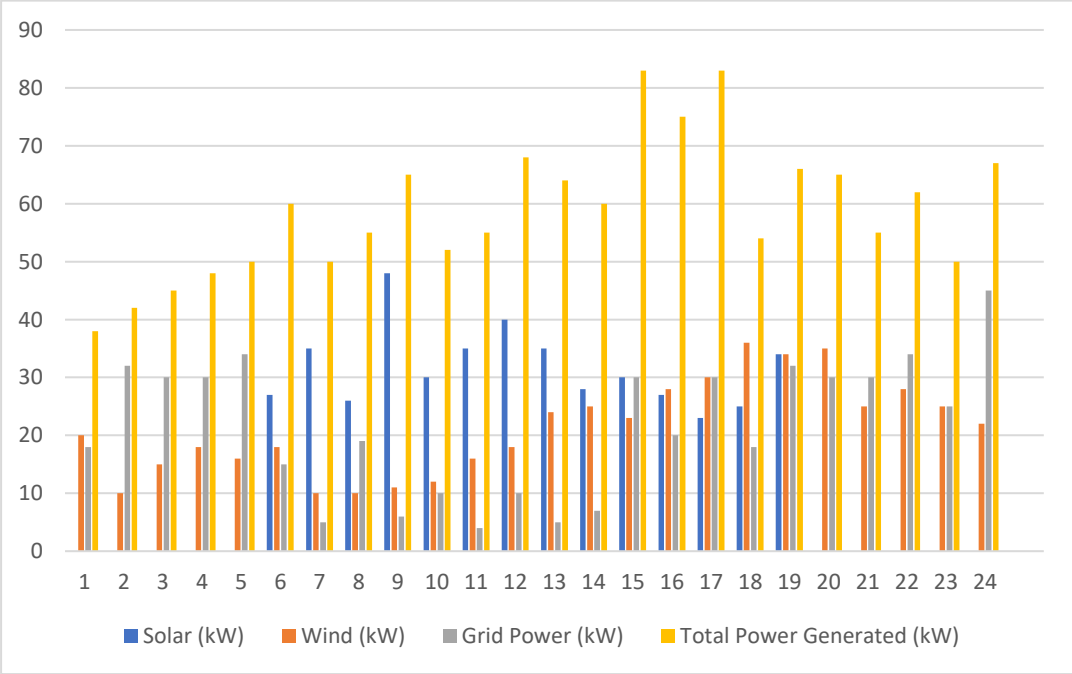

Figure 3.7. Energy management strategies of grid-tied HS

In its place, with higher electricity prices from the grid, the WTs will supply EVCS load before obtaining power from the grid. WTs will be at full capacity from 15:00 to 05:00 due to the higher availability.

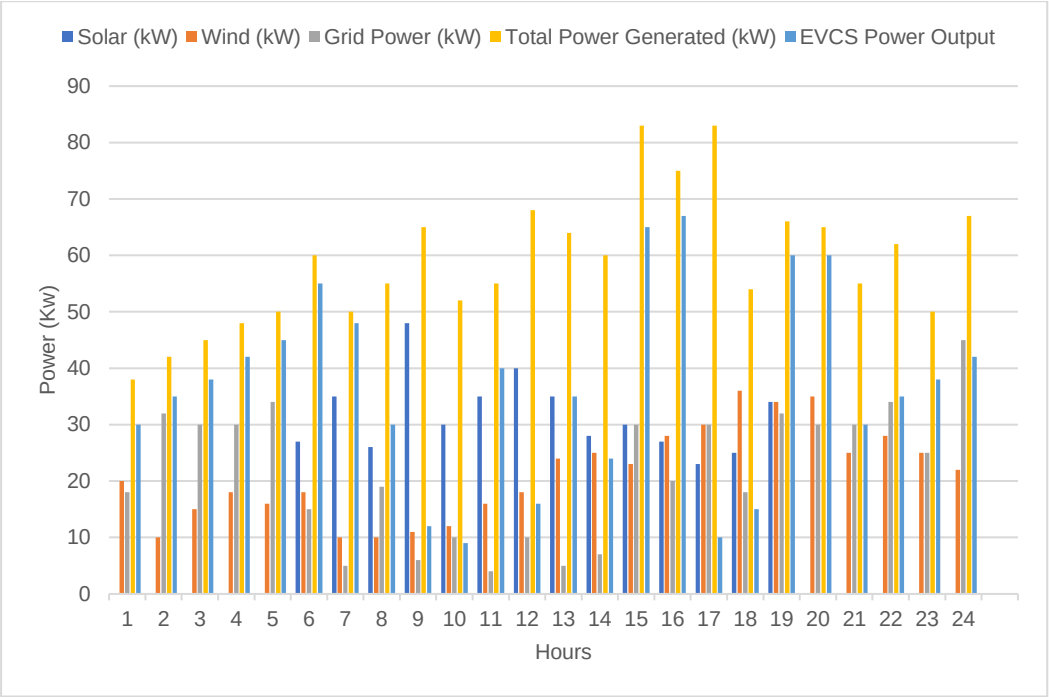

Figure 3.8. Grid-tied HS Energy management at EV charging station loading

3.4 Chapter Summary

In this chapter, the MINLP classical technique is used to develop hybrid system EMSs for grid-tied RES. The FMINCON approach is used in MATLAB simulation to resolve the hybrid system EMS's supply and demand mismatch of a grid-tied renewable energy system. The accepted method is significant in the context of RES self-consumption methods, as it uses a baseline method that considers operational costs, battery SOC charge, and recharge rate. Based on the simulation results, the proposed EMS optimization proved effective in lowering the costs of the grid-connected RES hybrid system while improving self-consumption of renewable energy sources. The created MINLP classical approach effectively demonstrated an essential cost reduction using the baseline line strategy. The proposed methodology considerably enhances the self-consumption of renewable energy. Simulated grid-connected, solar PV-based energy management systems were shown. Energy management systems were used to demonstrate grid-tied renewable energy systems under MATLAB-simulated weather conditions with seasonal changes for optimal solar PV and grid output.

.

CHAPTER FOUR

PSO METHOD FOR ECONOMIC POWER DISPATCH PROBLEM OF A GRID-TIED RES-BASED-HS SYSTEM

4.1 Introduction

Economic power dispatch is a significant segment of power system's continuous operation and scheduling. EPD produces energy at the lowest cost considering operational limits concerning generation and transmission. This chapter solves the EPD problem with the PSO algorithm. The literature (Sit et al., 2022), (Zhou et., 2021), (Fu et al., 2019) and (Suresh and Suresh, 2015), solve EPD problems by minimizing both fuel costs and emissions using combinatorial energy management system, case studies, and artificial intelligence algorithm (AIA) where the combined solution is given by the co-optimization and validated on a standard IEEE bus distribution testbed. Different power system network cost analysis variabilities are interconneed with RES-based hybrid system are mentioned in the literature as solar PV, wind turbine, fuel cell, and biogas regarding EMSs of HS (explained in Chapter 3), and they are now employed to solve the EPD problem. Until now, the literature on PSO and hybrid PSO methods application for EPD has exclusively used the cost coefficient functions for conventional thermal units, but renewable energy sources uncertainty cost function inclusion is rare. This chapter recommends using the quadratic uncertainty cost coefficient function for renewable energy with or without RESs, in addition to formulating and solving the EPD issue using the PSO method. The impact of RES uncertainty cost function factors on the solution of the EPD problem is evaluated using IEEE 14-bus, IEEE 30-bus and IEEE 118-bus distribution testbed case study. This chapter describes economic power dispatch problem in section 4.2, PSO model formulation for solving the EPD problem in section 4.3, EPD problem with a fuel cost objective function in section 4.4, and f the developed PSO method application for solving the EPD are presented in section 4.5 with section 4.6 as conclusions.

4.2 Economic Power Dispatch Problem

The power system's economic challenges depend on key problems which hinge on power dispatch and power flow. This chapter addresses the economic power dispatch. required to find out the generating plants that are better to use in the planning of electricity supplies to customers. RESs integration in electricity generation matrices is essential to be included in the economic power dispatch planning. Though RES supply is uncertain, so are the quadratic cost functions employed in economic power dispatch. However, the

non-inclusion of quadratic cost functions for renewable energy is rare while the study of uncertainty costs for renewable generation is due to their inherent stochastic nature and their application on economic power dispatch.

4.3 Particle Search Optimisation Model Formulation EPD Problem

Economic power dispatch was primarily adopted with equal incremental costs, transmission loss and penalty elements were introduced later (Hasibuan et al., 2021). PSO, DE, GA, and EP are instances of intelligent techniques used to tackle complex dispatch difficulties involving valve points, prohibited zones, and quadratic cost functions (Roy and Das, 2021). For entire transmission and distribution systems, incorporating RESs for energy supply without interfering with distribution operation scheme and economically workable. Joint supply side and load side controller have been proposed in the literature to aid grid systems power balance and frequency regulation (Silva, et al., 2022; Kusakana, 2015). The liberalization of the energy market creates new forms of competition and paradigm shifts in the process of producing electricity. Then, in terms of energy contribution to total electric power generation, distributed generation has piqued the curiosity of many. The concept of microgrids is now emerging as a natural replacement for traditional electric power systems, with large synchronous generators in remote locations accompanied by smaller generators and shorter transmission lines close to the loads, providing an efficient and sustainable alternative for fully utilizing renewable energy (Silva, et al., 2022). Microgrids can use both traditional generators (e.g., thermal generators or diesel engines) and renewable energy source generating units. It is critical to remember that the operations of RES projects are unpredictable and subject to disturbances, making it difficult to determine the best dynamic solution to an economic dispatch problem (Pandey et al., 2022). For physically confined new-generation and conventional systems, energy management in grids looks to maximize the anticipated system's objective function cost efficiency, and dependability. RES connectivity to large energy systems acts as a technological solution for restraining deficiency or excess generated energy in grids while accounting for capacity changes (Pandey et al., 2022; Xu et al., 2022). These studies frequently neglect the transmission system structure at the grid bus level, instead focusing on distribution system dynamics by treating load buses as mobile nodes. With fewer transmission-level studies during the last ten years, much more effort has been put into optimizing RESs in distribution networks. Several approaches have been presented to successfully coordinate RESs loss minimization, dispatch signal, and so on (Iweh et al., 2021). Kempener et al., 2013 indicated that smart grids adoption is economically feasible over conventional systems, considering renewable grid injection and any grid optimization requirements. Grid

reforms required manageable renewable energy, such as low, medium, and high with numerous studies concentrating on a distinctive RES problem regarding their integration into the grid. Several studies were conducted on the co-optimization of transmission and energy management systems. In (Bhattacharyya et al., 2016), models for transmission and distribution networks with RESs are provided, and a multi level technique is proposed to address each layer subproblems in turn. (Peres et al., 2021) proposes a coordinating strategy based on resolving the related subproblems for both levels.

4.4 Economic power dispatch problem with a fuel cost objective function

The EPD formulation is to determine the generation unit dispatch to minimize the immediate operating cost, subject to total generation minus total load plus losses constraints. The EPD objective function can be formulated as,

$$\text{Minimize } F_c = \sum_{t=1}^{N_G} F_i\,(P_{Gi}) = \sum_{t-1}^{N_G}\left(aP_i^{\,2} + b_iP_i + c_i\right)\,[\$/hr] \tag{4.1}$$

Where

F_c= Total Fuel Cost

$F_i(P_{Gi})$ = Fuel cost of the generator

P_i = Real power generation of unit i

a_i, b_i, c_i = Cost coefficients of generating for unit i

N_G = Number of generating units

Subject to the following constraints

1. Power balance

$$\sum_{t=1}^{N} P_i = P_G = P_D + P_L\,[MW] \tag{4.2}$$

where

P_G = Entire system Power generation

P_D = Entire system Power demand

The expression for transmission loss is,

$$P_L = \sum_{i=1}^{N}\sum_{j=i}^{N} P_{i,}B_{i,j}P_j + \sum_{i=1}^{N} B_{0i,}P_i + B_{00}\,[MW] \tag{4.3}$$

Where

P_i = Active power generation of unit i

P_j = Active power generation of unit j

$B_{i,j}, B_{0i,}, B_{00}$ = Transmission loss coefficients

2. Generator operational constraints

$$P_{i,min} \le P_i \le P_{i,max}, p = \overline{1,n} \qquad [MW] \tag{4.4}$$

where

$P_i\,, min$ = Real power minimum value at generator i

P_i, max = Real power maximum value at generator i

A multiobjective optimisation conversion into a single objective problem via introduction of renewable energy sources uncertainty cost coefficient function is.

$$F_T = \sum_{i=1}^{T}(\sum_{g=1}^{N_G}(aP_{Ui}{}^2 + b_{Ui}P_{Ui} + c_{Ui}) + (aP_{ri}{}^2 + b_iP_{ri} + c_{ri}) + (aP_{vi}{}^2 + b_iP_{vi} + c_{vi}) + (aP_{mi}{}^2 + b_iP_{mi} + c_{mi}) + E_{batt} + \gamma \quad (4.5)$$

F_T = EPD fuel cost

P_{Ui} = Real power generation of conventional generators

P_{ri} = Real power generation of grid transmission line spinning reserve

P_{vi} = Real power generation of solar PV generators

P_{mi} =Real power generation of wind turbine generators

E_{batt} = Battery model equation

γ = Percentage renewable-based penalty requirement on grid transmission line

4.4.1 PSO's method for the solution of the economic power dispatch

The method for the EPD solution using the PSO algorithm solves the aforementioned difficulty by mapping the EPD structure in equations (4.1) and (4.2) for position and velocity. The process is as follows:

- It is acknowledged that generators number is equivalent to individual's number within a distinct swarm particle. The particle positions of the members represent the active generated power by the dispatch generators.
- Although they are utilized to conduct searches in the constraint's domain, the variable velocities have active power connotation.
- Presumably, the swarm has Np particles in total. Equations (4.1) to (4.4) provide the developed PSO method for solving economic dispatch.

The first stage is to model EPD, which should include "cost" and "zero plant", specified in the preceding section. To model EPD, combine data from algorithms must prioritize recognizing forbidden zones, UR, and DR. It's crucial to include this section as a key component of the model's limitations. In the second stage, the B matrix and plant attributes are required for the algorithm. Each plant's cost is independent of its power cost, with one utilized for internal PSO and the other for external PSO of EPD. Modelling yields two parse solutions: external and internal, which can be used in distinct cost functions. Parsing solution mentioned in the preceding section can be represented as the following codes.

The iteration procedure's first step begins at I=1.

Step 1: Set the PSO initial values for the parameters, including maximum iterations number, uniform random values rand1, rand2, and inertia weight max and min. Itermax

Step 2: Using generator restriction limits in equation (4.6), determine the lowest and maximum initial velocities, which are provided in Equation (4.7) as follows:

$$-0.5P_{pi}^{min} \leq V_{pi} \leq +0.5P_{pi}^{max}, p = \overline{1, N_p}, i = \overline{1, n-1} \quad (4.6)$$

Where

Np Swarm particles number

n Members number in one particle and equal to entire generators.

Because one generator is assumed as a slack one, particle velocity calculation and there is (n-1) generators location.

Step 3: Using equation (4.5), initial velocity is computed for each particle excluding the slack bus.

$$V_{pi} = V_{pi}^{min}\, rand\,()\left(V_{pi}^{max} - V_{pi}^{min}\right), p = \overline{1, N_p}, i = \overline{1, n-1} \quad (4.7)$$

Where

$V_{pi}^{min}, V_{pi}^{max}$ previously computed velocity minimum pi and maximum pi.

Step 4: Calculate initial particle position of the members using equation (4.7)

$$P_{pi} = P_{pi}^{min}\, rand\,()\left(P_{pi}^{max} - P_{pi}^{min}\right), p = \overline{1, N_p}, i = \overline{1, n-1} \quad (4.8)$$

The estimated position falls within the restrictions indicated by equation (4.4), as described.

$$P_{pi} = \left\{ \begin{matrix} P_{pi}^{min}, P_{pi} \leq P_{pi}^{min} \\ P_{pi}^{max}, P_{pi} \leq P_{pi}^{max} \\ P_{pi}, P_{pi}^{min} \leq P_{pi} \leq P_{pi}^{max} \end{matrix} \right\}, p = \overline{1, N_p}, i = \overline{1, n-1} \quad (4.9)$$

The power system buses are categorised as:

(i) slack buses,

(ii) generator buses (solar PV), and

(iii) load buses.

In a categorised system, any bus connected to a generator with the maximum power generation capability is referred as slack bus, which bus serves as voltage and angle reference for real and reactive powers. The slack bus is unregulated; it provides whatsoever real or reactive power that is required to balance system's power flows. The generation scheduling is done to solve the economic dispatch, without considering the real power of the slack bus generator. PSO algorithm meets the power balance condition in the specified slack bus in equation (3.2). Step 5 explains how to use the PSO algorithm to calculate the slack bus generator's true power.

Step 5: The generator on the slack bus is considered a reliant on highest power-generating capacity generator. The bus voltage size and phase angle are quantified as references and the power balance constraint (Kothari and Dhillon, 2011) are calculated by initial active power P_{pd} as follows.

Where

$$P_{pd} + \sum_{\substack{i=1 \\ i\neq d}}^{n} P_{pi} = \left[\sum_{\substack{i=1 \\ i\neq d}}^{n}\sum_{\substack{j=1 \\ j\neq d}}^{n} P_{pi}B_{ij}P_{pj} + \sum_{\substack{j=1 \\ j\neq d}}^{n} P_{pj}\left(B_{jd}+B_{dj}\right)P_{pd} + B_{dd}P_{pd}^{2} + \sum_{\substack{i=1 \\ i\neq d}}^{n} B_{io}P_{pi} + B_{do}P_{pd} + B_{oo} + P_{D}\right], p = \overline{1, N_p} \quad (4.10)$$

Where

P_{pd} is the slack bus power produced by the generator

P_D is the entire system power demand

$\sum_{\substack{i=1 \\ i\neq d}}^{n} P_{pi}$ is the entire active power excluding the slack bus

Equation (4.10) conversion to quadratic form, where unknown variable P_{pd} is:

$$XP_{pd}^{2} + YP_{pd} + Z = 0 \quad (4.11)$$

Where

$$X = B_{pd} \quad (4.12)$$

$$Y = \sum_{\substack{i=1 \\ i\neq d}}^{n}\left(B_{jd}+B_{dj}\right)P_{pd} + B_{do} - 1 \quad (4.13)$$

$$Z = P_D + B_{oo} + \sum_{\substack{i=1 \\ i\neq d}}^{n}\sum_{\substack{j=1 \\ j\neq d}}^{n} P_{pi}B_{ij}P_{pj} + \sum_{\substack{i=1 \\ i\neq d}}^{n} B_{io}P_{pi} + \sum_{\substack{i=1 \\ i\neq d}}^{n} P_{pi} \quad (4.14)$$

Equation (4.11) positive root is derived as follows:

$$P_{pd} = \frac{-Y+\sqrt{Y^2-4XZ}}{2X}, where\ Y^2 - 4XZ \geq 0 \quad (4.15)$$

Now, real vector power is created as $P_p = \left[P_{pd,}P_{pi,}i = 1, n, i \neq d\right]$ while $p = \overline{1, N_p}$

Step 6: Calculating the particles' initial positions objective functions.

i) Thermal generator cost function,

$$F_{Cp} = \sum_{t-1}^{\mathrm{n}}\left(aP_i^{\,2} + b_iP_i + c_i\right)\ [\$/hr]\ \ p = \overline{1, N_p} \quad (4.16)$$

Introducing RES cost function into conventional thermal cost function,

$$F_{Tp} = \sum_{i=1}^{T}\left(\sum_{g=1}^{N_G}\left(aP_{Ui}^{\,2} + b_{Ui}P_{Ui} + c_{Ui}\right) + \left(aP_{ri}^{\,2} + b_iP_{ri} + c_{ri}\right) + \left(aP_{vi}^{\,2} + b_iP_{vi} + c_{vi}\right) + \left(aP_{mi}^{\,2} + b_iP_{mi} + c_{mi}\right),\ p = \overline{1, N_p} \quad (4.17)$$

Cost values F_{Tp} for all particles is arranged in increasing command. The first number in the command is chosen as the best T.

Step 7: Select the initial best position and initial best global position as follows:

i) The initial particles positions in the swarm are regarded as the optimal positions $P_p{}^{\text{best}} = min\ P_p{}^{\text{best}}, i = \overline{1, N_p};\ p = \overline{1, N_p}$

ii) The optimal position among the best particles. $min\ P_p{}^{\text{best}}, p = \overline{1, N_p}$ is taken

$$G_p{}^{\text{best}} = G_p{}^{\text{best}}, p = \overline{1, N_p}$$

i^{th} iteration step procedure begins, where *I = I+1*

Step 8: Use equation (4.17) to calculate new velocity

$$V_{pi}^{new1} = \omega . V_{pi}^{I-1} + c1 . rand1\left(P_p^{bestI-1} - P_{pi}^{I-1}\right) + c2 . rand2\left(G^{best1-1} - P_{pi}^{I-1}\right),$$
$$p = \overline{1, N_p}, i = \overline{1, n-1} \quad (4.18)$$

The velocity's constraint minimum value at generator i and maximum value value at generator i.

$$V_{pi}^{newI} > V_{pi}^{maxI-1}, V_{pi}^{newI} = V_{pi}^{maxI-1} \text{ and}$$

$$\text{If } V_{pi}^{newI} > V_{pi}^{maxI-1}, V_{pi}^{newI} = V_{pi}^{maxI-1}, p = \overline{1, N_p}, i = \overline{1, n-1} \quad (4.19)$$

Step 9: Calculate the generators new position in the particles using equation (4.18).

$$P_{pi}^{newI} = V_{pi}^{I-1} + V_{pi}^{newI}, p = \overline{1, N_p}, i = \overline{1, n-1} \quad (4.20)$$

Step 10: Use constraint equation (4.9) to determine the generators new position in the particles.

$$P_{pi}^{newI} = \left\{ \begin{matrix} P_{pi}^{min}, P^{newI} \leq P_{pi}^{min} \\ P_{pi}^{max}, P^{newI} \leq P_{pi}^{max} \\ P^{newI}, P_{pi}^{min} \leq P^{newI} \leq P_{pi}^{max} \end{matrix} \right\}, p = \overline{1, N_p}, i = \overline{1, n-1} \quad (4.21)$$

Step 11: Calculate the generator's slack bus new real power. From the real power, P_{pd}^{I}vector based on Step 5 equations. Check the slack bus generator new position in the particles using equation (4.23) as constraint:

$$P_{pd}^{newI} = \left\{ \begin{matrix} P_{pd}^{min}, P^{newI} \leq P_{pd}^{min} \\ P_{pd}^{max}, P^{newI} \leq P_{pd}^{max} \\ P^{newI}, P_{pd}^{min} \leq P^{newI} \leq P_{pd}^{max} \end{matrix} \right\} \quad (4.22)$$

Step 12: The lth iteration vector entire active power is:

$$P_p^{newI} = \left[P_{pd}^{newI}, P_{pi}^{newI}, i = \overline{1, n}, i \neq d\right],\ p = \overline{1, N_p} \quad (4.23)$$

Step 13: Calculate the new functions, F_T^{new}, from Step 6.

Step 14: Check the new function F_T^{new}, which is defined as

$$\text{If } F_T^{newI} < F_T^{bestI-1}\ then\ F_T^{bestI} = F_T^{newI}\ and\ F_{pi}^{bestI} = P_{pi}^{newI}$$

$$\text{Else } F_T^{bestI} = F_T^{bestI-1}\ and\ P_{pi}^{newI} = P_{pi}^{besti-I} \quad (4.24)$$

$G_{pi}^{bestI} = P_p^{bestI}, p = \overline{1, N_p}$

where i represents iterations number.

The best solution, Gbest is only one for the entire system.

The best solution for each particle is $P_p^{best} = \min P_{pi}, \ i = \overline{1, n}$

The best solution for the entire system is $P_p^{best} = P_1^{best}, P_2^{best} \ldots \ldots, P_{Np}^{best},$

Then $\text{Gbest} = \min P_p^{best}, \ for \ p = \overline{1, Np}$

Step 15: Repeat steps 5, 8, and 13 until the iterations maximum number is reached.

The flowchart of the PSO method is shown in Figure 4.1.

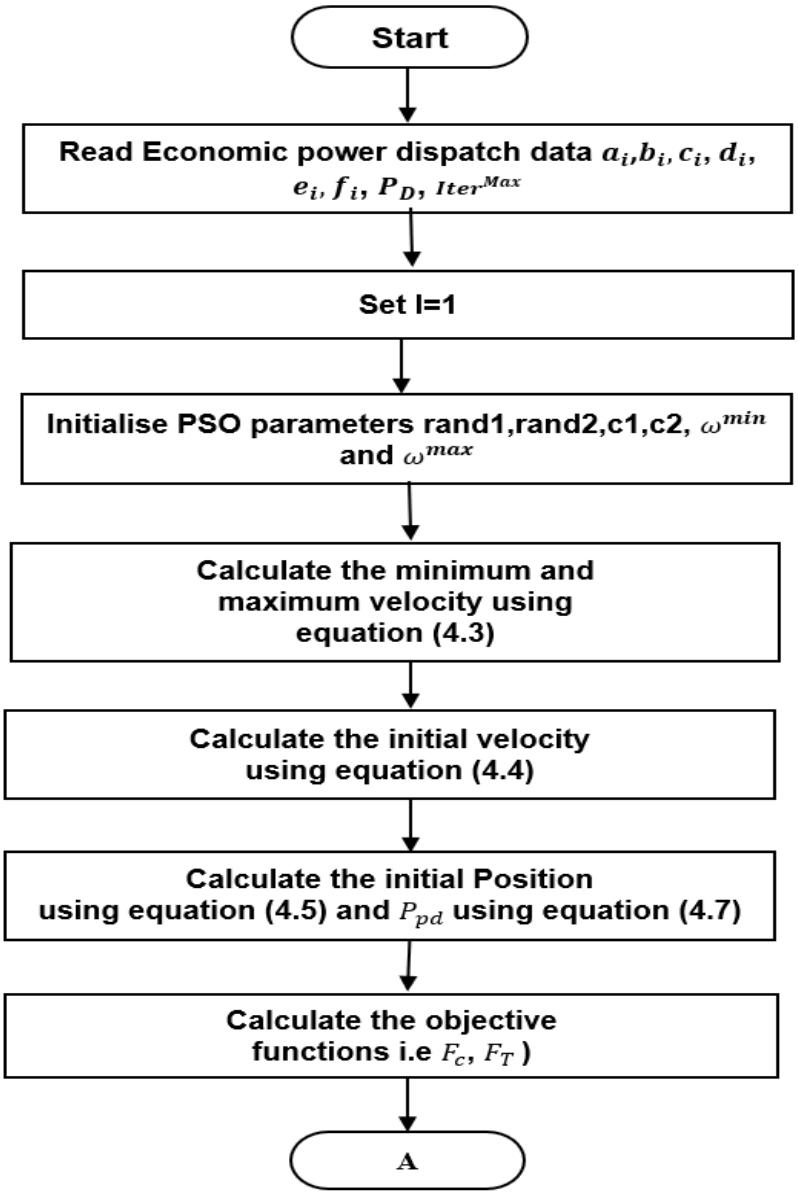

Figure 4.1. Flowchart for EPD problems solution using PSO method

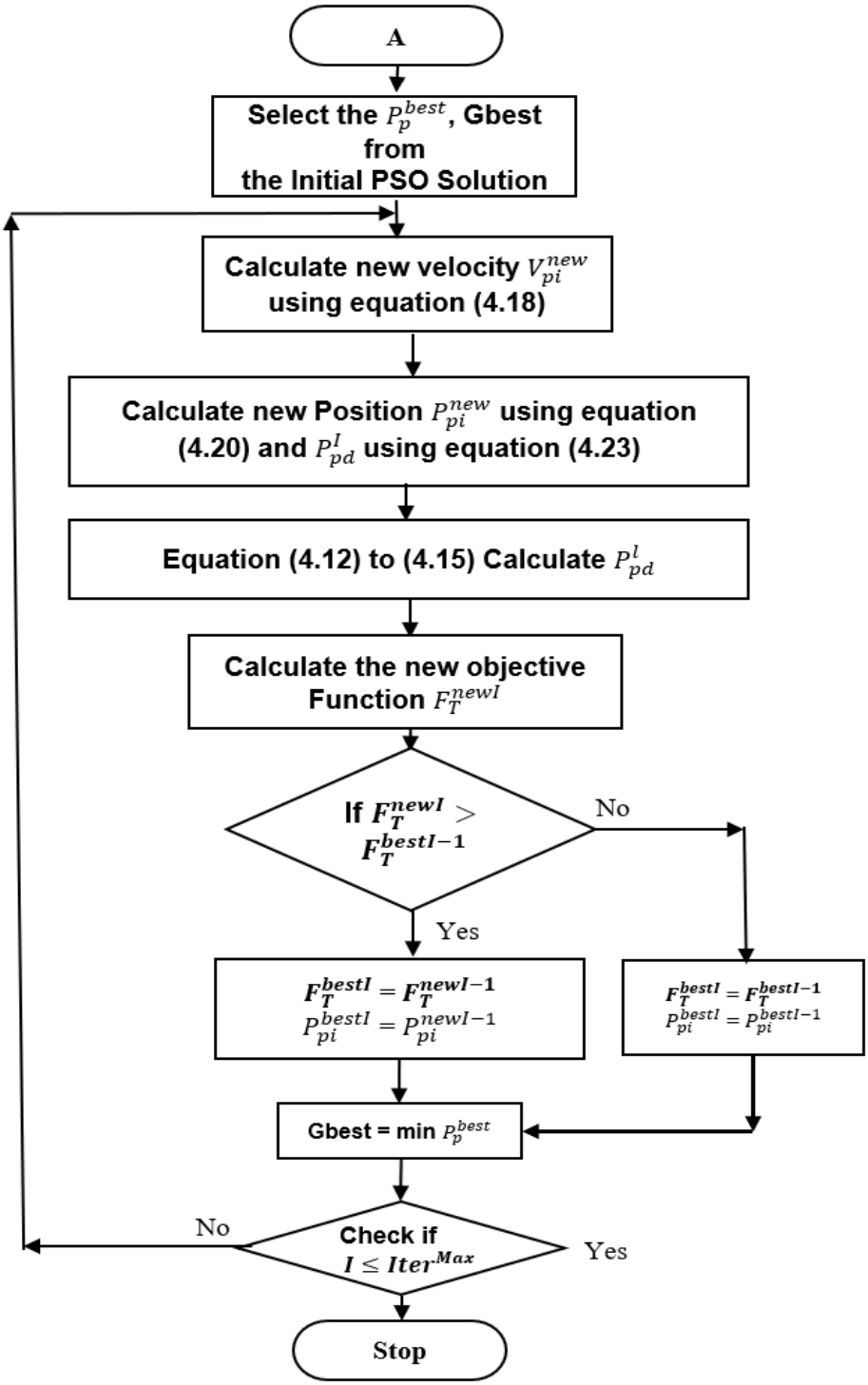

Figure 4.2: Flowchart for EPD problems solution using PSO method continuation

4.4.2 PSO Algorithm Steps to solve EPD problems (Heris, 2016)

Step 1 - Problem definition

- Z=F(X) = P=PminActual +(PmaxActual minus PminActual). *x
- Create a parse.m function, P=ParseSolution(x,model).

- Input Pmin = model.Plants.Pmin; Pmax = model.Plants.Pmax; and P = Pmin + (Pmax - Pmin).*x; PZ=model.Plants.PZ; nPlant=model.nPlant; for i=1:nPlant; forj=1:numel(PZ{i})if P(i) > PZ{i}{j}(1) && P(i) < PZ{i}{j}(2)% Correction
- Create a model for 3, 6, and 15 committed generator variables, with uniformly random distributions of Pmin, Pmax, alpha, beta, gamma, P0, UR, DR, transmission loss, and over X (position).
- Developed CostFunction -@(x) MyCost (x, Model).
- Develop a model calculation. C=alpha+beta.*P+gamma.*P.*P, PL=P*B*P'+B0*P'+B00;
- Decision variables nVar = Model. nPlant (lower and upper limits for 3, 6, 15 units) Committed generator variables

Step 2 - PSO Parameters

- MaxIt - number of iterations; nPop - swarm size; Constriction Coefficient (C1 = chi*phi 1 as personal coefficient, C2 = chi*Phi 2 as global coefficient); Velocity Limit.

Step 3 - Initialisation

- BestSol.Cost = inf; for i=1; nPop, initialize position and velocity;
- Evaluate each generator's cost model based on the objective function value.
- Z=F(X) = P=PminActual+(PmaxActual-PminActual). *x; with or without prohibited zones.
- Evaluate; update personal and global bests; BestSol = Particle(1)'Best.

Step 4 - PSO Main Loop

- For i=1, use It-1 and MaxIt to update velocity, apply velocity limits, update position, apply position limits, evaluate, and update personal best.
- Run PSO Matlab routines by calling functions for issue creation, PSO parameters, constriction coefficients, velocity limits, particle initialization, position, and evaluation, as well as updating personal best and global 'Best Cost'.
- Results: Plot (Best Cost, x and y labels)
- Update generator velocities.
- Move particles to their new positions using CostFunction(particle(i).Position);
- If the current position of all generators is better than the prior best position, update the value particle(i).Cost<particle(i).Best.Cost
- Find the best generator update. BestCost(it)=BestSol

4.5 Developed PSO Method Application for solving EPD problem.

The proposed economic power dispatch is resolved for the IEEE 14-bus distribution testbed (Kennedy and Eberhart, 1995; Yoshida et al., 2000; Heris, 2016;) and IEEE 30-bus distribution testbed (Gaing, 2003; Krishnamurthy and Tzoneva, 2012; Heris, 2016; Al-Roomi, 2016).

4.5.1 Test system 1: IEEE 14-bus, IEEE 30-bus and IEEE 118-bus distribution testbed with 3, 6, and 15 generator units using zero RESs cost coefficients.

The EPD simulation includes coal thermal unit's data from South Africa's energy company (Eskom) as well as from South Africa Solar PV Installation Company's website. The power demand for 850MW, 1263MW, and 2630MW IEEE 14-bus, IEEE 30-bus and IEEE 118-bus distribution testbed respectively, with external PSO having 2 maximum iterations for and internal PSO is 100. The thermal generated power cost functions were based on plant input-output features obtained from the literature, whereas solar PV plant input-output is free of charge. The anticipated expenses are the operating costs that are the focus of this research. In the simulation, MATLAB 2020b was used to program the PSO algorithm, which runs on Windows 10 and Intel Core i7. Two unimodal functions and multimodal functions each were applied to minimize objective function via maximum iteration transformation into a value of 200. The EPD problems with modifying load demand and generating unit numbers are examined using 3-units, 6-units, and 15-units case studies scenarios. without. The following cases for all thermal generators and solar PV units' generation zero coefficient values are presented:

4.5.1.1 Case 1: 3-unit generator demand of 850 MW

The 3-unit generator system case study of 850 MW load demand data (Gaing, 2003) was simulated. In minimal circumstances, the swarm's ability does not call for numerous particles to identify the best solution; though, in maximal circumstances, rapid space increases call for numerous particles explored to accurately identify the best solution issue. Table 4.1 shows PSO for EPD with the intended ramp-down and ramp-up limits restrictions, with banned zone creation. Figure 4.3 illustrates convergence feature approaches.

Table 4.1. IEEE 14-bus cost coefficient data of 3-Unit testbed (Heris, 2016; Kennedy and Eberhart, 1995; Yoshida et al., 2000)

Bus Number	Generator limits [MW]		Fuel cost coefficients without RESs			Fuel cost coefficients with RESs		
	P_{max}	P_{min}	a_i [\$/MW^{2}h]	b_i [\$/MWh]	c_i [\$/h]	a_i [\$/MW^{2}h]	b_i [\$/MWh]	c_i [\$/h]
1	100	600	561	7.92	0.0016	561	7.92	0.0016
2	100	400	310	7.85	0.0019	0	0	0
5	50	200	78	7.97	0.0048	78	7.97	0.0048

Transmission loss coefficients					
B_{01}			B		
0.01890	-0.00342	-0.007660	0.0002940	0.0000901	-0.0000507
			0.0000901	0.0005210	0.0000953
B_{00}=0.000014			-0.0000507	0.0000953	0.0006760

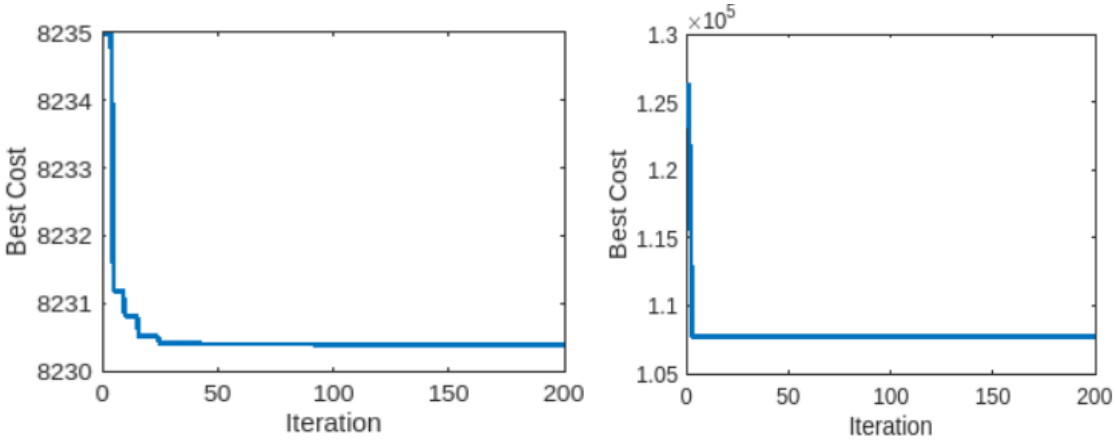

(a) (b)

Figure 4.3. 3-Unit testbed simulation for EPD (best cost) (a) minimum cost (best cost) 3 thermal units convergence; (b) minimum cost (best cost) 2 thermal and 1 solar PV units convergence.

4.5.1.2 Case 2: 6-unit generator demand of 1263 MW

The 6-unit generator case scenario of 1263 MW load data demand uses a B-loss coefficient from Ref. (Gaing, 2003). The IEEE 30-bus testbed consists of 26 buses and 46 transmission lines for 6x100 thermal and RESs units (Yoshida et al., 2000). Table 4.2 demonstrates the proposed PSO for the EPD evolutionary process applying ramp-up limits ramp-down limits and generator forbidden zones as the primary algorithm model limitation, and parse solution for unit commitment as the main cost function. Each separately performed function has a fitness rating of 99.0, eliminating unpredictability in the algorithm. The graphic illustrates a sampling of the restricted zones of the unit number's production factories. Figure 4.4 shows the 6-unit simulation for EPD at the lowest cost (best cost).

Table 4.2. IEEE 30-bus cost coefficient data of 6-Unit testbed (Heris, 2016; Al-Roomi, 2016; Gaing, 2003)

Bus Number	Generator limits [MW]		Fuel cost coefficients without RESs			Fuel cost coefficients with RESs		
	P_{max}	P_{min}	a_i [\$/MW^{2}h]	b_i [\$/MWh]	c_i [\$/h]	a_i [\$/MW^{2}h]	b_i [\$/MWh]	c_i [\$/h]
1	100	500	240	7.00	0.0070	240	7.00	0.0070
2	50	200	200	10.0	0.0095	0	0	0
5	80	300	220	8.5	0.0090	0	0	0
8	50	150	200	11.0	0.0090	0	0	0
11	50	200	220	10.5	0.0080	0	0	0
13	50	120	190	12.0	0.0075	190	12.0	0.0075

Transmission loss coefficients								
B_{01}			B					
-0.3908	-0.1279	0.7047	0.0017	0.0012	0.0007	-0.0001	-0.0005	-0.0002
			0.0012	0.0014	0.0009	0.0001	-0.0006	-0.0001
0.0591	0.2161	-0.6635	0.0007	0.0009	0.0031	0.0000	-0.0010	-0.0006
			-0.0001	0.0001	0.0000	0.0024	-0.0006	-0.0008
B_{00}=0.056			-0.0005	-0.0006	-0.0010	0.0006	0.0129	-0.0002
			-0.0002	-0.0001	-0.0006	0.0008	-0.0002	0.0150

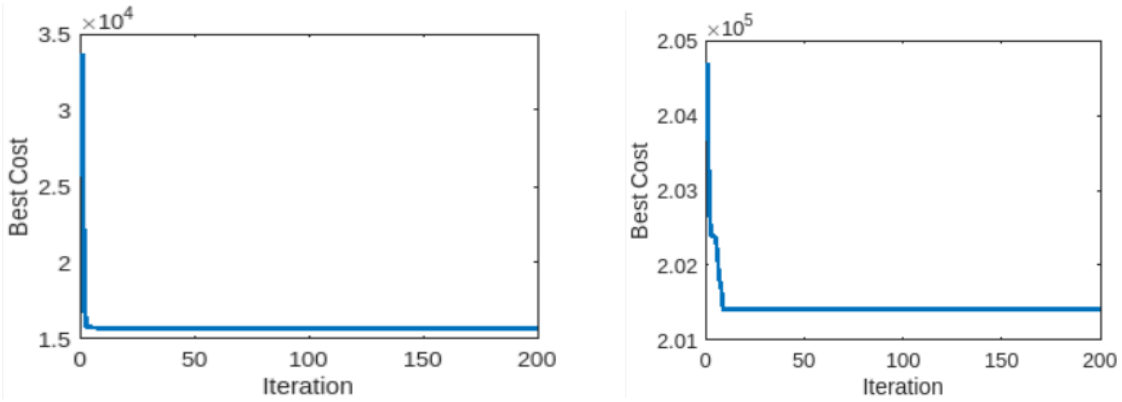

(a) (b)

Figure 4.4. 6-Unit testbed simulation for EPD (best cost) (a) minimum cost (best cost) 6 thermal units convergence; (b) minimum cost (best cost) 2 thermal and 4 solar PV units convergence.

4.5.1.3 Case 3: 15-unit generator demand of 2630 MW

Table 4.3 displays input-output characteristics for 15 thermal units with a population dimension of 15x100 in case 3. Figure 4.5 displays the evolving PSO proposed process for EPD with up-ramp limits and down-ramp restrictions and generators forbidden zones of 15 x 15. Figure 4.5 depicts the 15-unit EPD simulation at the lowest cost convergence. The ideal plant selection is expected to be at the grid operator's discretion to schedule the suitable plants.

Table 4.3. IEEE 118-bus cost coefficient data of 15-Unit testbed (Heris, 2016; Al-Roomi, 2016; Gaing, 2003; Yoshida et al., 2000)

Bus Number	Generator limits [MW]		Fuel cost coefficients without RESs			Fuel cost coefficients with RESs		
	P_{max}	P_{min}	a_i [\$/MW^{2}h]	b_i [\$/MWh]	c_i [\$/h]	a_i [\$/MW^{2}h]	b_i [\$/MWh]	c_i [\$/h]
1	150	455	671	10.10	0.0003	671	10.10	0.0003
2	150	455	574	10.20	0.0001	574	10.20	0.0001
5	20	130	374	8.80	0.0011	0	0	0
4	20	130	374	8.80	0.0011	0	0	0
4	150	470	461	10.40	0.0002	461	10.40	0.0002
5	135	460	630	10.10	0.0003	630	10.10	0.0003
8	135	465	548	9.80	0.0003	548	9.80	0.0003
10	60	300	227	11.20	0.0003	227	11.20	0.0003
25	25	162	173	11.20	0.0008	0	0	0
26	25	160	175	10.70	0.0012	0	0	0
30	20	80	186	10.20	0.0035	0	0	0
37	20	80	230	9.90	0.0055	0	0	0
38	25	85	225	13.10	0.0003	0	0	0
63	15	55	309	12.10	0.0019	0	0	0
64	15	55	323	12.40	0.0044	323	12.40	0.0044

Transmission loss coefficients													
B													
0.0014	0.0012	0.0007	-0.0001	-0.0003	-0.0001	-0.0001	-0.0001	0.0003	0.0005	-0.0003	-0.0002	0.0004	0.0003	-0.0001
0.0012	0.0015	0.0013	0.0000	-0.0005	-0.0002	0.0000	0.0001	-0.0002	0.0004	-0.0001	-0.0000	-0.0004	0.0010	-0.0002
0.0001	0.001	0.0076	-0.0001	--0.0013	-0.0009	0.0001	0.0000	-0.0008	-0.0012	-0.0017	-0.0000	-0.0026	-0.0111	-0.0028
-0.0001	0.0000	-0.0001	-0.0001	0.0034	-0.0007	-0.0001	0.0011	0.0050	0.0029	0.0032	-0.0000	0.0001	0.0001	0.0026
-0.0003	-0.0005	-0.0013	-0.0007	0.0090	0.0014	-0.0003	-0.0012	-0.0010	-0.0013	-0.0007	-0.0002	-0.0002	-0.0024	-0.0003
-0.0001	-0.0002	-0.0009	-0.0004	0.0014	0.0016	-0.0000	-0.0006	-0.0005	-0.0008	-0.0011	-0.0001	-0.0002	-0.0017	0.0003
-0.0001	0.0000	-0.0001	0.0011	0.0003	-0.0000	0.0015	0.0017	0.0015	0.0009	-0.0005	-0.0007	-0.0000	-0.0002	0.0008
-0.0001	0.0001	0.0000	0.0050	0.0012	-0.0006	0.0017	0.0168	0.0082	0.0079	-0.0023	-0.0036	-0.0001	0.0005	-0.0078
-0.0003	-0.0002	-0.0008	0.0029	-0.0010	-0.0005	0.0015	0.0082	0.0129	0.0116	-0.0021	-0.0025	0.0007	0.0012	-0.0072
-0.0003	-0.0004	-0.0017	0.0011	-0.0007	0.0011	-0.0005	-0.0023	-0.0021	-0.0127	-0.0140	-0.0001	0.0004	0.0038	0.0168
-0.0002	-0.0000	-0.0000	-0.0000	-0.0002	-0.0001	0.0007	-0.0036	-0.0025	-0.0003	-0.0001	0.0051	-0.0001	-0.0004	0.0028
0.0004	0.0004	-0.0026	0.0001	-0.0002	-0.0002	-0.0000	-0.0001	0.0007	0.0009	0.0004	-0.0001	0.0103	-0.0101	0.0028

0.0003	0.0010	0.0111	0.0001	-0.0024	-0.0017	-0.0002	0.0005	-0.012	-0.011	-0.0038	-0.004	-0.0101	0.0578	-0.0094
-0.0001	-0.0002	-0.0028	-0.0026	-0.0003	0.0003	-0.0008	-0.0078	-0.072	-0.088	0.0168	0.0024	-0.0028	-0.0094	0.1283
B_{01}														
-0.0001	-0.0002	-0.0028	-0.0001	0.0001	-0.0003	-0.0002	-0.0002	0.006	0.039	-0.0017	-0.0000	-0.0032	0.0067	-0.0064
B00=0.055														

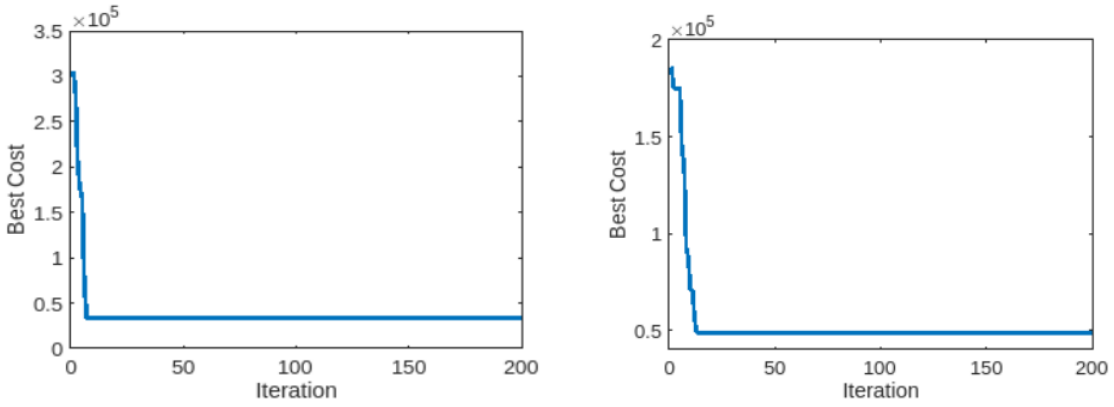

(a) (b)

Figure 4.5. 15-Unit testbed simulation for EPD (best cost) (a) minimum cost (best cost) 15 thermal units convergence; (b) minimum cost (best cost) 7 thermal and 8 solar PV units convergence.

In simple cases, numerous particles are not required to find small scale best answer, but in medium and for large scales, particles number increases the speed and swarm's search precision through issue space. Table 4 lists maximum results obtained using the suggested technique as well as previous findings.

4.5.2 Test system 2: IEEE 14-bus, IEEE 30-bus and IEEE 118-bus distribution testbed with 3, 6, and 15 generator units using Monte Carlo uncertainty cost coefficients for RESs (Mart´ınez, 2018)

Modeling the uncertainty cost function (UCF) as in economic power dispatch may be problematic since the cost function variable utilized in this chapter is determined by the analytical formula for the expected cost of uncertainty mathematically, considering probability distributions for each major RESs. Modeling the availability of primary RESs for these technologies allows for power programming. The generator stochastic tendencies may be different from dispatched real power $W_{av,i}$ and the planned power by system operator $W_{s,i}$. This requires considering the cost of uncertainty through underestimating ($W_{s,i} < W_{av,i}$) or overestimation ($W_{s,i} > W_{av,i}$).

$$UCF = C_{u,i}(W_{s,i}, W_{av,i}) + C_{o,i}(W_{s,i}, W_{av,i}) \quad (4.25)$$

This is done using Monte Carlo simulation (Mendez, 2017) which is accurate in (Ar´evalo et al., 2019) and (Sanchez et al., 2017). The following are the key steps in performing the simulation:

1. A power cost represents the solar generator power i as designed by economic dispatch model $W_{PV.s.i}$. The Monte Carlo simulation yielded an arbitrary irradiance value expressive of uncertainty cost relating to RESs function.

2. A Monte Carlo setting of random irradiance value is created using Log-normal probability distribution for the generator i(G_i).

3. The generated power $W_{PV.s.i}$equations are calculated using random irradiance.

4. The uncertainty cost is estimated as follows: if $W_{PV.s.i} < W_{PV..i}$ then use underestimated condition to; if $W_{PV..i} < W_{PV.s.i}$ then overestimated condition.

5. Steps 2-4 are repeated for set number of Monte Carlo settings.

6. The predicted cost of the entire accrued cost is calculated; which is uncertainty cost function.

7. Steps 1–6 is performed for every possible economic dispatch power cost programmed by the model ($W_{PV.s.i}$).

The quadratic function models provide the best approximation by using the MATLAB tool to program EPD uncertainty cost function while the optimization problem at hand is resolved. The simulation was created to address optimal power flow problems which are predominantly intended for researchers and educators (Mendez, 2017). The uncertainty cost function approximation for solar PV and with the best representation are:

$$f(W_{PV.s.i}) = 0{:}331(W_{PV.s.i})^2 + 33{:}544\,(W_{PV.s.i}) - 918{:}558 \quad (4.26)$$

For inclusion in economic dispatch models, uncertainty cost function must meet criterion.

$$W_{PV.s.i} \geq 25\ [MW] \quad (4.27)$$

With this knowledge, modelling the uncertainty cost function is possible as a polynomial with programmed power as approximated quadratic independent variable (Equation 4.28) for wind turbines as:

$$f(W_{m.s.i}) = 1{:}744\,(W_{m.s.i})^2 + 3{:}643\,(W_{m.s.i}) - 183{:}851 \quad (4.28)$$

Although this function appropriately captures the expected value behavior of uncertainty cost in economic dispatch model's usage might stand impossible or troublesome because the cost functions used in it are similar to the function. This is why the setting of the plant has a dispatched power value $W_{PV.s.i}$ and $W_{m.s.i}$ been offered, as uncertainty cost function may therefore have specific quadratic function and incorporated into the economic power dispatch models.

4.5.2.1 Case 4: 3-unit generator demand of 850 MW with RESs using Monte Carlo uncertainty cost functions

The 3-unit generator of 850 MW case study load demand data (Gaing, 2003) was simulated using Monte Carlo uncertainty cost functions with RESs. In minimal circumstances, the swarm's ability does not call for numerous particles to identify the best solution; though, in maximal circumstances, rapid space increases call for numerous particles explored to accurately identify the best solution issue. Table 4.4 shows PSO for EPD with the intended ramp-down and ramp-up restrictions, with banned zone creation. Figure 4.6 illustrates convergence feature approaches.

Table 4.4. IEEE 14-bus of 3-Unit with RESs cost coefficient data (Heris, 2016; Al-Roomi, 2016; Gaing, 2003; Yoshida et al., 2000)

Bus Number	Generator limits [MW]		Fuel cost coefficients without RESs			Fuel cost coefficients with RESs		
	P_{max}	P_{min}	a_i [\$/MW^{2}h]	b_i [\$/MWh]	c_i [\$/h]	a_i [\$/MW^{2}h]	b_i [\$/MWh]	c_i [\$/h]
1	100	600	561	7.92	0.0016	561	7.92	0.0016
2	100	400	310	7.85	0.0019	918.558	33.544	0.331
5	50	200	78	7.97	0.0048	183.851	3.643	1.744
Transmission loss coefficients								
B_{01}			B					
0.01890	-0.00342	-0.007660	0.0002940		0.0000901		-0.0000507	
			0.0000901		0.0005210		0.0000953	
B_{00}=0.000014			-0.0000507		0.0000953		0.0006760	

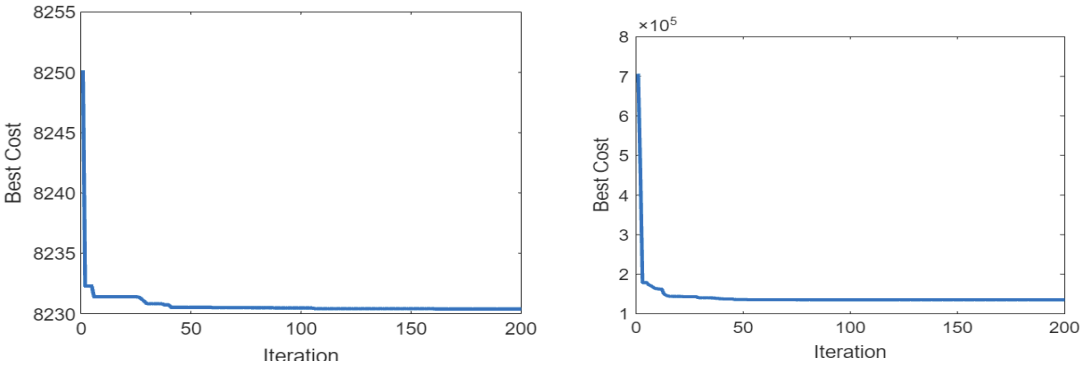

(a) Best Cost = \$8230.3883 (b) Best Cost = \$135229.9905

Figure 4.6. 3-Unit with RESs cost coefficient data testbed simulation for EPD (best cost) (a) minimum cost (best cost) 3 thermal units convergence; (b) minimum cost (best cost) 2 thermal and 1 solar PV units convergence.

4.5.2.2 Case 5: 6-unit generator demand of 1263 MW with RESs using Monte Carlo uncertainty cost functions

The 6-unit generator case study of 1263 MW load demand data uses a loss coefficient from Ref. Gaing (2003) with Monte Carlo uncertainty cost functions with RESs. The IEEE

30-bus testbed consists of 26 buses and 46 transmission lines for 6x100 thermal and RESs units Monte Carlo uncertainty cost functions. Table 4.5 demonstrates the proposed PSO for the EPD evolutionary process, applying ramp-up limits, ramp-down limits, and generator forbidden zones as the primary algorithm model limitation and a parse solution for unit commitment. Figure 4.7 shows the 6-unit EPD with RESs cost coefficient data simulation at the lowest cost (best cost).

Table 4.5. IEEE 30-bus of 6-Unit with RESs cost coefficient data (Heris, 2016; Al-Roomi, 2016, Gaing, 2003)

Bus Number	Generator limits [MW]		Fuel cost coefficients without RESs			Fuel cost coefficients with RESs		
	P_{max}	P_{min}	a_i [\$/MW^{2}h]	b_i [\$/MWh]	c_i [\$/h]	a_i [\$/MW^{2}h]	b_i [\$/MWh]	c_i [\$/h]
1	100	500	240	7.00	0.0070	240	7.00	0.0070
2	50	200	200	10.0	0.0095	918.558	33.544	0.331
5	80	300	220	8.5	0.0090	183.851	3.643	1.744
8	50	150	200	11.0	0.0090	918.558	33.544	0.331
11	50	200	220	10.5	0.0080	183.851	3.643	1.744
13	50	120	190	12.0	0.0075	190	12.0	0.0075

Transmission loss coefficients								
B_{01}			B					
-0.3908	-0.1279	0.7047	0.0017	0.0012	0.0007	-0.0001	-0.0005	-0.0002
			0.0012	0.0014	0.0009	0.0001	-0.0006	-0.0001
0.0591	0.2161	-0.6635	0.0007	0.0009	0.0031	0.0000	-0.0010	-0.0006
			-0.0001	0.0001	0.0000	0.0024	-0.0006	-0.0008
B_{00}=0.056			-0.0005	-0.0006	-0.0010	0.0006	0.0129	-0.0002
			-0.0002	-0.0001	-0.0006	0.0008	-0.0002	0.0150

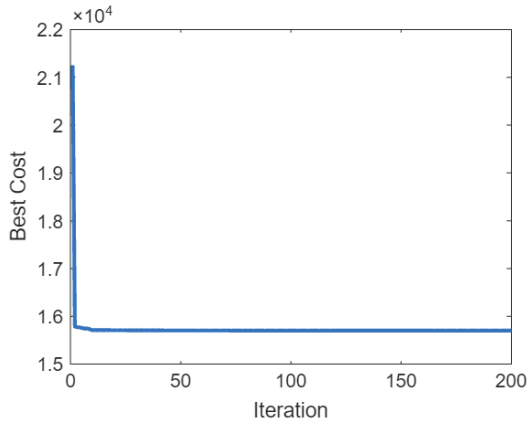

(a) Best Cost = \$15700.447

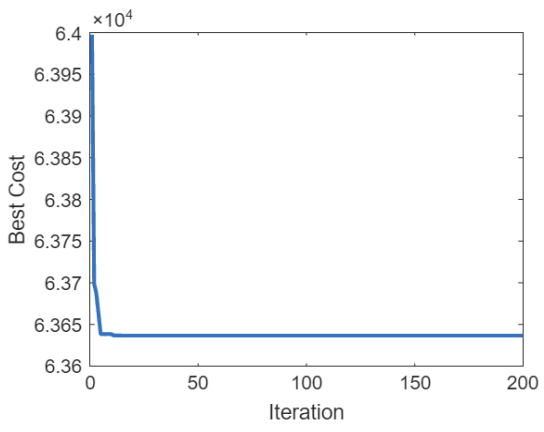

(b) Best Cost = \$63636.6183

Figure 4.7. 6-Unit with RESs cost coefficient data testbed simulation for EPD (best cost) (a) minimum cost (best cost) 6 thermal units convergence; (b) minimum cost (best cost) 2 thermal and 4 solar PV units convergence.

4.5.3.3 Case 6: 15-unit generator demand of 2630 MW with RESs Monte Carlo uncertainty cost functions

Table 4.6 displays the input-output characteristics for 15 thermal and RESs Monte Carlo uncertainty cost functions with a population dimension of 15x100 in case 3. Figure 6 displays the evolving proposed EPD PSO process with up-ramp limits and down-ramp restrictions and generating forbidden zones of 15 x 15. Figure 4.8 depicts the convergence EPD property for a 15-unit PSO simulation at the lowest cost. The ideal plant selection is expected to be at the grid operator's discretion to schedule the suitable plants.

Table 4.6. IEEE 118-bus of 15-Unit with RESs cost coefficient data (Heris, 2016; Al-Roomi, 2016; Gaing, 2003; Yoshida et al., 2000)

Bus Number	Generator limits [MW]		Fuel cost coefficients without RESs			Fuel cost coefficients with RESs		
	P_{max}	P_{min}	a_i [\$/MW^{2}h]	bi [\$/MWh]	ci [\$/h]	a_i [\$/MW^{2}h]	bi [\$/MWh]	ci [\$/h]
1	150	455	671	10.10	0.0003	671	10.10	0.0003
2	150	455	574	10.20	0.0001	574	10.20	0.0001
5	20	130	374	8.80	0.0011	918.558	33.544	0.331
4	20	130	374	8.80	0.0011	183.851	3.643	1.744
4	150	470	461	10.40	0.0002	461	10.40	0.0002
5	135	460	630	10.10	0.0003	630	10.10	0.0003
8	135	465	548	9.80	0.0003	548	9.80	0.0003
10	60	300	227	11.20	0.0003	227	11.20	0.0003
25	25	162	173	11.20	0.0008	918.558	33.544	0.331
26	25	160	175	10.70	0.0012	183.851	3.643	1.744
30	20	80	186	10.20	0.0035	918.558	33.544	0.331
37	20	80	230	9.90	0.0055	183.851	3.643	1.744
38	25	85	225	13.10	0.0003	918.558	33.544	0.331
63	15	55	309	12.10	0.0019	183.851	3.643	1.744
64	15	55	323	12.40	0.0044	323	12.40	0.0044

Transmission loss coefficients
B

0.0014	0.0012	0.0007	-0.0001	-0.0003	-0.0001	-0.0001	-0.0001	0.0003	0.005	-0.0003	-0.0002	0.0004	0.0003	-0.001
0.0012	0.0015	0.0013	0.0000	-0.0005	-0.0002	0.0000	0.0001	-0.0002	0.004	-0.0001	-0.0000	-0.0004	0.0010	-0.002
0.0001	0.001	0.0076	-0.0001	--0.0013	-0.0009	0.0001	0.0000	-0.0008	-0.012	-0.0017	-0.0000	-0.0026	-0.0111	-0.028
-0.0001	0.0000	-0.0001	-0.0001	0.0034	-0.0007	-0.0001	0.0011	0.0050	0.029	0.0032	-0.0000	0.0001	0.0001	0.026
-0.0003	-0.0005	-0.0013	-0.0007	0.0090	0.0014	-0.0003	-0.0012	-0.0010	-0.013	-0.0007	-0.0002	-0.0002	-0.0024	-0.003
-0.0001	-0.0002	-0.0009	-0.0004	0.0014	0.0016	-0.0000	-0.0006	-0.0005	-0.008	-0.0011	-0.0001	-0.0002	-0.0017	0.003
-0.0001	0.0000	-0.0001	0.0011	0.0003	-0.0000	0.0015	0.0017	0.0015	0.009	-0.0005	-0.0007	-0.0000	-0.0002	0.008
-0.0001	0.0001	0.0000	0.0050	0.0012	-0.0006	0.0017	0.0168	0.0082	0.079	-0.0023	-0.0036	-0.0001	0.0005	-0.078
-0.0003	-0.0002	-0.0008	0.0029	-0.0010	-0.0005	0.0015	0.0082	0.0129	0.116	-0.0021	-0.0025	0.0007	0.0012	-0.072
-0.0003	-0.0004	-0.0017	0.0011	-0.0007	0.0011	-0.0005	-0.0023	-0.0021	-0.0127	-0.0140	-0.0001	0.0004	0.0038	0.0168
-0.0002	-0.0000	-0.0000	-0.0000	-0.0002	-0.0001	0.0007	-0.0036	-0.0025	-0.0003	-0.0001	0.0051	-0.0001	-0.0004	0.028
0.0004	0.0004	-0.0026	0.0001	-0.0002	-0.0002	-0.0000	-0.0001	0.0007	0.009	0.0004	-0.0001	0.0103	-0.0101	0.028
0.0003	0.0010	0.0111	0.0001	-0.0024	-0.0017	-0.0002	0.0005	-0.0012	-0.0011	-0.0038	-0.004	-0.0101	0.0578	-0.0094
-0.0001	-0.0002	-0.0028	-0.0026	-0.0003	0.0003	-0.0008	-0.0078	-0.0072	-0.0088	0.0168	0.0024	-0.0028	-0.0094	0.1283
B_{01}														
-0.0001	-0.0002	-0.0028	-0.0001	0.0001	-0.0003	-0.0002	-0.0002	0.0006	0.039	-0.0017	-0.0000	-0.0032	0.0067	-0.0064
B00=0.055														

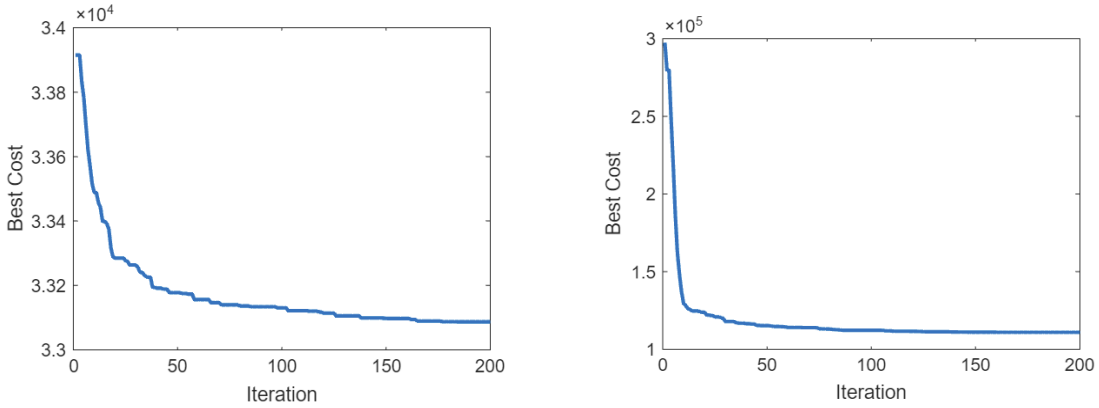

(a) Best Cost = $33087.0709 (b) Best Cost = $110922.1851

Figure 4.8. 15-Unit with RESs cost coefficient data testbed simulation for EPD (best cost) (a) minimum cost (best cost) 15 thermal units convergence; (b) minimum cost (best cost) 7 thermal and 8 solar PV units convergence.

Table 4.7. Comparative results of simulated IEEE 14-bus, 30-bus and 118-bus testbed with buses and transmission lines data

	PSO plants Model	Best cost ($)	Difference	% Best cost/day ($)	Compared Best cost
3- Units	3 Thermal	8230.38	4.5932	0.055	8234.07 (Al-Betar et. al., 2022)
	2 Thermal and 1 PV	95283.67	107709.5	91.87	8194.35 (Rajashree and Upadhyay, 2016)
					8242
6- Units	6 Thermal	15709.8	29396.0	46.55	15447 (Gaing, 2003; Kuo, 2008)
	2 Thermal and 4 PV	201411.1	7920.48	3.784	15450.00 (Kuo, 2008)
					15465.83
15- Units	15 Thermal	33330.2	137487.9	89.10	33049 (Gaing, 2003; Kuo, 2008)
	7 Thermal and 8 PV	48653.8	272723.7	73.86	32708 (Rahmani et al., 2012)
					32858.00 (Al-Betar et. al., 2022)

4.6 Results Discussion

The developed PSO successfully demonstrated maximum yearly cost savings and cost reduction that significantly enhanced the self-consumption of solar PV and cost benefit ratio significance compared to the baseline method. However, several particles are not required to find PSO optimal convergence for 3-unit (small scale), but required for 6 unit (medium scale) and 118-unit (large scale). The particle number increases the swarm's search accuracy and speed of the problem space. To build RESs's best capacity scale, we presented a novel particle PSO method. Operating transmission line losses, energy, and cost are the known optimum solar PV generator objective functions for allocation and sizing. The optimization approach uses particle swarm optimization with varied set-

ups to achieve optimal performance beneath a variety of operational conditions. This chapter contributes to knowledge by using a novel PSO algorithm.

4.7 Chapter Summary

The objective of Chapter 4 is to present the PSO method for the economic power dispatch problem of a grid-tied RES-based-HS scheme, to minimize the operational costs while meeting limitations for non-contingency and contingency circumstances. The developed PSO method has effectively demonstrated a yearly operational cost reduction with substantial cost savings and cost-benefit as shown in comparative results of simulated IEEE 14-bus, IEEE 30-bus, and IEEE 118-bus testbeds of generator units with buses and transmission lines system data (Table 4, 7). The proposed optimization method can enhance the baseline method in comparison to the self-consumption ratio. Chapter 5 will cover the integration of an electric vehicle charge station to further enhance a self-consumption ratio in comparison to the baseline method.

CHAPTER FIVE

PSO METHOD FOR HYBRID SYSTEM WITH ELECTRIC VEHICLE CHARGING STATION

5.1 Introduction

Hybrid systems (HS) combine multiple forms of energy-producing equipment, including generators, storage, and renewable energy sources. Energy planning and decision-making need major resource allocation that affects all economic actors. Hybrid systems in an isolated or grid-connected mode for restricted applications can be used in modern HS research on planning considering renewable power output uncertainties and load demands. HS planning optimizes generation and transmission approaches for energy-producing equipment optimum system utilization, which is crucial in towards global energy efficiency. The charging infrastructure required by electric vehicles poses a fundamental problem that must be overcome before significant deployment of RESs can occur. However, the introduction of numerous charging stations portends a negative effect on the consistency and distribution network smooth operation. The electric vehicle charging station (EVCS) operating parameters will be impaired via lack of reliability, power losses, voltage deviation of buses, harmonics distortions, voltage instability, and high peak demand. The literature proposed PSO of an electric vehicle charging station provides the best bus location and sizes for both RES and EV considering capacity constraints. Monte Carlo simulation of the quadratic cost uncertainty value from the reviewed literature was adopted for PVs/WTs. Power flow analysis with Newton Raphson methodology (NPM) to locate several electric vehicles and optimize RESs grid-tied system power dispatch. Power optimization was established as objective function, which includes minimizing losses in active and reactive power considering cost, power flow, and voltage, in a multi-objective formulation. Chapter 5 of the thesis aims to propose a particle swarm optimization method for a hybrid system of an electric vehicle charging station (EVCS). To provide best value for uncertainty cost functions for both RES and location, sizes for EVCS considering active, reactive power losses considering cost, power flow, and voltage deviation constraints in a multi-objective formulation. The chapter presents test cases in MATLAB where EVs were integrated with optimally sized RESs in the IEEE 14-bus, IEEE 30-bus and IEEE 118-bus testbeds. The outcomes of using this approach for the IEEE distribution testbeds demonstrate validity and efficacy of the PSO method in identifying the optimal locations for EVCS unit installation in the distribution grid. The noteworthy contributions outlined in the thesis chapter are:

1. To reach fast and precise convergence by using a PSO search algorithm.

2. Optimize active power, power flow, and EVCS location to minimize power losses and maximiza power system steadiness.
3. Examine the problem of minimizing power losses by merging EVs and RES to achieve the highest feasible active power output from RESs in terms of distribution network voltage and power loss coefficients.
4. The IEEE 14-bus, IEEE 30-bus and IEEE 118-bus distribution testbeds demonstrate the efficacy and validity of the proposed PSO method for determining EV charging stations best on the distribution grid.

5.2 Energy Management of The Hybrid System

Energy management systems (EMS) aid in optimizing the usages of hybrid systems in grids, mainly when generation and flexible pricing are involved. The development of an optimization uses loading conditions and estimated pricing to optimally sell or store energy from battery system in a grid-tied RESs. Two methods are established: a heuristic and the multi integer nonlinear program-based optimization. The study of EMS optimization can benefit from breakthroughs in computational and mathematical programming methodologies, which predate the invention of digital computers and have revolutionized numerical optimization and computation. Many practical applications require design variables to adhere to specific electrical or physical limitations; thus, they cannot take random values. These limitations, also known as design constraints, are critical to guaranteeing the system's stability and security. The following is a list of the mathematical modeling restrictions characteristic of the multi-objective function's inputs for hybrid energy systems. (Fan et. al., 2019).

HS is traditionally contemplated to have four key elements in this thesis: a grid, a solar PV, a wind turbine, and an energy storage system. The hybrid system's factors cooperate adaptively to meet load demand. The ESS acts as a backup storage when solar PV or wind turbine output is inadequate to meet the load requirement. The best element of a hybrid system is that it maximizes energy efficiency by storing excess solar PV or wind turbine energy in the ESS. The energy flow from solar PV and ESS is inadequate to meet load requirement, the wind turbine is planned. By reducing excessive grid use, the hybrid system's techno-economic feasibility is maximized. The proposed simulation process is depicted in Figure 1 in terms of the simulation model, input, output, and associated constraints. According to Figure 1, the hybrid system power flow has been defined in this study. P_{RES} - P_{ESS} and P_{ESS} - P_{LOAD} indicate energy flow from P_{PV} to the battery and from the battery bank to the load, respectively, whilst $P_G - P_L$ and P_{RES} - P_{LOAD} reflect the energy flow from the grid and the PV grid to the load. To be clear, we shall refer to the energy flow to and from the battery reserve as positive. During inadequate energy supply

to meet the load requirement, the wind turbine is planned as energy flow from P_{WT} reflect the grid energy flow and P_{WT} grid to the load. Both P_{PV} and P_{WT} can also be planned simultaneously.

5.3 Energy Management for the Hybrid System of an EVCS

The lack of readily available electric vehicle charging stations on electrical network slows the swift electric vehicles adoption as a more cost-effective means of transportation, predominantly in developing countries. Sequel to this challenge, EV owners use a home connection to recharge their EV batteries, triggering a substantial energy system loss and a worse profitability index in the power sector (Sivaraman and Sharmeela, 2021). Likewise, several EV charging stations created distribution grid power quality issues, such as power loss and voltage variations, due to the system's non-linear behavior (Surbhi et al., 2020). The unorganized and inefficient EV charging energy is associated with power problems in the distribution network (Sridevi et al., 2022). These problems can be solved by adding renewable resources (Ashish Kumar et al., 2019), improving converter topologies (Radha and Singh, 2019), and modifying charging patterns (Qiyun, 201) using energy management systems (Viet Thang et al., 2019). Despite intermittent nature and high capital requirements for renewable power-generation infrastructure, there have been increases in popularity due to their environmental benefits, cost-effectiveness, and low maintenance (Wang, 2020). However, using RESs for EV charging has system stability impact and security issues because of their inconsistency and uncertainty. There are not enough EV charging stations in developing countries, therefore many charges from home, resulting in substantial system loss and a lower viability index, these limitations can be overcome by utilizing the hybrid system for EV charging stations (Asif et al., 2019).

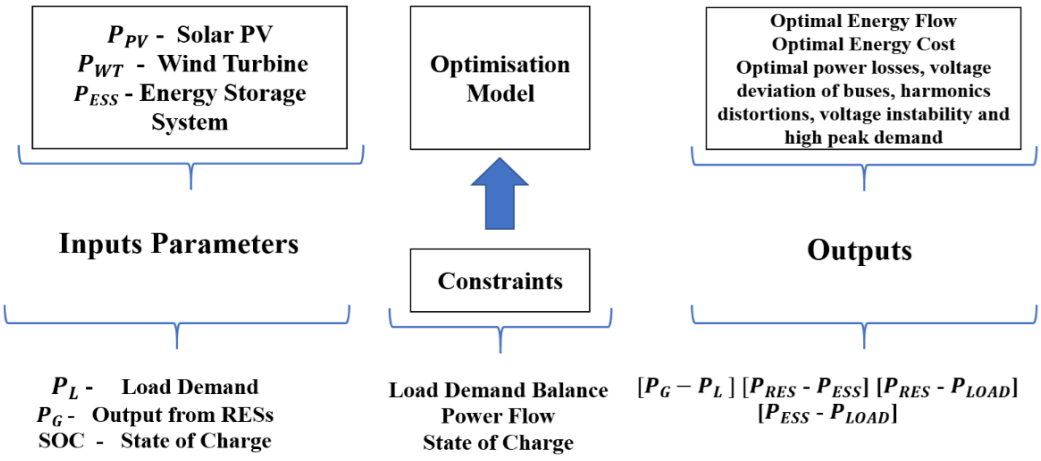

Figure 5.1. Energy Management structure for the Hybrid System of an EVCS

As a result, an EV charging station energy management strategy is required to maximize use of RESs. There has been EVCS optimization research, considering EV power demand, charging priority, location, and charging duration (Shahid et al., 2020). Although solar PV energy is an electricity generation valuable source, it can be harnessed for a few hours per day. In contrast, wind energy resources may provide electricity when sun energy is unavailable (Natasha and Warren, 2020). As a result, combining these resources can help the power generation reliability and efficiency improvements. Research on hybrid systems using RESs has proven that it is energy efficient, cost-effective, and environmentally beneficial (Eltoumi, 2020). However, the lack of a hybrid system energy management scheme significantly limits electric vehicle adoption. Nonetheless, most hybrid system adoption for EV charging lacks an energy management strategy. Supplementary research is required to optimize the EVCS in terms of off-peak/peak hours for the charging cycle, EV power consumption, real-time charging cost, and RES integration.

5.4 Hybrid System of an Electric Vehicle Charging Station

The increased use of electric vehicles necessitates the construction of efficient charging stations capable of providing adequate charging rates. Combining on-site RES would reduce grid load, improving charging station effectiveness. In this thesis, a solar PV system is used in conjunction with the grid to power an electric vehicle. Solar PV is known for its irregular character, which is greatly impacted by location and weather conditions. To compensate for the irregular nature of solar PV, an energy storage system is combined with a grid-tied RESs scheme to assure the continuous operation of a hybrid solar PV-based charging station. In general, hybrid-source-based charging stations should be affordable, efficient, and dependable enough to meet the varying needs of EV loads in a variety of situations. This thesis develops and utilizes the MINLP approach to optimize on-site PV energy and satisfy the changing load of EVs while considering the ESS's fast reaction and reducing grid stress. The proposed formulation tries to lower the expected cost of operation.

$$min\ F_{C_{total}} = \alpha_i + \beta_i P_{s,i} + c_i P_{s,i}^2 \tag{4.1}$$

Where α_i, β_i, c_i are the cost coefficients of generator i .

$$C_{total} = \sum_{i=1}^{N_T}(\sum_{g=1}^{N_g} C_g(P_{g,i}) + \sum_{r=1}^{N_r} C_r(P_{r,i}) + \sum_{v=1}^{N_v} C_{v,i}(P_{v,i}) + \sum_{m=1}^{N_m} C_{m,i}(P_{m,i}) + \sum_{ev=1}^{N_{ev}} C_{evcs,i}(P_{evcv.i}) + \gamma) \tag{5.2}$$

The variables N_g , $N_r, N_{v,} N_m, N_{evcs}$ represent the number of conventional generators, spinning reserves, solar PV, wind power generators, and buses with EV charging stations, respectively. The penalty function, $\boldsymbol{\gamma}$, ensures a minimum renewable obligation

during dispatch to meet energy mix requirements. In the applied method, solar PV generator have a cost function, with P_{gi} being the scheduled generator power output i, and the direct cost is provided by:

$$P_{gi} = P_{v,i} + P_{evcs.i} \tag{5.3}$$

The power flow solver considered optimization algorithm's constraints. Furthermore, the must slack bus chosen in the formulation, including PV bus, and PQ bus.

5.5 Energy management strategies at an electric vehicle charging station

The EMS strategies (Figure 5.3) at charging station stations used are intended to maximize the use of solar PV supply for the EVCS charging cycle. The priority is to reducing reduce reliance on grid electricity supply steadily with significant purpose of increasing renewable energy usage, and carbon footprint reduction. The dynamically controlled EMS power flow prioritize prioritizes EVCS charging periods using sola PV available power to reduce operational costs by exploiting self-consumption of energy generated, which is largely more cost-effective than grid electricity, mostly when considering solar PV infrastructure long-term investment factor. EMS allocates power proportionately between the EVCSs based on discrete EV necessities as represented in equation (5.4), making it simpler to estimate each EV charging power as shown in equation (5.2). Equation (5.3) presents the total EVCS power requisite, calculated by separate EVCS charging powers.

$$P_{evcs(t)} = \left(SOC_{evcs(\min)} < SOC_{ess(t)} < SOC_{evcs(\max)}\,(t)\right) C_{evcs(t)} \tag{5.4}$$

$$P_{v,i} = \frac{\left(SOC_{evcs(\min)} < SOC_{ess(t)} < SOC_{evcs(\max)}\,(t)\right) C_{evcs(t)}}{t_{di} - t - \Delta t} \tag{5.5}$$

$$P_{evcs(t)\,-limit} = P_{v,i(t)}\, X\, P_{max} \tag{5.6}$$

$$P_{demand} = \sum_{i=1}^{T_{evcs}} P_{ss(t)} \tag{5.7}$$

$P_{ess(t)}$ denotes EVCS charging power, $SOC_{evcs(\max)}$ is the maximum EVCS state of charge, $SOC_{evcs(\min)}$ is the minimum EVCS state of charge, $SOC_{evcs(t)}$ denotes the current charging station state of charge, $C_{evcs(t)}$ signifies battery capacity, t is the current time, T_{evcs} is duspatch horizon (24 hours), tdi signifies the departure time, and Δt is dispatching resolution (1 hour), EMS's EV charging strategy to maximize solar energy consumption. Following that, it discusses charging the energy storage system. The EMS's overarching control strategy prioritizes EV charging, intending to maximize solar energy utilization. Following that, it discusses ESS charging. Any extra electricity is dynamically distributed to supplementary loads in the system or supplied back to grid. When the energy in the ESS is depleted (SOC less than 20%), the EMS will draw power from the grid to ensure uninterrupted functioning.

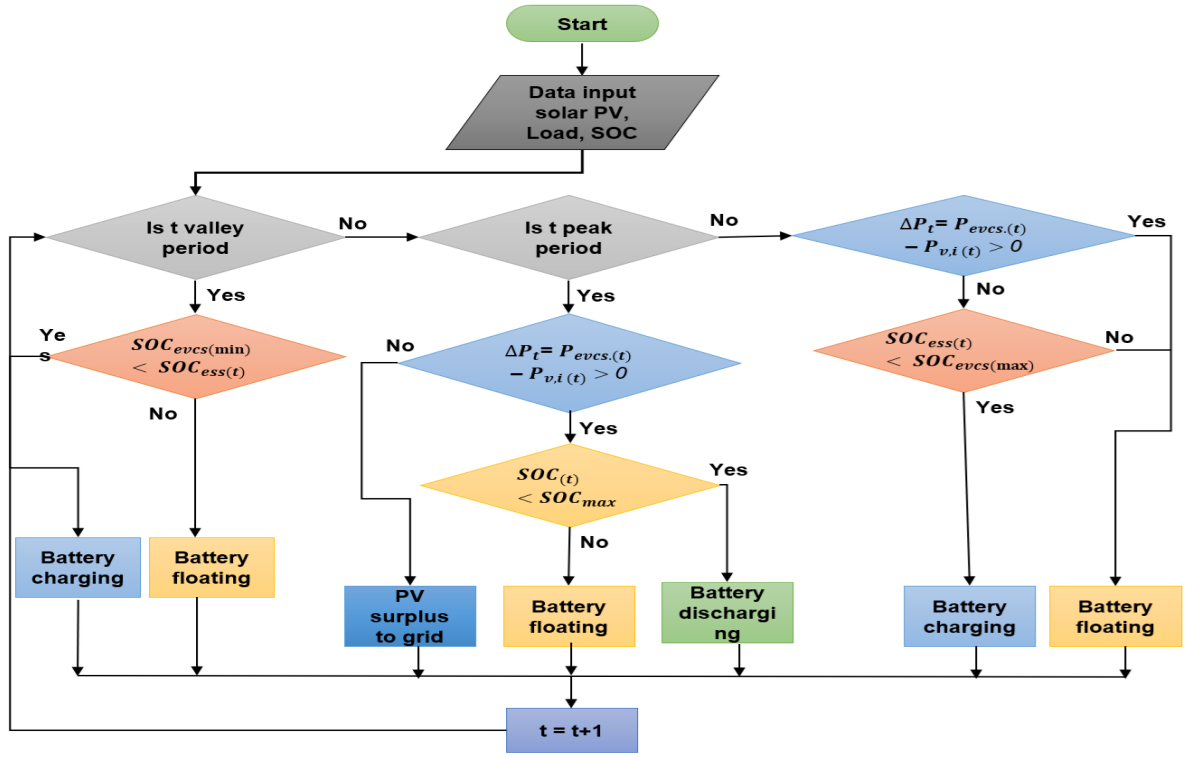

Figure 5.2. Energy management strategies at EV charging station

5.6 Optimal Active–Reactive Power Flow Considering RESs and EV charging stations station using multi-objective PSO optimization

Optimal power flow is a key issue in hybrid system operation, analysis, and planning, with extensive research over the last 50 years (Sau-Bassols et al., 2019). OPF is a constrained, nonlinear, nonconvex, and large-scale optimization with continuous and discrete control variables. The OPF aims to optimize a precise objective function, such as reliability or cost, by handling power flow within an electrical network while adhering to operating limits and network restrictions (Wang and Song, 2023). OPF has been designed to address detailed concerns, such as reactive power dispatch, which are critical for ensuring efficient and secure power system operation. Technical systems of measurement, such as voltage variation can serve as objectives for system boundaries in transmission network loss capacity, and generation compensation. This thesis considers voltage stability in short-term operational planning. The aim is to find the best preventive action to improve power stability while remaining within operational limitations. The thesis focuses on optimizing reactive and active power dispatch and by minimizing total power transmission losses. The optimal power flow is treated as a multi-objective function while meeting equality and inequality constraints as

$$P_i + jQ_i = V_i^* \sum_{j-1}^{n} Y_{ij} V_j \qquad i = 1,2,\ldots\ldots,n \tag{5.8}$$

Where P and Q are real and reactive powers. V is voltage and Y is the bus admittance.

5.6.1 Equality constraints considered with a power flow inside the optimization Algorithm

The fundamental reason for the equality constraints is that the generator's active power must match both active load demand and power loss. The active power flow equality criteria balancing equation are as follows:

$$P_{gi} - P_{di} - v_i \sum_{j \in N_i} v_j \left(g_{ij} \cos \delta i - \delta j - \theta_{ij} + B_{ij} \sin \delta i - \delta j - \theta_{ij} \right) \quad (5.9)$$

$$Q_{gi} - Q_{di} - v_J \sum_{j \in N_i} v_j \left(g_{ij} \sin \delta i - \delta j - \theta_{ij} + B_{ij} \cos \delta i - \delta j - \theta_{ij} \right) \quad (5.10)$$

where i = 1,…, Ni (total buses number), g_{ij} and B_{ij} are branch conductance and susceptance between buses i and j; v_i and v_J are voltage magnitudes at buses i and j; and θ_{ij} is load angle difference between buses i and j. P_{gi} and P_{di} represent generated and active power demand by bus i. Q_{gi} and Q_{di} represent generated reactive power and power needed by bus i.

5.6.2 Inequality Constraints Related to the Fitness Function Inside of the Optimization Algorithm

These constraints are provided by slack bus active produced power limit (5.11), the generation reactive power limit at each generator bus (5.12), each load bus voltage magnitude limit (5.13), and each transmission line power flow limit constraint (5.14).

$$P_{slack} \leq P_{slack}^{max} \quad (5.11)$$

$$Q_{slack} \leq Q_{gi} \leq Q_{slack}^{max}, \; i \in N_g \quad (5.12)$$

$$v_{gi}^{min} \leq v_{loadi} \leq v_{gi}^{max}, \; i \in N_B \quad (5.13)$$

$$S_1 \leq vS_1^{max}, \; l \in N_1 \quad (5.14)$$

where N_B represents load buses number, i.e., buses with P_{di} greater than zero, and N_1 indicates network branches number. The fitness function includes a penalty factor (ρ) to account for non-contingency and contingency circumstances (N − 1). The PF is calculated for (N - 1) scenarios. After a maximum iterations number, best fitness function cost solution will be chosen. The heuristic search strategy for each element power flow is given, based on the population-based optimization techniques employed in this thesis presented.

$$PF = \rho \Big\{ (P_{slack}^{max} - P_{slack})^2 + \sum_{i=1}^{N_g} \left[(Q_{gi} - Q_{gi}^{min})^2 + (Q_{gi}^{max} - Q_{gi})^2 \right] + \sum_{i=1}^{N_g} \left[(v_{loadi} - v_{loadi}^{min})^2 + (v_{loadi}^{max} - v_{loadi})^2 \right] + \sum_{l=1}^{N_l} (s_{slack}^{max} - s_l) \Big\} \quad (5.15)$$

The recent advancements in digital computer technology have resulted in the creation of several solutions for handling power flow challenges. Gauss-Seidel and Newton-Raphson are most often utilized iterative algorithms today (Nur and Kaygusuz, 2021).

Although these approaches are efficient, comparing them is challenging due to computers differences, methods and languages used in programming, and testing challenges. However, the Newton-Raphson approach is commonly used method for big load flow analysis for of its computational simplifications, fast convergence, and accurate results (Noureddine and Djamel, 2021). In this thesis, the NR approach is applied to solve the line flow equations in the applied IEEE distribution testbeds. Power losses, voltage variations and each bus active and reactive power flows calculation can be determined by the voltage at the sending and receiving end to allow for optimal system operation (Flaten, 1988). Same iterative method is performed until a predefined tolerance threshold is obtained for smaller solution (Ashida, 2021). Similarly, the NR approach can be extended to a nonlinear equations collection. In this scenario, the solution is Jacobian J matrix is (n×n) with all derivative elements.

$$F(X^K) = -J^K \Delta X^K, \tag{5.16}$$

$$X^{K+1} = X^K + \Delta X^K \tag{5.17}$$

The Newton-Raphson technique can also be used to analyse load flow in rectangular or polar dimensions (Seng et al., 2015). The NR approach can also be used to discover the solution for a rectangular coordinate system.

5.6.3 Electric Vehicle Charging Station Load Profiles-Based Methods

Electric vehicles (EVs) have high efficiency and can minimize transportation energy use while transitioning from fossil fuels to renewable energy. Managing renewable energy output through energy storage and dispatchable load is a common challenge in non-dispatchable RESs management contribute significantly to system instability (Pearre and Swan, 2020). Governments and utilities are interested in applying the EV charging benefits to fulfill definite grid management objectives (Rwamurangwa et al., 2022). This case study, with defined grid limits and exact loading data, particularly useful to policymakers. EVs interaction with electrical system is fully dependent on an accurate understanding of how much energy consumed while in EVs are use, and when returned to a charging station. The potential effects of EVs on the energy system are addressed in (Connected EVs, 2021) based on the importance of electric car driving habits.. If charging rates and timing are not restricted, there is a risk of unwanted night-time spike "convenience charging". The situation is envisioned as similar to how mobile phones are used in cars, with plugging in and charging immediately upon arrival at a charging station, independent of time of day or impact on the grid. In this instance, EVs are most likely plugged in as soon as they get at their destination, which is usually home, and charged to capacity. To investigate EV energy usage impact daily on the grid, (NHTS, 2023) data

for 1616 EV classes was adopted to approximate the EV penetration rate. Table 5.1 shows the EVs category in class by EVCS which require an average of 15 kWh per day, based on driving patterns and energy consumption. Table 5.2, Table 5.3 and Table 5.3 are simulation data for IEEE 14-bus, IEEE 30-bus and IEEE 118-bus testbeds data (Heris, 2016; Al-Roomi, 2016, Gaing, 2003).

Table 5.1. Parameters for Charging Load Model by EV Consumer Classes and Type

Data (NHTS, 2023)	**Electric Car**	**Electric SUV**	**Electric Van**	**Electric Pickup Truck**
EV Class	**Compact**	**Economy**	**Mid-size Van**	**Light Truck**
BCap, kWh	8 - 12	10 - 14	14 - 18	19 - 23
EC, kWh/km	15-25	25-40	40-55	55-60
Consumption	90	105	120	120
(km for 24kWh	1480	80	48	8

Table 5.2. IEEE 14-bus 3-Unit cost data and constraints (Heris, 2016; Al-Roomi, 2016, Gaing, 2003)

Bus Number	Generator limits [MW]		Fuel cost coefficients without RESs			Fuel cost coefficients with RESs		
	P_{max}	P_{min}	a_i [$/MW^{2}h]	b_i [$/MWh]	c_i [$/h]	a_i [$/MW^{2}h]	b_i [$/MWh]	c_i [$/h]
1	100	500	240	7.00	0.0070	240	7.00	0.0070
2	50	200	200	10.0	0.0095	918.558	33.544	0.331
5	80	300	220	8.5	0.0090	183.851	3.643	1.744

Table 5.3. IEEE 30-bus 6-Unit cost data and constraints (Heris, 2016; Al-Roomi, 2016, Gaing, 2003)

Bus Number	Generator limits [MW]		Fuel cost coefficients without RESs			Fuel cost coefficients with RESs		
	P_{max}	P_{min}	a_i [$/MW^{2}h]	b_i [$/MWh]	c_i [$/h]	a_i [$/MW^{2}h]	b_i [$/MWh]	c_i [$/h]
1	100	500	240	7.00	0.0070	240	7.00	0.0070
2	50	200	200	10.0	0.0095	918.558	33.544	0.331
5	80	300	220	8.5	0.0090	183.851	3.643	1.744
8	50	150	200	11.0	0.0090	918.558	33.544	0.331
11	50	200	220	10.5	0.0080	183.851	3.643	1.744
13	50	120	190	12.0	0.0075	190	12.0	0.0075

Table 5.4. IEEE 118 Bus 15-Unit cost data and constraints (Heris, 2016; Al-Roomi, 2016, Gaing, 2003)

Bus Number	Generator limits [MW]		Fuel cost coefficients without RESs			Fuel cost coefficients with RESs		
	P_{max}	P_{min}	a_i [\$/MW^{2}h]	bi [\$/MWh]	ci [\$/h]	a_i [\$/MW^{2}h]	bi [\$/MWh]	ci [\$/h]
4	150	455	671	10.10	0.0003	671	10.10	0.0003
6	150	455	574	10.20	0.0001	574	10.20	0.0001
15	20	130	374	8.80	0.0011	918.558	33.544	0.331
24	20	130	374	8.80	0.0011	183.851	3.643	1.744
31	150	470	461	10.40	0.0002	461	10.40	0.0002
66	135	460	630	10.10	0.0003	630	10.10	0.0003
70	135	465	548	9.80	0.0003	548	9.80	0.0003
77	60	300	227	11.20	0.0003	227	11.20	0.0003
82	25	162	173	11.20	0.0008	918.558	33.544	0.331
87	25	160	175	10.70	0.0012	183.851	3.643	1.744
90	20	80	186	10.20	0.0035	918.558	33.544	0.331
99	20	80	230	9.90	0.0055	183.851	3.643	1.744
70	25	85	225	13.10	0.0003	918.558	33.544	0.331
110	15	55	309	12.10	0.0019	183.851	3.643	1.744
116	15	55	323	12.40	0.0044	323	12.40	0.0044

5.7 Particle Swarm Optimization for Hybrid Systems of an Electric Vehicle Charging Station

In modern days, the optimization model has witnessed numerous new meta-heuristic algorithms. Engineering real-world problems are non-linear and challenging to resolve with classical methods. The EVCS problem is a multiple variable and difficult problem including, nonlinear objective functions, and constraints. To create effective and speedy solutions it is critical to build the best evolutionary algorithms for charging stations. Each method employs a heuristic search technique to monitor inequality constraints based on active power generation output variables, generator bus voltage set-points and EVs, tap positions of stepwise adjustable on-load transformers, and the status of switchable shunt compensation devices. Each resolution in each population receives a power flow, objective assessment, and fitness function score. The power flow calculation considers limits, requiring the formulation to select a slack bus, PV bus, and PQ bus. The objective evaluation is compatible with the estimated total generating cost, as stated in the section. The objective function and penalty function (PF) construct the fitness function value in the technique, considering limitations (5.7) - (5.10) via a penalty factor (ρ). The PF is

calculated for both the non-contingency and the contingency (N - 1) scenarios. After a maximum number of iterations, the solution with the best fitness function value is chosen. This study employs four population-based optimization techniques. Figure 5.2 describes the energy management tactics for an EV charging station using the PSO method.

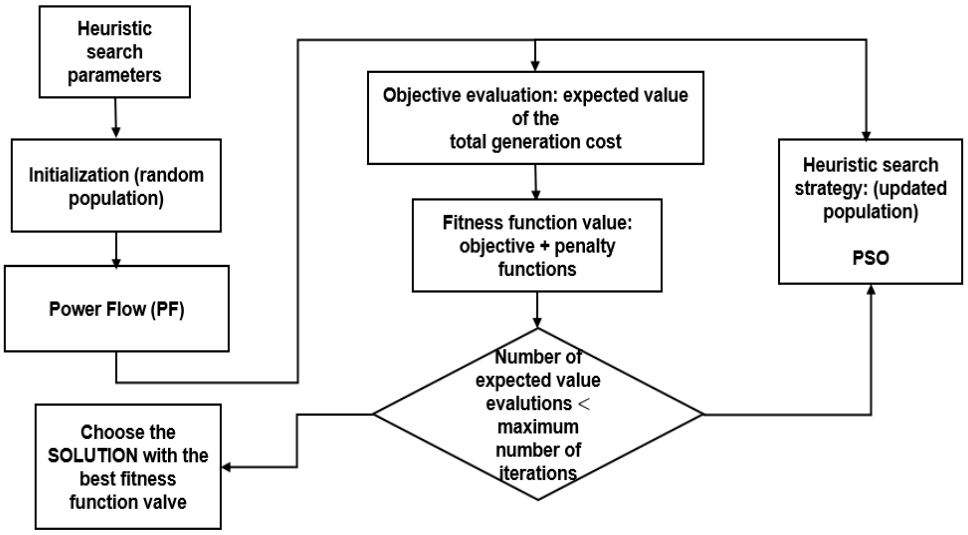

Figure 5.3. Energy management strategies at EV charging station flowchart

5.8 Results of Optimal Active–Reactive Power Flow Considering RESs and EV Charging Stations using multi-objective PSO Algorithm

The analysis is carried out using IEEE14 and IEEE 30 distribution bus system simulation considering solar PV generation serving EVCS loads supplied via the substation at bus-1, 2, 5, 8, 11, 13. The simulation assumes that an EVCS is randomly located on buses, with no loss of generality. The PSO is used to model the EVCS controllable load in terms of EV Class and Type factors and variables as viewed by the EV owner. The case scenario infers EVs to be charged proposed model on the distribution system remains continuous irrespective of the EV class capacity constraint. EVs are optimally allocated to charging stations throughout the day, although with limited load consumption during hours 9:00 – 17:00 due to high arrival/parking rates, due to the selection of the objective function even if the EVCS capacity is not reached. The results are presented in Figure 5.4, with EV charging station Best Total System Cost at Buses and Figure 5.5. EV charging station Voltage profile at Buses. Figure 5.6 is the Apparent Line Power Flow demand without optimal EVCS demand. The systems losses are presented in Figure 5.7. Real Power Loss of the System demand without optimal EVCS demand and Figure 5.8. Reactive Power Loss demand without optimal EVCS demand.

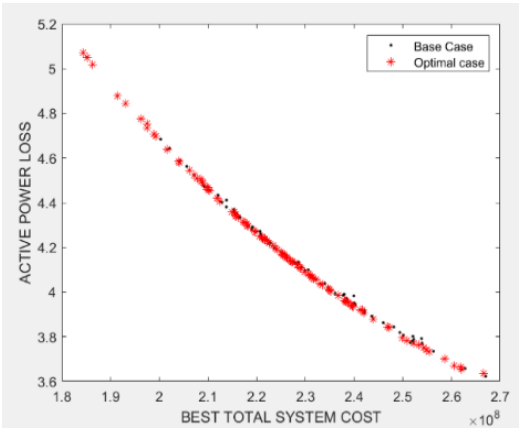

(a) IEEE14

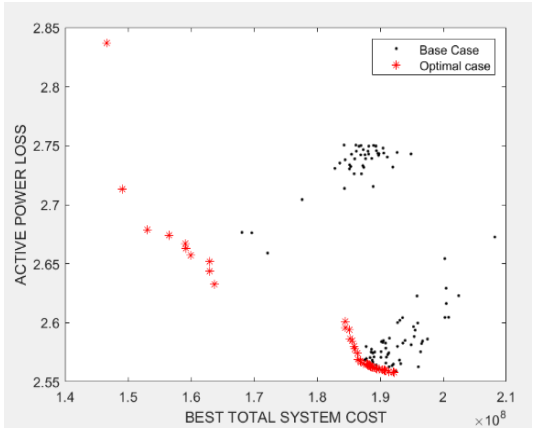

(b) IEEE 30

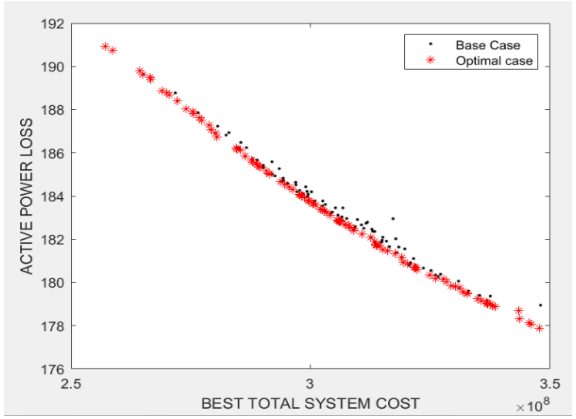

(c) IEEE 118

Figure 5.4. Best Total System Cost at Buses without optimal EVCS demand

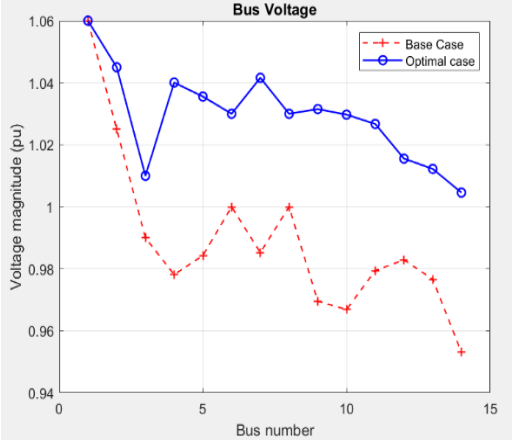

(a) IEEE14

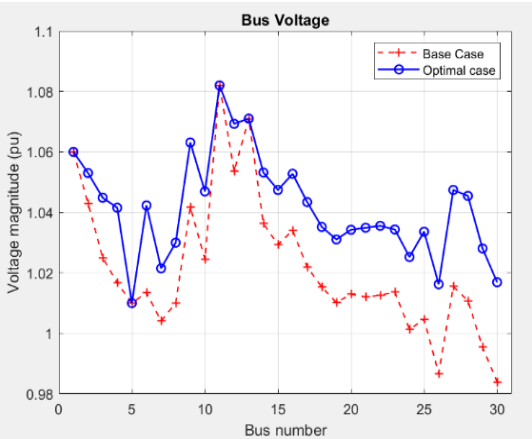

(b) IEEE 30

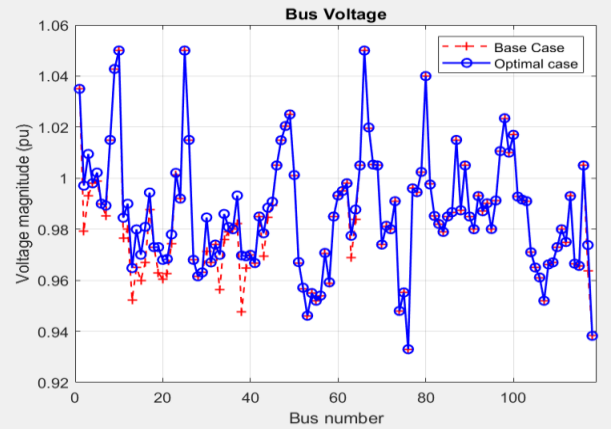

(c) IEEE 118

Figure 5.5. Voltage profile at Buses without optimal EVCS demand

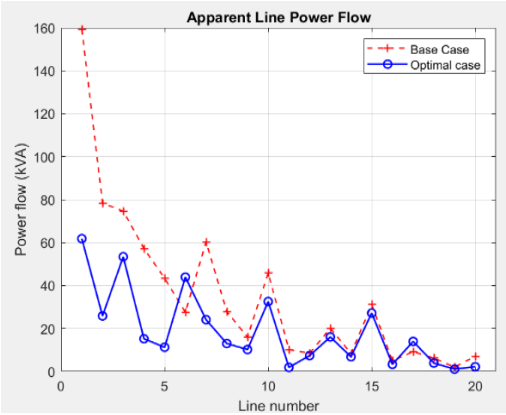

(a) IEEE14

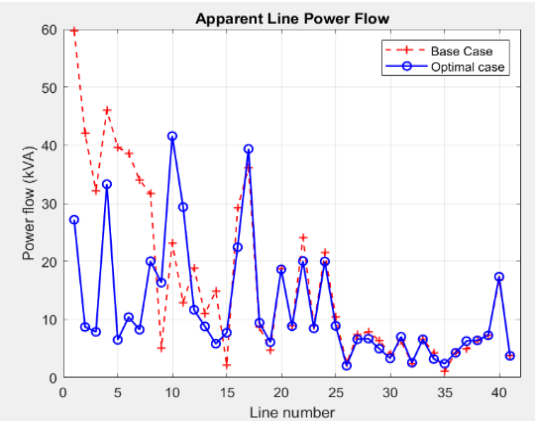

(b) IEEE 30

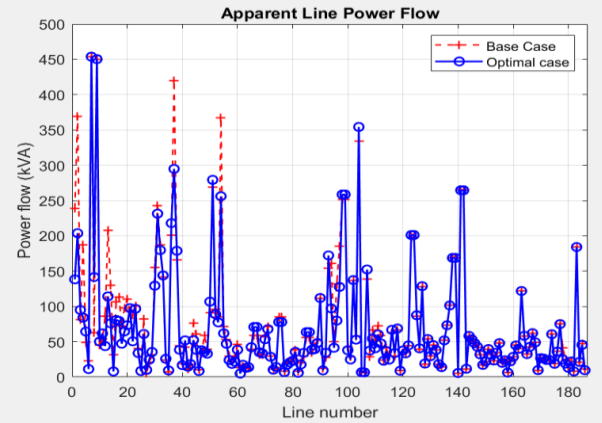

(c) IEEE 118

Figure 5.6. Apparent Line Power Flow without optimal EVCS demand

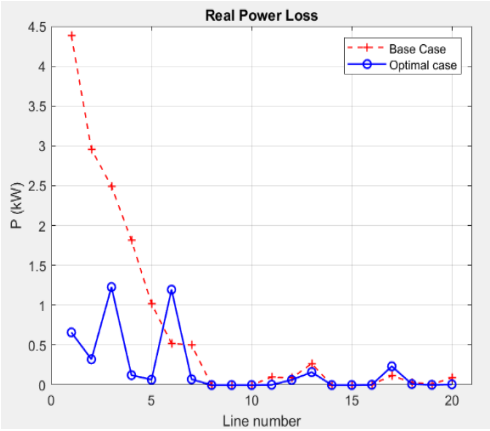

(a) IEEE14

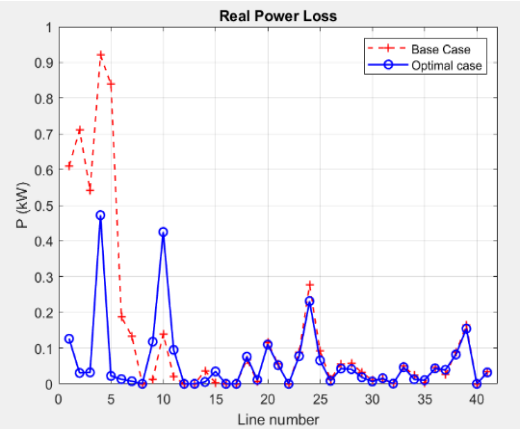

(b) IEEE 30

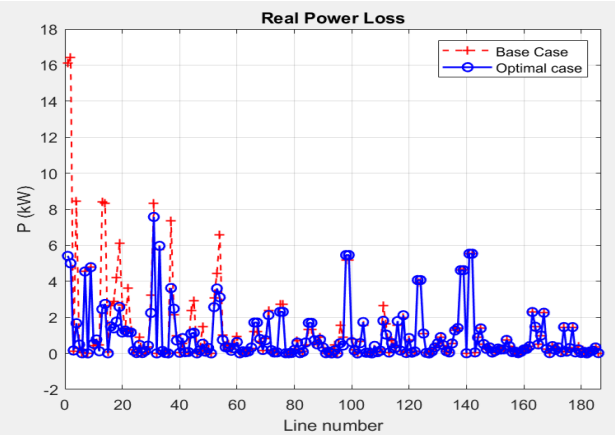

(c) IEEE 118

Figure 5.7. Real Power Loss without optimal EVCS demand

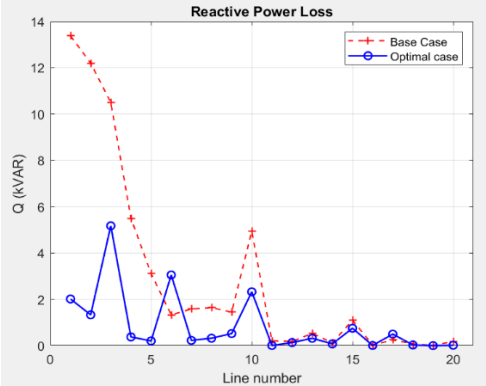

(a) IEEE14

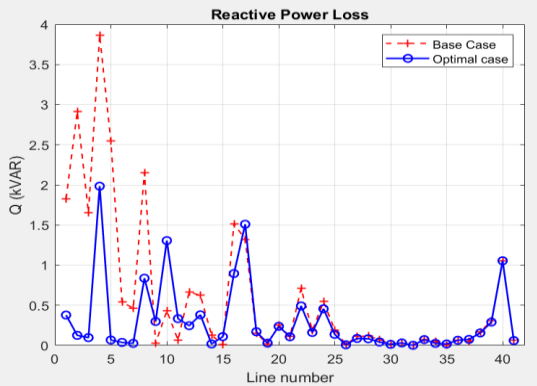

(b) IEEE 30

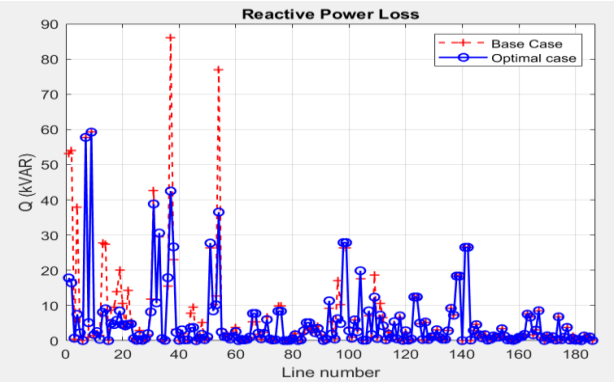

(c) IEEE 118

Figure 5.8. Reactive Power Loss without optimal EVCS demand

5.9 Validation of optimal active–reactive power flow considering RESs and EVCS using PSO algorithm on IEEE 14, IEEE 30 and IEEE 118 bus network

This section uses an IEEE 14-bus, IEEE 30-bus and IEEE 118-bus testbeds network for validation of optimal active–reactive power flow considering RESs with EV charging stations using PSO algorithm. The generator system transmission lines data, power flow data, and dynamic load data may be found in (Illinois Center for a Smarter Electric Grid, 2013). However, EV charging station dynamic load demands negative impact on power distribution network cannot be overlooked. This thesis analyses how EV charging station load affects IEEE testbeds network technical and cost factors. This thesis thoroughly examined the EV charging stations impact on total system cost, bus voltage, and apparent line real and reactive power loss in this chapter using grid-tied Solar PV data and grid-tied wind turbines with EVCS loading. Key conclusions are presented. The IEEE 14-bus test system can endure five charging stations on buses 4, 5, 7, 9, and 10, while the IEEE 30-bus test system can endure five charging stations on 4, 6, 9,12, and 28, IEEE 118-bus on 8, 26, 30, 38 and 63 are the system's strongest bus. Distributing EVCS across numerous buses improved voltage variations, and reduced power loss while combining robust distribution nodes allows for greater accessibility to EV's dependability and compared to a single bus. This will alleviate high traffic concentrations on bus routes with concentrated EVCSs.

5.9.1 IEEE 14 bus test system

The IEEE 14-bus test case is a simple approximation of the American Electric Power System. It contains 14 buses, 5 generators, and eleven loads. The analysis was performed on the IEEE 14-bus test system. The IEEE 14-bus test case is a radial network a simplified representation of the network's branch and line data that were sourced from literature. The solar PV demand for under various loading factors increases as the bus voltage deviates from its fundamental values.

5.9.2 IEEE 30 bus test system

The IEEE 30-bus test case is a basic model of the American Electric Power system. The corresponding system contains 30 buses, six generators, and three synchronous condensers. Each generator is characterized as a voltage source, with 10 Ohms impedance. Each source's properties, use a [100 MVA] base per unitizing. In this experiment, an IEEE 30-bus distribution testbeds was investigated and assessed, and the steps were taken throughout testing in sequential order. The distribution systems

significance rests in their ability to enhance voltage profiles, reduce power losses, and increase system load capability performance with optimal allocation of dispatched generations.

5.9.3 IEEE 118-bus test system

The IEEE 118-bus test case is the midwestern American Electric Power system representation model. The corresponding system contains 19 generators, 177 lines, 9 transformers, 35 synchronous condenser, and 91 loads.

5.9.4 IEEE 14, IEEE 30 and IEEE 118 bus test analytical algorithm

The standard IEEE 14-bus, 30-bus and 118-bus testbeds are balanced three-phase loop systems made up of 14 buses, 20 branches, 30 buses, 32 branches and 118 buses, 177 branches respectively. t is believed that all loads are supplied by the substation at node i. The loads for one segment are located at the end of each section. This proposed system, like any other power system, consists of nodes or buses associated with four distinct quantities: magnitude of voltage, phage angle of voltage, active or real power, and reactive power. Four of these numbers are presented, while the other two require an equation solution. This system is commonly used for both voltage stability and low-frequency oscillatory stability studies. Unlike previous systems, the 30-bus and 118-bus test case has no line limitations. It also has a low base voltage and plenty of voltage control options. According to the aforementioned equations, the analytical algorithm is as follows:

Step 1: The first step is to number all of the system's nodes from 14, 30 and 118 Node 1 is the reference node.

Step 2: Replace equivalent current sources with generators admittance.

Step 3: Detect all bus kinds and numbers using the bus data provided by the IEEE standard bus testbeds, then set all bus voltages to an initial value.

Step 4: Calculate the required parameters as follows.

1. Calculate the actual and reactive power for each bus.
2. Determine the bus voltage and voltage angle.
3. Update voltage magnitude (V) and angle.
4. Increase the iteration counter (iter = iter + 1).
5. If the number of iterations is less than the maximum, go to step 2.
6. Evaluate the power flow solution and determine line flow and losses.

The study used two different test systems consisting of 14 and 30 buses. The goal is to be able to observe the impact of EV charging stations in networks of varying sizes.

Tables 5.5, 5.6, and 5.7 illustrate the loads for 14-bus, 30-bus, and 118-bus systems, respectively. Power system analysis uses per-unit system values. This system is constructed by proportioning real physical quantities to certain values based on load values. As a result, the values utilized to analyze power systems will be smaller, making the study easier. The actual system values can be determined by using the base values specified in the simulation scripts.

Table 5.5. Load bus data for the IEEE 14-bus testbed using NR method (Al-Roomi, 2015; Olcay et al., 2023)

	Without EVCS Demand (kW)		**With EVCS Demand (kW)**	
Bus	**Pload (p.u.) PLi**	**Qload (p.u.) QLi**	**Pload (p.u.) PLi**	**Qload (p.u.) QLi**
1	0	0	0	0
2	0.217	0.217	0.217	0.127
3	0.0942	0.191	0.094	0.019
4	0.478	-0.039	0.5518	0.050
5	0.076	0.016	0.5518	0.050
6	0.112	0.075	11.2	7.5
7	0	0.109	0.1119	0.0251
8	0	0	0.0	0.0
9	0.295	0	0.4614	0.094
10	0.09	0.166	0.4774	0.100
11	0.035	0.058	0.0035	0.0018
12	0.061	0.016	0.0614	0.016
13	0.135	0.058	0.0135	0.058
14	0.149	0.050	0.0149	0.0050

Table 5.6. IEEE 30-bus Load data using the NR method (Al-Roomi, 2015; Olcay et al., 2023)

	Without EVCS Demand (kW)		**With EVCS Demand (kW)**	
Bus	**Pload (p.u.) PLi**	**Qload (p.u.) QLi**	**Pload (p.u.) PLi**	**Qload (p.u.) QLi**
1	0	0	0	0
2	0.217	0.127	0.217	0.127
3	0.024	0.012	0.024	0.012
4	0.076	0.016	0.5518	0.050
5	0.942	0.19	0.942	0.19
6	0	0	0.5518	0.050
7	0.228	0.109	0.228	0.109
8	0.3	0.3	0.3	0.3

9	0	0	0.119	0.0251
10	0.058	0.02	0.058	0.02
11	0	0	0	0
12	0.112	0.075	0.4614	0.097
13	0	0	0	0
14	0.062	0.016	0.062	0.016
15	0.082	0.025	0.082	0.025
16	0.035	0.018	0.035	0.018
17	0.09	0.058	0.09	0.058
18	0.032	0.009	0.032	0.009
19	0.095	0.034	0.095	0.034
20	0.022	0.007	0.022	0.007
21	0.175	0.112	0.175	0.112
22	0	0	0	0
23	0.032	0.016	0.032	0.016
24	0.087	0.067	0.087	0.067
25	0	0	0	0
26	0.035	0.023	0.035	0.023
27	0	0	0	0
28	0	0	0.4774	0.100
29	0.024	0.009	0.024	0.009
30	0.106	0.019	0.106	0.019

Table 5.7. IEEE 118-bus selected Load data using the NR method (Al-Roomi, 2015; Olcay et al., 2023)

	Without EVCS Demand (kW)		**With EVCS Demand (kW)**	
Bus	**Pload (p.u.) PLi**	**Qload (p.u.) QLi**	**Pload (p.u.) PLi**	**Qload (p.u.) QLi**
1	0.5414	0.0866	0.5414	0.0866
2	0.4140	0.1062	0.4140	0.1062
3	0.2123	0.0955	0.2123	0.0955
4	0.2123	0.0849	0.5518	0.050
5	0.4989	0.1962	0.4989	0.1962
8	0.7431	0.2442	0.5518	0.050
10	0.2654	0.1062	0.119	0.0251
25	0.26369	0.3609	0.5518	0.050
26	0.1911	0.0318	0.1911	0.0318

30	0.1486	0.0849	0.4614	0.097
37	0.1062	0.0531	0.4614	0.097
38	0.0743	0.0318	0.5518	0.050
63	0.6600	0.2000	0.4614	0.097
64	0.6800	0.2700	0.4614	0.097
68	0.4700	0.1100	0.5518	0.050
71	0.3300	0.1500	0.119	0.0251
81	0.6800	0.3600	0.5518	0.050
87	0.7100	0.2600	0.5518	0.050
111	0.3900	0.3200	0.4614	0.097

5.10 Results of IEEE Distribution Test Bus with RESs and EVCS (NHTS, 2024)

We investigated the effect of EV charging on daily load demand and developed a PSO method for optimizing charging operations. This study looks at the negative impacts of EV charging stations on the distribution network, including as overall system cost, bus voltage, apparent line real, and reactive power loss. To achieve optimal system performance, the power flow analysis for the IEEE 14, IEEE 30, and IEEE 118 bus testbeds considers voltage magnitudes, active and reactive powers, as well as generation and load costs.

5.10.1 Test system 1: IEEE 14 using zero cost coefficients for RESs and Monte Carlo cost coefficients for RESs with optimal EVCS load demand

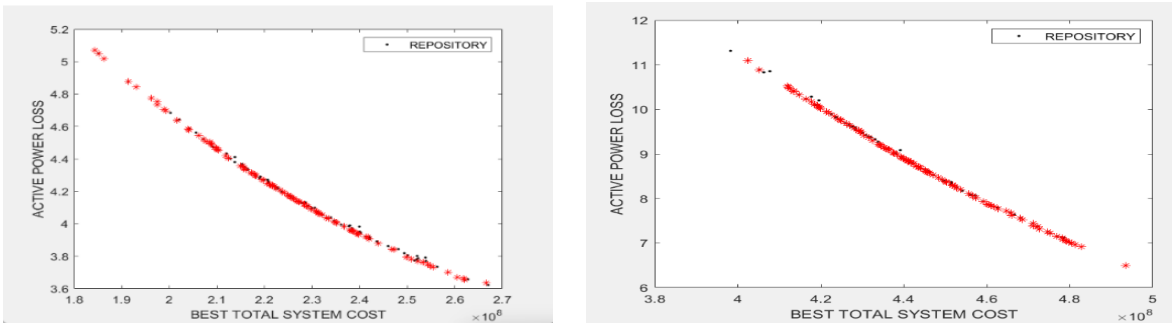

(a) (b)

Figure 5.9. *IEEE 14 Best Total System Cost at Buses with optimal EVCS load demand (a) using zero cost coefficients for RESs (b) using Monte Carlo uncertainty cost coefficients for RESs.*

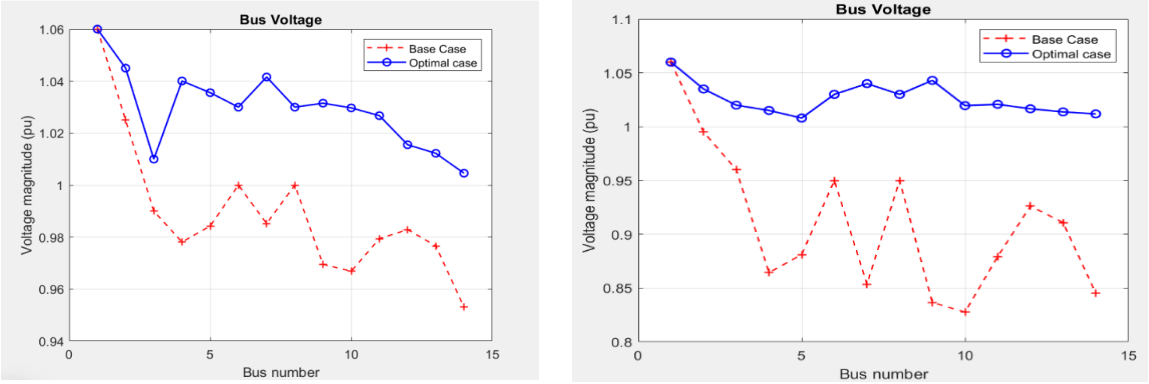

(a) (b)

Figure 5.10. *IEEE 14 Bus Voltage profile with optimal EVCS load demand (a) using zero cost coefficients for RESs (b) using Monte Carlo uncertainty cost coefficients for RESs*

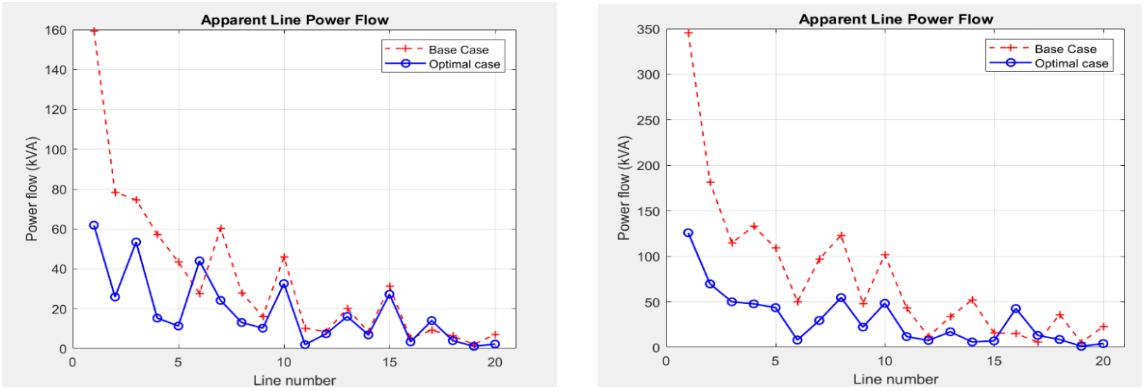

(a) (b)

Figure 5.11. IEEE 14 Apparent Line Power Flow with optimal EVCS load demand (a) using zero cost coefficients for RESs (b) using Monte Carlo uncertainty cost coefficients for RESs

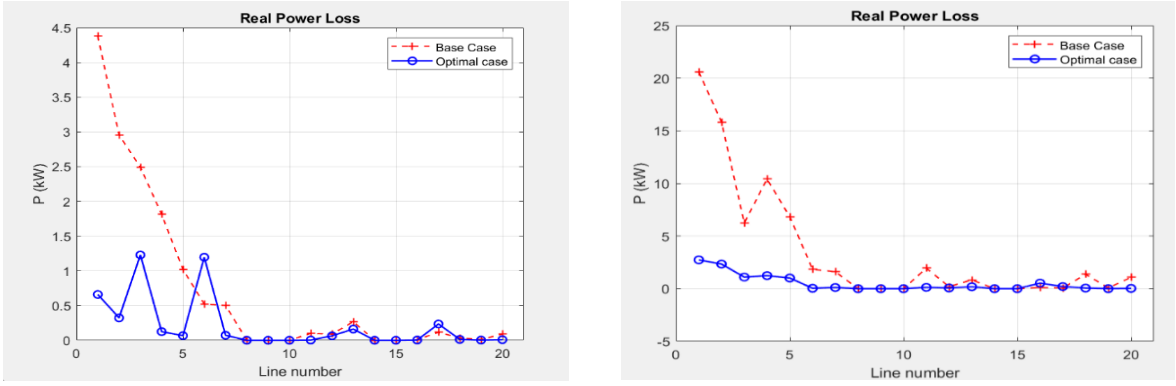

(a) (b)

Figure 5.12. IEEE 14 Real Power Loss with optimal EVCS load demand (a) using zero cost coefficients for RESs (b) using Monte Carlo uncertainty cost coefficients for RESs

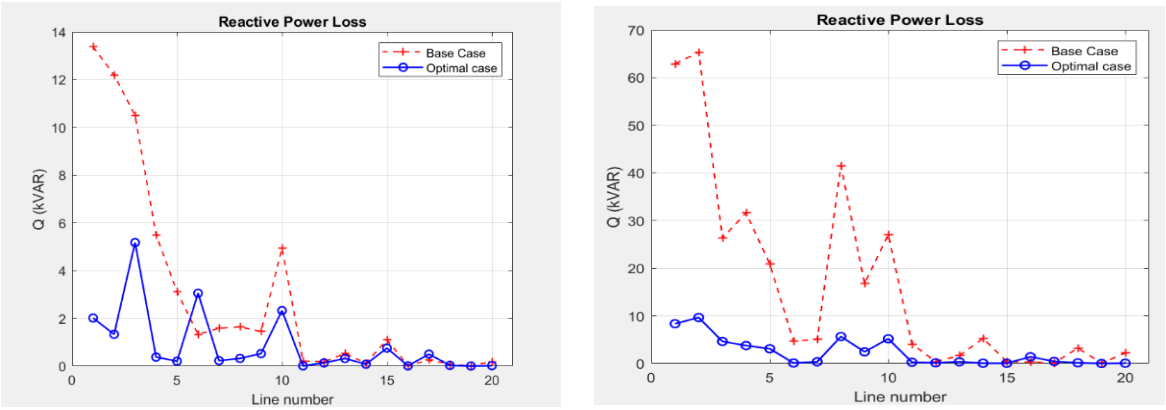

(a) (b)

Figure 5.13. IEEE 14 Reactive Power Loss with optimal EVCS load demand (a) using zero cost coefficients for RESs (b) using Monte Carlo uncertainty cost coefficients for RESs

5.10.2 Results of IEEE 14-bus testbed without using and using RESs Data

The real power loss at IEEE 14-bus without using RESs data is 14.394 kW and IEEE 14 bus using RESs data 16.157 kW respectively, a drop of 1.763 kW in the bus. The reactive power loss at IEEE 14 bus without using RESs data is 3.889 kVAR and IEEE 14 bus using RESs data 58.308 kVAR respectively, a significant increase of 54.419 kVAR in the bus (Table 5.8).

Table 5.8. Compared Results of IEEE 14-bus testbed

IEEE 14 without using RESs Data	IEEE 14 using RESs Data
BestSolution = $ 235,920,000	BestSolution = $ 226,070,000
Total Qloss = 3.889 kVAR	Total Qloss = 58.308 kVAR
Total Ploss = 16.157 kW	Total Ploss = 14.394 kW

5.10.3 Discussion of Results of IEEE 14-bus testbed without using and using RESs Data

The proposed work is tested on the IEEE 14 bus testbed system with charge criteria for each region consider the number of EVs at charging stations. DC and AC chargers were used to meet the demands of these EVCS. Charge profiles for buses 4, 5, 7, 9, and 10 are modified based on infrastructure requirements and EV numbers. Direct load flow analysis determines voltage and power losses in the distribution network. The best cost is 235,920 million dollars without using RESs data and 226,07 million dollars, a gain of 9,850 million dollars. The system's true power loss is 16.157 kW without using RESs data and 14.394 kW using RESs data, improvement of 1.763 kW, 10.91% real power savings. The reactive power loss of 3.889 kVAR without using RESs and 58.308 kVAR using RESs data, negative of 54.419 kW, 0.93%. The negative reactive power created indicates that reactive power is flowing from grid-tied RESs (caused by EV batteries) to

the generator, which is equivalent to transferring power from EVCS to a capacitive load. Installing EVCSs leads to increased power losses in the system. RESs are deployed in the system to offset power losses.

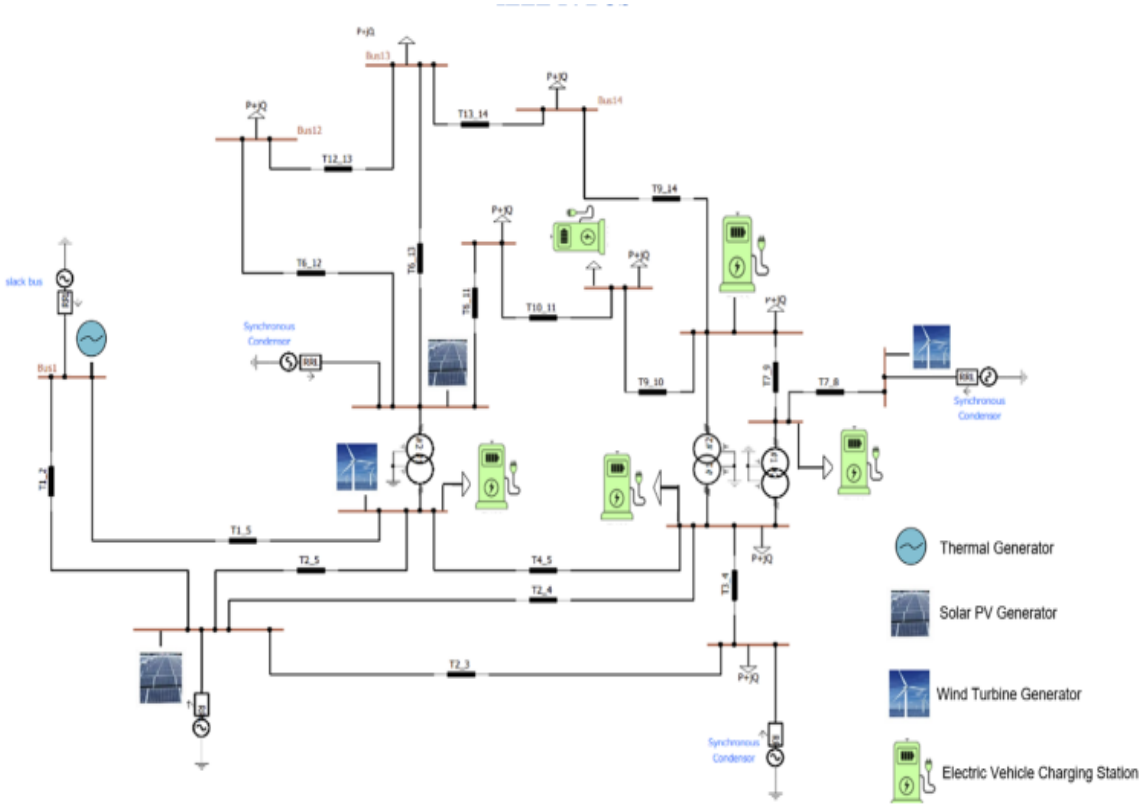

Figure 5.14: Simulated Model of IEEE 14-bus system with Optimal RESs and EV Location

5.10.4 Test system 2: IEEE 30 using Monte Carlo cost coefficients for RESs with optimal EVCS load demand

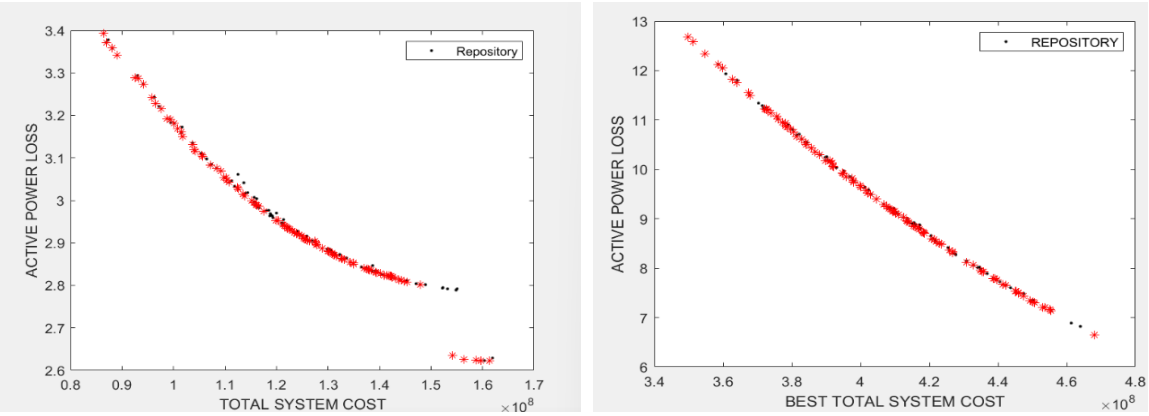

(a) (b)

Figure 5.15. IEEE 30 Best Total System Cost at Buses with optimal EVCS load demand (a) using zero cost coefficients for RESs (b) using Monte Carlo uncertainty cost coefficients for RESs

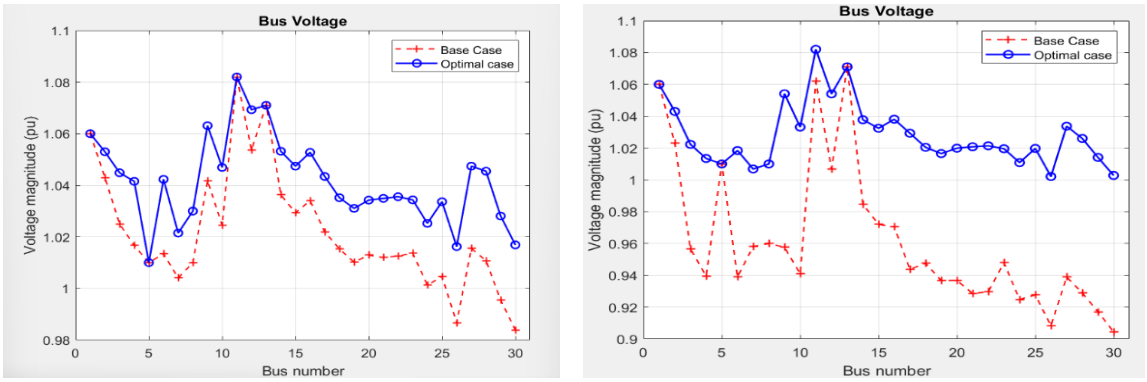

(a) (b)

Figure 5.16. IEEE 30 Bus Voltage profile with optimal EVCS load demand (a) using zero cost coefficients for RESs (b) using Monte Carlo uncertainty cost coefficients for RESs

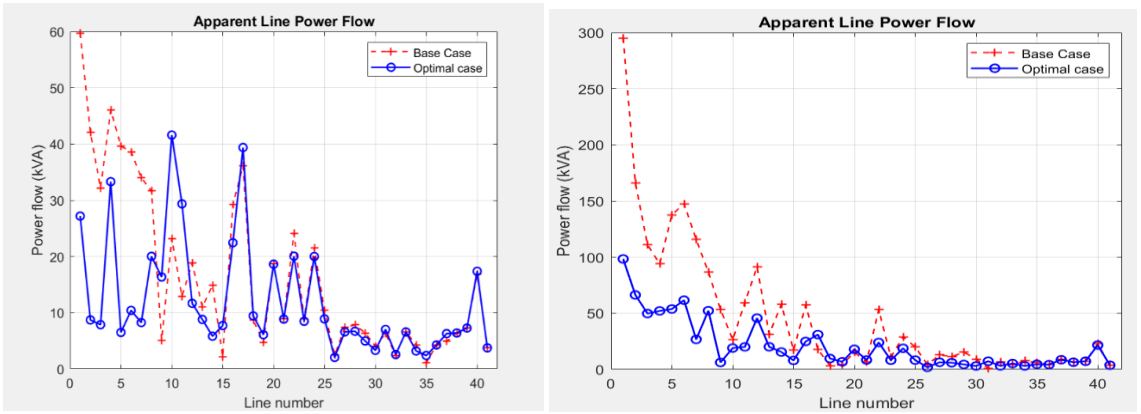

(a) (b)

Figure 5.17. IEEE 30 Apparent Line Power Flow with optimal EVCS load demand (a) using zero cost coefficients for RESs (b) using Monte Carlo uncertainty cost coefficients for RESs

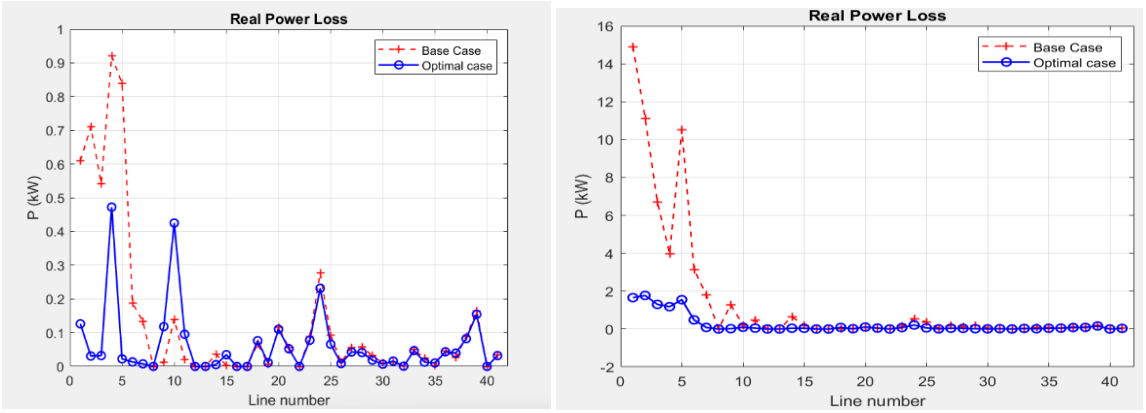

(a) (b)

Figure 5.18. IEEE 30 Real Power Loss with optimal EVCS load demand (a) using zero cost coefficients for RESs (b) using Monte Carlo uncertainty cost coefficients for RESs

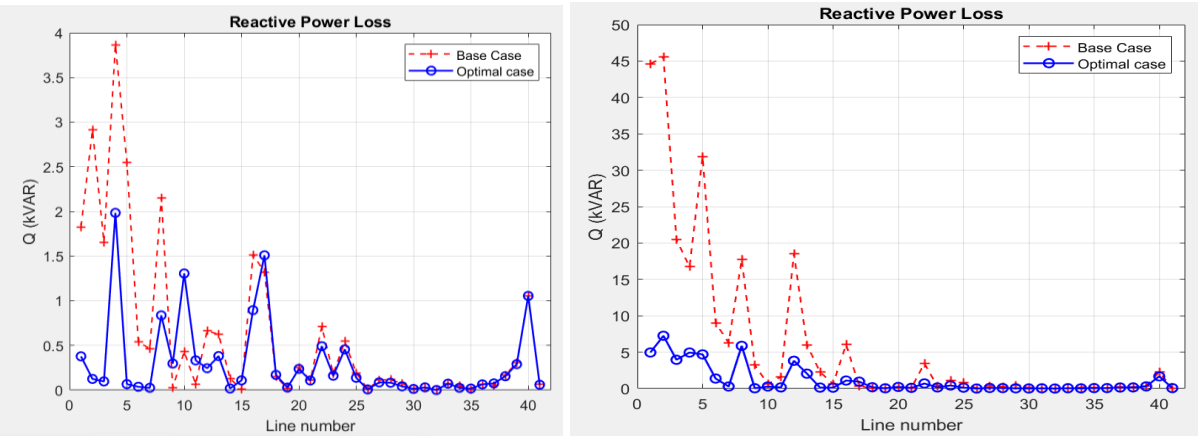

(a) (b)

Figure 5.19. IEEE 30 Reactive Power Loss with optimal EVCS load demand (a) using zero cost coefficients for RESs (b) using Monte Carlo uncertainty cost coefficients for RESs

5.10.5 Results of IEEE 30-bus testbed without using and using RESs Data

The real power loss at IEEE 30 bus without using RESs data is 58.308 kW and IEEE 30 bus using RESs data 5.470 kW respectively, a significant power loss of 52.838 kW in the bus. The reactive power loss at IEEE 30 bus without using RESs data is 14.394 kVAR and IEEE 30 bus using RESs data 25.120 kVAR respectively, an increase of 10.816 kVAR in the bus system (Table 5.9).

Table 5.9. Compared Results of IEEE 30-bus system

IEEE 30 without using RESs Data	**IEEE 30 using RESs Data**
Best Cost = $ 8,077,900	Best Cost = $ 190.560,000
Total Qloss = 14.394 kVAR	Total Qloss = 25.120 kVAR
Total Ploss 58.308 kW	Total Ploss 5.470 kW

5.10.6 Discussion of Results of IEEE 30-bus testbed without using and using RESs Data

The proposed work is tested on the IEEE 30 bus testbed system with charge criteria for each region consider the number of EVs at charging stations. DC and AC chargers were used to meet the demands of these EVCS. Charge profiles for buses 4, 6, 9,12, and 28 are modified based on infrastructure requirements and EV numbers. Direct load flow analysis determines voltage and power losses in the distribution network. The best cost is 8,077.9 million dollars without using RESs data and 190,560 million dollars, a loss of 182,482,100 million dollars. The system's true power loss is 58.838 kW without using RESs data and 5.470 kW using RESs data, improvement of 53.368 kW, 9.07% real power savings. The reactive power loss of 14.394 kVAR without using RESs and 25.120 kVAR using RESs data, negative of 10.726 kVAR, 74.517%. The negative reactive power

created indicates that reactive power is flowing from grid-tied RESs (caused by EV batteries) to the generator, which is equivalent to transferring power from EVCS to a capacitive load. Installing EVCSs leads to increased power losses in the system. RESs are deployed in the system to offset power losses.

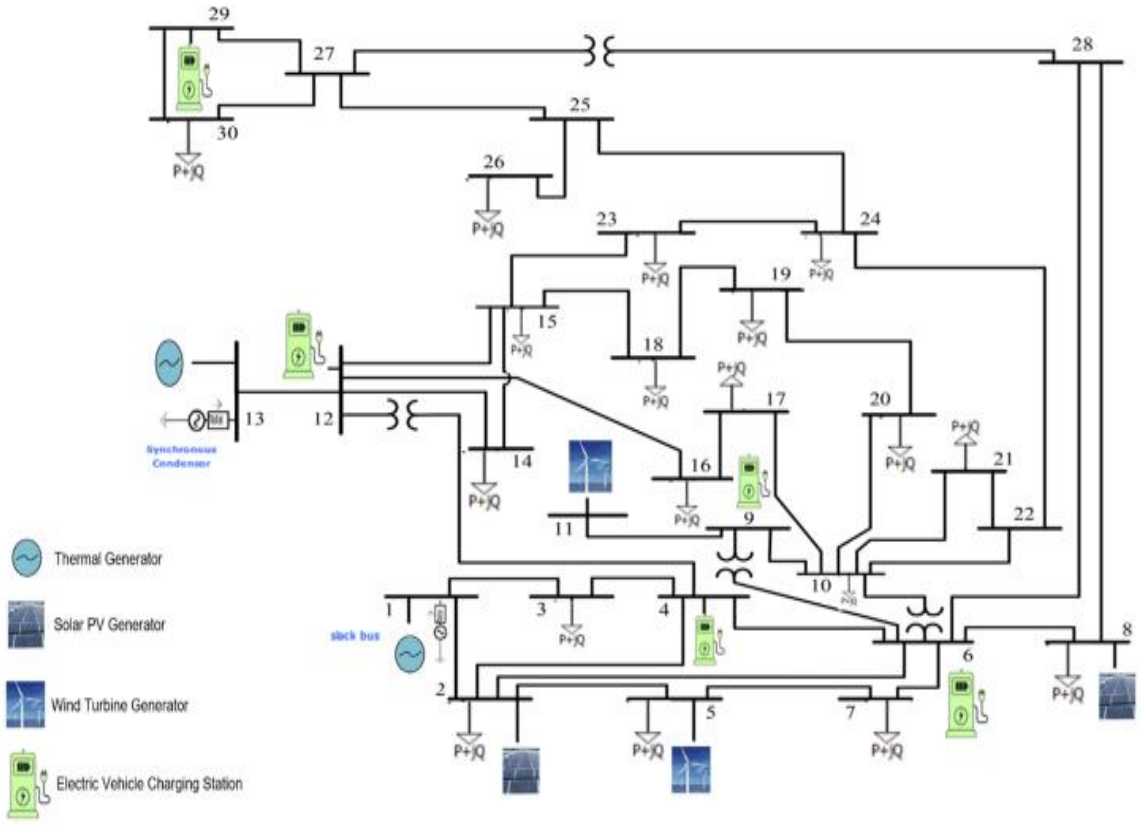

Figure 5.20: Simulated Model of IEEE 30-bus with Optimal RESs and EV Location

5.10.7 Test system 3: IEEE 118 using Monte Carlo uncertainty cost coefficients for RESs with optimal EVCS load demand

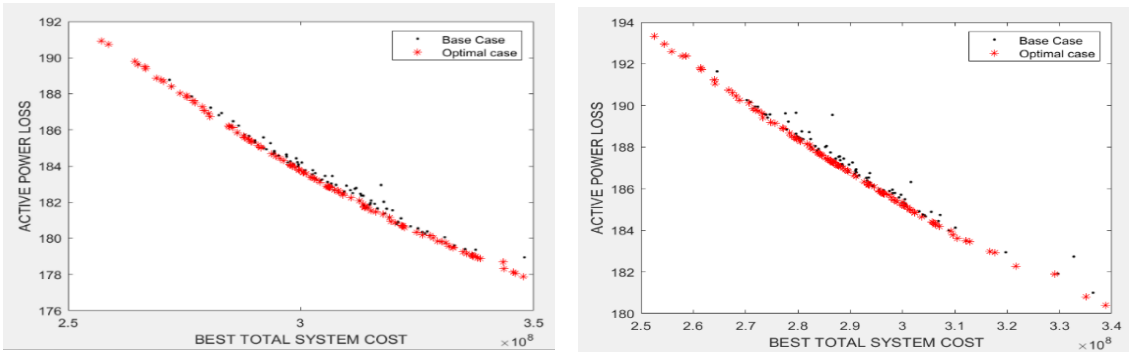

(a) (b)

Figure 5.21. IEEE 118 Best Total System Cost at Buses with optimal EVCS load demand (a) using zero cost coefficients for RESs (b) using Monte Carlo uncertainty cost coefficients for RESs

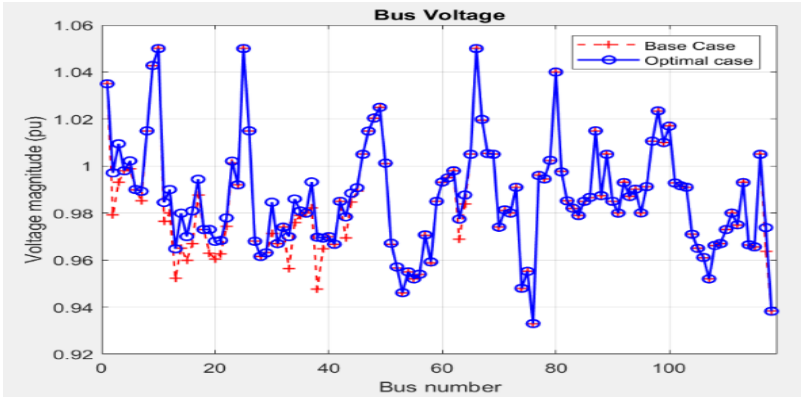

(a)

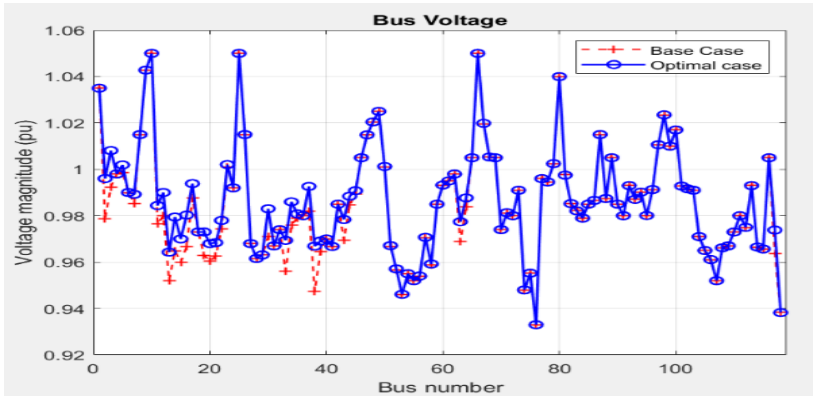

(b)

Figure 5.22. IEEE 118 Bus Voltage profile with EVCS loading demand (a) using zero cost coefficients for RESs (b) using Monte Carlo uncertainty cost coefficients for RESs

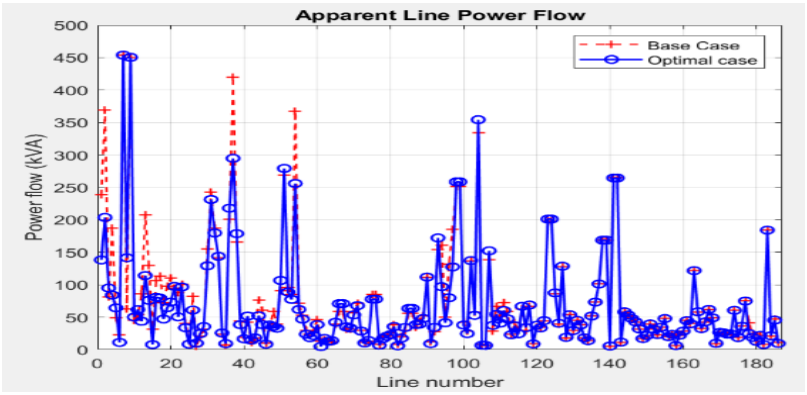

(a)

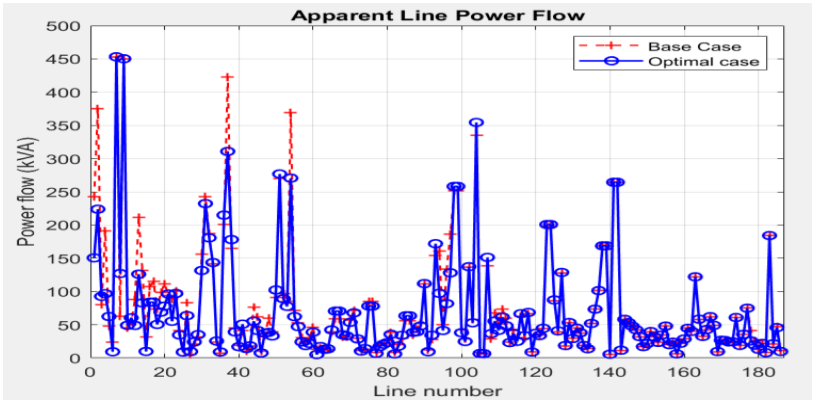

(b)

Figure 5.23. IEEE 118 Apparent Line Power Flow with optimal EVCS load demand (a) using zero cost coefficients for RESs (b) using Monte Carlo uncertainty cost coefficients for RESs

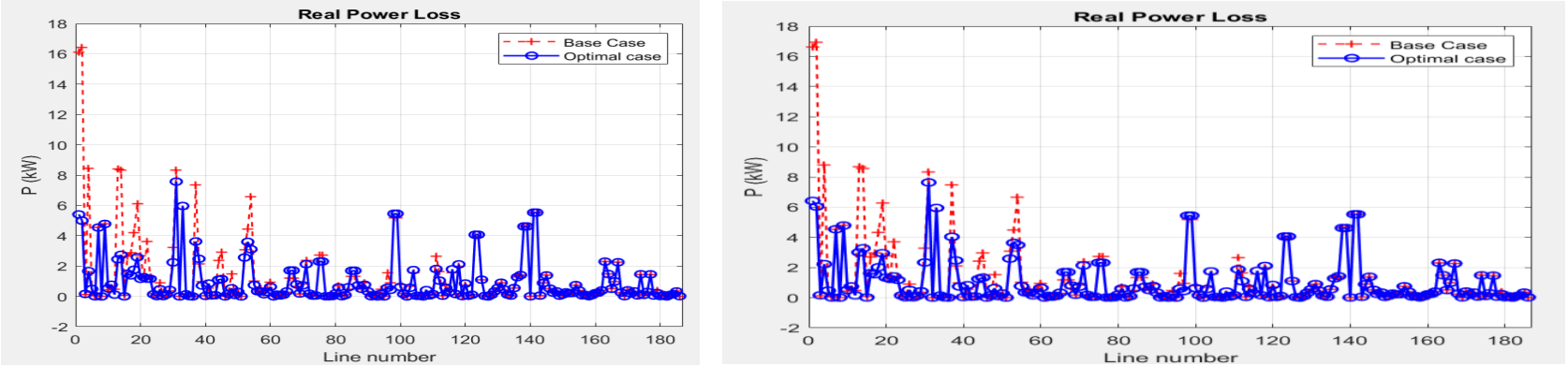

(a) (b)

Figure 5.24. IEEE 118 Real Power Loss with optimal EVCS load demand (a) using zero cost coefficients for RESs (b) using Monte Carlo uncertainty cost coefficients for RESs

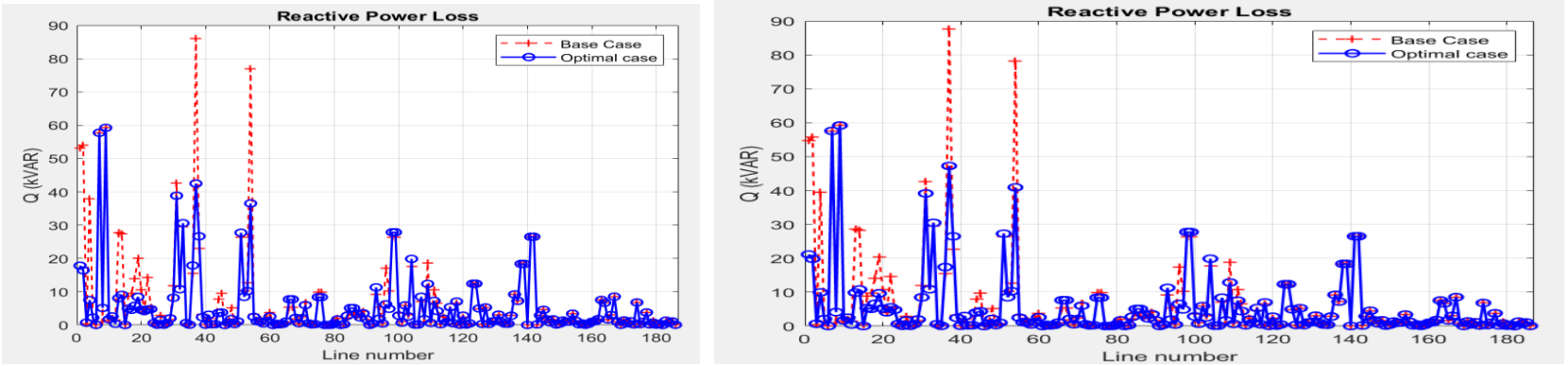

(a) (b)

Figure 5.25. IEEE 118 Reactive Power Loss with optimal EVCS load demand (a) using zero cost coefficients for RESs (b) using Monte Carlo uncertainty cost coefficients for RESs

5.10.8 Results of IEEE 118-bus testbed without using and using RESs Data

The real power loss at IEEE 118 bus without using RESs data is 250.606 kW and IEEE 118 bus using RESs data 253.489 kW respectively, a very low power loss of 28 kW in the bus. The reactive power loss at IEEE 118 bus without using RESs data is 1293.525 kVAR and IEEE 118 bus using RESs data 1305.845 kVAR respectively, a significantly low reactive loss of 120 kVAR in the bus system (Table 6.0).

Table 5.10. Compared Results of IEEE 118-bus testbed

IEEE 118 without using RESs Data	**IEEE 118 using RESs Data**
Best Cost = $ 269,630,000.0	Best Cost =$ 289,480,000
Total Qloss = 1,293.525 kVAR	Total Qloss = 1,305.845 kVAR
Total Ploss = 250.606 kW	Total Ploss = 253.489 kW

5.10.9 Discussion of Results of IEEE 118-bus testbed without using and using RESs Data

The proposed work is tested on the IEEE 118 bus testbed system with charge criteria for each region consider the number of EVs at charging stations. DC and AC chargers were used to meet the demands of these EVCS. Charge profiles for buses 8, 26, 30, 38 and 63 are modified based on infrastructure requirements and EV numbers. Direct load flow analysis determines voltage and power losses in the distribution network. The best cost is 269.63 million dollars without using RESs data and 289.48 million dollars, a loss of 19,85 million dollars. The system's true power loss is 250.606 kW without using RESs data and 253.489 kW using RESs data, loss of 2.883 kW, 1.15% real power losses. The reactive power loss of 1293.525 kVAR without using RESs and 1305.845 kVAR using RESs data, negative of 12.320 kW, 0.0009%. The negative reactive power created indicates that reactive power is flowing from grid-tied RESs (caused by EV batteries) to the generator, which is equivalent to transferring power from EVCS to a capacitive load. Installing EVCSs leads to increased power losses in the system. RESs are deployed in the system to offset power losses.

5.11 Chapter Summary

This chapter present PSO method for hybrid system energy management of an electric vehicle charging station. The created PSO technique has effectively demonstrated a reduction in operational total costs of EVCS load modeling by employing manageable variables such as the number of EVs charging concurrently, total charging current, arrival rate, and parking rate time. The study also investigated the contribution of such EVCS loads to demand response and their integration into the distribution system operations

framework. The controlled EVCS load profile was obtained using a line-up model that considered different classes of electric vehicles, arriving/parking at EVCS offices as a non-homogeneous, and determining the charging load for each EV. The optimal charging decisions were combined with the EVCS charging load model from a distribution bus optimal operations model. The target functions studied were decreasing overall EVCS distribution feeder losses and maximizing the number of EVs charged concurrently, as represented by the EVCS owner's perspective. The chapter discussed EVCS controlled operation loading and its contribution to demand response using IEEE 14-bus, IEEE 30-bus, and IEEE 118-bus distribution systems as test cases. The study found that the EVCS owner's goal of boosting the number of EVs charged concurrently can result in bus voltage fluctuations and substantial EVCS distribution feeder losses while requiring additional EVs to charge. The distribution of electric vehicle charging stations was more advantageous in terms of voltage fluctuations and power loss over multiple buses than in a single bus. In some cases, when distribution network strong nodes and road network nodes with high traffic concentrations are combined, the routes leading to that node become crowded. The results from the study shows that the real power loss at IEEE 14 without or with RESs data with EVCS load at 1.763 kW, with reactive power loss at IEEE 14 without or with RESs data with EVCS load at 54.419 kVAR. The real power loss at IEEE 30 without or with RESs data without or with EVCS load at 52.838 kW with reactive power loss at IEEE 30 using RESs data with EVCS load at 10.816 kVAR. The real power loss at IEEE 118 without or with RESs data without or with EVCS load at 0.028 kW with reactive power loss at IEEE 118 using RESs data with EVCS load at 0.012 kVAR. The compared results are

For IEEE 14

i. A gain of 9,850 million dollars.
ii. Real power loss improvement of 1.763 kW, 10.91% real power savings.
iii. Negative reactive power of 54.419 kW, 0.93%.

For IEEE 30

i. A loss of 182,482,100 million dollars.
ii. Real power loss improvement of 53.368 kW, 9.07% real power savings.
iii. Negative reactive power of 10.726 kVAR, 74.517%.

For IEEE 118

i. A loss of 19,85 million dollars was realised in IEEE 118 simulation.
ii. Real power loss of 2.883 kW, 1.15%.

iii. Negative reactive power of 12.320 kVAR, 0.0009%kW, 0.0009%.

From the values, it shows that IEEE 14 system enables the optimization of operational cost gain and real power loss improvements with less reactive losses. Its applications will contribute to a judicious and cost-effective deployment strategy for the optimization effect of the PSO approach for inclusion in the economic dispatch of renewable energy production plants.

CHAPTER SIX

CONCLUSION AND FUTURE RECOMMENDATIONS

6.1 Introduction

The foundation for the work developed and presented in this thesis was laid by means of a thorough state-of-the-art investigation of the problem formulation and solution techniques for hybrid energy management systems with electric vehicles considering both classical (MINLP) and heuristic (PSO) optimization methods. Chapter 3 presents the developed MINLP method to solve grid-tied RES hybrid system network objective functions and constraint limitations for economic power dispatch problems. The developed MINLP algorithms can minimize total operational costs and grid dependency while also optimizing grid voltage and power flow and maximizing renewable energy sources used by electric vehicle charging stations. The proposed approach, which is based on energy management of hybrid system strategies for grid-tied RES systems, is capable of resolving EVCS loading strategies through evaluation of optimal active and reactive power losses for likely voltage and EVCS loading in grid-tied RES. Chapter 4 introduces the Particle Swarm Optimisation method and outline how it was developed for the EPD problem. The algorithm is tested using multiple IEEE 14-bus, IEEE 30-bus and IEEE 118-bus test benchmark models in the Matlab environment. Chapter 5 provides the PSO method for a hybrid system with an electric vehicle charging station. The developed PSO method has successfully demonstrated an operational total cost reduction of EVCS load modeling of using manageable EVs number variables being total charging current, charged concurrently, arrival rate, and parking rate time. Chapter 6 discusses the thesis conclusion and concludes with thesis results, future work, and a list of author publications.

6.2 Aim and Objectives of the research

The thesis developed PSO & MINLP method for hybrid system energy management algorithms of electric vehicle charging stations is outlined in the following objectives:

1. Analyse hybrid system energy management algorithms of EV charging stations and develop a suitable hybrid system of an electric vehicle charging station.
2. To formulate the uncertainty cost function for RESs from the conducted literature review and investigate economic dispatch impacts on the solution.
3. Optimize active power, and power flow, and analyze the problem of lowering power losses by integrating grid/RES for the best possible output.

4. Minimize power losses on the distribution grid, due to non-linear behavior by adopting EVs as a more cost-effective method of transportation.
5. Particle swarm optimization and MINLP methods are developed for hybrid system energy management of an electric vehicle charging station to reach convergence quickly and accurately.
6. Use IEEE 14-bus, IEEE 30-bus and IEEE 118-bus testbed distribution networks to demonstrate developed PSO & MINLP methods validity for the suggested strategy in identifying optimal EV charging stations locations on the distribution grid.

These objectives have been accomplished, and are detailed in the previous chapters of this thesis. In the following section, the deliverables of the research as outlined in section 1.8 are presented.

6.3 Thesis deliverables

6.3.1 Comprehensive literature study and review of the main aspects of the optimization methods for the Hybrid energy management with Electric Vehicles

Chapter 2 of the thesis presents the energy management system as a crucial component of the smart grid that offers all the functionality required to guarantee the supply of energy at the lowest possible operational costs from generation, distribution, and transmission. The intermittent nature of RESs adds uncertainty to the hybrid system, reducing optimizing renewable generation profile usage, ensure grid stability, improve EVCS load profiles, and the enforced real-time equality constraint. The difficulties in achieving a high penetration rate for renewable energy sources include the need for prior knowledge of the underlying stochastic processes in the hybrid system state to achieve AI monitoring of electric vehicles. Electric vehicle-enabled hybrid systems present grid integration of renewable energy and optimal energy monitoring system scheme challenges, including instability, integrability, modularity, dependability, interoperability, and uncertainties like imprecise optimization of energy demand and generation. The review finding provides that Optimization-based energy management will offer artificial intelligence (AI) that needs autonomy, intellect, and proprietary protocols to interface with coordinated EV charging in a heterogeneous way. The grid-connected HS operates more steadily under unbalanced loading conditions in comparison to traditional grid-interfaced hybrid renewable energy systems.

6.3.2 Theoretical development and design of the algorithms used in solving the dispatch optimization problem of the grid-tied RES hybrid system

The Thesis developed MINLP & PSO algorithms to solve the economic dispatch of the grid-tied RES hybrid system, the detailed achieved deliverables of those two optimization methods is described in sections 6.3.2.1 and 6.3.2.2 respectively as follows:

6.3.2.1 MINLP method for the Economic dispatch of the grid-tied RES hybrid system

In Chapter 3, novel MINLP algorithm to solve grid-tied RES hybrid system network objective functions and constraint limitations has been developed for economic power dispatch problems. The MINLP algorithms were created to reduce total operating costs and grid dependency, consequently increasing grid voltage and power flow and maximizing renewable energy source use by electric vehicle charging stations. Based on the energy management of hybrid system strategies for grid-tied RES systems, the suggested approach to resolve EVCS loading strategies via optimal active and reactive power losses for determining the probable voltage and EVCS loading violations in grid-tied RES. The novel method is achieved by the MINLP problem decomposition of economic power dispatch nonlinear network optimization, which leads to an iterative process with MINLP solver variable constraints in each step and application of different P/Q/EPD modifications of RES units until the desired voltage profile and energy management requirements are met. The increase in electric vehicle usage requires charging stations' efficient design to provide appropriate charging rates. Combining on-site RES would reduce the stress on the grid, which can enhance charging station performance. In this thesis, a solar PV system is used in conjunction with the grid to power an electric vehicle. However, the PV is known for its intermittent nature, which is greatly controlled by terrain and weather. To compensate for solar PV's intermittent nature, an energy storage system is combined with PV in a grid-tied system to assure the stable operation of a hybrid PV-based charging station. In general, hybrid-source-based charging stations should be affordable, efficient, and dependable enough to meet the varying needs of EV loads in a variety of situations. These techniques include using ESS as backup storage when solar PV or wind turbine output is insufficient to fulfill load requirements. The best part of a hybrid system is that it maximizes energy efficiency by storing excess solar PV in the ESS or wind turbine energy. When the energy flow from solar PV and ESS is insufficient to satisfy the load requirement, the wind turbine is scheduled to compensate for the insufficiency subject to favour wind speed. By reducing excessive grid use, the hybrid system's techno-economic feasibility is maximized. This thesis develops and utilizes the MINLP approach to optimize on-site PV energy and

satisfy the changing load of EVs while considering the ESS's fast reaction and reducing grid stress. The proposed formulation tries to lower the predicted value of the overall operational cost.

6.3.2.2 PSO method for the Economic dispatch of the grid-tied RES hybrid system

Chapter 4 examines numerous approaches for the optimization of energy management of hybrid system EVCS, including meta-heuristics or evolutionary computation optimization methods for considering RESs and EVCS as applicable to the distribution network and the EV user approach with different objective functions, constraints, and their combinations. Hence, the review of the sizing approach and optimal citation for charging stations with EMSs and RESs integration to minimize the EV peak demand from the grid. In addition, different EVCS placement optimization strategies with objective functions are discussed. PSO method was adopted for EDP problem of a grid-tied RES-HS system, to minimize the operational costs while meeting limitations for non-contingency and contingency circumstances. The developed PSO method has successfully demonstrated an operational costs reduction of yearly maximum cost savings and substantial cost-benefit as shown in comparative results of simulated IEEE 14-bus, IEEE 30-bus and IEEE 118-bus test of generator units with buses and transmission lines system data. PSO method for energy management of the hybrid system of an electric vehicle charging station. The created PSO technique effectively confirmed an operational total cost reduction of EVCS load modelling by using manageable variables such as the number of EVs total charging current, charged concurrently, arrival rate, and parking rate time. The investigation also investigated the contribution of such EVCS loads to demand response and their integration into the distribution system operations framework. The target functions studied were decreasing overall EVCS distribution feeder losses and maximizing the number of EVs charged concurrently, as represented by the EVCS owner's perspective. The chapter discussed EVCS controlled operation loading and its contribution to demand response using IEEE 14-bus, IEEE 30-bus, and IEEE 118-bus distribution systems as test cases. The study found that the EVCS owner's goal of maximizing the number of EVs being charged concurrently can result in bus voltage variations and substantial EVCS distribution feeder losses, while requiring extra EVs to charge.

6.3.2.3 PSO method for the Economic dispatch of the grid-tied RES hybrid system with Electric Vehicles

Chapter 5 of the thesis investigates the EV charging impact on daily load demand and develops a PSO method to optimize charging operations. It considers total system cost, bus voltage, apparent line real, and reactive power loss for optimal system performance. Voltage-independent loads have less commutative voltage magnitude than voltage dependent loads, with active power generation more definite when voltage magnitude is greater than 1 p.u. Swing bus active power reduces power generation and operational cost, reliant on phase angle and voltage difference, difficult to predict without voltage-dependent loads integration. The reactive power difference in a generator bus is greater than the active power swing bus difference, affecting the EVCS load and voltage magnitudes. Load active power consumption varies between independent and voltage dependent loads, with voltage dependent loads consuming less power, promoting system stability and reducing power loss. Reactive power, a measure of voltage-dependent loads, varies across different buses and does not follow a specific pattern. Electric vehicle charging station distribution improves voltage deviation and power loss between buses, but merging strong nodes with high traffic concentration can cause congestion in routes. In dealing with EV charging stations optimal location problem, all the above-mentioned results voltage deviation, power loss reliability indices degradation with EV charging station loads must be considered. The novelty of the study is presented as formulation for EV charging stations optimal location problem with validation on IEEE 14 and IEEE 30 distribution network, which lies in the capability of considered power loss, voltage stability, and reliability formulation together under established the effectiveness of the using VSI index. The results from the study shows that the real power loss at IEEE 14 without or with RESs data with EVCS load at 1.763 kW, with reactive power loss at IEEE 14 without or with RESs data with EVCS load at 54.419 kVAR. The real power loss at IEEE 30 without or with RESs data without or with EVCS load at 52.838 kW with reactive power loss at IEEE 30 using RESs data with EVCS load at 10.816 kVAR. The real power loss at IEEE 118 without or with RESs data without or with EVCS load at 0.028 kW with reactive power loss at IEEE 118 using RESs data with EVCS load at 0.012 kVAR.

6.3.3 Software development for the implementation of the developed MLIP & PSO algorithms

The algorithms developed as detailed in section 6.3.2 (MNLIP and particle swarm optimization algorithm) have been implemented in the MATLAB numerical and technical

computing environment. The MATLAB programs for these algorithms are presented in Appendices are enumerated in Table (6.1).

Table 6.1: Software programs developed and implemented in this thesis

Chapter 3	
Program description	**Program description Appendix**
Energy management system for hybrid system scripts help to optimize the use of RESs by minimizing the cost of grid power while meeting load with power from PV, battery, and grid, especially when variable pricing and generation involve heuristic state machine strategy and a linear program-based optimization method approach.	A. MINLP Scripts for Energy Management System for Hybrid System
EPD PSO method for different function model=CreateModel() using PSO with specific parameter for optimal allocation of all connected generating units to achieve the lowest total generation cost considering B-Coefficient for Transmission loss, and integration of RES units for an optimal solution	B. PSO Method for EPD Problem of a Grid-tied RES-HS Scripts
PSO method provide the best value for uncertainty cost functions for both RES and location, sizes for EVCS considering active, reactive power losses considering cost, power flow, and voltage deviation constraints in a multi-objective formulation. Power flow analysis with Newton Raphson methodology (NPM) to locate several electric vehicles charging stations and optimize RESs grid-tied system power dispatch. Power optimization was exhibited as the objective function, which includes minimizing active and reactive power losses while considering cost, power flow, and voltage for a hybrid system of an electric vehicle charging station (EVCS).	C. Scripts for PSO Method for Energy Management of The Hybrid System of an Electric Vehicle Charging Station

The energy management system algorithm optimizes the size of a PV-Bat-Grid in a standalone system through particle swarm optimization.	D. PSO scripts for PV-Bat-Grid energy management of the hybrid system

Chapter 6 present the conclusion and future recommendations. The study examines the impact of EVCS load models on load flow analysis, focusing on voltage magnitude variation of active and reactive power demands. Simulations on IEEE 14-bus, IEEE 30-bus and IEEE 118-bus systems showed increased system stability and security. Active power modeling improved, while reactive power modeling significantly affected voltage differences. EVCS load models reduce system losses and generation costs. The study presents a novel EV fast charging system structure with lower costs and higher efficiency. It compares the bus system and EV charging under fair efficiency analysis, including power loss comparisons. Results show that placing fast charging stations at weak buses affects power distribution network smooth operation and incurs economic loss.

6.4 Contribution of the Thesis

The economic power dispatch for defined systems is based on a collection of realistic methodological and economic models of grid-tied components (RES, ESS, and EVCS Load), considering network operator-planned strategies and mechanisms for fluctuating sun irradiation, wind, EVCS load, and dynamic electricity profiles. In the scope of this thesis, the deliverables can be classified as follows:

- The study involves the development of novel MINLP algorithms to solve hybrid system network objective functions and constraint limitations to minimize total operating costs and reduce grid dependency, while increasing grid voltage and power flow and boosting renewable energy source use. This is accomplished by integrating the MINLP solver with a grid-based HS network calculating tool. Because the network limitations are nonlinear, they are incorporated into mathematical calculations via an iterative procedure with varying constraints for the MINLP solver at each stage until the necessary voltage and power flow requirements are reached. This program is clever enough to try several tactics for predicting voltage and EVCS loading violations on the grid distribution bus while also generating optimized RES and ESS planning, making it suitable for managing future networks with a high integration of RES units. These solutions

involve active and reactive power supply from RES power dispatch, iteratively modifying MINLP limitations, and curtailment of renewable energy..

- The second significant contribution of this thesis originates from development of PSO algorithm, which solves EPD optimization problems in a grid-tied RES hybrid system. The main novelty of this PSO method is the optimization process that incorporates the network restrictions' impact on the solution of the economic dispatch problem. In addition, uncertainty cost function for RESs from the conducted literature review using simulated monte carlo RESs uncertainty fuel cost function from the conducted literature review to optimize active and reactive power losses, voltage and power flow by integrating grid-tied RES to guarantee a fast convergence for the best possible output.
- The last contribution is the development of particle swarm optimization method that employs a RESs uncertainty cost function to minimize the unit's operational costs with minimizing the transmission losses and validation of the developed PSO methods for energy management of the hybrid systems of an electric vehicle charging station using IEEE 14-bus, IEEE 30-bus and IEEE 118-bus test systems to reduce active and reactive power losses, voltage and power flow of the EVCS.

6.5 Possible applications of the research outputs

The methods, algorithms and software programs developed in this thesis can find application in industry as well as in academia:

- A renewable energy (RE) solutions provider such as Scatec, an electricity distribution company in South can adopt PSO method in deliverable of dispatchable power of 225MW/1,140MWh battery storage capacity to the national grid year-round usually from 5 a.m. to 9.30 p.m.
- The novel PSO methods for Solar PV & Battery dispatchable power can be used as AI simulation software for training the operators and technicians to have an insight on how units to minimize grid-tied RESs operational costs with while minimizing the transmission losses.
- The developed PSO method can find its usefulness in the postgraduate research and undergraduate teaching course on grid energy management and EVCS that requires real-time EPD solutions for decision-making on hybrid systems and distribution networks.

6.6 Future research

Further study will focus on wind turbine integration, while electric vehicle charging station loading is discussed in the next chapters to obtain a far greater self-consumption ratio than the baseline method. Testing the developed algorithms in a closed loop optimisation of the dispatch problem using Real Time Digital Simulator (RTDS) using Power Hardware in the loop simulation (PHIL), interfacing the renewable energy components with RTDS via the power amplifier, and testing and validating the developed MNLIP & PSO algorithms for the hybrid energy management system.

6.7 Publication

1. Adenuga, O.T.; Krishnamurthy, S. Economic Power Dispatch of a Grid-Tied Photovoltaic-Based Energy Management System: Co-Optimization Approach. Mathematics 2023, 11, 3266. https://doi.org/10.3390/math11153266.
2. Optimized EVCS demand to minimize active and reactive power losses of the dispatchable hybrid energy management system multi-objective formulation. 54TH Earthday Indexed IGEN ENERGATHON 2024. Institution of Green Engineers. 17 SDG-17 Institutions -17 Institution Heads. Hosted online from India, from May 18th to 19th, 2024.
3. A particle swarm optimisation method for electric vehicle charging station using dispatchable PV and wind energy of the south Africa network. Anticipated to submit the paper to IEEE open acces Journal by July 2024.

BIBLIOGRAPHY

Abdellatif Elmouatamid, E. Ouladsine, R. Bakhouya, M. El Kamoun, N. Khaidar, M. and Zine-Dine, K. 2021. Review of Control and Energy Management Approaches in Micro-Grid Systems, Energies, 14, 168. https://dx.doi.org/10.3390/en14010168.

Abdulrahman, I. 2020. MATLAB-Based Programs for Power System Dynamic Analysis, Journal of Power and Energy, IEEE Open Access, Volume 7.

Abrishambaf, O. Ghazvini, M. Gomes, L. Faria, P. Vale, Z. and Corchado, J. 2016. Application of a Home Energy Management System for Incentive-Based Demand Response Program Implementation, 27th International Workshop on Database and Expert Systems.

Adefarati, T. Bansal, R. C. Bettayeb, M. and Naidoo, R. 2021. Optimal energy management of a PV-WTG-BSS-DG microgrid system, Energy, 217.

Adenuga, O.T. Mpofu, K. and Ramatsetse, B.I. 2019. Energy efficiency analysis modelling system for manufacturing in the context of industry 4.0, Procedia CIRP; 80:735-740.

Adenuga, O.T. Mpofu, K. and Ramatsetse, B.I. 2020. Exploring energy efficiency prediction method for Industry 4.0: a reconfigurable vibrating screen case study, Procedia Manufacturing, 51, Pages 243-250.

Adenuga, O.T., Krishnamurthy, S., 2023. Economic Power Dispatch of a Grid-Tied Photovoltaic-Based Energy Management System: Co-Optimization Approach. Mathematics 11, 3266.

Adeyemo, A. A. Amusan, O. T. 2022. Modelling and multi-objective optimization of hybrid energy storage solution for photovoltaic powered off-grid net zero energy building, Journal of Energy Storage, Volume 55, Part A, 105273, https://doi.org/10.1016/j.est.2022.105273.

Ahmad, A. Khan, A. Javaid, N. Hussain, H.M. Abdul, W. Almogren, A. Alamri, A. and Niaz, I.A. 2017. An Optimized Home Energy Management System with Integrated

Renewable Energy and Storage Resources, Energies, 10, 549; doi:10.3390/en10040549.

Ahmad, E. Osama M. and El-Kishky, H. 2022. Efficient operation of battery, 2nd ed. Hoboken, NJ, USA: Wiley.

Ahmadi, M. Colak, K. I. and Eguchi, K. 2021. Optimal energy management of distributed generation in micro-grids using artificial bee colony algorithm. Mathematical Biosciences and Engineering, Volume 18, Issue 6, 7402–7418. MBE, 18(6): 7402–7418. DOI: 10.3934/mbe.2021366.

Ahmadi, S. Moghaddam, M. S. Ranjbar, S. 2022. New model of PEV parking lots in the presence of demand response uncertainties, Sustain. Energy Grids Netw. 30, 100641.

Akbarabadi, L. M.; Sirjani, R. 2023. Achieving Sustainability and Cost-Effectiveness in Power Generation: Multi-Objective Dis-patch of Solar, Wind, and Hydro Units. Sustainability 15, 2407. https://doi.org/10.3390/su15032407.

Akhtar H., Lee, J. and Kim, H. 2016. An Optimal Energy Management Strategy for Thermally Networked Microgrids in Grid-Connected Mode, International Journal of Smart Home, Vol. 10, No. 3, pp. 239-258. http://dx.doi.org/10.14257/ijsh.2016.10.3.24.

Albadr, M.A., Tiun, S., Ayob, M., AL-Dhief, F., 2020. Genetic Algorithm Based on Natural Selection Theory for Optimization Problems. Symmetry 12, 1758.

Alhasnawi, B. N. Jasim, B. H. Siano, P. and Guerrero, J. M. 2021. A Novel Real-Time Electricity Scheduling for Home Energy Management System Using the Internet of Energy, Energies, vol. 14, no.11, pp. 3191-3220, doi: 10.3390/en14113191.

Alkhalifa, L. and Mittelmann, H. 2022. New Algorithm to Solve Mixed Integer Quadratically Constrained Quadratic Programming Problems Using Piecewise Linear Approximation, Mathematics, 10, 198. https://doi.org/10.3390/math10020198.

Allan, R., Billinton, R., Sjarief, I. et al. 1991. A reliability test system for educational purposes-basic distribution system data and results. IEEE Transactions on Power Systems 6 (2): 813–820.

Altaf, M., Yousif, M., Ijaz, H., Rashid, M., Abbas, N., Khan, M.A., Waseem, M., Saleh, A.M.: PSO-based optimal placement of electric vehicle charging stations in a distribution network in smart grid environment incorporating backward forward sweep method. IET Renew. Power Gener. 1–15 (2023). https://doi.org/10.1049/rpg2.12916.

An, L. N. and Quoc-Tuan, T. 2015. Optimal energy management for grid connected microgrid by using dynamic programming method, in Proc. IEEE Power Energy Soc. Gen. Meeting, Denver, CO, USA, pp. 1–5.

Anglani, N. Oriti, G. and Colombini, M. 2017. Optimized energy management system to reduce fuel consumption in remote military microgrids, IEEE Trans. Ind. Appl., vol. 53, no. 6, pp. 5777–5785.

Ar´evalo, J. Santos, F. and Rivera, S. 2019. Uncertainty Cost Functions for Solar Photovoltaic Generation, Wind Energy Generation, and Plug-In Electric Vehicles: Mathematical Expected Value and Verification by Monte Carlo Simulation, International Journal of Power and Energy Conversion, pp 171-207. https://doi.org/10.1504/IJPEC.2019.098620.

Arash Dizqah, M. Maheri, A. Busawon, K. and Kamjoo. A. 2015. A Multivariable Optimal Energy Management Strategy for Standalone DC Microgrids, IEEE TRANSACTIONS ON POWER SYSTEMS, VOL. 30, NO. 5.

Asghari, M. Fathollahi-Fard, A.M. S. Mirzapour, M. Al-e-hashem, J. Dulebenets, M.A. 2022. Transformation and Linearization Techniques in Optimization: A State-of-the-Art Survey, Mathematics, 10, 283. https://doi.org/10.3390/math10020283.

Ashida, S., 2021. Finiteness of The Number of Critical Values of The Hartree-Fock Energy Functional ESS Than A Constant Smaller Than The First Energy Threshold. Kyushu Journal of Mathematics 75, 277–294.

Ashish Kumar, K. Roy, S. and Ahmed M. R. 2019.Analysis of the impact of electric vehicle charging station on power quality issues. In 2019 international conference on electrical, computer and communication engineering (ECCE), pp. 1-6. IEEE.

Asif, K. Memon, S. Sattar, T. and Karmaker P. 2019. Challenges for electric vehicle adoption in Bangladesh. In 2019 International Conference on Electrical, Computer and Communication Engineering (ECCE), pp. 1-6. IEEE.

Azaroual, M. Ouassaid, M. and Maaroufi, M. 2021. Optimum Energy Flow Management of a Grid-Tied Photovaolatic-Wind-Battery System considering Cost, Reliabilty, and CO2 Emission. Hidawi, International Journal of Photoenergy, vol 2021, Article ID 5591456.

Balamurugan, R., and Subramanian, S. 2007. A Simplified Re-cursive Approach to Combined Economic Emission Dispatch. Electric Power Components and Systems, Vol. 36, No. 1, pp. 17-27.

Baldi, F. Ahlgren, F. Melino, F. Gabrielii, C. and Andersson, K. 2016. Optimal load allocation of complex ship power plants, Energy Convers. Manage., vol. 124, pp. 344–356.

Balu, K. and Mukherjee, V. 2023. Optimal allocation of electric vehicle charging stations and renewable distributed generation with battery energy storage in radial distribution system considering time sequence characteristics of generation and load demand, J. Energy Storage 59 (), 106533.

Barbato A. and Capone, A. 2014. Optimization Models and Methods for Demand-Side Management of Residential Users: A Survey, Energies, 7, 5787-5824; doi:10.3390/en7095787.

Barua, S. and Mohammad, N. 2021. Optimization-based Energy Management System to Minimize Electricity Bill for Residential Customer, 3rd International Conference on Electrical & Electronic Engineering (ICEEE), 22-24, EEE, RUET, Bangladesh.

Bhattacharyya, B. and Kumar, S. 2016. Approach for the solution of transmission congestion with multi-type FACTS devices. IET Generation, Transmission & Distribution 10(11), pp. 2802–2809. doi.org/10.1049/iet-gtd.2015.1574.

Biegler, L.T. and Grossmann, I.E. 2004. Retrospective on optimization, Comput. Chem. Eng., 28, 1169–1192.

Bigdeli, N. 2015. Optimal management of hybrid pv/fuel cell/battery power system: A comparison of optimal hybrid approaches," Renew Sust Energ Rev. 42:377–93. https://doi.org/10.1016/j.rser.2014.10.032.

Bishwajit D.; Shyamal K. R.; Biplab B. 2019. Solving multi-objective economic emission dispatch of a renewable integrated microgrid using latest bio-inspired algorithms, Engineering Science and Technology, an International Journal, Volume 22, Issue 1, pp. 55-66, https://doi.org/10.1016/j.jestch.2018.10.001.

Blaabjerg, F. Yang, Y. Yang, D. Wang, X. 2017. Distributed Power-Generation Systems and Protection, Proceedings of the IEEE Vol. 105, No. 7. DOI: 10.1109/JPROC.2017.2696878.

Burlacu, R. Geißler, B. and Schewe, L. 2020. Solving mixed-integer nonlinear programmes using adaptively refined mixed-integer linear programmes, Optim. Methods Softw., 35, 7–64.

Byrne, R. H. Nguyen, T. A. Copp, D. A. Chalamala, B. R. and Gyuk, I. 2018. Energy Management and Optimization Methods for Grid Energy Storage Systems, IEEE Access, vol. 6, pp. 13231-13260.

Cao, Y. Li, D. Zhang, Y. Tang, Q. Khodaei, A. and Zhan, H. 2022. Optimal Energy Management for Multi-Microgrid Under a Transactive Energy Framework with Distributionally Robust Optimization, in IEEE Transactions on Smart Grid, vol. 13, no. 1, pp. 599-612, doi: 10.1109/TSG.2021.3113573.

Cecilia, A. Carroquino, J. Roda, V. Costa-Castelló, R. and Barreras. F. 2020. Optimal Energy Management in a Standalone Microgrid, with Photovoltaic Generation, Short-Term Storage, and Hydrogen Production, Energies, 13, 1454; doi:10.3390/en13061454.

Chow, J. and Rogers, G. 2008. Power System Toolbox Manual, Version 3.0, Tech. Rep., 2008. Available Online: https://www.ecse.rpi.edu/~chowj/

Chow, J. H. and Cheung, K. W. 1992. A toolbox for power system dynamics and control engineering education and research, IEEE Trans. Power Syst.,

Cole, S. and Belmans, R. 2011. MatDyn, a new MATLAB-based toolbox for generation to reduce constraints on distribution networks, EVS27 Barcelona, Spain, November 17-20.

Connected EVs, 2021. Electric and Hybrid Vehicle Technology International, 128–128.

Davarzani, S. Ahmadi, A. R., Manandhar, T. Shaw, R. Georgiopoulos, S. Martinez, I. and Stojkovska, B. 2020. Coordination trial of novel distributed energy resources management system to provide reactive power services to address transmission constraints. CIRED – Open Access Proceedings Journal, (1), 143–146. https://doi.org/10.1049/oap-cired.2021.0291.

Derong Liu, et al., 2020. Adaptive dynamic programming for control: a survey and recent advances, IEEE Trans. Syst. Man Cybern. Syst. Hum. 51 (1) 142–160.

Dhillon, J.S., Parti, S.C., and Kothari, D.P. 1993. Stochastic economic emission load dispatch. Electric Power Systems Research, Vol. 26, pp. 179-186.

Dinc Yalcin, G., Curtis, F.E., 2024. Incremental quasi-Newton algorithms for solving a nonconvex, nonsmooth, finite-sum optimization problem. Optimization Methods and Software 1–23.

Ding, Z. Lu, Y. Lai, K. Yang, and Lee, W. 2020. Optimal coordinated operation scheduling for electric vehicle aggregator and charging stations in an integrated electricity-transportation system, Electrical Power and Energy Systems 121, 106040.

Dinh, H. T. and Kim, D. 2021. An Optimal Energy-Saving Home Energy Management Supporting User Comfort and Electricity Selling with Different Prices, in IEEE Access, vol. 9, pp. 9235-9249, doi: 10.1109/ACCESS.2021.3050757.

Dizqah, A. M. Maheri, A. Busawon K. and Kamjoo, A. 2015. A Multivariable Optimal Energy Management Strategy for Standalone DC Microgrids, in IEEE Transactions on Power Systems, vol. 30, no. 5, pp. 2278-2287, doi: 10.1109/TPWRS.2014.2360434.

Djete, M. F. Possamaï, D. Tan, X. Vlasov, M. 2022. optimal control: the dynamic programming principle, Ann. Probab. 50, 2,791–833.

Dorahaki, S. Dashti, R. and Reza Shaker, H. 2020. Optimal energy management in the smart microgrid considering the electrical energy storage system and the demand-side energy efficiency program, Journal of Energy Storage, Volume 28, 101229, https://doi.org/10.1016/j.est.2020.101229.

Dorigo, M., 2007. Ant colony optimization. Scholarpedia 2, 1461.

Dupin, N. 2019. Column generation for the discrete UC problem with min-stop ramping constraints. IFAC-PapersOnLine, 52(13), 529–534. https://doi.org/10.1016/j.ifacol.2019.11.186.

Economic dispatch in power system networks including renewable energy resources using various optimization techniques, 2023. Archives of Electrical Engineering.

Ekinci, S. Demiroren, A. and Zeynelgil, H. 2017. PowSysGUI: A new educational
Ekramul, K. Assi, M. Hossain, C. Tushar, M. K. and Yan, J. 2017. Optimal scheduling of EV charging at a solar power-based charging station. IEEE Systems Journal 14, no. 3 (2020): 4221-4231. IEEE Access. volume XX.

Elkazaz, M. Summer, M. and Thomas, D. 2020. Energy management system for hybrid PV-wind-battery microgrid using convex programming model predictive and rolling horizon predictive control with experimental validation. International Journal of Electrical Power & Energy Systems, vol. 115. P.105483.

Eltoumi, F. 2020. Charging station for electric vehicle using hybrid sources. PhD diss., Bourgogne Franche-Comté. energy storage systems, electric-vehicle charging stations and renewable energy.

Erenoğlu, A. K. Şengör, İ. Erdinç, O. Taşcıkaraoğlu, A. J. and Catalão, P.S. 2022. Optimal energy management system for microgrids considering energy storage, demand response and renewable power generation, International Journal of Electrical Power & Energy Systems, Volume 136, 107714, https://doi.org/10.1016/j.ijepes.2021.107714.

Eslami, E. and Kamarposhti, M. A. 2019. Optimal design of solar–wind hybrid system-connected to the network with cost-saving approach and improved network reliability index, SN Appl. Sci., 1, 1–12.

Fan, M. Zhang, Z. and Wang, C. 2019. Mathematical Models and Algorithms for Power System Optimization, Modeling Technology for Practical Engineering Problems, An imprint of Elsevier. China Electric Power Press. Published by Elsevier Inc.

Fathy, A. Alanazi, T. Rezk, M. H. and Yousri, D. 2021. Optimal energy management of micro-grid using sparrow search algorithm, Energy Reports 8, 758–773. https://doi.org/10.1016/j.egyr.2021.12.022.

Fernandes, F. Morais, H. Vale Z. and Ramos, C. 2014. Dynamic load management in a smart home to participate in demand response events, Energy and Buildings, vol. 82, pp. 592-606.

Filho G. P.R., Villas, L.A. Gonçalves, V.P. Pessin, G. Loureiro, A.A.F. and Ueyama. J. 2019. Energy-efficient smart home systems: Infrastructure and decision-making process, Internet of Things, Vol. 5, pp. 153–167.

Finding the best strategy in 2-player games through iteration, 2023. International Research Journal of Modernization in Engineering Technology and Science.

Flaten, D.L., 1988. Distribution system losses calculated by percent loading. IEEE Transactions on Power Systems 3, 1263–1269.

Fodstad, M. del Granado, P. Hellemo, C. L. Rugstad Knudsen, B Pisciella, P. Silvast, A. Bordin, C. Schmidt, S. Straus, J. 2022. Next frontiers in energy system modelling: A review on challenges and the state of the art, Renewable and Sustainable Energy Reviews, Volume 160, 112246, https://doi.org/10.1016/j.rser.2022.112246.

Fouladfar, M.H. Saeed, N. Marzband, M. and Franchini, G. 2021. Home-Microgrid Energy Management Strategy Considering EV's Participation in DR. Energies, 14, 5971. https://doi.org/ 10.3390/en14185971.

Fu, C. Zhang, S. and Chao K. 2020. Energy Management of a Power System for Economic Load Dispatch Using the Artificial Intelligent Algorithm, Electronics 9, 108; doi:10.3390/electronics9010108.

Gao, X. and Fu, L. 2020. SOC Optimization Based Energy Management Strategy for Hybrid Energy Storage System in Vessel Integrated Power System, IEEE Access. Vol 8. Digital Object Identifier 10.1109/ACCESS.2020.2981545.

Garcia Vera, Y. Dufo-Lopez E. R. and Bernal-Agustin, J. L. 2019. Energy Management in Microgrids with Renewable Energy Sources: A Literature Review, Appl. Sci, vol. 9, no. 18, pp. 225-253.

Gbadegesin, A.O. 2020. Optimal Energy Management of Microgrids Incorporating Hybrid Energy Storage Systems," (Doctoral Research Thesis) Johannesburg: University of Johannesburg. Available from: http://hdl.handle.net/102000/0002. Accessed: 22 September 2022.

Ghasemi, A. and Enayatzare, M. 2018.Optimal energy management of a renewable-based isolated microgrid with pumped-storage unit and demand response, Renewable Energy, vol. 123, pp. 460-474.

Ghiasi, M. Niknam, T. Dehghani, M. Siano, P. Haes Alhelou, H. and Al-Hinai, 2021. A. Optimal Multi-Operation Energy Management in Smart Microgrids in the Presence of RESs Based on Multi-Objective Improved DE Algorithm: Cost-Emission Based Optimization. Appl. Sci., 11, 3661. https://doi.org/10.3390/app11083661.

Gielen, D. Boshell, D. F, Saygin, D, Bazilian, M.D. Wagner, N. and Gorini, R. 2019. The role of renewable energy in the global energy transformation, Energy Strategy Reviews, Volume 24, pp 38-50, https://doi.org/10.1016/j.esr.2019.01.006.

Glover, F. and Kochenberger, G.A. 2003. Handbook of Metaheuristics, Springer: Berlin/Heidelberg, Germany.

Gnanadass, R. NOV 2005. Optimal power dispatch and pricing for deregulated power industry. PhD Thesis, Pondicherry University, India.

Gomes, I. Bot, K. Ruano, M.G. and Ruano, A. 2022. Recent Techniques Used in Home Energy Management Systems: A Review. Energies, 15, 2866. https://doi.org/10.3390/en15082866.

Guerrero, R.P. 2004. Differential Evolution based power dispatch algorithms, M.S. Thesis, Electrical Engineering Department, University of Puerto Rico, and Mayaguez Campus.

Gürdal, Z. R. Haftka, T. and Hajela. P. 1999. Design and Optimization of Laminated Composite Materials. John Wiley and Sons.

Hamid, K. and Shahram, J. 2020. Optimal energy management for multi-microgrid considering demand response programs: A stochastic multi-objective framework, Energy, Elsevier, 2020. vol. 195(C).

Hasibuan, A. Kurniawan, R. Isa, M. Mursalin, M. 2021. Economic Dispatch Analysis Using Equal Incremental Cost Method with Linear Regression Approach. Journal of Renewable Energy, Electrical, and Computer Engineering. 2021.1(1):16. doi.org/10.29103/jreece.v1i1.3617.

Heris, M. K. Particle Swarm Optimization (PSO) in MATLAB — Video Tutorial (URL: https://yarpiz.com/440/ytea101-particle-swarm-optimization-pso-in-matlab-video-tutorial), Yarpiz, 2016

Hirsch, A. Parag, Y. and Guerrero, J. 2018. Microgrids: A review of technologies, key drivers, and outstanding issues, Renew Sust Energ Rev. 2018. 90:402–411. https://doi.org/10.1016/j.rser.2018.03.040.

Hossain, M. R. and Ginn, H. L. 2017. Real-time distributed coordination of power electronic converters in a dc shipboard distribution system, IEEE Trans. Energy Convers., vol. 32, no. 2, pp. 770–778.

Hu, W. Wang, P. and Gooi, H. B. 2018. Toward optimal energy management of microgrids via robust two-stage optimization, IEEE Trans. Smart Grid, vol. 9, no. 2, pp. 1161–1174.

Huang, W. Wang, Jianguo, Wang, Jianping, Zeng, H. Zhou, M. Cao, J. 2024. EV charging load profile identification and seasonal difference analysis via charging sessions data of charging stations. Energy 288, 129771.

Hussain, H. Javaid, N. Iqbal, S. Hasan, Q. Aurangzeb, K. and Alhussein, M. 2018. An efficient demand side management system with a new optimized home energy management controller in smart grid, Energies, vol. 11, no. 1, p. 190.

Igualada, L. Corchero, C. Cruz-Zambrano, M. and Heredia, F. J. 2014. Optimal Energy Management for a Residential Microgrid Including a Vehicle-to-Grid System, in IEEE Transactions on Smart Grid, vol. 5, no. 4, pp. 2163-2172, doi: 10.1109/TSG.2014.2318836.

Illinois Center for a Smarter Electric Grid. 2013. Available Online at FTP:http://publish.illinois.edu/smartergrid/

Ishigaki, Y. Kimura, Y. Matsusue, I. Miyoshi, H. and Yamagishi. K. 2014. Optimal Energy Management System for Isolated Micro Grids, ENVIRONMENT and ENERGY. SEI TECHNICAL REVIEW · NUMBER 78.

Iweh, C.D. Gyamfi, S. Tanyi, E. and Effah-Donyina, E. 2021. Distributed Generation and Renewable Energy Integration into the Grid: Prerequisites, Push Factors, Practical Options, Issues and. Merits. Energies 14, 5375. https:// doi.org/10.3390/en14175375.

Jahic, A. Eskander, M. and Schulz, D. 2019. Charging Schedule for Load Peak Minimization on Large-Scale Electric Bus Depots. Applied Sciences 9, 1748.

Jamborsalamati, Hossain, P. Taghizadeh, M. J. Konstantinou, S. Manbachi, G. M. and Dehghanian, P. 2020. Enhancing Power Grid Resilience Through an IEC61850-Based EV-Assisted Load Restoration, in IEEE Transactions on Industrial Informatics, vol. 16, no. 3, pp. 1799-1810, doi: 10.1109/TII.2019.2923714. 2020.

Jaurola, M. Hedin, A. Tikkanen, S. and Huhtala, K. 2019. Topti: A flexible framework for optimising energy management for various ship machinery topologies, J. Mar. Sci. Technol., vol. 24, no. 4, pp. 1183–1196, 2019.

Jiawen, B. Tao D. Zhe, W. and Ianhua C. 2019. Day-Ahead Robust Economic Dispatch Considering Renewable Energy and Con-centrated Solar Power Plants, Energies, 12(20), pp. 3832; https://doi.org/10.3390/en12203832.

K. 2019. Real-Time Optimal Energy Management Controller for Electric Vehicle Integration in Workplace Microgrid, in IEEE Transactions on Transportation Electrification, vol. 5, no. 1, pp. 174-185, March 2019, doi: 10.1109/TTE.2018.2869469.

Karmaker, A. K. Hossain, M. Alamgir Pota, H. R. Onen, A and Jung J. Energy Management System for Hybrid Renewable Energy-based Electric Vehicle Charging Station,

Karmellos, M. and Mavrotas, G. 2019. Multi-objective optimization and comparison framework for the design of Distributed Energy Systems, Energy Conversion and Management, Volume 180, Pages 473-495, https://doi.org/10.1016/j.enconman.2018.10.083.

Kassim, A.M., 2022. The Efficiency of Hybridised Genetic Algorithm and Ant Colony Optimisation (HGA-ACO) in a Restaurant Recommendation System. ASM Science Journal 17, 1–11.

Kempener, R. Komor, P. and Hoke, A. 2013. Smart Grids and Renewables—A Guide for Effective Deployment; International Renewable Energy Agency (IRENA): Abu Dhabi, UAE.

Khan, A.A., Malik, S.K., 2017. A semi search algorithm towards semantic search using domain ontologies. International Journal of Autonomic Computing 2, 191.

Khan, M. Wang, W. J. Ma, M. Xiong, L. Li, P. and Wu, F. 2019. Optimal energy management and control aspects of distributed microgrid using multi-agent systems, Sustainable Cities and Society, Volume 44, Pages 855-870, https://doi.org/10.1016/j.scs.2018.11.009.

Khorram, M. Faria, P. and Vale, Z. 2018. Optimization-based Home Energy Management System Under Different Electricity Pricing Schemes, 2018 IEEE 16th Int. Conf. Industrial Informatics (INDIN), Porto, Portugal, Jul. 18-20, pp. 508-513.

Kleinert, T. Labbé, M. Ljubić, I. and Schmidt, M. 2021. A Survey on Mixed-Integer Programming Techniques in Bilevel Optimization, EURO Journal on Computational Optimization, Volume 9, 100007, https://doi.org/10.1016/j.ejco.2021.100007.

Koubaa, R. and Krichen, L. 2016.Ant Colony Optimization Based Optimal Energy Management for an FC/UC Electric Vehicle. 17th international conference on Sciences and Techniques of Automatic control & computer engineering, STA'2016, Sousse, Tunisia, December 19-21.

Koyuncu, H., Ceylan, R., 2018. A PSO based approach: Scout particle swarm algorithm for continuous global optimization problems. Journal of Computational Design and Engineering 6, 129–142.

Krishnamurthy, N.K.; Sabhahit, J.N.; Jadoun, V.K.; Gaonkar, D.N.; Shrivastava, A.; Rao, V.S.; Kudva, G. 2023. Optimal Placement and Sizing of Electric Vehicle Charging Infrastructure in a Grid-Tied DC Microgrid Using Modified TLBO Method. Energies 16, 1781. https://doi.org/10.3390/en16041781.

Krishnamurthy, S., and Tzoneva, R. 2012e. Application of the Particle Swarm Optimization Algorithm to a Combined Economic Emission Dispatch Problem using a new penalty factor. IEEE PES Power Africa 2012 – Conference and Exhibition, Johannesburg, South Africa, pp 1-7.

Kumar, M. and Tyagi, B. 2021. Optimal energy management and sizing of a community smart microgrid using demand side management with load uncertainty, ECTI-CIT, 15, 186–197.

Kusakana, K. 2015. Optimal scheduled power flow for distributed photovoltaic/wind/diesel generators with battery storage sys-tem. IET Renewable Power Generation. 9(8): pp. 916–924. doi.org/10.1049/iet-rpg.2015.0027.

Lai, K. and Illindala, M. S. 2018. A distributed energy management strategy for resilient shipboard power system, Appl. Energy, vol. 228, pp. 821–832, 2018.

Lakshminarayanan, V. V. Chemudupati, G. S. Pramanick S. K. and Rajashekara, Lebrouhi, B.E. et al., 2021. Key challenges for a large-scale development of battery electric vehicles: a comprehensive review, J. Energy Storage 44, 103273.

Leyffer S. and Linderoth. J. 2007. Introduction to Integer Nonlinear Optimization, Nonlinear Branch-and-Cut," Theoretical and Computational Challenges. Argonne National Laboratory. http://science.energy.gov/~/media/ascr/pdf/workshops-conferences/mathtalks/Leyffer.pdf.

Li, H. Eseye, A.T Zhang, J. and Dehua, Z. 2017. Optimal energy management for industrial microgrids with high penetration renewable. Prot Cont Modern Power Syst 2017; 2: 12.

Li, J., Xing, Y., Zhang, D., 2022. Planning Method and Principles of the Cloud Energy Storage Applied in the Power Grid Based on Charging and Discharging Load Model for Distributed Energy Storage Devices. Processes 10, 194.

Li, M. Shahidehpour, F. Aminifar, A. Alabdulwahab, and Y. Al-Turki, 2017. Networked microgrids for enhancing the power system resilience, Proc IEEE;105 (7):1289–310. https://doi.org/10.1109/jproc.2017.2685558.

Li, Y. He, H. Peng, J. and Wang, H. 2019. Deep Reinforcement Learning-Based Energy Management for a Series Hybrid Electric Vehicle Enabled by History Cumulative Trip Information, in IEEE Transactions on Vehicular Technology, vol. 68, no. 8, pp. 7416-7430, doi: 10.1109/TVT.2019.2926472.

Li, Z. Xu, Y. Fang, S. Zheng, X. and Feng, X. 2020. Robust coordination of a hybrid ac/dc multi-energy ship microgrid with flexible voyage and thermal loads, IEEE Trans. Smart Grid, vol. 11, no. 4, pp. 2782–2793.

Lim, S.M., Sultan, A.B.Md., Sulaiman, Md.N., Mustapha, A., Leong, K.Y., 2017. Crossover and Mutation Operators of Genetic Algorithms. International Journal of Machine Learning and Computing 7, 9–12.

Lin, W. M. Tu, C. S. and Tsai, M. T. 2016. Energy management strategy for microgrids by using enhanced bee colony optimization, Energies, 9.

Liu, H., Lee, A., Lee, W., Guo, P., 2023. DAACO: adaptive dynamic quantity of ant ACO algorithm to solve the traveling salesman problem. Complex & Intelligent Systems 9, 4317–4330.

Luna, A. C. Diaz, N. Graells, L. M. Vasquez, J. C. and Guerrero, J. M. 2016. Mixer-Integer-Linear-Programming Based Energy Management System for Hybrid PV-wind-battery Microgrids: Modelling, Design and Experimental Verification, IEEE Trans. Power Electron., vol. 32, no. 4, doi: 10.1109/TPEL.2016.2581021.

Lv, T. and Qian, A. 2016. Interactive energy management of networked microgrids based active distribution system considering large-scale integration of renewable energy resources, Appl Energy.; 163:408–22. 2016.

M. Dorigo and L. M. Gambardella, “Ant colonies for the traveling salesman problem,” Bio-systems, Vol. 43, pp. 73–81, 1997.

Ma, Y., 2024. Optimization of basic PID control algorithm based on genetic algorithm and Matlab. Theoretical and Natural Science 30, 178–186.

Mandal, S. and Mandal, K. K. 2020. Optimal energy management of microgrids under environmental constraints using chaos enhanced differential evolution, Renewable Energy Focus, Volume 34. https://doi.org/10.1016/j.ref.2020.05.002.

Mart´ınez, C. Rivera S. Revista, M. 2018. Quadratic Modelling of Uncertainty Costs for Renewable Generation and its Application on Economic Dispatch; Del Programa De Matem´aticas VOL: V, p´gina: 37–61.

Marzband, M. Azarinejadian, F. Savaghebi, M. and Guerrero, J. M. 2017. An Optimal Energy Management System for Islanded Microgrids Based on Multiperiod Artificial Bee Colony Combined with Markov Chain, in IEEE Systems Journal, vol. 11, no. 3, pp. 1712-1722, doi: 10.1109/JSYST.2015.2422253.

Masrur, H., Sharifi, A., Islam, Md.R., Hossain, Md.A., Senjyu, T., 2021. Optimal and economic operation of microgrids to leverage resilience benefits during grid outages. International Journal of Electrical Power & Energy Systems 132, 107137.

Mehdi, H.M., Azeem, M.K., Ahmad, I., 2023. Artificial intelligence based nonlinear control of hybrid DC microgrid for dynamic stability and bidirectional power flow. Journal of Energy Storage 58, 106333.

Meiling, Y. Samir, J. Rafael, G, and Noureddine, Z. 2019. Review on health-conscious energy management strategies for fuel cell hybrid electric vehicles: Degradation models and strategies, International journal of hydrogen energy 44, 6844-6861.

Mendez, C. 2017.Direcci´on: Sergio Rivera, Modelaci´on cuadr´atica de los costos de incertidumbre parageneraci´on renevobles E´olica y Solar y su aplicaci´on en el Despacho Econ´omico, Tesis Pregrado Universidad.

Milano, F. 2005. An open source power system analysis toolbox, IEEE Trans.

Modise, R.K. Mpofu, K. and Adenuga, O.T. 2021. Energy and Carbon Emission Efficiency Prediction: Applications in Future Transport Manufacturing, Energies, 14, 8466. https://doi.org/10.3390/ en14248466. 2021.

Montero, L. Bello, A. and Reneses, J. 2022. A Review on the Unit Commitment Problem: Approaches, Techniques, and Resolution Methods, Energies, 15, 1296. https://doi.org/10.3390/en15041296.

Morais, H. Vale, Z. A. Soares, J. and Sousa. T. 2020. Chapter 6: INTEGRATION OF RENEWABLE ENERGY IN SMART GRID in Applications of Modern Heuristic Optimization Methods in Power and Energy Systems, First Edition. Edited by Kwang Y. Lee and Zita A. Vale. The Institute of Electrical and Electronics Engineers, Inc. Published by John Wiley & Sons, Inc.

Murty, V. V. V. S. N. and Kumar, A. 2020. Optimal Energy Management and Techno-economic Analysis in Microgrid with Hybrid Renewable Energy Sources, in Journal of Modern Power Systems and Clean Energy, vol. 8, no. 5, pp. 929-940. doi: 10.35833/MPCE.2020.000273.

Naidu, B.R, Panda, G, and Siano, P. 2018. A self-reliant dc microgrid: Sizing, control, adaptive dynamic power management, and experimental analysis, IEEE Trans Ind Inform. 14 (8) :3300–13. https://doi.org/10.1109/TII.2017.2780193.

Nasir, M.B. Hussain, A. K. Niazi, A.K. Nasir, M. 2022. An Optimal Energy Management System (EMS) for Residential and Industrial Microgrids, Energies, 15, 6266. https://doi.org/10.3390/ en15176266.

Natasha, J. and Warren P. 2020.Innovation and distribution of solar home systems in Bangladesh. Climate and Development: 1-13.

Naz, K. Zainab, F. Mehmood, K.K. Bukhari, S.B.A. Khalid, H.A. and Kim, C.H. 2021. An Optimized Framework for Energy Management of Multi-Microgrid Systems, Energies, 14, 6012. https://doi.org/10.3390/en14196012.

Nguyen, D.T. and Le, L. B. 2013. Optimal energy management for cooperative microgrids with renewable energy resources, 2013 IEEE International Conference on Smart Grid Communications (Smart Grid Comm), pp. 678-683, doi: 10.1109/SmartGridComm.2013.6688037.

Nikolaos, V. and Sahinidis. 2019. Mixed-integer nonlinear programming, Optimization and Engineering 20:301–306. part of Springer Nature 2019. https://doi.org/10.1007/s11081-019-09438-1.

Nisha, K. Dattatraya, S. Gaonkar, N. and Jayalakshmi, N.S. 2023. Operation and control of multiple electric vehicle load profiles in bipolar microgrid with photovoltaic and battery energy systems, J. Energy Storage 57, 106261.

Nocedal, J. and Wright, S. 2006. Numerical Optimization, 2rd ed.; Springer: New York, NY, USA.

Noureddine, T. and Djamel, L. 2021. Load flow analysis using newton raphson method in presence of distributed generation. International Journal of Power Electronics and Drive Systems (IJPEDS) 12, 489.

Nur, A. and Kaygusuz, A. 2021. Load Flow Analysis with Newton–Raphson and Gauss–Seidel Methods in a Hybrid AC/DC System. IEEE Canadian Journal of Electrical and Computer Engineering 44, 529–536.

Nyong-Bassey, B. E. 2022. A Concise Review of Energy Management Strategies for Hybrid Energy Storage Systems. European Journal of Engineering and Technology Research, Vol 7, Issue 3. DOI: http://dx.doi.org/10.24018/ejeng.2022.7.3.2815 ISSN: 2736-576X.

Olcay, K.; Çetinkaya, N. 2023. Analysis of the Electric Vehicle Charging Stations Effects on the Electricity Network with Artificial Neural Network. Energies, 16, 1282. https://doi.org/10.3390/en16031282.

Optimized Generation Scheduling of Thermal Generators Integrated to Wind Energy System with Storage. 2018. International Journal of Renewable Energy Research. (v8i2). doi.org/10.20508/ijrer.v8i2.7084.g7359.

Pandey, A.C. Das, V. Kumar, P. Singh, R. and Maurya, S.K. 2022. AEFA Based Optimal Dynamic Economic Load Dispatch Problem Considering Penetration of Renewable Energy Systems. Distributed Generation & Alternative Energy Journal doi.org/10.13052/dgaej2156-3306.3745.

Pappas, I. Avraamidou, S. Katz, J. Burnak, B. Beykal, B. Türkay, M. and Pistikopoulos, E.N. 2021. Multiobjective Optimization of Mixed-Integer Linear Programming Problems: A Multiparametric Optimization Approach, Ind Eng Chem Res. 16;60 (23): 8493-8503. doi: 10.1021/acs.iecr.1c01175. Epub 2021 Jun 4. PMID: 34219916; PMCID: PMC8248908.

Pearre, N. and Swan, L. 2020. Reimagining renewable electricity grid management with dispatchable generation to stabilize energy storage. Energy 203, 117917.

Peilin, X. Josep, M. Sen Tan, G., Bazmohammadi, N. Juan Vasquez, C. Mehrzadi, M. and Al-Turki, Y. 2021. Optimization-Based Power and Energy Management System in Shipboard Microgrid, A Review. IEEE SYSTEMS JOURNAL, 1937-9234.

Peres, F. and Castelli, M. 2021. Combinatorial Optimization Problems and Metaheuristics: Review, Challenges, Design, and Development. Appl. Sci. 11, 6449. https:// doi.org/10.3390/app11146449.

Petit, M. and Perez, Y. 2013.Coordination of EV fleet charging with distributed

Phani Raghav, L. Seshu Kumar, R. Koteswara Raju, D. and Singh, A. R. Optimal Energy Management of Microgrids Using Quantum Teaching Learning Based Algorithm, IEEE TRANSACTIONS ON SMART GRID, VOL. 12, NO. 6..
Power Syst., vol. 20, no. 3, pp. 1199-1206.

Prudhviraj, D. P. Kiran, B. S. and Pindoriya, N. M. 2020. Stochastic energy management of microgrid with nodal pricing, Journal of Modern Power Systems and Clean Energy, vol. 8, no. 1, pp. 102-110.

Pruitt, K.A. Braun, R.J. and Newman, A.M. 2013. Evaluating shortfalls in mixed-integer programming approaches for the optimal design and dispatch of distributed generation systems, Appl. Energy, 102, 386–398.

Qiyun. D. 2018. Electric Vehicle (EV) charging management and relieve impacts in grids." In 2018 9th IEEE International Symposium on Power Electronics for Distributed Generation Systems (PEDG), pp. 1-5. IEEE.

Radha, K. and Singh B. 2019. A power quality improved EV charger with bridgeless Cuk converter." IEEE Transactions on Industry Applications 55, no. 5: 5190-5203.

Ray, S. Kasturi, K. Patnaik, S. and Nayak, M. R. 2023. Review of electric vehicles integration impacts in distribution networks: Placement, charging/discharging strategies, objectives and optimisation models. Journal of Energy Storage 72, 108672.

REN21. 2017. Renewable Global Status Report (Paris: REN21 Secretariat), Renewable Energy Policy Network for the 21st Century. 2017ISBN 978-3-9818107-6-9.

Rivera, M.M., Guerrero-Mendez, C., Lopez-Betancur, D., Saucedo-Anaya, T., 2023. Dynamical Sphere Regrouping Particle Swarm Optimization: A Proposed Algorithm for

Dealing with PSO Premature Convergence in Large-Scale Global Optimization. Mathematics 11, 4339.

Rolan, A., Bogarra, S., Bakkar, M., 2022. Integration of Distributed Energy Resources to Unbalanced Grids Under Voltage Sags with Grid Code Compliance. IEEE Transactions on Smart Grid 13, 355–366.

Roy, C.; Das, D.K. 2021. A hybrid genetic algorithm (GA)–particle swarm optimization (PSO) algorithm for demand side management in smart grid considering wind power for cost optimization. Sādhanā. 46(2). doi.org/10.1007/s12046-021-01626-z.

Rwamurangwa, E. Gonzalez, J.D. and Butare, A. 2022. Integration of EV in the Grid Management: The Grid Behavior in Case of Simultaneous EV Charging-Discharging with the PV Solar Energy Injection. Electricity 3, 563–585.

Sahinidis, N.V. 2018. Mixed-integer nonlinear programming, Optim Eng. 20, 301–306 (2019). https://doi.org/10.1007/s11081-019-09438-1.

Sai Thirumala Baba, K. and Srinivas, V. 2016. Optimal Energy Management Strategy for Renewable Energy DC Microgrids, Vol-2 Issue-5, IJARIIE-ISSN(O)-2395-4396.

Sanchez, F.S.M. Sichac´, S.J.P. Rodriguez, S.R.R. 2017. Formulaci´on de funciones de Costo de Incertidumbre enPeque˜nas Centrales Hidroel´ectricas dentro de una Microgrid, Ingenier´ıas USBmed 8 (1), 29-36.

Sau-Bassols, J. Zhao, Q. García-González, J. Prieto-Araujo, E. and Gomis-Bellmunt, O. 2019. Optimal power flow operation of an interline current flow controller in an hybrid AC/DC meshed grid. Electric Power Systems Research 177, 105935.

Sauer, P. M. Pai, A. and Chow, J. H. 2017.Power System Dynamics and Stability,
Selvaraj, S., Choi, E., 2022. Dynamic Sub-Swarm Approach of PSO Algorithms for Text Document Clustering. Sensors 22, 9653.

Seng, C.K. Tien, T.L. Nanda, J. and Masri, S. 2015. Load Flow Analysis Using Improved Newton-Raphson Method. Applied Mechanics and Materials 793, 494–499.

Şengör, I. Erdinç, O. Yener, B. Taşcikaraoglu, A. and Catalão, J. P. 2018. Optimal energy management of EV parking lots under peak load reduction based dr programs considering uncertainty, IEEE Trans. on Sustain. Energy. doi: 10.1109/TSTE.2018.2859186.

Shaffer, B., Tarroja, B., Samuelsen, S., 2015. Dispatch of fuel cells as Transmission Integrated Grid Energy Resources to support renewables and reduce emissions. Applied Energy 148, 178–186.

Shafie-Khah, M. and Siano, P. 2018. A Stochastic Home Energy Management System Considering Satisfaction Cost and Response Fatigue, IEEE Transactions on Industrial Informatics, vol. 14, no. 2, pp. 629-638.

Shaheen, M. A. M., Hasanien, H. M., Mekhamer, S. F., and Talaat, H. E. A. 2019. Optimal Power Flow of Power Systems Including Distributed Generation Units Using Sunflower Optimization Algorithm. IEEE Access, 7, 109289–109300. https://doi.org/10.1109/access.2019.2933489.

Shahid, H. Ahmed, M. A. Lee, K. and Kim Y. 2020. Fuzzy logic weight-based charging scheme for optimal distribution of charging power among electric vehicles in a parking lot. Energies 13, no. 12: 3119.

Shahrabi, E. S. Hakimi, M. Hasankhani, A Derakhshan, G. and Abdi, B. 2021. Developing optimal energy management of energy hub in the presence of stochastic renewable energy resources, Sustain. Energy Grids Netw., 26.

Shayeghi, H. and Asefi, S. 2017. Optimal energy management in a microgrid applying renewable sources and demand response, The 5th Iranian Conference on Renewable Energy & Distributed Generation (ICREDG2017) – University of Gu.

Shekari, T. Gholami, A. and Aminifar, F. 2019. Optimal energy management in multi-carrier microgrids: an MILP approach, in Journal of Modern Power Systems and Clean Energy, vol. 7, no. 4, pp. 876-886, doi: 10.1007/s40565-019-0509-6.

Shi, W. Xie, X. Chu, C. and Gadh, R. 2015. Distributed Optimal Energy Management in Microgrids, IEEE Transactions on Smart Grid, vol.6, no.3, pp.1137-1146.

Sihotang, H.T., 2021. Determination of the Shortest Path Using the Ant Colony Optimization (ACO) Algorithm Approach. ComTech: Computer, Mathematics and Engineering Applications 12, 123–133.

Silva, H.G. Coelho, A.L.M. Faria, I.P. Araujo, B.G. 2022. ANN based impedance trajectory detection approach for loss of excitation protection of synchronous generators connected to transmission lines with SVCs. Electric Power Systems Research. 213:108766. doi.org/10.1016/j.epsr.2022.108766.

Sitek, P. and Wikarek, J. 2018. A multi-level approach to ubiquitous modeling and solving constraints in combinatorial optimization problems in production and distribution, Appl Intell 48, 1344–1367. https://doi.org/10.1007/s10489-017-1107-9.

Siti, M.W. Mbungu, N.T. Tungadio, D.H. Banza, B.B. Ngoma, L Tiako, R. 2022. Economic dispatch in a stand-alone system using a combinatorial energy management system, Journal of Energy Storage 55, 105695.

Sivaraman, P. and Sharmeela, C. 2021. Power quality problems associated with electric vehicle charging infrastructure. In Power Quality in Modern Power Systems, pp. 151-161. Academic Press.

Song, N.O. Lee, J.H. Kim, H.M. Im, Y.H. and Lee, J.Y. 2015. Optimal Energy Management of Multi-Microgrids with Sequentially Coordinated Operations. Energies 2015, 8, 8371-8390. https://doi.org/10.3390/en8088371.

Sridevi, T. Gu, M. and Meegahapola, L. 2022. Reaping the Benefits of Smart Electric Vehicle Charging and Vehicle-to-Grid Technologies: Regulatory, Policy and Technical Aspects. IEEE Access.

Srivastava, A.; Das, D.K. 2022. An adaptive chaotic class topper optimization technique to solve economic load dispatch and emission economic dispatch problem in power system. Soft Computing., 26(6), 2913–2934. doi.org/10.1007/s00500-021-06644-x.

Stochastically coordinated transmission and distribution system operation with large-scale wind farms. 2020. CSEE Journal of Power and Energy Systems. doi.org/10.17775/cseejpes.2020.02150.

Stojiljković, M.M. Stojiljković, M.M and Blagojević, B.D. 2014. Multi-Objective Combinatorial Optimization of Trigeneration Plants Based on Metaheuristics. Energies 2014, 7, 8554-8581. https://doi.org/10.3390/en7128554.

Sulaiman, N. Hannan, M.A. Mohamed, A. Majlan, E.H. and WanDaud, W.R. 2015. A review on energy management system for fuel cell hybrid electric vehicle: Issues and challenges, Renewable and Sustainable Energy Reviews 52, 802–814.

Sultana, U. Mujahid, A. Jilani, H.A. and Perveen, U. 2022. Cost Minimization in Radial Distribution System Integrated with Commercial Electric Vehicle Charging Station. Eng. Proc. 20, 15. https:// doi.org/10.3390/engproc2022020015.

Summary of travel trends: 2024. National Household Travel Survey, Federal Highway Administration, USA, Available Online: https://nhts.ornl.gov/vehicle-trips. Accessed 29042024.

Sundstr̆om O. and Stefanopoulou, A. 2006. Optimal power split in fuel cell hybrid electric vehicle with different battery sizes, drive cycles, and objectives, In: Proceedings of the international conference on control applications; pp. 1681–8.

Sunny, J. C and Thomas, J. P. 2017. An Optimal Energy Management Strategy for Standalone DC Microgrids. International Journal of Engineering Research & Technology (IJERT), Vol. 6 Issue 04, April-2017.http://www.ijert.org ISSN: 2278-0181.

Surbhi, P. Sujil, A. Ratra, S. and Kumarm R. 2020. Electric vehicle charging station Challenges and opportunities: a future perspective." In 2020 International Conference on Emerging Trends in Communication, Control and Computing (ICONC3), pp. 1-6. IEEE.

Suresh, V. and Suresh, S. 2015. Economic Dispatch and Cost Analysis on a Power System Network Interconnected with Solar Farm, International Journal of Renewable Energy Research, Vol.5, No.4.

Taslimi, M. Ahmadi, P. Ashjaee, M. and Rosen, M. 2021. Design and mixed integer linear programming optimization of a solar/battery-based Conex for remote areas and various climate zones, Sustainable Energy Technologies and Assessments. 45. 101104. 10.1016/j.seta.2021.101104.

Ton, D.T. and Smith, M.A. 2012. The USA department of energy's microgrid initiative, Electr J. 25(8):84–94.

Tuani, A.F., Keedwell, E., Collett, M., 2020. Heterogenous Adaptive Ant Colony Optimization with 3-opt local search for the Travelling Salesman Problem. Applied Soft Computing 97, 106720.

Tuladhar, S.R. Singh, J.G. Ongsakul, W. 2016.Multi-objective approach for distribution network reconfiguration with optimal DG power factor using NSPSO. IET Generation, Transmission & Distribution 10(12), pp. 2842–2851. doi.org/10.1049/iet-gtd.2015.0587.

Vanderbei, R. J. Linear Programming, Springer International Publishing, 2020.

Viet Thang, T. Islam, M. R. Muttaqi, K. M. and Sutanto D. 2019. An efficient energy management approach for a solar-powered EV battery charging facility to support distribution grids. IEEE Transactions on Industry Applications 55, no. 6: 6517-6526.

Wang, B. Chen, J. Wang, J. Kim, and Begovic, M. 2018. Robust optimization based optimal dg placement in microgrids, IEEE Trans Smart Grid. 5(5): 2173–82. 2018.
Wang, Bo. 2020.Advanced Control and Energy Management Schemes for Power Grids with High Proliferation of Renewables and Electric Vehicles." PhD diss., The George Washington University.

Wang, J. and Song, Y. 2023. Distributionally robust OPF in distribution network considering CVaR-averse voltage security. International Journal of Electrical Power & Energy Systems 145, 108624.

Wang, L. Yang, Z. Sharma, S. Mian, A. Lin, T.E. Tsatsaronis G. Maréchal, F. and Yang, Y. 2019. 2019. A Review of Evaluation, Optimization and Synthesis of Energy Systems, Methodology and Application to Thermal Power Plants. Energies, 12, 73. https://doi.org/10.3390/en12010073.

Wang, S. Liu, X. and Ha, J. Optimal IoT-based decision-making of smart grid dispatchable generation units using blockchain technology considering high uncertainty of system, Ad Hoc Networks 127 (2022) 102751.

Wang, X. Ji, Y. Wang, J. Wang, Y. and Qi, L. 2020. Optimal energy management of microgrid based on multi-parameter dynamic programming. Intelligent IoT - Artificial Intelligence for Future Internet of Things - Research Article, International Journal of Distributed Sensor Networks, Vol. 16(6). https://doi.org/10.1177/1550147720937141.

Wu, D. and Lisser, A. 2022. A deep learning approach for solving linear programming problems, Neurocomputing 520 (2022) 15–24.

Wu, H. Li, H. and Gu, X. 2020. Optimal energy management for microgrids considering uncertainties in renewable energy generation and load demand, Processes, 8.

Wu, K.Y. Tai, T.C. Li, B.H. and Kuo, C.C. 2024. Dynamic Energy Management Strategy of a Solar-and-Energy Storage M -Integrated Smart Charging Station. Appl. Sci.2024, 14, 1188. https://doi.org/ 10.3390/app14031188.

Xie, P. Guerrero, J. M. Tan, S. Bazmohammadi, N. Vasquez, J.C. Mehrzadi, M. and Al-Turki, Y. 2022.Optimization-Based Power and Energy Management System in Shipboard Microgrid: A Review, IEEE SYSTEMS JOURNAL, VOL. 16, NO. 1.

Xu, J. Liu, A. Qin, Y. Xu, G. and Tang, Y. 2022. A Cost-Effective Solution to Dynamic Economic Load Dispatch Problem Using Improved Chimp Optimizer. Frontiers in Energy Research 10. doi.org/10.3389/fenrg.2022.952354.

Xu, Q. Yang, B. Han, Q. Yuan, Y. Chen, C. and Guan, X. 2019. Optimal power management for failure mode of MV dc microgrids in all-electric ships, IEEE Trans. Power Syst., vol. 34, no. 2, pp. 1054–1067, Mar. 2019.

Yu, X. Li, W. Maleki, A. Rosen, M.A. Birjandi, A.K. and Tang, L. 2021. Selection of optimal location and design of a stand-alone photovoltaic scheme using a modified hybrid methodology, Sustain. Energy Technol. Assessments, 45, 101071. 2021.

Yuan, Y. Zhang, T. Shen, B. Yan X., and Long, T. A fuzzy logic energy management strategy for a photovoltaic/diesel/battery hybrid ship based on experimental database, Energies, vol. 11, no. 9, p. 2211. 2018.

Zhang, W. Maleki, A. Pourfayaz, F. and Shadloo, 2021. M.S. An artificial intelligence approach to optimization of an off-grid hybrid wind/hydrogen system, Int. J. Hydrogen Energy, 46, 12725–12738. 2021.

Zhou, X. Chang, C. Bernstein, A. Zhao, C. and Chen, L. 2021. Economic Dispatch with Distributed Energy Resources: Co-Optimization of Transmission and Distribution Systems, IEEE CONTROL SYSTEMS LETTERS, VOL. 5, NO. 6.

APPENDICES

A. MINLP Scripts for Energy Management System for Hybrid System

batterySolarOptimize

```
function [Pgrid,Pbatt,Ebatt] =
battSolarOptimize(N,dt,Ppv,Pload,Einit,Cost,FinalWeight,batteryMinMax)
% battSolarOptimize - function to optimize usage of energy storage for a
% small-scale grid.
%
% [Pgrid,Pbatt,Ebatt] = battSolarOptimize(N,dt,Ppv,Pload,Einit,Cost,...
%                       FinalWeight,batteryMinMax)
%
%   Inputs:
%       N       - Optimization step horizon, number of discrete steps
%       dt      - Time between optimization calls [s]
%       Ppv     - Vector of Current and Forecast PV Power [W]
%       Pload   - Vector of Current and Forecast Grid Load [W]
%       Einit   - Initial Battery Energy [J]
%       Cost    - Cost Vector of Current and Forecast Grid Price [$/kWh]
%       FinalWeight   - Tunable Weight for Final Energy storage
%       batteryMinMax - Structure of simplified battery properties
%
%   Outputs:
%       Pgrid   - Optimal vector of grid power usage [W]
%       Pbatt   - Optimized battery usage [W]
%       Ebatt   - Total battery energy over optimization horizon [J]
%
% Power offset - battery/grid make up the difference
d = Pload - Ppv;

% Sub-matrices for optimization constraints
eyeMat = eye(N);
zeroMat = zeros(N);

battPower = diag(ones(N-1,1),-1)*dt;
battEnergy = diag(-ones(N-1,1),-1) + eye(N);

% Generate the equivalent constraint matrices
Aeq = [eyeMat   eyeMat     zeroMat;
       zeroMat  battPower   battEnergy];
beq = [d; Einit; zeros(N-1,1)];

% Generate the objective function
f = [(Cost*dt)' zeros(1,N) zeros(1,N-1) -FinalWeight];

% Constraint equations
A = [zeroMat    eyeMat      zeroMat;
     zeroMat    -eyeMat     zeroMat;
     zeroMat    zeroMat     eyeMat;
     zeroMat    zeroMat     -eyeMat];
b = [batteryMinMax.Pmax*ones(N,1);
```

```
    -batteryMinMax.Pmin*ones(N,1);
    batteryMinMax.Emax*ones(N,1);
    -batteryMinMax.Emin*ones(N,1)];

% Perform Linear programming optimization
options = optimset('Display','none');
xopt = linprog(f,A,b,Aeq,beq,[],[],[],options);

% Parse optmization results
if isempty(xopt)
    Pgrid = zeros(N,1);
    Pbatt = zeros(N,1);
    Ebatt = zeros(N,1);
else
    Pgrid = xopt(1:N);
    Pbatt = xopt(N+1:2*N);
    Ebatt = xopt(2*N+1:end);
end
```

batterySolarOptimize

```
function [Pgrid,Pbatt,Ebatt] =
battSolarOptimize(N,dt,Ppv,Pload,Einit,Cost,FinalWeight,batteryMinMax)

% Minimize the cost of power from the grid while meeting load with power
% from PV, battery and grid

prob = optimproblem;

% Decision variables
PgridV = optimvar('PgridV',N);
PbattV =
optimvar('PbattV',N,'LowerBound',batteryMinMax.Pmin,'UpperBound',batteryMinMax.Pmax);
EbattV =
optimvar('EbattV',N,'LowerBound',batteryMinMax.Emin,'UpperBound',batteryMinMax.Emax);

% Minimize cost of electricity from the grid
prob.ObjectiveSense = 'minimize';
prob.Objective = dt*Cost'*PgridV - FinalWeight*EbattV(N);

% Power input/output to battery
prob.Constraints.energyBalance = optimconstr(N);
prob.Constraints.energyBalance(1) = EbattV(1) == Einit;
prob.Constraints.energyBalance(2:N) = EbattV(2:N) == EbattV(1:N-1) - PbattV(1:N-1)*dt;

% Satisfy power load with power from PV, grid and battery
prob.Constraints.loadBalance = Ppv + PgridV + PbattV == Pload;

% Solve the linear program
options = optimoptions(prob.optimoptions,'Display','none');
[values,~,exitflag] = solve(prob,'Options',options);

% Parse optmization results
if exitflag <= 0
    Pgrid = zeros(N,1);
```

```
    Pbatt = zeros(N,1);
    Ebatt = zeros(N,1);
else
    Pgrid = values.PgridV;
    Pbatt = values.PbattV;
    Ebatt = values.EbattV;
end
```

energyOptimizationScript.m

```
% Load Power Data from Existing PV array
load pvLoadPriceData;

% Set up Optimization Parameters
numDays = 1;            % Number of consecutive days
FinalWeight = 1;      % Final weight on energy storage
timeOptimize = 5;       % Time step for optimization [min]

% Battery/PV parameters
panelArea = 2500;
panelEff = 0.3;

battEnergy = 2500*3.6e6;
Einit = 0.5*battEnergy;
batteryMinMax.Emax = 0.8*battEnergy;
batteryMinMax.Emin = 0.2*battEnergy;
batteryMinMax.Pmin = -400e3;
batteryMinMax.Pmax = 400e3;

% Rescale data to align with desired time steps
stepAdjust = (timeOptimize*60)/(time(2)-time(1));
cloudyPpv = panelArea*panelEff*repmat(cloudyDay(2:stepAdjust:end),numDays,1);
clearPpv = panelArea*panelEff*repmat(clearDay(2:stepAdjust:end),numDays,1);

% Adjust and Select Loading
loadSelect = 3;
loadBase = 350e3;
loadFluc = repmat(loadData(2:stepAdjust:end,loadSelect),numDays,1) + loadBase;

% Grid Price Values [$/kWh]
C = repmat(costData(2:stepAdjust:end),numDays,1);

% Select Desired Data for Optimization
Ppv = clearPpv;
% Ppv = cloudyPpv;
Pload = loadFluc;

% Setup Time Vectors
dt = timeOptimize*60;
N = numDays*(numel(time(1:stepAdjust:end))-1);
tvec = (1:N)'*dt;

% Optimize Grid Energy Usage
[Pgrid,Pbatt,Ebatt] = battSolarOptimize(N,dt,Ppv,Pload,Einit,C,FinalWeight,batteryMinMax);
```

```
% Plot Results
figure;
subplot(3,1,1);
thour = tvec/3600;
plot(thour,Ebatt/3.6e6); grid on;
xlabel('Time [hrs]'); ylabel('Battery Energy [kW-h]');
subplot(3,1,2);
plot(thour,C); grid on;
xlabel('Time [hrs]'); ylabel('Grid Price [$/kWh]');

subplot(3,1,3);
plot(thour,Ppv/1e3,thour,Pbatt/1e3,thour,Pgrid/1e3,thour,Pload/1e3);
grid on;
legend('PV','Battery','Grid','Load')
xlabel('Time [hrs]'); ylabel('Power [W]');
```

Resources

battSolarOptimize

```
function [Pgrid,Pbatt,Ebatt] =
battSolarOptimize(N,dt,Ppv,Pload,Einit,Cost,FinalWeight,batteryMinMax)

% Minimize the cost of power from the grid while meeting load with power
% from PV, battery and grid

prob = optimproblem;

% Decision variables
PgridV = optimvar('PgridV',N);
PbattV =
optimvar('PbattV',N,'LowerBound',batteryMinMax.Pmin,'UpperBound',batteryMinMax.Pmax);
EbattV =
optimvar('EbattV',N,'LowerBound',batteryMinMax.Emin,'UpperBound',batteryMinMax.Emax);

% Minimize cost of electricity from the grid
prob.ObjectiveSense = 'minimize';
prob.Objective = dt*Cost'*PgridV - FinalWeight*EbattV(N);

% Power input/output to battery
prob.Constraints.energyBalance = optimconstr(N);
prob.Constraints.energyBalance(1) = EbattV(1) == Einit;
prob.Constraints.energyBalance(2:N) = EbattV(2:N) == EbattV(1:N-1) - PbattV(1:N-1)*dt;

% Satisfy power load with power from PV, grid and battery
prob.Constraints.loadBalance = Ppv + PgridV + PbattV == Pload;

% Solve the linear program
options = optimoptions(prob.optimoptions,'Display','none');
[values,~,exitflag] = solve(prob,'Options',options);

% Parse optmization results
if exitflag <= 0
```

```
    Pgrid = zeros(N,1);
    Pbatt = zeros(N,1);
    Ebatt = zeros(N,1);
else
    Pgrid = values.PgridV;
    Pbatt = values.PbattV;
    Ebatt = values.EbattV;
end
```

compareCosts.m

```
% mdl = 'microgrid_WithESSOpt';
mdl = bdroot;

% Heuristic-based EMS Control
in(1) = Simulink.SimulationInput(mdl);
in(1) = in(1).setBlockParameter([mdl ...
    '/Energy Management System/Energy Management Mode'],'Value','0');

% Optimization-based EMS Control
in(2) = Simulink.SimulationInput(mdl);
in(2) = in(2).setBlockParameter([mdl ...
    '/Energy Management System/Energy Management Mode'],'Value','1');

% No Battery Storage
in(3) = Simulink.SimulationInput(mdl);
in(3) = in(3).setBlockParameter([mdl ...
    '/Energy Management System/Energy Management Mode'],'Value','2');

% Perform Simulations
out = sim(in,'ShowProgress','off');

% Plot Results
subplot(2,1,1)
for i = 1:numel(in)
    plot(out(i).logsout{4}.Values.Time/3600,...
        out(i).logsout{4}.Values.Data,'LineWidth',2); hold on;
end
title('Cumulative Grid Cost ($)');
xlabel('Time (hours)'); ylabel('Rolling Cost ($)');
legend('Heuristic','Optimization','No Storage','Location','northwest');
grid on;

subplot(2,1,2)
for i = 1:numel(in)
    plot(out(i).logsout{2}.Values.Time/3600,...
        out(i).logsout{2}.Values.Data,'LineWidth',2); hold on;
end
title('Cumulative Grid Usage (kW-h)');
xlabel('Time (hours)'); ylabel('Grid Usage (kW-h)');
legend('Heuristic','Optimization','No Storage','Location','northwest');
grid on; hold off;

% Compare Final Cost
```

```
costHeuristic = out(1).logsout{4}.Values.Data(end);
costOpt = out(2).logsout{4}.Values.Data(end);
perDiff = (costOpt-costHeuristic)/costHeuristic;

disp(['Heuristic EMS Cost: $ ' num2str(costHeuristic)]);
disp(['Optimization EMS Cost: $ ' num2str(costOpt)]);
disp(['Difference (%) between Methods: ' num2str(perDiff*100) '%']);
```

InitialConditions.m

```
load pvLoadPriceData.mat;
costDataOffset = costData + 5;

% Grid Settings
panelArea = 2500;   % Area of PV Array [m^2]
panelEff = 0.3;     % Efficiency of Array
loadBase = 350e3;   % Base Load of Microgrid [W]

BattCap = 2500;     % Energy Storage Rated Capacity [kWh]
batteryMinMax.Pmin = -400e3;    % Max Discharge Rate [W]
batteryMinMax.Pmax = 400e3;     % Max Charge Rate [W]

% Online optimization parameters
FinalWeight = 1;    % Final weight on energy storage
timeOptimize = 5;    % Time step for optimization [min]
timePred = 20;        % Predict ahead horizon [hours]

% Compute PV Array Power Output
cloudyPpv = panelArea*panelEff*cloudyDay;
clearPpv = panelArea*panelEff*clearDay;

% Select Load Profile
loadSelect = 3;
loadFluc = loadData(:,loadSelect);

% Battery SOC Energy constraints (keep between 20%-80% SOC)
battEnergy = 3.6e6*BattCap;
batteryMinMax.Emax = 0.8*battEnergy;
batteryMinMax.Emin = 0.2*battEnergy;

% Setup Optimization time vector
optTime = timeOptimize*60;
stepAdjust = (timeOptimize*60)/(time(2)-time(1));
N = numel(time(1:stepAdjust:end))-1;
tvec = (1:N)'*optTime;

% Horizon for "sliding" optimization
M = find(tvec > timePred*3600,1,'first');
numDays = 2; % Repeat data for end of day forcasts
loadSelect = 3;
clearPpvVec = panelArea*panelEff*repmat(clearDay(2:stepAdjust:end),numDays,1);
for loadSelect = 1:4
   loadDataOpt(:,loadSelect) = repmat(loadData(2:stepAdjust:end,loadSelect),numDays,1) +
loadBase;
```

```
end
C = repmat(costData(2:stepAdjust:end),numDays,1);

CostMat = zeros(N,M);
PpvMat = zeros(N,M);
PloadMat = zeros(N,M);

% Construct forecast vectors for optimization (N x M) matrix
for i = 1:N
   CostMat(i,:) = C(i:i+M-1);
   PpvMat(i,:) = clearPpvVec(i:i+M-1);
   PloadMat(i,:) = loadDataOpt(i:i+M-1,loadSelect);
End

CostForecast.time = tvec;
CostForecast.signals.values = CostMat;
CostForecast.signals.dimensions = M;

PpvForecast.time = tvec;
PpvForecast.signals.values = PpvMat;
PpvForecast.signals.dimensions = M;

PloadForecast.time = tvec;
PloadForecast.signals.values = PloadMat;
PloadForecast.signals.dimensions = M;

%Clean up unneeded Variables
clear clearDay cloudyDay BattCap panelArea panelEff loadBase;
clear M N i loadSelect numDays stepAdjust timeOptimize;
clear CostMat PloadMat PpvMat clearPpvVec C;
clear batteryMinMax timePred tvec loadData loadDataOpt FinalWeight


compareCosts_Multi.mix

clear;
initialConditions;
mdl = 'microgrid_WithESSOpt';
pvDataSet = [0;1];
numOffset = 5;
offset = linspace(1,25,numOffset);
offset = repmat(offset,1,2)';
[xVec,yVec] = meshgrid(offset,pvDataSet);
inputVec = [xVec(:) yVec(:)];
numSim = size(inputVec,1);
inputVec(numOffset*numel(pvDataSet)+1:end,3) = 1;
for i = 1:numSim
   in(i) = Simulink.SimulationInput(mdl);
   in(i) = in(i).setVariable('emsMode',inputVec(i,3));
   in(i) = in(i).setVariable('pvSelect',inputVec(i,2));

   costDataOffset = [costData(inputVec(i,1):end); costData(1:inputVec(i,1)-1)];
   in(i) = in(i).setVariable('costDataOffset',costDataOffset);
end
in(1)
```

```
ans =
  SimulationInput with properties:

         ModelName: 'microgrid_WithESSOpt'
      InitialState: [0×0 Simulink.SimState.ModelSimState]
     ExternalInput: []
   ModelParameters: [0×0 Simulink.Simulation.ModelParameter]
   BlockParameters: [0×0 Simulink.Simulation.BlockParameter]
         Variables: [1×3 Simulink.Simulation.Variable]
         PreSimFcn: []
        PostSimFcn: []
        UserString: ''
out = sim(in, 'ShowSimulationManager', 'on','UseFastRestart',true,'ShowProgress','off');
Warning: Connected variable 'emsMode' not found for 'Slider Switch'
Warning: Connected variable 'pvSelect' not found for 'Combo Box'
heuristicCost = [];
optCost = [];
for i = 1:numSim
   if i <= numOffset*numel(pvDataSet)
      heuristicCost(end+1) = out(i).logsout{1}.Values.Data(end);
   else
      optCost(end+1)= out(i).logsout{1}.Values.Data(end);
   end
end
histogram(heuristicCost); hold on;
histogram(optCost);
legend('Heuristic','Optimization');
xlabel('Cost per Day ($)'); hold off;
```

B. PSO Method for EPD Problem of a Grid-tied RES-HS Scripts

```
%
function model=CreateModel()
    model.PD=1263;

    model.Plants.Pmin=[100 50 80 50 50 50];
    model.Plants.Pmax=[500 200 300 150 200 120];
    model.Plants.alpha=[240 200 220 200 220 190];
    model.Plants.beta=[7 10 8.5 11 10.5 12];
    model.Plants.gamma=[0.007 0.0095 0.009 0.009 0.008 0.0075];
    model.Plants.P0=[440 170 200 150 190 110];
    model.Plants.UR=[80 50 65 50 50 50];
    model.Plants.DR=[120 90 100 90 90 90];

    model.Plants.PminActual = max(model.Plants.Pmin,model.Plants.P0-model.Plants.DR);
    model.Plants.PmaxActual = min(model.Plants.Pmax,model.Plants.P0+model.Plants.UR);

    model.Plants.PZ{1}={[210 240],[350 380]};
    model.Plants.PZ{2}={[90 110],[140 160]};
    model.Plants.PZ{3}={[150 170],[210 240]};
    model.Plants.PZ{4}={[80 90],[110 120]};
    model.Plants.PZ{5}={[90 110],[140 150]};
    model.Plants.PZ{6}={[75 85],[100 105]};

    model.nPlant=numel(model.Plants.alpha);

    model.B=[ 0.0017  0.0012  0.0007 -0.0001 -0.0005 -0.0002
              0.0012  0.0014  0.0009  0.0001 -0.0006 -0.0001
              0.0007  0.0009  0.0031  0.0000 -0.0010 -0.0006
             -0.0001  0.0001  0.0000  0.0024 -0.0006 -0.0008
             -0.0005 -0.0006 -0.0010 -0.0006  0.0129 -0.0002
             -0.0002 -0.0001 -0.0006 -0.0008 -0.0002  0.0150]/40;
    model.B0=1e-3*[-0.3908 -0.1279 0.7047 0.0591 0.2161 -0.6635];

    model.B00=0.056;
end



%
function model=CreateModel1()
    model.PD=850;
    model.Plants.Pmin=[100 100 50];
    model.Plants.Pmax=[600 400 200];
    model.Plants.alpha=[561 310 78];
    model.Plants.beta=[7.92 7.85 7.97];
    model.Plants.gamma=[0.001562 0.001940 0.004820];
    model.Plants.P0=[440 350 170];
    model.Plants.UR=[80 80 50];
    model.Plants.DR=[120 120 90];

    model.Plants.PminActual = max(model.Plants.Pmin,model.Plants.P0-model.Plants.DR);
    model.Plants.PmaxActual = min(model.Plants.Pmax,model.Plants.P0+model.Plants.UR);
```

```
    model.Plants.PZ{1}={[210 240],[350 380]};
    model.Plants.PZ{2}={[90 110],[140 160]};
    model.Plants.PZ{3}={[150 170],[210 240]};

    model.nPlant=numel(model.Plants.alpha);

    model.B=[ 0.0002940  0.0000901  -0.0000507
              0.0000901  0.0005210  0.0000953
              -0.0000507  0.0000953  0.0006760]/40;

    model.B0=1e-3*[0.01890,-0.00342,-0.007660];

    model.B00=0.40357;
end



%
function model=CreateModel2()
    model.PD=1263;
    model.Plants.Pmin=[100 50 80 50 50 50];
    model.Plants.Pmax=[500 200 300 150 200 120];
    model.Plants.alpha=[240 918.558 183.851 918.558 183.851 190];
    model.Plants.beta=[7 33.544 3.643  33.544 3.643 12];
    model.Plants.gamma=[0.007 0.331 1.744 0.33 1.744 0.0075];
    model.Plants.P0=[440 150 75 100 50 110];
    model.Plants.UR=[80 25 25 25 25 50];
    model.Plants.DR=[120 25 25 25 25 90];

    model.Plants.PminActual = max(model.Plants.Pmin,model.Plants.P0-model.Plants.DR);
    model.Plants.PmaxActual = min(model.Plants.Pmax,model.Plants.P0+model.Plants.UR);

    model.Plants.PZ{1}={[210 240],[350 380]};
    model.Plants.PZ{2}={[90 110],[140 160]};
    model.Plants.PZ{3}={[150 170],[210 240]};
    model.Plants.PZ{4}={[80 90],[110 120]};
    model.Plants.PZ{5}={[90 110],[140 150]};
    model.Plants.PZ{6}={[75 85],[100 105]};

    model.nPlant=numel(model.Plants.alpha);

    model.B=[ 0.0017  0.0012  0.0007 -0.0001 -0.0005 -0.0002
              0.0012  0.0014  0.0009  0.0001 -0.0006 -0.0001
              0.0007  0.0009  0.0031  0.0000 -0.0010 -0.0006
             -0.0001  0.0001  0.0000  0.0024 -0.0006 -0.0008
             -0.0005 -0.0006 -0.0010 -0.0006  0.0129 -0.0002
             -0.0002 -0.0001 -0.0006 -0.0008 -0.0002  0.0150]/40;
    model.B0=1e-3*[-0.3908 -0.1279 0.7047 0.0591 0.2161 -0.6635];

    model.B00=0.056;
end



%
```

```
function model=CreateModel3()
    model.PD=850;
    model.Plants.Pmin=[100 20 50];
    model.Plants.Pmax=[600 100 200];
    model.Plants.alpha=[561 918.558 183.851];
    model.Plants.beta=[7.92 33.544 3.643];
    model.Plants.gamma=[0.001562 0.331 1.744];
    model.Plants.P0=[440 50 110];
    model.Plants.UR=[80 25 50];
    model.Plants.DR=[120 25 90];

    model.Plants.PminActual = max(model.Plants.Pmin,model.Plants.P0-model.Plants.DR);
    model.Plants.PmaxActual = min(model.Plants.Pmax,model.Plants.P0+model.Plants.UR);

     model.Plants.PZ{1}={[210 240],[350 380]};
    model.Plants.PZ{2}={[40 50],[50 90]};
    model.Plants.PZ{3}={[150 170],[210 240]};

    model.nPlant=numel(model.Plants.alpha);

    model.B=[ 0.0002940  0.0000901  -0.0000507
            0.0000901  0.0005210  0.0000953
            -0.0000507  0.0000953  0.0006760]/40;

    model.B0=1e-3*[0.01890,-0.00342,-0.007660];

    model.B00=0.40357;
end



%
function model=CreateModel15()
    model.PD=2630;

    model.Plants.Pmin=[150 150 20 20 150 135 135 60 25 25 20 20 25 15 15];
    model.Plants.Pmax=[455 455 130 130 470 460 465 300 162 160 80 80 85 55 55];
    model.Plants.alpha=[671 574 374 374 461 630 548 227 173 175 186 230 225 309 323];
    model.Plants.beta=[10.10 10.20 8.80 8.80 10.40 10.10 9.80 11.20 11.20 10.70 10.20 9.90
13.10 12.10 12.40];
    model.Plants.gamma=[0.0002990 0.0001830 0.0011260  0.0011260 0.0002050
0.0003010 0.0003640 0.0003380 0.0008070 0.0012030 0.0035860 0.0055130 0.0003710
0.0019290 0.0044470];
    model.Plants.P0=[400 300 105 100 90 400 350 95 105 110 60 40 30 30 20];
    model.Plants.UR=[80 80 130 130 80 80 80 65 60 60 80 80 80 55 55];
    model.Plants.DR=[120 120 130 130 120 120 120 100 100 100 80 80 80 55 55];

    model.Plants.PminActual = max(model.Plants.Pmin,model.Plants.P0-model.Plants.DR);
    model.Plants.PmaxActual = min(model.Plants.Pmax,model.Plants.P0+model.Plants.UR);

    model.Plants.PZ{1}={[210 240],[350 380]};
    model.Plants.PZ{2}={[210 240],[350 380]};
    model.Plants.PZ{3}={[90 110],[140 160]};
    model.Plants.PZ{4}={[80 90],[110 120]};
    model.Plants.PZ{5}={[210 240],[350 380]};
```

```
    model.Plants.PZ{6}={[210 240],[350 380]};
    model.Plants.PZ{7}={[210 240],[350 380]};
    model.Plants.PZ{8}={[150 170],[210 240]};
    model.Plants.PZ{9}={[080 090],[110 120]};
    model.Plants.PZ{10}={[080 090],[110 120]};
    model.Plants.PZ{11}={[065 075],[060 80]};
    model.Plants.PZ{12}={[065 075],[060 75]};
    model.Plants.PZ{13}={[065 075],[060 75]};
    model.Plants.PZ{14}={[030 055],[040 50]};
    model.Plants.PZ{15}={[030 055],[040 50]};


    model.nPlant=numel(model.Plants.alpha);

    model.B=[ 0.0014  0.0012  0.0007 -0.0001 -0.0003 -0.0001 -0.0001 -0.0001 -0.0003
0.0005 -0.0003 -0.0002 0.0004 0.0003 -0.0001
            0.0012 0.0015 0.0013 0.0000 -0.0005 -0.0002 0.0000 0.0001 -0.0002 -0.0004 -
0.0001 -0.0000 0.0004 0.0010 -0.0002
            0.0007 0.0013 0.0076 -0.0001 -0.0013 -0.0009 0.0001 0.0000 -0.0008 -0.0012 -
0.0017 -0.0000 -0.0026 0.0111 -0.0028
            -0.0001 0.0000 -0.0001 0.0034 -0.0007 -0.0001 0.0011 0.0050 0.0029 0.0032 -
0.0011 -0.0000 0.0001 0.0001 -0.0026
            -0.0003 -0.0005 -0.0013 -0.0007 0.0090 0.0014 -0.0003 -0.0012 -0.0010 0.0013 -
0.0007 -0.0002 -0.0002 -0.0024 -0.0003
            -0.0001 -0.0002 -0.0009 -0.0004 0.0014 0.0016 -0.0000 -0.0006 -0.0005 -0.0008
0.0011 -0.0001 -0.0002 -0.0017 0.0003
            -0.0001 0.0000 -0.0001 0.0011 0.0003 -0.0000 0.0015 0.0017 0.0015 0.0009 -
0.0005 -0.0007 -0.0000 -0.0002 0.0008
            -0.0001 0.0001 0.0000 0.0050 0.0012 -0.0006 0.0017 0.0168 0.0082 0.0079 -
0.0023 -0.0036 0.0001 0.0005 -0.0078
            -0.0003 -0.0002 -0.0008 0.0029 -0.0010 -0.0005 0.0015 0.0082 0.0129 0.0116 -
0.0021 -0.0025 0.0007 0.0012 -0.0072
            -0.0005 -0.0001 -0.0012 0.0032 -0.0013 -0.0008 0.0009 0.0079 0.0116 0.0200 -
0.0027 -0.0031 0.0009 -0.0011 -0.0088
            -0.0003 -0.0004 -0.0017 0.0011 -0.0007 0.0011 -0.0005 -0.0023 -0.0021 -0.0027 -
0.0140 0.0001 0.0004 0.0038 0.0168
            -0.0002 -0.0000 -0.0000 -0.0000 -0.0002 -0.0001 0.0007 -0.0036 -0.0025 -0.0003
0.0001 0.0051 -0.0001 -0.0004 0.0028
            0.0004 0.0004 -0.0026 0.0001 -0.0002 -0.0002 -0.0000 0.0001 0.0007 0.0009
0.0004 -0.0001 0.0103 -0.0101 0.0028
            0.0003 0.0010 0.0111 0.0001 -0.0024 -0.0017 -0.0002 0.0005 -0.0012 -0.0011 -
0.0038 -0.0004 -0.0101 0.0578 -0.0094
            -0.0001 -0.0002 -0.0028 -0.0026 -0.0003 0.0003 -0.0008 -0.0078 -0.0072 -0.0088
0.0168 0.0028 0.0028 -0.0094 0.1283]/40;

     model.B0=1e-3*[-0.0001, -0.0002, 0.0028, -0.0001, 0.0001, -0.0003, -0.0002, -0.0002,
0.0006, 0.0039, -0.0017, -0.0000, -0.0032, 0.0067, -0.0064];

    model.B00=0.055;
end
```

```
%
function model=CreateModel16()
    model.PD=2630;

    model.Plants.Pmin=[150 150 20 20 150 135 135 60 25 25 20 20 25 15 15];
    model.Plants.Pmax=[455 455 130 130 470 460 465 300 162 160 80 80 85 55 55];
    model.Plants.alpha=[671 574 918.558 183.851 461 183.851 548 918.558 918.558
183.851 918.558 183.851 918.558 183.851 323];
    model.Plants.beta=[10.10 10.20 33.544 3.643 10.40 3.643 9.80 33.544 33.544 3.643
33.544 3.643 33.544 3.643 12.40];
    model.Plants.gamma=[0.0002990 0.0001830 0.331  1.744 0.0002050 1.744 0.0003640
0.331 0.331 1.744 0.331 1.744 0.331 1.744 0.0044470];
    model.Plants.P0=[400 300 105 100 90 400 350 95 105 110 60 40 30 30 20];
    model.Plants.UR=[80 80 25 25 80 80 80 65 25 25 25 25 25 25 55];
    model.Plants.DR=[120 120 25 25 120 120 120 100 25 25 25 25 25 25 55];


    model.Plants.PminActual = max(model.Plants.Pmin,model.Plants.P0-model.Plants.DR);
    model.Plants.PmaxActual = min(model.Plants.Pmax,model.Plants.P0+model.Plants.UR);

     model.Plants.PZ{1}={[210 240],[350 380]};
    model.Plants.PZ{2}={[210 240],[350 380]};
    model.Plants.PZ{3}={[90 110],[140 160]};
    model.Plants.PZ{4}={[80 90],[110 120]};
    model.Plants.PZ{5}={[210 240],[350 380]};
    model.Plants.PZ{6}={[210 240],[350 380]};
    model.Plants.PZ{7}={[210 240],[350 380]};
    model.Plants.PZ{8}={[150 170],[210 240]};
    model.Plants.PZ{9}={[080 090],[110 120]};
    model.Plants.PZ{10}={[080 090],[110 120]};
    model.Plants.PZ{11}={[065 075],[060 80]};
    model.Plants.PZ{12}={[065 075],[060 75]};
    model.Plants.PZ{13}={[065 075],[060 75]};
    model.Plants.PZ{14}={[030 055],[040 50]};
    model.Plants.PZ{15}={[030 055],[040 50]};


    model.nPlant=numel(model.Plants.alpha);

    model.B=[ 0.0014  0.0012  0.0007 -0.0001 -0.0003 -0.0001 -0.0001 -0.0001 -0.0003
0.0005 -0.0003 -0.0002 0.0004 0.0003 -0.0001
            0.0012 0.0015 0.0013 0.0000 -0.0005 -0.0002 0.0000 0.0001 -0.0002 -0.0004 -
0.0001 -0.0000 0.0004 0.0010 -0.0002
            0.0007 0.0013 0.0076 -0.0001 -0.0013 -0.0009 0.0001 0.0000 -0.0008 -0.0012 -
0.0017 -0.0000 -0.0026 0.0111 -0.0028
            -0.0001 0.0000 -0.0001 0.0034 -0.0007 -0.0001 0.0011 0.0050 0.0029 0.0032 -
0.0011 -0.0000 0.0001 0.0001 -0.0026
            -0.0003 -0.0005 -0.0013 -0.0007 0.0090 0.0014 -0.0003 -0.0012 -0.0010 0.0013 -
0.0007 -0.0002 -0.0002 -0.0024 -0.0003
            -0.0001 -0.0002 -0.0009 -0.0004 0.0014 0.0016 -0.0000 -0.0006 -0.0005 -0.0008
0.0011 -0.0001 -0.0002 -0.0017 0.0003
            -0.0001 0.0000 -0.0001 0.0011 0.0003 -0.0000 0.0015 0.0017 0.0015 0.0009 -
0.0005 -0.0007 -0.0000 -0.0002 0.0008
```

```
        -0.0001 0.0001 0.0000 0.0050 0.0012 -0.0006 0.0017 0.0168 0.0082 0.0079 -
0.0023 -0.0036 0.0001 0.0005 -0.0078
        -0.0003 -0.0002 -0.0008 0.0029 -0.0010 -0.0005 0.0015 0.0082 0.0129 0.0116 -
0.0021 -0.0025 0.0007 0.0012 -0.0072
        -0.0005 -0.0001 -0.0012 0.0032 -0.0013 -0.0008 0.0009 0.0079 0.0116 0.0200 -
0.0027 -0.0031 0.0009 -0.0011 -0.0088
        -0.0003 -0.0004 -0.0017 0.0011 -0.0007 0.0011 -0.0005 -0.0023 -0.0021 -0.0027 -
0.0140 0.0001 0.0004 0.0038 0.0168
        -0.0002 -0.0000 -0.0000 -0.0000 -0.0002 -0.0001 0.0007 -0.0036 -0.0025 -0.0003
0.0001 0.0051 -0.0001 -0.0004 0.0028
         0.0004 0.0004 -0.0026 0.0001 -0.0002 -0.0002 -0.0000 0.0001 0.0007 0.0009
0.0004 -0.0001 0.0103 -0.0101 0.0028
         0.0003 0.0010 0.0111 0.0001 -0.0024 -0.0017 -0.0002 0.0005 -0.0012 -0.0011 -
0.0038 -0.0004 -0.0101 0.0578 -0.0094
        -0.0001 -0.0002 -0.0028 -0.0026 -0.0003 0.0003 -0.0008 -0.0078 -0.0072 -0.0088
0.0168 0.0028 0.0028 -0.0094 0.1283]/40;



   model.B0=1e-3*[-0.0001, -0.0002, 0.0028, -0.0001, 0.0001, -0.0003, -0.0002, -0.0002,
0.0006, 0.0039, -0.0017, -0.0000, -0.0032, 0.0067, -0.0064];

   model.B00=0.055;
end
```

C. Scripts for PSO Method for Energy Management of The Hybrid System of an Electric Vehicle Charging Station

Main_Start.m

```
clear all
close all
clc


global nbus
global busdata
global linedata
global gendata
global Bdg
global LFl
global lineIV
global busIV
global baseMVA

baseMVA = 100;
nbus = 30;
busdata = busdatas(nbus);
linedata = linedatas(nbus);
gendata = gendatas(nbus);


nBR=length(linedata(:,1));
LFl = linedata(:,7);

[LFs Lpij Lqij J KT KTid VM Pgen Qgen del npq] = updatebus();


%% BASE/NON-OPTIMAL POWER FLOW RESULTS ANALYSIS
VM_mag   = abs(VM);    %%VoltageMag
VM_angle = del;

SFLOW = LFs;          %%LineFlow in kVA

PLOSS = Lpij;         %%RealLINELoss
QLOSS = Lqij;         %%ReactiveLINELoss


TOTAL_PLOSS = sum(PLOSS);
TOTAL_QLOSS = sum(QLOSS);


%% EV PLACEMENT PARAMETERS
n = 5; %%SELECT NUMBER OF BUSES:-  any integer, 1 to maximum number of system
buses, depennding on choice of Number of RES
```

```
LSFactor = KT;              %% determines the top candidate lines with the least LSF
Bdg0 = linedata(KTid,1);    %% determines the sending end buses of the candidate lines

[b,i,j]=unique(Bdg0, 'first');
Bdg1=Bdg0(sort(i));
Bdg2 = Bdg1(Bdg1~=1);       %% remove bus 1 from the sending end buses of the candidate
lines
Bdg = Bdg2(1:n);            %%the "n" selected candidate buses

%--------------mopso optimization with power flow analysis------------------
CostFunction=@(K) CostFun(K);
nVar=length(Bdg);

VarMin=   10*ones(1,nVar);     % Lower Bound of Variables
VarMax=  100*ones(1,nVar);     % Upper Bound of Variables



VarSize=[1 nVar];

VelMax=(VarMax-VarMin)/10;

%% MOPSO Settings

nPop  = 100;   % Population Size

nRep  = 100;   % Repository Size

MaxIt = 150;  % Maximum Number of Iterations


%%Basic PSO parameters
phi1=2.00;
phi2=2.00;
chi = 1;


%%Constricted Coefficient PSO parameters
% phi1=2.05;
% phi2=2.05;
% phi=phi1+phi2;
% chi=2/(phi-2+sqrt(phi^2-4*phi));


%%Other PSO initilaization parameters
w= chi;            % Inertia Weight
wdamp=1;           % Inertia Weight Damping Ratio
c1=chi*phi1;       % Personal Learning Coefficient
c2=chi*phi2;       % Global Learning Coefficient


alpha=0.1;  % Grid Inflation Parameter
```

```
nGrid=1000;   % Number of Grids per each Dimension

beta=8;     % Leader Selection Pressure Parameter

gamma=6;    % Extra (to be deleted) Repository Member Selection Pressure

% Initialization

particle=CreateEmptyParticle(nPop);

for i=1:nPop
   particle(i).Velocity=0;
   particle(i).Position=unifrnd(VarMin,VarMax,VarSize);

   particle(i).Cost=CostFunction(particle(i).Position);

   particle(i).Best.Position=particle(i).Position;
   particle(i).Best.Cost=particle(i).Cost;
end

particle=DetermineDomination(particle);

rep=GetNonDominatedParticles(particle);

rep_costs=GetCosts(rep);
G=CreateHypercubes(rep_costs,nGrid,alpha);

for i=1:numel(rep)
   [rep(i).GridIndex rep(i).GridSubIndex]=GetGridIndex(rep(i),G);
end

% MOPSO Main Loop

for it=1:MaxIt
   for i=1:nPop
      rep_h=SelectLeader(rep,beta);
   w = (0.9 - (0.5*it/MaxIt));
      particle(i).Velocity=w*particle(i).Velocity ...
                     +c1*rand*(particle(i).Best.Position - particle(i).Position) ...
                     +c2*rand*(rep_h.Position -  particle(i).Position);

      particle(i).Velocity=min(max(particle(i).Velocity,-VelMax),+VelMax);

      particle(i).Position=particle(i).Position + particle(i).Velocity;

      flag=(particle(i).Position<VarMin | particle(i).Position>VarMax);
      particle(i).Velocity(flag)=-particle(i).Velocity(flag);

      particle(i).Position=min(max(particle(i).Position,VarMin),VarMax);

      particle(i).Cost=CostFunction(particle(i).Position);

      if Dominates(particle(i),particle(i).Best)
         particle(i).Best.Position=particle(i).Position;
```

```
            particle(i).Best.Cost=particle(i).Cost;

        elseif ~Dominates(particle(i).Best,particle(i))
            if rand<0.5
                particle(i).Best.Position=particle(i).Position;
                particle(i).Best.Cost=particle(i).Cost;
            end
        end

    end

    particle=DetermineDomination(particle);
    nd_particle=GetNonDominatedParticles(particle);

    rep=[rep
         nd_particle];

    rep=DetermineDomination(rep);
    rep=GetNonDominatedParticles(rep);

    for i=1:numel(rep)
        [rep(i).GridIndex rep(i).GridSubIndex]=GetGridIndex(rep(i),G);
    end

    if numel(rep)>nRep
        EXTRA=numel(rep)-nRep;
        rep=DeleteFromRep(rep,EXTRA,gamma);

        rep_costs=GetCosts(rep);
        G=CreateHypercubes(rep_costs,nGrid,alpha);

    end

    disp(['Iteration ' num2str(it) ': Number of Repository Particles = ' num2str(numel(rep))]);

   w=w*wdamp;
end

% Results

costs=GetCosts(particle);
rep_costs=GetCosts(rep);


figure(1)
plot(costs(1,:),costs(2,:),'k.');
hold on;
plot(rep_costs(1,:),rep_costs(2,:),'r*');
legend('Base Case','Optimal case');
xlabel('BEST TOTAL SYSTEM COST')
ylabel('ACTIVE POWER LOSS')

BestSolution = rep_h.Cost
```

```
Optimal_EV_Location = Bdg
K = rep_h.Position;
Optimal_EV_Size = K


[F, VMp, delp, Lpijp, Lqijp,Pgenp, Qgenp, LFsp] = CostFun(K);



%% cpf=0.25;                    % site capacity factor
Niv = 0.95;                  %inverter's efficiency
Npv = 0.85;                    % PV derating factor



VM_mag_opt = abs(VMp);                  %%VoltageMag
VM_angle_opt = delp;

SFLOW_opt = LFsp;          %%LineFlow in KVA

PLOSS_opt = Lpijp;         %%RealLINELoss
QLOSS_opt = Lqijp;         %%ReactiveLINELoss


TOTAL_PLOSS_opt = sum(Lpijp);
TOTAL_QLOSS_opt = sum(Lqijp);




%% FIGURES
figure(2)
plot(VM_mag,'r+--','LineWidth',1.0);
hold on
plot(VM_mag_opt,'bo-','LineWidth',1.25);
hold off
legend('Base Case','Optimal case')
xlim([0 nbus+1])
xlabel('Bus number')
ylabel('Voltage magnitude (pu)')
title('Bus Voltage')
grid on


figure(3)
plot(SFLOW,'r+--','LineWidth',1.0);
hold on
plot(SFLOW_opt,'bo-','LineWidth',1.25);
hold off
legend('Base Case','Optimal case')
legend('Base Case','Optimal case')
xlim([0 nBR+1])
xlabel('Line number')
ylabel('Power flow (kVA)')
```

```
title('Apparent Line Power Flow')
grid on


figure(4)
plot(PLOSS,'r+--','LineWidth',1.0);
hold on
plot(PLOSS_opt,'bo-','LineWidth',1.25);
hold off
legend('Base Case','Optimal case')
xlim([0 nBR+1])
xlabel('Line number')
ylabel('P (kW)')
title('Real Power Loss')
grid on

figure(5)
plot(QLOSS,'r+--','LineWidth',1.0);
hold on
plot(QLOSS_opt,'bo-','LineWidth',1.25);
hold off
legend('Base Case','Optimal case')
xlim([0 nBR+1])
xlabel('Line number')
ylabel('Q (kVAR)')
title('Reactive Power Loss')
grid on
%%%
```

Gendatas.m

```
% Returns Initial Bus datas of the system...

function gendt = gendatas(num)


gendata14  =  [1  0.0070   7.00   240       50      200     -20     250    50   0.0630 ;
%slackbus
           2  0.331           33.544        918.558     20      80      -20     100    40   0.0980;
           3  1.744   3.643   183.851    15      50      -15      80    0     0 ;
           6  0.331           33.544        918.558   10      35      -15      60    0     0;
           8  1.744    3.643  183.851   10      30      -10      50    0     0 ];



gendata30  =    [1        0.0070           7.00    240      50      200   -20   250;
%slack bus
             2    1.744   3.643   183.851   20      80    -20   100;
                    5    0.331         33.544        918.558  15      50    -15    80;
                    8    1.744   3.643   183.851    10      35    -15    60;
```

```
                11    0.331       33.544       918.558  10      30    -10    50;
                13    0.0075 12.0     190      12      40    -15    60];

gendata118  =  [4     1.744      3.643        183.851        5        30       -300    300
              6    0.331      33.544       918.558        5        30       -13     50
              8    0.069663       26.2438        31.67  5        30       -300    300
             10    0.010875       12.8875        6.78   150      300      -147    200
             12    0.010875       12.8875        6.78   100      300      -35     120
             15    1.744      3.643        183.851        10       30       -10     30
             18    0.0128     17.82        10.15  25       100      -16     50
             19    0.069663       26.2438        31.67  5        30       -8      24
             24    0.331      33.544       918.558        5        30       -300    300
             25    0.010875       12.8875        6.78   100      300      -47     140
             26    0.003      10.76        32.96  100      350      -1000   1000
             27    0.069663       26.2438        31.67  8        30       -300    300
             31    1.744      3.643        183.85 8        30       -300    300
             32    0.0128     17.82        10.15  25       100      -14     42
             34    0.069663       26.2438        31.67  8        30       -8      24
             36    0.0128     17.82        10.15  25       100      -8      24
             40    0.069663       26.2438        31.67  8        30       -300    300
             42    0.069663       26.2438        31.67  8        30       -300    300
             46    0.0128     17.82        10.15  25       100      -100    100
             49    0.002401       12.3299        28     50       250      -85     210
             54    0.002401       12.3299        28     50       250      -300    300
             55    0.0128     17.82        10.15  25       100      -8      23
             56    0.0128     17.82        10.15  25       100      -8      15
             59    0.0044     13.29        39     50       200      -60     180
             61    0.0044     13.29        39     50       200      -100    300
             62    0.0128     17.82        10.15  25       100      -20     20
             65    0.01059    8.3391       64.16  100      420      -67     200
             66    0.331      33.544       918.558        100      420      -67     200
             69    0.010875       12.8875        6.78   80       300      -99999  99999
             70    1.744      3.643        183.85 30       80       -10      32
             72    0.069663       26.2438        31.67  10       30       -100    100
             73    0.069663       26.2438        31.67  5        30       -100    100
             74    0.028302       37.6968        17.95  5        20       -6      9
             76    0.0128     17.82        10.15  25       100      -8      23
             77    0.331      33.544       918.558        25       100      -20     70
             80    0.010875       12.8875        6.78   150      300      -165    280
             82    1.744      3.643        183.851        25       100      -9900   9900
             85    0.069663       26.2438        31.67  10       30       -8      23
             87    0.331      33.544       918.558        100      300      -100    1000
             89    0.010875       12.8875        6.78   50       200      -210    300
             90    1.744      3.643        183.851        8        20       -300    300
             91    0.009774       22.9423        58.81  20       50       -100    100
             92    0.010875       12.8875        6.78   100      300      -3      9
             99    0.331      33.544       918.558                 100      300     -100    100
            100 0.010875       12.8875        6.78   100      300      -50     155
            103 1.744      3.643        183.851        8        20       -15     40
            104 0.0128     17.82        10.15  25       100      -8      23
            105 0.0128     17.82        10.15  25       100      -8      23
            107 0.028302       37.6968        17.95  8        20       -200    200
            110 0.331      33.544       918.5581       25       50       -8      23
            111 0.0128     17.82        10.15  25       100      -100    1000
```

```
        112 0.0128    17.82      10.15  25    100    -100   1000
        113 0.0128    17.82      10.15  25    100    -100   200
        116 1.744     3.643      183.85 25    50     -1000  1000];


switch num
   case 14
      gendt = gendata14;

   case 30
      gendt = gendata30;

   case 118

      gendt = gendata118;

end
```

Load Flow.m

```
% Program for Bus Power Injections, Line & Power flows (p.u)...

function [LFs Lpij Lqij VM Pi Qi Pg Qg Pgen Qgen] = loadflow(nbus,V,del,baseMVA)
global busdata
global linedata
global lineIV
global busIV
% global Ppvall

baseMVA = 100;

Y = ybusppg();

type = busdata(:,2);
Vm = pol2rect(V,del);     % Converting polar to rectangular..
Del = del*180/pi;         % Bus Voltage Angles in Degree...
fb = linedata(:,1);       % From bus number...
tb = linedata(:,2);       % To bus number...
nl = length(fb);          % No. of Branches..
PG = busdata(:,5);        % PGi..
QG = busdata(:,6);        % QGi..
PL = busdata(:,7);        % PLi..
QL = busdata(:,8);        % QLi..
%Qsh = busdata(:,11);              %2-30
Qsh = zeros(nbus, 1);


Iij = zeros(nbus,nbus);
Sij = zeros(nbus,nbus);
Si  = zeros(nbus,1);

% Bus Current Injections..
 I  = Y*Vm;
```

```
 Im = abs(I);
 Ia = angle(I);

%Line Current Flows..
for m = 1:nl
    p = fb(m); q = tb(m);
    Iij(p,q) = -(Vm(p) - Vm(q))*Y(p,q); % Y(m,n) = -y(m,n)..
    Iij(q,p) = -Iij(p,q);
end

Iij  = sparse(Iij);
Iijm = abs(Iij);
Iija = angle(Iij);

% Line Power Flows..
for m = 1:nbus
    for n = 1:nbus
        if m ~= n
            Sij(m,n) = Vm(m)*conj(Iij(m,n))*baseMVA;
        end
    end
end
Sij = sparse(Sij);
Pij = real(Sij);
Qij = imag(Sij);

% Line Losses..
Lij = zeros(nl,1); S_ij = zeros(nl,1); S_ji = zeros(nl,1);
for m = 1:nl
    p = fb(m); q = tb(m);
    Lij(m) = Sij(p,q) + Sij(q,p);
    S_ij(m) = abs(Sij(p,q));
    S_ji(m) = abs(Sij(q,p));
end

Lpij = real(Lij);
Lqij = imag(Lij);
LFs  = full(max(S_ij, S_ji));
%LFl = linedata(:,7);                    %2-30

% Bus Power Injections..
for i = 1:nbus
    for k = 1:nbus
        Si(i) = Si(i) + conj(Vm(i))* Vm(k)*Y(i,k)*baseMVA;
    end
end

Pi = real(Si);
Qi = -imag(Si);
Pg = Pi+PL;
Qg = Qi+QL-Qsh;

for m = 1:nbus
    busIV(m,1) = m;
```

```
    busIV(m,2) = V(m);
    busIV(m,3) = Del(m);
    busIV(m,4) = Pg(m);
    busIV(m,5) = Qg(m);
    busIV(m,6) = Pi(m);
end
for m = 1:nl
    p = fb(m); q = tb(m);
    lineIV(m, 1) = p;
    lineIV(m, 2) = q;
    lineIV(m, 3) = Pij(p,q);
    lineIV(m, 4) = Qij(p,q);
    lineIV(m, 5) = q;
    lineIV(m, 6) = p;
    lineIV(m, 7) = Pij(q,p);
    lineIV(m, 8) = Qij(q,p);
    lineIV(m, 9) = S_ij(m);
    lineIV(m, 10) =S_ji(m);
end




 k=0;

for n = 1:nbus
     if type(n) == 1
     k=k+1;
     Si(n)= (Pi(n)+1j*Qi(n));
     Pg(n) = (Pi(n) + PL(n));
     Qg(n) = (Qi(n) + QL(n) - Qsh(n));
     Pgg(k)=Pg(n);
     Qgg(k)=Qg(n);     % April 2017
     elseif  type(n) ==2
     k=k+1;
     Si(n)=(Pi(n)+1j*Qi(n));
     Qg(n) = (Qi(n) + QL(n) - Qsh(n));
     Pgg(k)=PG(n);
     Qgg(k)=Qg(n);  % April 2017
     end
end
```

busdata.m

```
% Returns Initial Bus datas of the system...

function busdt = busdatas(num)

% Type....
% 1 - Slack Bus..
```

```
% 2 - PV Bus..
% 3 - PQ Bus..

%       |Bus | Type | Vsp | theta | PGi | QGi | PLi | QLi |  Qmin | Qmax |

busdata14 = [1    1   1.060   0    232.4   -16.9  0    0      0      0  0;
         2    2   1.045   0     40      0  21.7   12.7   -40    50  0;
         3    2   1.010   0      0      0  94.2   19.1    0     40  0;
         4    3   1.0     0      0      0  47.8    3.9    0      0  0;
         5    3   1.0     0      0      0   7.6    1.6    0      0  0;
         6    2   1.000   0      0      0  11.2    7.5    -6     24  0;
         7    3   1.0     0      0      0   0.0    0.0    0      0  0;
         8    2   1.000   0      0      0   0.0    0.0    -6     24  0;
         9    3   1.0     0      0      0  29.5   16.6    0      0  0;
         10   3   1.0     0      0      0   9.0    5.8    0      0  0;
         11   3   1.0     0      0      0   3.5    1.8    0      0  0;
         12   3   1.0     0      0      0   6.1    1.6    0      0  0;
         13   3   1.0     0      0      0  13.5    5.8    0      0  0;
         14   3   1.0     0      0      0 14.9    5.0    0      0  0];

busdata30=[1   1    1.06    0.0     0.0   0.0    0.0   0.0   -20  250      0
        2   2    1.043   0.0     80     0    21.70 12.7   -20  100      0
        3   3    1.0     0.0     0     0     2.4   1.2     0    0       0
        4   3    1.06    0.0     0     0     7.6   1.6     0    0       0
        5   2    1.01    0.0     50     0    94.2  19.0   -15   80       0
        6   3    1.0     0.0     0.0   0.0    0.0   0.0     0    0       0
        7   3    1.0     0.0     0     0    22.8  10.9     0    0       0
        8   2    1.01    0.0     20     0    30.0  30.0   -15   60       0
        9   3    1.0     0.0     0.0   0.0    0.0   0.0     0    0       0
        10   3    1.0     0.0     0     0     5.8   2.0     0    0       0
        11   2    1.082   0.0     20.0   0.0    0.0   0.0   -10   50       0
        12   3    1.0     0       0     0    11.2   7.5     0    0       0
        13   2    1.071   0       20    0.0     0     0    -15   60       0
        14   3    1       0       0     0     6.2   1.6     0    0       0
        15   3    1       0       0     0     8.2   2.5     0    0       0
        16   3    1       0       0     0     3.5   1.8     0    0       0
        17   3    1       0       0     0     9.0   5.8     0    0       0
        18   3    1       0       0     0     3.2   0.9     0    0       0
        19   3    1       0       0     0     9.5   3.4     0    0       0
        20   3    1       0       0     0     2.2   0.7     0    0       0
        21   3    1       0       0     0    17.5  11.2     0    0       0
        22   3    1       0       0    0.0     0     0      0    0       0
        23   3    1       0       0     0     3.2   1.6     0    0       0
        24   3    1       0       0     0     8.7   6.7     0    0      4.3
        25   3    1       0       0    0.0     0     0      0    0       0
        26   3    1       0       0     0     3.5   2.3     0    0       0
        27   3    1       0       0    0.0     0     0      0    0       0
        28   3    1       0       0    0.0     0     0      0    0       0
        29   3    1       0       0     0     2.4   0.9     0    0       0
        30   3    1       0       0     0    10.6   1.9     0    0       0];

busdata118 =   [1       1        1.035   0        516.4   0        0        0        -300    300
           2     3        0.971   0        0        0        20       9        0        0
           3     3        0.968   0        0        0        39       10       0        0
```

4	2	0.998	0	0	0	39	12	-300	300	
5	3	1.002	0	0	-40	0.5518		0.050	0	0
6	2	0.99	0	0	0	52	22	-13	50	
7	3	0.989	0	0	0	19	2	0	0	
8	2	1.015	0	0	0	28	0	-300	300	
9	3	1.043	0	0	0	0.5518	0.050	0	0	
10	2	1.05	0	450	0	0.119	0.0251	-147	200	
11	3	0.985	0	0	0	70	23	0	0	
12	2	0.99	0	85	0	47	10	-35	120	
13	3	0.968	0	0	0	34	16	0	0	
14	3	0.984	0	0	0	14	1	0	0	
15	2	0.97	0	0	0	90	30	-10	30	
16	3	0.984	0	0	0	25	10	0	0	
17	3	0.995	0	0	0	11	3	0	0	
18	2	0.973	0	0	0	60	34	-16	50	
19	2	0.963	0	0	0	45	25	-8	24	
20	3	0.958	0	0	0	18	3	0	0	
21	3	0.959	0	0	0	14	8	0	0	
22	3	0.97	0	0	0	10	5	0	0	
23	3	1	0	0	0	7	3	0	0	
24	2	0.992	0	0	0	13	0	-300	300	
25	2	1.05	0	220	0	0.5518	0.050	-47	140	
26	2	1.015	0	314	0	0.1911	0.0318	-1000	1000	
27	2	0.968	0	0	0	71	13	-300	300	
28	3	0.962	0	0	0	17	7	0	0	
29	3	0.963	0	0	0	24	4	0	0	
30	3	0.968	0	0	0	0.4614		0.097	0	0
31	2	0.967	0	7	0	43	27	-300	300	
32	2	0.964	0	0	0	59	23	-14	42	
33	3	0.972	0	0	0	23	9	0	0	
34	2	0.986	0	0	14	59	26	-8	24	
35	3	0.981	0	0	0	33	9	0	0	
36	2	0.98	0	0	0	31	17	-8	24	
37	3	0.992	0	0	-25	0.4614		0.097	0	0
38	3	0.962	0	0	0	0.5518	0.050	0	0	
39	3	0.97	0	0	0	27	11	0	0	
40	2	0.97	0	0	0	66	23	-300	300	
41	3	0.967	0	0	0	37	10	0	0	
42	2	0.985	0	0	0	96	23	-300	300	
43	3	0.978	0	0	0	18	7	0	0	
44	3	0.985	0	0	10	16	8	0	0	
45	3	0.987	0	0	10	53	22	0	0	
46	2	1.005	0	19	10	28	10	-100	100	
47	3	1.017	0	0	0	34	0	0	0	
48	3	1.021	0	0	15	20	11	0	0	
49	2	1.025	0	204	0	87	30	-85	210	
50	3	1.001	0	0	0	17	4	0	0	
51	3	0.967	0	0	0	17	8	0	0	
52	3	0.957	0	0	0	18	5	0	0	
53	3	0.946	0	0	0	23	11	0	0	
54	2	0.955	0	48	0	113	32	-300	300	
55	2	0.952	0	0	0	63	22	-8	23	
56	2	0.954	0	0	0	84	18	-8	15	
57	3	0.971	0	0	0	12	3	0	0	

58	3	0.959	0	0	0	12	3	0	0	
59	2	0.985	0	155	0	277	113	-60	180	
60	3	0.993	0	0	0	78	3	0	0	
61	2	0.995	0	160	0	0	0	-100	300	
62	2	0.998	0	0	0	77	14	-20	20	
63	3	0.969	0	0	0	0.4614		0.097	0	0
64	3	0.984	0	0	0	0.4614		0.097	0	0
65	2	1.005	0	391	0	0	0	-67	200	
66	2	1.05	0	392	0	39	18	-67	200	
67	3	1.02	0	0	0	28	7	0	0	
68	3	1.003	0	0	0	0.5518	0.050	0	0	
69	2	0.955	0	0	0	51	27	-5	15	
70	2	0.984	0	0	0	66	20	-10	32	
71	3	0.987	0	0	0	0.119	0.0251	0	0	
72	2	0.98	0	0	0	12	0	-100	100	
73	2	0.991	0	0	0	6	0	-100	100	
74	2	0.958	0	0	12	68	27	-6	9	
75	3	0.967	0	0	0	47	11	0	0	
76	2	0.943	0	0	0	68	36	-8	23	
77	2	1.006	0	0	0	61	28	-20	70	
78	3	1.003	0	0	0	71	26	0	0	
79	3	1.009	0	0	20	39	32	0	0	
80	2	1.04	0	477	0	130	26	-165	280	
81	3	0.997	0	0	0	0.5518	0.050	0	0	
82	3	0.989	0	0	20	54	27	0	0	
83	3	0.985	0	0	10	20	10	0	0	
84	3	0.98	0	0	0	11	7	0	0	
85	2	0.985	0	0	0	24	15	-8	23	
86	3	0.987	0	0	0	21	10	0	0	
87	2	1.015	0	4	0	0.5518	0.050	-100	1000	
88	3	0.987	0	0	0	48	10	0	0	
89	2	1.005	0	607	0	0	0	-210	300	
90	2	0.985	0	0	0	163	42	-300	300	
91	2	0.98	0	0	0	10	0	-100	100	
92	2	0.993	0	0	0	65	10	-3	9	
93	3	0.987	0	0	0	12	7	0	0	
94	3	0.991	0	0	0	30	16	0	0	
95	3	0.981	0	0	0	42	31	0	0	
96	3	0.993	0	0	0	38	15	0	0	
97	3	1.011	0	0	0	15	9	0	0	
98	3	1.024	0	0	0	34	8	0	0	
99	2	1.01	0	0	0	42	0	-100	100	
100	2	1.017	0	252	0	37	18	-50	155	
101	3	0.993	0	0	0	22	15	0	0	
102	3	0.991	0	0	0	5	3	0	0	
103	2	1.001	0	40	0	23	16	-15	40	
104	2	0.971	0	0	0	38	25	-8	23	
105	2	0.965	0	0	20	31	26	-8	23	
106	3	0.962	0	0	0	43	16	0	0	
107	2	0.952	0	0	6	50	12	-200	200	
108	3	0.967	0	0	0	2	1	0	0	
109	3	0.967	0	0	0	8	3	0	0	
110	2	0.973	0	0	6	39	30	-8	23	
111	2	0.98	0	36	0	0.4614		0.097	-100	1000

```
112 2 0.975 0 0 0 68 13 -100 1000
113 2 0.993 0 0 0 6 0 -100 200
114 3 0.96 0 0 0 8 3 0 0
115 3 0.96 0 0 0 22 7 0 0
116 2 1.005 0 0 0 184 0 -1000 1000
117 3 0.974 0 0 0 20 8 0 0
118 3 0.949 0 0 0 33 15 0 0];
```

```
%%IEEE STANDARD TEST SYSTEM

 switch num

       case 14
       busdt = busdata14;

       case 30
       busdt = busdata30;

           case 118

       busdt = busdata118;


end


end
```

CreateEmptyParticles.m

```
function particle=CreateEmptyParticle(n)

   if nargin<1
      n=1;
   end

   empty_particle.Position=[];
   empty_particle.Velocity=[];
   empty_particle.Cost=[];
   empty_particle.Dominated=false;
   empty_particle.Best.Position=[];
   empty_particle.Best.Cost=[];
   empty_particle.GridIndex=[];
   empty_particle.GridSubIndex=[];

   particle=repmat(empty_particle,n,1);
```

```
end
```

CreateHypercubes.m

```
function G=CreateHypercubes(costs,ngrid,alpha)

    nobj=size(costs,1);

    empty_grid.Lower=[];
    empty_grid.Upper=[];
    G=repmat(empty_grid,nobj,1);

    for j=1:nobj

        min_cj=min(costs(j,:));
        max_cj=max(costs(j,:));

        dcj=alpha*(max_cj-min_cj);

        min_cj=min_cj-dcj;
        max_cj=max_cj+dcj;

        gx=linspace(min_cj,max_cj,ngrid-1);

        G(j).Lower=[-inf gx];
        G(j).Upper=[gx inf];

    end
```

GetCosts.m

```
function costs=GetCosts(pop)

    nobj=numel(pop(1).Cost);
    costs=reshape([pop.Cost],nobj,[]);

end
```

Linedata.m

```
%UNTITLED2 Summary of this function goes here
%   Detailed explanation goes here
% Returns Line datas of the system...

function linedt = linedatas(num)
```

```
%          | From | To   |  R    |  X    |    B/2  | X'mer  | LFl |
%          | Bus  | Bus  |  pu   |  pu   |    pu   | TAP (a)|  MVA |
linedata14 = [1     2     0.01938   0.05917    0.0264       1    120    1
          1     5     0.05403   0.22304    0.0219       1    65    2
          2     3     0.04699   0.19797    0.0187       1    36    3
          2     4     0.05811   0.17632    0.0246       1    65    4
          2     5     0.05695   0.17388    0.0170       1    50    5
          3     4     0.06701   0.17103    0.0173       1    65    6
          4     5     0.01335   0.04211    0.0064       1    45    7
          4     7     0.0       0.20912    0.0        0.978    55    8
          4     9     0.0       0.55618    0.0        0.969    32    9
          5     6     0.0       0.25202    0.0        0.932    45   10
          6    11     0.09498   0.19890    0.0          1     18   11
          6    12     0.12291   0.25581    0.0          1     32   12
          6    13     0.06615   0.13027    0.0          1     32   13
          7     8     0.0       0.17615    0.0          1     32   14
          7     9     0.0       0.11001    0.0          1     32   15
          9    10     0.03181   0.08450    0.0          1     32   16
          9    14     0.12711   0.27038    0.0          1     32   17
          10   11     0.08205   0.19207    0.0          1     12   18
          12   13     0.22092   0.19988    0.0          1     12   19
          13   14     0.17093   0.34802    0.0          1     12   20];


linedata30  =  [1    2     0.0192   0.0575     0.02640      1     130     1
           1    3     0.0452   0.1852            0.02040      1     130     2
           2    4     0.0570   0.1737     0.01840      1     65     3
           2    5     0.0472   0.1983     0.02090      1     130     4
           2    6     0.0581   0.1763     0.01870      1     65     5
           3    4     0.0132   0.0379     0.00420      1     130     6
           4    6     0.0119   0.0414     0.00450      1     90     7
           4    12       0     .2560     0          0.932    65     8
           5    7     0.0460   0.1160     0.01020      1     70     9
           6    7     0.0267   0.0820     0.00850      1     130    10
           6    8     0.0120   0.0420     0.00450      1     32    11
           6    9       0.0   0.2080     0.0        0.978    65    12
           6    10       0    0.5560     0          0.969    32    13
           6    28     .0169     .0599     0.065        1      32    14
           8    28     .0636     .2000     0.0214       1      32    15
           9    11       0     0.2080     0            1      65    16
           9    10       0      .1100     0            1      65    17
          10    20     .0936     .2090     0            1      32    18
          10    17     .0324     .0845     0            1      32    19
          10    21     .0348     .0749     0            1      32    20
          10    22     .0727     .1499     0            1      32    21
          12    13       0      .1400     0            1      65    22
          12    14     .1231     .2559     0            1      32    23
          12    15     .0662     .1304     0            1      32    24
          12    16     .0945     .1987     0            1      32    25
          14    15     .2210     .1997     0            1      16    26
          15    18     .1073     .2185     0            1      16    27
          15    23     .1000     .2020     0            1      16    28
          16    17     .0824     .1923     0            1      16    29
```

```
18    19    .0639    .1292    0        1      16    30
19    20    .0340    .0680    0        1      32    31
21    22    .0116    .0236    0        1      32    32
22    24    .1150    .1790    0        1      16    33
23    24    .1320    .2700    0        1      16    34
24    25    .1885    .3292    0        1      16    35
25    26    .2544    .3800    0        1      16    36
25    27    .1093    .2087    0        1      16    37
27    29    .2198    .4153    0        1      16    38
27    30    .3202    .6027    0        1      16    39
28    27      0      .3960    0      0.968    65    40
29    30    .2399    .4533    0        1      16    41];


%%IEEE STANDARD TEST SYSTEM

switch num


    case 14                    %
    linedt = linedata14;

    case 30                    %
    linedt = linedata30;

end
end
```

Ybusppg.m

```
%UNTITLED Summary of this function goes here
%   Detailed explanation goes here
% Program to for Admittance And Impedance Bus Formation....

function Y = ybusppg()  % Returns Y

global linedata

fb = linedata(:,1);          % From bus number...
tb = linedata(:,2);          % To bus number...
r = linedata(:,3);           % Resistance, R...
x = linedata(:,4);           % Reactance, X...
b = linedata(:,5);           % Ground Admittance, B/2...
a = linedata(:,6);           % Tap setting value..
z = r + i*x;                 % z matrix...
y = 1./z;                    % To get inverse of each element...
b = i*b;                     % Make B imaginary...

nb = max(max(fb),max(tb));   % No. of buses...
nl = length(fb);             % No. of branches...
Y = zeros(nb,nb);            % Initialise YBus...
```

```
% Formation of the Off Diagonal Elements...
for k = 1:nl
   Y(fb(k),tb(k)) = Y(fb(k),tb(k)) - y(k)/a(k);
   Y(tb(k),fb(k)) = Y(fb(k),tb(k));
end

% Formation of Diagonal Elements....
for m = 1:nb
   for n = 1:nl
      if fb(n) == m
         Y(m,m) = Y(m,m) + y(n)/(a(n)^2) + b(n);
      elseif tb(n) == m
         Y(m,m) = Y(m,m) + y(n) + b(n);
      end
   end

%Y;                % Bus Admittance Matrix
%Z = inv(Y);       % Bus Impedance Matrix

end
```

solar PV CostFun.m

```
function [F, VMp, delp, Lpijp, Lqijp,Pgenp, Qgenp, LFsp] = CostFun(K)

global busdata
global linedata
global gendata
global Bdg
global nbus
global LFl
global lineIV
global busIV


Pgenmin=gendata(:,5);
Pgenmax=gendata(:,6);

Qgenmin=gendata(:,7);
Qgenmax=gendata(:,8);
%%%%%%%%%%%%%%%%%%   PV array parameters
%%%%%%%%%%%%%%%%%%%%%%
Cstinv = 1748;              % Investment/initial Cost pf PV with storage [$/kW]
Ompv   = 33.67;             % yearly operating and maintenance cost     [$/kW-Yr]
spv    = 0.25*Cstinv;       % reselling price [$/kW]
%ibat  = 353;
%epv   = 0.14;              % efficiency
cpf    = 0.25;              % site capacity factor
TY     = 8760;              % area of land
Npv    = 0.85;              % derating factor/conversion efficiency
int    = 0.10;              % interest rate
```

```
infl   = 0.04;                 % Inflation rate
esc    = 0.075;                 % Escalation rate
Gstd   = 1000;
Rc     = 150;
Niv    = 0.95;                 %inverter's efficiency
%%%%%%%%%%%%%%%%%%%%%%%%%%%%%%%%%%%%%%%%%%%%%%%%%%%%%%%%%%%%%%%%%%%%%%%%%%%%%%%%%%%%%%%%%%%%%%%%%%

%%%%%%%%%%%%%Daily solar insolation data [w/m2]  %%%%%%%%%%%%%%%
Id=     [0
        0
        0
        0
        0
    8.0000
   11.7288
  156.6027
  368.9123
  578.1808
  735.6849
  834.0000
  872.7973
  839.2630
  735.6466
  577.1973
  377.5205
  154.2548
   11.3425
        0
        0
        0
        0
        0];



%%%%%%%%%%%%%%%%%%%%%%%%GRID OPERATION WITH DG%%%%%%%%%%%%%%%%%%%%%%%%%%%%%

Ndg=length(Bdg);

for bt=1:Ndg
for     t=1:24
    if      Id(t)  >= 0 & Id(t) <= Rc
            Ppv(bt,t)= K(bt)*Id(t)^2/(Gstd*Rc);
    elseif  Id(t)>Rc
            Ppv(bt,t)= K(bt)*Id(t)/Gstd;
    end
end

end

PPV = (mean(Ppv,2)./cpf)*Niv*Npv;                        %%capacity factor (cpf) for finding the effective DG size for Power Flow analysis
```

```
%PPV = cpf*Niv*Npv*mean(Ppv,2);                    %%Niv is the inverter efficiency

busdata = busdatas(nbus);
busdata(Bdg, 7) = busdata(Bdg, 7) - PPV;           %NEGATIVE LOAD MODEL
FOR DG AT SELECTED BUSES

QPV = tan(acos(0.9))*PPV;
busdata(Bdg, 8) = busdata(Bdg, 8) - QPV;           %Assume inverter at PF = 0.90
and 95% efficiency


PLT=sum(busdata(:,7));

nbus = length(busdata(:,1));  nl=length(linedata(:,1));



[LFs Lpij Lqij J KT KTid VM Pgen Qgen del npq] = updatebus();
% % %%==========Real power generaed
limit==========================================
% % % %
% %
% %        k1 = 1*(sum((Pgen > Pgenmax).*(Pgen - Pgenmax).*(Pgen - Pgenmax)) +
sum((Pgen < Pgenmin).*(Pgenmin - Pgen).*(Pgenmin - Pgen)));
% %
% %
% % %%==========Reactive power generaed
limit==========================================
% %
% %
% %        k2 = 1*(sum((Qgen > Qgenmax).*(Qgen - Qgenmax).*(Qgen - Qgenmax)) +
sum((Qgen < Qgenmin).*(Qgenmin - Qgen).*(Qgenmin - Qgen)));
% %
% %
% % %%==========Bus voltage
limit==========================================
% %
% %
% %        k3 = 10^3*(sum((VM > 1.05).*(VM - 1.05).*(VM - 1.05)) + sum((VM < 0.95).*(0.95
- VM).*(0.95 - VM)));
% %
% %
% % %%=====================Line flow
limit=======================================
% %
% %        k4 = 100*sum((LFs > LFl).*(LFs - LFl).*(LFs - LFl));
% %
% %
% %
% % lam=1500*abs(sum(Pgen) - sum(Lpij) - PLT) + k1 + k2 + k3 + k4;



  %% COST MODEL FOR ECONOMIC ANALYSIS (FOR MULTIOBJECTIVE)
```

```
  % FOR PV SYSTEM
   Cinv= sum(K)*Cstinv;                % capital cost of the investment for 25 years [$]

   for j=1:25
   OMpv(j)= (Ompv*sum(K)*cpf*TY)*((1+esc)/(1+int))^j;
   end
   OMpv=sum(OMpv);        % Total operation and maintainence cost for 25 years [$]


   Spv=(spv*sum(K))*(((1+infl)/(1+int))^25);                % resale price after 25 years [$]



TotalPVSetuPcost= (Cinv + OMpv - Spv);  % Total PV cost per hour

%% POSIBLE OBJECTIVE FUNCTIONS
a = TotalPVSetuPcost;  %% TOTAL INVESTMENT COST (ECONOMIC)
b = sum(Lpij);         %% TOTAL LINE LOSS (TECHNICAL)
d = sum(abs(VM - 1.0));  %% TOTAL ABSOLUTE VOLTAGE DEVIATION (TECHNICAL)




%=%==================single-objective problem
formulation==================================================
 F1 = a; %+lam; % total cost with violation...
 F2 = b;


F = [F1 F2]';



 VMp   = VM;
 delp  = del;
 Lpijp = Lpij;
 Lqijp = Lqij;
 Pgenp = Pgen;
 Qgenp = Qgen;
 LFsp  = LFs;

end
```

D. PSO scripts for PV-Bat-Grid energy management of the hybrid system

```
clear;clc;close all;tic;
% Note that the energy management system (EMS) is a dummy system.
% This algorithm is used to learn how to size a PV-Bat-Grid
% standalone system using particle swarm optimization.

%% PSO Setting

set.Nparticle=50;
set.Niteration=200;
set.w=1;
set.c1=2.05;
set.c2=2.05;

set.weight_LGS=100;             %LGS Weightage
set.weight_COESS=100;           %COESS Weightage
set.desired_LGS=-100;           %Desired LGS
set.Normal_COESS=1000;          %Normalize COESS

set.Npv_min=6600;
set.Npv_max=350e3;
set.Nbat_min=6600;
set.Nbat_max=400e3;
set.Ngrid_min=6600;
set.Ngrid_max=350e3;


%% Initiate Particle
particle.position=[];
particle.velocity=[];
particle.best_position=[];
particle.best_LGS=[];
particle.best_COESS=[];
particle.best_Mark=[];
particle=repmat(particle,1,set.Nparticle);

best_global.position=[];
best_global.LGS=[];
best_global.COESS=[];
best_global.Mark=[];
log_global=repmat(best_global,1,set.Niteration);


%% Initiate initial Condition
temp_InitiateP(:,1)=randi([set.Npv_min,set.Npv_max],set.Nparticle,1);
temp_InitiateP(:,2)=randi([set.Nbat_min,set.Nbat_max],set.Nparticle,1);
temp_InitiateP(:,3)=randi([set.Ngrid_min,set.Ngrid_max],set.Nparticle,1);

for n_par=1:set.Nparticle
    particle(n_par).position=temp_InitiateP(n_par,:);
    particle(n_par).velocity=[0 0 0];
```

```
end
clear n_par temp_InitiateP


%% Main PSO
for n_ite=1:set.Niteration
   for n_par=1:set.Nparticle
      [LGS,COESS]=EMS(particle(n_par).position(1),...
         particle(n_par).position(2),...
         particle(n_par).position(3));
      %% Calculate Mark
      Mark=set.weight_LGS*abs(LGS-set.desired_LGS)+...
         set.weight_COESS*COESS/set.Normal_COESS;
      %% Best Particle
      if isempty(particle(n_par).best_Mark) || particle(n_par).best_Mark>Mark
         particle(n_par).best_position=particle(n_par).position;
         particle(n_par).best_LGS=LGS;
         particle(n_par).best_COESS=COESS;
         particle(n_par).best_Mark=Mark;
      end
      %% Best Global
      if (n_ite==1 && n_par==1) || best_global.Mark>Mark
         best_global.position=particle(n_par).position;
         best_global.LGS=LGS;
         best_global.COESS=COESS;
         best_global.Mark=Mark;
      end
      log_global(n_ite)=best_global;

      %% Velocity and New Position
      particle(n_par).velocity=set.w*particle(n_par).velocity...
         +set.c1*(particle(n_par).best_position-particle(n_par).position)...
         +set.c2*(best_global.position-particle(n_par).position);
      particle(n_par).position=particle(n_par).position...
         +particle(n_par).velocity;

      %% Round Position
      particle(n_par).position(1)=round(particle(n_par).position(1));
      particle(n_par).position(2)=round(particle(n_par).position(2));
      particle(n_par).position(3)=round(particle(n_par).position(3));

      %% Limit Position
      if particle(n_par).position(1)<set.Npv_min
         particle(n_par).position(1)=set.Npv_min;
      end
      if particle(n_par).position(2)<set.Nbat_min
         particle(n_par).position(2)=set.Nbat_min;
      end
      if particle(n_par).position(3)<set.Ngrid_min
         particle(n_par).position(3)=set.Ngrid_min;
      end
      if particle(n_par).position(1)>set.Npv_max
         particle(n_par).position(1)=set.Npv_max;
      end
```

```
        if particle(n_par).position(2)>set.Nbat_max
            particle(n_par).position(2)=set.Nbat_max;
        end
        if particle(n_par).position(3)>set.Ngrid_max
            particle(n_par).position(3)=set.Ngrid_max;
        end
    end
end
clear LGS COESS Mark n_ite n_par

%% Show Result
for n_ite=1:set.Niteration
    LGS(n_ite)=log_global(n_ite).LGS;
    COESS(n_ite)=log_global(n_ite).COESS;
end
subplot(2,1,1);
plot(LGS);
grid on;
xlabel('n-th Iteration')
ylabel('Loss of Grid Supply, LGS');

subplot(2,1,2);
plot(COESS);
grid on;
xlabel('n-th Iteration')
ylabel('Cost of ESS, COESS ($)');

tpro=toc;
fprintf('The optimum system size is:\n   Npv=%d\n   Nbat=%d\n   Ngrid=%d\nwith the LGS =
%.3f%% and COESS = $%.2f\nCompute in %.2f s\n',...
    best_global.position,best_global.LGS*100,best_global.COESS,tpro);
beep;
```

EMS.m

```
function [LGS,COESS]=EMS(Npv,Nbat,Ngrid)
% This is just a dummy EMS System
LGS = 1/(0.5*Npv+0.3*Nbat+0.1*Ngrid);
COESS = 0.1*(0.3*Npv+0.2*Nbat+0.4*Ngrid);
```